Note: CD on back

CHARACTERISATION OF "WILLIN", A SCIATIC NERVE-DERIVED NOVEL MEMBER OF THE FERM DOMAIN-CONTAINING FAMILY OF PROTEINS.

By

Frances E. Brannigan BSc.(Hons)

School of Biology

University of St Andrews

A thesis submitted in partial fulfillment of the requirements

for the degree of Doctor of Philosophy

April 2006

Declarations

I, Frances Brannigan, hereby certify that this thesis, which is approximately 45,000 words in length, has been written by me, that it is the record of work carried out by me and that it has not been submitted in any previous application for a higher degree.

Date 12/4/06 Signature of candidate..

I was admitted as a research student in October 1999 and as a candidate for the degree of Doctor of Philosophy in October 1999; the higher study for which this is a record was carried out in the University of St Andrews between 1999 and 2006.

Date 12/4/06 Signature of candidate.

I hereby certify that the candidate has fulfilled the conditions of the Resolution and Regulations appropriate for the degree of Doctor of Philosophy in the University of St Andrews and that the candidate is qualified to submit this thesis in application for that degree.

Date 12/4/06 Signature of co-supervisor.

Date 12/4/06 Signature of co-supervisor

In submitting this thesis to the University of St Andrews I understand that I am giving permission for it to be made available for use in accordance with the regulations of the University Library for the time being in force, subject to any copyright vested in the work not being affected thereby. I also understand that the title and abstract will be published, and that a copy of the work may be made available and supplied to any bona fide library or research worker.

Date 12/4/06 Signature of candidate.

ACKNOWLEDGEMENTS

I would firstly like to say an all-encompassing thank you to my long-suffering family and friends.

I am hugely and permanently indebted to Professor Pat Willmer for becoming my second supervisor, despite the inherent heavy workload which this step would entail; for constant encouragement during the fairly numerous tough times; and for an incalculable level of support.

I would like to say an emphatic thank you to Ailsa Ritchie of Student Support Services for all her assistance during my time in St Andrews. Thanks also to Chris Lusk and the rest of the Student Support Services Team.

My warmest thanks to Tina Briscoe for being a great, great friend, and for an incredible amount of help, both inside and outside of the lab.

I would like to extend my thanks to the following people who helped me in a large number of ways, and, due to the circumstances, probably helped me a lot more than I ever helped them (!):

Fleur Davey

Lorraine Hughes

Heidi Mendoza

Margaret Taylor

Claire Phillips

I am very grateful to Professor Keith Sillar for his assistance during my PhD.

To the technical, secretarial and support staff in the Bute, who provided much assistance and who always had time to help – thank you:

Murray Coutts

Moira Dodds

Ian Grieve

Jane Mackie

Joyce Strachan

Alex Taylor

I would like to thank Professor Jeremy Tavaré and all in the Tavaré lab for affording me the warmest of welcomes during my visit to the University of Bristol. I would particularly like to thank Gavin Welsh for donating his time and offering his expert assistance during the live cell imaging work.

Thank you to Alex Houston for all the DNA sequencing, and to Tony Vaughan for all the assistance with the Deltavision.

Thanks also to Kieren Allinson, who assisted with some of the western blots shown in Chapter 3.

I would finally like to convey my thanks to: Jo Avis and Jackie Platt at the former UMIST, Vanessa Cowton, Frank Gunn-Moore, Maria Hill, Michelle McRobbie, Colin Sinclair and Jean Young.

This PhD was funded by:

BBSRC

University of St Andrews School of Biology

William Ramsay Henderson Trust

Abstract

The partial DNA sequence of a new gene of neurological origin – "willin" – had been discovered. Bioinformatics searches classified the new gene as a member of the ERM family of proteins. These proteins are known to act as membrane-cytoskeletal linkers; to be involved in cell shape and movement; and to participate in cell signalling pathways.

Whole and partial segments of the willin gene were cloned into various expression vectors. Cultured cell lines were analysed to assay for the possible presence of the native protein and, along with the expressed protein, to characterise two anti-willin antibodies. EGFP-tagged versions of the protein were expressed in different cell lines to examine their localisation and effect on the cells. Attempts were made to purify the expressed protein. Live cell imaging experiments were conducted to observe the movement of willin in response to stimuli.

A band corresponding to the possible full length protein was detected in certain cell lines. Full length willin was found to localise in a similar manner to the other members of the ERM family; furthermore, it localised in a different manner to that observed in cells expressing constructs containing its N-terminus only, or its C-terminus only. Transfection of the willin N- or C-termini into HEK cells caused pronounced aberrant cell morphology. A protocol was successfully developed to enable the extraction of viable amounts of the protein from induced cells. Microscope images were captured which showed changes in the localisation of willin following treatment of the cells with EGF or ionomycin.

CONTENTS

CHAPTER 2: Experimental

Chapter 3: Analysis of anti-willin antibodies and examination of the expression of the native willin gene and protein.

Chapter 4: Imaging of the subcellular targeting of willin in mammalian cell lines using enhanced green fluorescent protein (EGFP) fusion proteins

Chapter 5: Investigation into willin's binding partners using protein lipid overlays and live cell imaging

List of Figures

Chapter 1

Chapter 3

List of tables

Abbreviations

~	Approximately
Å	Angstroms
aas	Amino acids
AGEs	Advanced glycation end products
AKAP78	cAMP-dependent protein kinase [A-kinase] anchoring protein 78
AP	Affinity purified
ARNO	ARF nucleotide-binding-site opener
Bc	Blue channel
BHK	Baby hamster kidney
bp	Base pairs
BSA	Bovine serum albumin
CD44	Cluster of differentiation 44
cDNA	Complementary DNA
CHO	Chinese hamster ovary
CK1	Anti-chicken 1 antibody
CLIC5	Chloride intracellular channel 5
CMC	Critical micelle concentration
C-terminus	Carboxy terminus
CW	C-terminus of willin
DABCO	4-diazabicyclo[2,2,2]octane
DAPI	2,4-diamindophenylindole
DAPP	Dual adaptor for phosphotyrosine and 3-phosphoinositides
dH_20	Distilled water
DMEM	Dulbecco's modified eagle's medium
DMF	Dimethyl formamide
DNA	Deoxyribonucleic acid
dNTP	2'deoxynucleotide 5'triphosphate
E.coli	*Escherichia coli*
E3KARP	NHE3 Kinase A Regulatory Protein
EBP50	ERM binding phosphoprotein 50
ECL	Enhanced chemiluminescence
EDTA	Ethylenediamine tetraacetic acid
EGF	Epidermal growth factor
EGFP	Enhanced green fluorescent protein
EPEC	Enteropathogenic *E.coli*
ERM	Ezrin radixin moesin
ERM-BMPs	ERM Binding Membrane Proteins
erv-1	Endogenous retrovirus-1
F-actin	Filamentous actin
FERM	Four point one ezrin radixin moesin
G-actin	Globular actin
Gc	Green channel
GDP	Guanosine 5'diphosphate
GFP	Green fluorescent protein
GST	Glutathione-s-transferase

GTP	Guanosine 5'triphosphate
H willin	Human willin
HEK	Human embryonic kidney
Hela	Helen Lane
HFL	Human full length willin
HGMP	Human genome mapping project
HRP	Horse radish peroxidase
ICAM	Intracellular adhesion molecule
Ig	Immunoglubulin
IP3	Inositol 1,4,5-trisphosphate
IPTG	Isopropylthio-β-D-galactoside
RNAi	Inhibition of ribonucleic acid
Kda	Kilodaltons
LB	Luria Bertani medium
MALDI-TOF	Matrix-Assisted Laser Desportion/Ionisation – Time of Flight
MDCK	Madin-Darby canine kidney
Micro-CALI	Micro-Chromophore Assisted Laser Inactivation
MQH_20	MilliQ water
MRC	Medical Research Council
mRNA	Messenger RNA
N-/C-ERMAD	N- or C-Ezrin-Radixin-Moesin association domain
Na-H	Sodium-hydrogen
NEB	New England Biolabs
NEP	Neutral endopeptidase 24.11
NF2	Neurofibromatosis Type 2
NGF	Nerve growth factor
NHE	Na^+/H^+ exchanger
NHERF	Na^+H^+ Exchanger Regulatory factor
N-terminus	Amino terminus
NW	N-terminal of willin
ORF	Open reading frame
p	Panned
P	Pellet fraction
PAGE	Polyacrylamide gel electrophoresis
PBS	Phosphate buffered saline
PCR	Polymerase chain reaction
PDZ	PSD95 discs large Zonula occludens
pI	Isoelectric point
PI	Phosphatidyl inositol
PI-3,4,5-P2	Phosphatidyl inositol-3,4,5-triphosphate
PI-3,4-P2	Phosphatidyl inositol-3,4-bisphosphate
PI-3,5-P2	Phosphatidyl inositol-3,5-bisphosphate
PI-3-P	Phosphatidyl inositol-3-phosphate
PI-4,5-P2	Phosphatidyl inositol-4,5-bisphosphate
PI-4-P	Phosphatidyl inositol-4- phosphate
PI-4-P-5K	Phosphatidyl inositol-4-phosphate 5-kinse
PI-5-P	Phosphatidyl inositol-5-phosphate
PIP2	Phosphatidyl inositol-4, 5-bisphosphate

PK	Protein kinase
PLC	Phospholipase C
PLO	Protein lipid overlay
PM	Plasma membrane
PMSF	Phenylmethylsulfonyl fluoride
PP	Polyproline
PSD95	Postsynaptic density protein 95
RANTES	Regulated upon activation, normal T cell-expressed and -secreted
Rc	Red channel
RER	Rough endoplasmic reticulum
Rho-GDI	Rho-GDP dissociation inhibitor
RNA	Ribonucleic acid
RNAi	RNA interference
ROCK	Rho-associated kinase
RPE	Retinal pigmented epithelial
RPEc5	RPE clone 5
RPEc5TCL1	RPE clone 5 tumour cell line 1
RT-PCR	Reverse transcription PCR
S	Supernatant fraction
S phase	Synthesis phase
S. cerevisiae	*Saccharomyces cerevisiae*
Sarcosyl	n-Lauroylsarcosine
SDS	Sodium dodecyl sulphate
Sf9	*Spodoptera frugiperda* insect cells
Taq	*Thermus aquaticus* [DNA polymerase]
TBE	Tris-borate/EDTA
TE	Tris EDTA
TEMED	N,N,N',N'-tetramethylethylenediamine
Triton	t-Octylphenoxypolyethoxyethanol
Tween	Polyoxyethylenesorbitan monolaurate
UV	Ultraviolet
VASP	Vasodilator-stimulated phosphoprotein
WCE	Whole cell extract
X-GAL	5-bromo-4-chloro-3-indolyl-β-D-galactoside
YT	Yeast terrific medium

Nucleotide abbreviations

A	Adenosine
C	Cytidine
T	Thymidine
G	Guanosine

Amino acid abbreviations

Amino acid	*Three letter code*	*One letter code*
Alanine	ala	A
Arginine	arg	R
Asparagine	asn	N
Aspartic acid	asp	D
Cysteine	cys	C
Glutamic acid	glu	E
Glutamine	gln	Q
Glycine	gly	G
Histidine	his	H
Isoleucine	ile	I
Leucine	leu	L
Lysine	lys	K
Methionine	met	M
Phenylalanine	phe	F
Proline	pro	P
Serine	ser	S
Threonine	thr	T
Tryptophan	trp	W
Tyrosine	tyr	Y
Valine	val	V

CHAPTER 1: Introduction

1.1.1 Introduction to the ERM family

Ezrin, radixin and moesin are collectively known as the ERM family of proteins. First identified as cell membrane-actin cytoskeleton linker proteins due to their homology to band 4.1 (figure 1.1), a protein with similar functions, they have since been revealed to play a role in a wide variety of cellular processes. Like band 4.1, the ERM proteins contain a FERM domain (Four point one Ezrin Radixin Moesin) which can bind to both proteins and lipids.

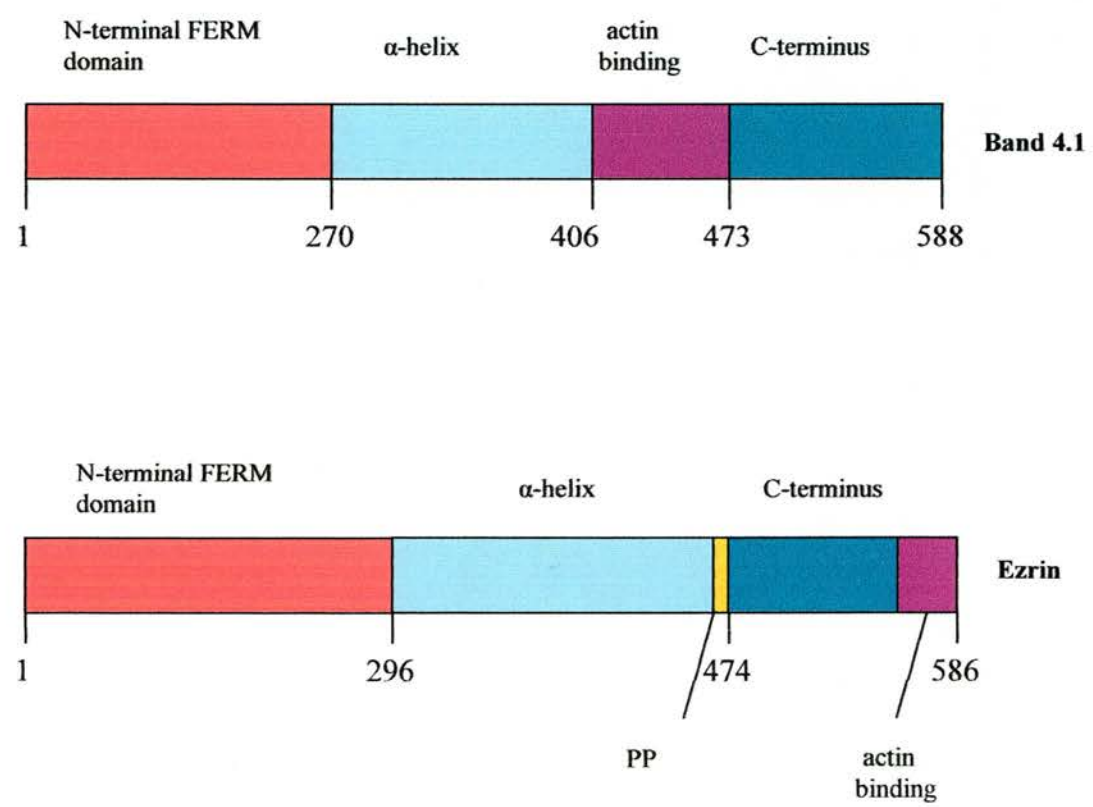

PP = stretch of polyproline residues at 468 to 474

Figure 1.1. The comparative structures of the proteins band 4.1 and ezrin. The main difference between the two proteins is that the actin binding domain is located just after the α-helix region in band 4.1, whereas it is located within the carboxy terminal final ~34 amino acids in ezrin, radixin and moesin. Radixin and moesin have a very similar structure to ezrin, except that moesin does not contain the polyproline stretch. N-terminus – amino terminus, C-terminus – carboxy terminus.

1.1.2 ERM family history

Ezrin was first identified as an 81kDa phosphotyrosine-containing protein that was isolated following the exposure of epidermal growth factor (EGF) to A431 cells (human epidermoid carcinoma cells) (Hunter and Cooper, 1981). It was later identified as an 80kDa component of the microvillus cytoskeleton and shown to be present in a variety of mammalian cells (Bretscher, 1983). In 1984, a 75kDa protein, initially called cytovillin, was isolated in response to an antibody directed against erv-1 (endogenous retrovirus-1), a human retroviral sequence (Suni et al, 1984). This protein was found to be enriched in microvilli (Pakkanen et al, 1987) and other cell surface protrusions (Pakkanen,1988) and was later found to be identical to ezrin.

Ezrin cDNA was cloned and sequenced in 1989 (Gould et al, 1989; Turunen et al, 1989) when its homology to band 4.1 was first noted. Containing 585 amino acids (aas), the molecular mass of the protein was calculated to be 69 kDa. The discrepancy between this figure and initial reports of 75-81kDa is possibly explained by the large percentage (38.5%) of charged amino acids present. Mouse ezrin cDNA shares 96.2% homology with human ezrin (Funayama et al, 1991).

Radixin was first identified as an 82kDa barbed end-capping protein localised in cell- to-cell adherens junctions (Tsukita et al, 1989). Cloned and sequenced in 1991, mouse radixin was found to contain 583aas, with a molecular mass of 68.5kDa, and mouse radixin shares 74.9% homology with mouse ezrin (Funayama et al, 1991).

In 1988 moesin was isolated from bovine uterine cells as a 78kDa heparin-binding protein (Lankes et al, 1988) and it was revealed that the protein localised to the surface of human

colon carcinoma cells. The amino acid sequence of mouse moesin shares 80.1% homology with mouse radixin and 71.7% homology with mouse ezrin (Sato et al, 1992).

1.1.3 Merlin

Merlin is a diverged member of the ERM family. Like the other ERM proteins, it contains an amino terminal FERM domain. Human merlin exhibits a 45% overall homology to human ezrin, but this similarity rises to 61% homology between the two FERM domains. Alternative splicing of the NF2 (Neurofibromatosis Type 2) transcript produces two isoforms of merlin (Hara et al, 1994) and these isoforms may be functionally distinct, as they are known to interact differently with ezrin (Meng et al, 2000).

1.1.4 Family tree

A family tree showing the members of the FERM superfamily is detailed below in figure 1.2.

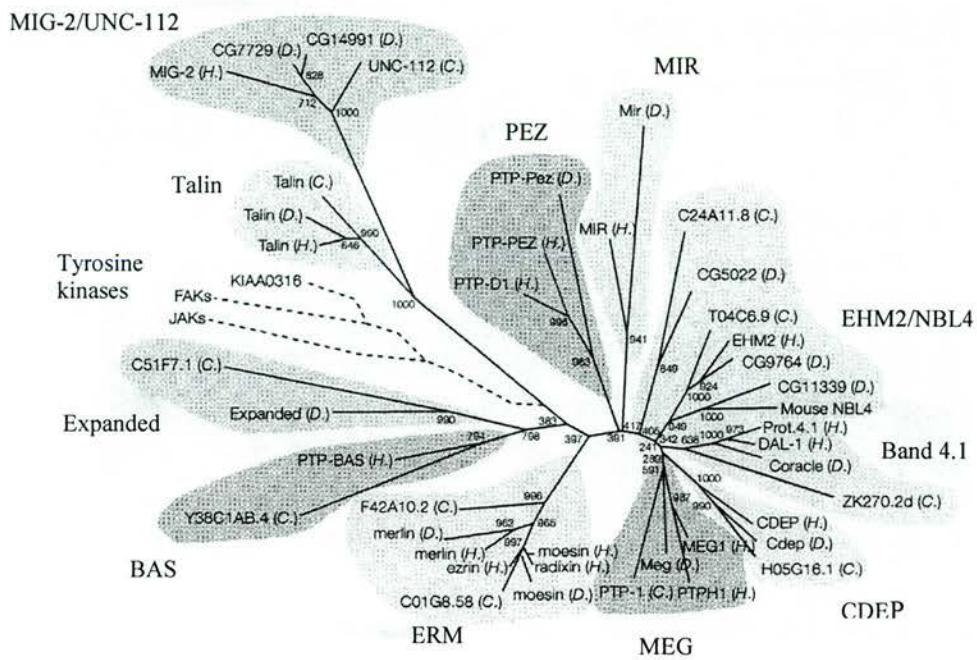

Figure 1.2. The FERM superfamily, as classified by Bretscher et al, 2002. The tree was constructed from an alignment of superfamily members using the region corresponding to human moesin residues 1-297. Bootstrap values, indicated at the nodes, denote the number of times a grouping occurs out of 1,000 random samples from the alignment. The tyrosine kinase portion of the superfamily was omitted from this alignment due to, according to Bretscher et al, its extremely low sequence similarity to the proteins shown, but the authors included it via a dotted line on the basis of a similar tree by Girault et al, 1998.

1.1.5 The discovery of willin

The willin gene was initially isolated from a rat sciatic nerve library following a yeast two hybrid screen (Gunn-Moore et al, 2005). The bait used was a transmembrane receptor named neurofascin. The results of the library screen indicated that neurofascin could bind to the ERM protein ezrin and also to what would later be revealed as another member of the ERM family, which was a cDNA sequence named 163scII. The 163scII cDNA was 981bp in length (Appendix III) and coded for 327aas, beginning at the initiating methionine codon, but no 3' stop codon was present.

1.1.6 The full length willin IMAGE clone

The 163scII clone was used in the initial experiments for this thesis, but bioinformatic searches then revealed that a full length human cDNA had been cloned which bore 85% homology at the DNA level and 91% homology at the protein level to the rat 163scII partial sequence. An alignment of the partial rat and human protein sequences is shown in figure 1.3.

```
RAT             MNKLTFHNNKVMQDRRRVCIFLPNDKSVSIIINVKILCHQLLVQVCDLLRLKDSHLFGLS 60
HUMAN           MNKLNFHNNRVMQDRRSVCIFLPNDESLNIIINVKILCHQLLVQVCDLLRLKDCHLFGLS 60
                ****.****:****** ********:*:.************************.****** 

RAT             VIQNNEHVYMELSQKLYKYCPKEWKKEASKGIDQFGPPMIIHFRVQYYVENGKLISDRIA 120
HUMAN           VIQNNEHVYMELSQKLYKYCPKEWKKEASKGIDQFGPPMIIHFRVQYYVENGRLISDRAA 120
                ************************************************:***** * 

RAT             RYYYYWHLRKQVLHSQCVLREEAYFLLAAFALQADLGNFKRKVHHGDYFEPEAYFPAWVV 180
HUMAN           RYYYYWHLRKQVLHSQCVLREEAYFLLAAFALQADLGNFKRNKHYGKYFEPEAYFPSWVV 180
                ****************************************: *:*.*********:*** 

RAT             SKRGKDYILKHIPNMHRDQFALTASEAYLKYIKEAVRLDDVAIHYYRLYKDKREVEGSLT 240
HUMAN           SKRGKDYILKHIPNMHKDQFALTASEAHLKYIKEAVRLDDVAVHYYRLYKDKREIEASLT 240
                ****************:**********:***************:***********:*.*** 

RAT             LGLTMRGIQIFQNLEEEKQLLYDFPWTNVGKLVFVGKKFEILPDGLPSARKLVYYTGCPT 300
HUMAN           LGLTMRGIQIFQNLDEEKQLLYDFPWTNVGKLVFVGKKFEILPDGLPSARKLIYYTGCPM 300
                **************:****************************************:****** 

RAT             RSRHLLQLLSNSHRLYMNLQPVLRHLR  327
HUMAN           RSRHLLQLLSNSHRLYMNLQPVLRHIR  327
                *************************:*
```

Figure 1.3. Sequence alignment of the rat willin protein sequence and the human willin sequence. The available rat sequence was only 327aa long whereas the human IMAGE clone contained a full length 614aa protein. * - identical residue, : - conserved residue, . – semiconserved residue. Colour code = red - small + hydrophobic (incl. aromatic), blue – acidic, magenta – basic, green - hydroxyl + amine + basic

A clone containing the human sequence, from uterine leiomyosarcoma tissue, was obtained from the MRC IMAGE Consortium DNA Bank. Since the IMAGE clone contained the full length willin gene, subsequent experiments were based mostly around this human DNA sequence, as opposed to the rat partial sequence.

The IMAGE cDNA sequence of willin is 1845bp in length (Appendix III) and contains 614aas, forming a predicted 71kDa protein. An alignment of ezrin and willin is shown in figure 1.4.

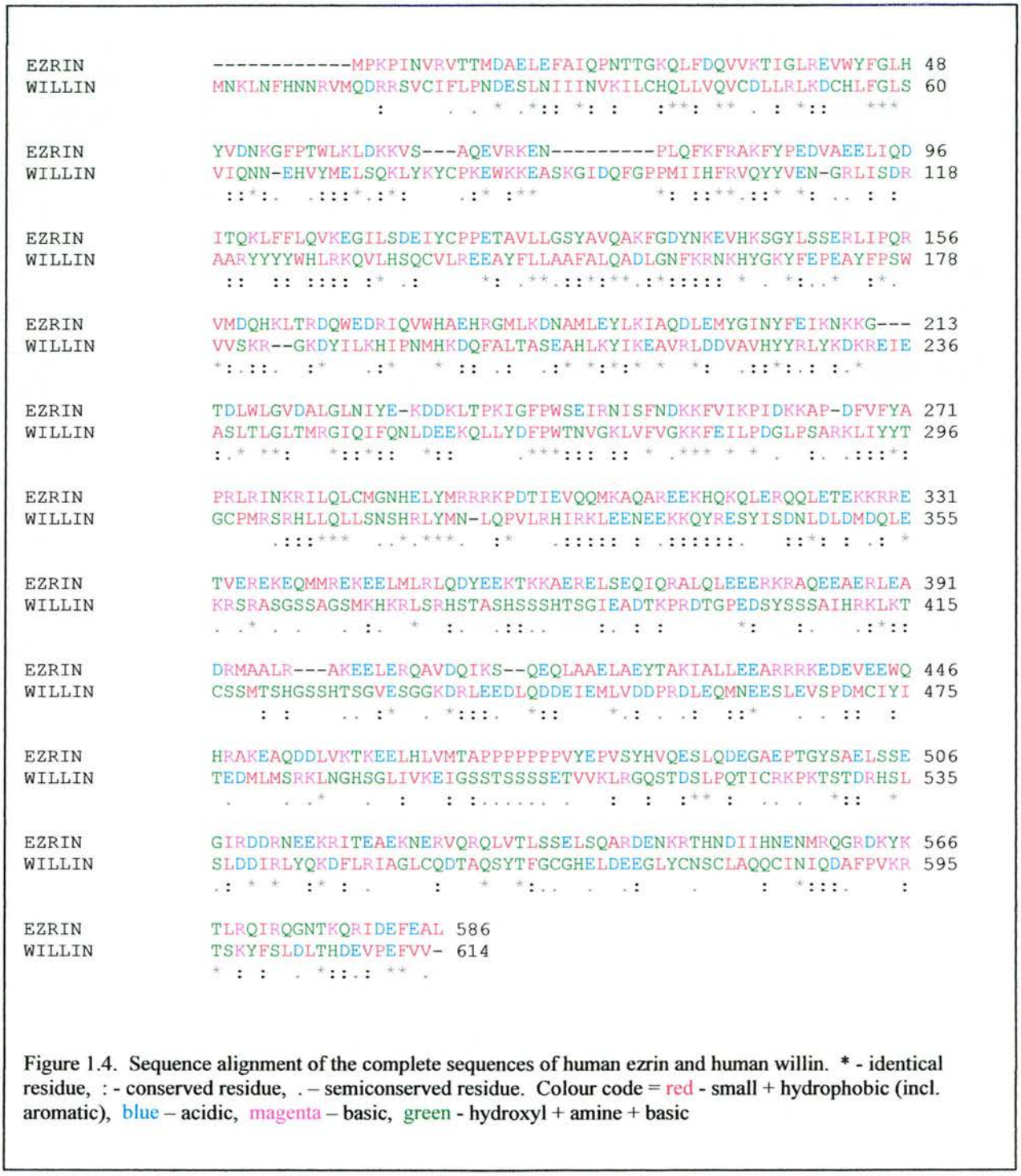

Figure 1.4. Sequence alignment of the complete sequences of human ezrin and human willin. * - identical residue, : - conserved residue, . – semiconserved residue. Colour code = red - small + hydrophobic (incl. aromatic), blue – acidic, magenta – basic, green - hydroxyl + amine + basic

Figure 1.5 shows an alignment of the four FERM domains of the human forms of ezrin, radixin, moesin and willin. A region of willin bearing very low homology to the three ERM proteins is highlighted in yellow. This is the section of the protein that was later used in antibody production for use in western blotting and other experiments (section 3.1).

```
RADIXIN          ------------MPKPINVRVTTMDAELEFAIQPNTTGKQLFDQVVKTVGLREVWFFGLQ 48
MOESIN           ------------MPKTISVRVTTMDAELEFAIQPNTTGKQLFDQVVKTIGLREVWFFGLQ 48
EZRIN            ------------MPKPINVRVTTMDAELEFAIQPNTTGKQLFDQVVKTIGLREVWYFGLH 48
WILLIN           MNKLNFHNNRVMQDRRSVCIFLPNDESLNIIINVKILCHQLLVQVCDLLRLKDCHLFGLS 60
                                :     . . * .*:: *: :   :**: ** . : *::   ***

RADIXIN          YVDSK--GYSTWLKLNKKVTQQDVKKEN----------PLQFKFRAKFFPEDVSEELIQEI 97
MOESIN           YQDTK--GFSTWLKLNKKVTAQDVRKES----------PLLFKFRAKFYPEDVSEELIQDI 97
EZRIN            YVDNK--GFPTWLKLDKKVSAQEVRKEN----------PLQFKFRAKFYPEDVAEELIQDI 97
WILLIN           VIQNNEHVYMELSQKLYKYCPKEWKKEASKGIDQFGPPMIIHFRVQYYVENG-RLISDRA 119
                   :.:   :    :   *   :: :**          *: ::**.::: *: :. : :

RADIXIN          TQRLFFLQVKEAILNDEIYCPPETAVLLASYAVQAKYGDYNKEIHKPGYLANDRLLPQRV 157
MOESIN           TQRLFFLQVKEGILNDDIYCPPETAVLLASYAVQSKYGDFNKEVHKSGYLAGDKLLPQRV 157
EZRIN            TQKLFFLQVKEGILSDEIYCPPETAVLLGSYAVQAKFGDYNKEVHKSGYLSSERLIPQRV 157
WILLIN           ARYYYYWHLRKQVLHSQCVLREEAYFLLAAFALQADLGNFKRNKHYGKYFEPEAYFPSWV 179
                 ::  :: :::: :* .:     *: .**.::*:*:. *::::: *   *:  :  :*. *

RADIXIN          LEQHKLTKEQWEERIQNWHEEHRGMLREDSMMEYLKIAQDLEMYGVNYFEIKNKKG---T 214
MOESIN           LEQHKLNKDQWEERIQVWHEEHRGMLREDAVLEYLKIAQDLEMYGVNYFSIKNKKG---S 214
EZRIN            MDQHKLTRDQWEDRIQVWHAEHRGMLKDNAMLEYLKIAQDLEMYGINYFEIKNKKG---T 214
WILLIN           VSKR--GKDYILKHIPNMHKDQFALTASEAHLKYIKEAVRLDDVAVHYYRLYKDKREIEA 237
                 :.::.  ::   .:*   * :: .:  .:: ::*:* *  *:  .::*: : :.*    :

RADIXIN          ELWLGVDALGLNIYE-HDDKLTPKIGFPWSEIRNISFNDKKFVIKPIDKKAP-DFVFYAP 272
MOESIN           ELWLGVDALGLNIYE-QNDRLTPKIGFPWSEIRNISFNDKKFVIKPIDKKAP-DFVFYAP 272
EZRIN            DLWLGVDALGLNIYE-KDDKLTPKIGFPWSEIRNISFNDKKFVIKPIDKKAP-DFVFYAP 272
WILLIN           SLTLGLTMRGIQIFQNLDEEKQLLYDFPWTNVGKLVFVGKKFEILPDGLPSARKLIYYTG 297
                 .* **:   *::*::  ::.     .***::: :: * .*** * * .  :. .:::*:

RADIXIN          RLRINKRILALCMGNHELYMRRRKP  297
MOESIN           RLRINKRILALCMGNHELYMRRRKP  297
EZRIN            RLRINKRILQLCMGNHELYMRRRKP  297
WILLIN           CPMRSRHLLQLLSNSHRLYMNLQPV  322
                     .:::* *  ..*.***. :
```

Figure 1.5. Sequence alignment of the FERM domains of human ezrin, human radixin, human moesin and human willin. The willin sequence that antibodies were later raised against (ref chapter) is highlighted in yellow. * - identical residue, : - conserved residue, . – semiconserved residue

1.2.1 Localisation of the ERM proteins

The imperative role played by the ERM family in cellular architecture and beyond would imply a necessarily ubiquitous distribution of these proteins, and this has proved to be correct. However, many cell types appear to express one or more ERM proteins whilst growing in culture, whereas the same cell types do not necessarily exhibit the same expression levels *in vivo*. A possible reason for this discrepancy has been proposed whereby cells growing in culture upregulate expression of the ERM proteins as an adaptive response to *in vitro* conditions (Berryman et al, 1993). This hypothesis appeared to have been validated when it was demonstrated that primary cultures of human umbilical vein endothelial cells, initially expressing only moesin, were shown to then express moesin and ezrin after eight to ten passages (Berryman et al, 1993).

In some instances, ERM proteins are found to be coexpressed *in vivo*. For example, lymphocytes, pancreatic intercalated duct cells, and the brush border microvilli that line the kidney proximal tubule are all enriched in both ezrin and moesin (Berryman et al, 1993). However, in an investigation comprised of approximately 50 different types of tissue, and with the exception of the kidney tissues studied, Berryman et al found a striking pattern of almost entirely mutually exclusive distribution patterns of ezrin and moesin (Berryman et al, 1993) (table 1.1).

Organ and cell type		Ezrin	Moesin
Placenta	Syncytiotrophoblast	+++	±
	Endothelium	-	++
Tongue	Stratified epithelium	++	-
	Endothelium	-	++
	Striated muscle	-	-
Oesophagus	Stratified epithelium	++	-
	Endothelium	-	++
	Smooth muscle	-	-
Stomach	Surface mucous	++	-
	Parietal	+++	-
	Chief	++	-
	Endothelium	-	++
	Smooth muscle	-	-
	Visceral mesothelium	+++	-
Small int.	Absorptive epithelium	+++	-
	Lymphocyte	+	+
	Endothelium	-	+
	Smooth muscle	-	-
	Visceral mesothelium	+++	-
Pancreas	Intercalated duct	++	+
	Interlobular duct	+++	-
	Endocrine cell	-	-
	Endothelium	-	++
Liver	Hepatocyte	-	++
	Sinusoid	-	+
	Large bile duct	+++	-
	Visceral mesothelium	+++	-
Heart	Cardiac muscle (myocardium)	-	-
	Endothelium (endocardium)	-	++
	Mesothelium (epicardium)	+++	-
Lung	Terminal bronchiole	+++	-
	Alveolar tissue	±‡	+++‡
	Pleural mesothelium	+++	-
Spleen	Lymphocyte	+	+
	Endothelium	-	++
	Visceral mesothelium	+++	-
Kidney	Renal corpuscle	++	+++‡
	Proximal tubule	+++	+++
	Distal tubule	+	±
	Collecting duct	+	±
	Endothelium	-	++
Bladder	Transitional epithelium	++	-
	Endothelium	-	+
	Smooth muscle	-	-
	Peritoneal mesothelium	+++	-

Table 1.1. Table adapted from Berryman et al (1993) showing the distribution of ezrin and moesin in various cell types. + and - denote relative staining intensities as judged visually by the authors using immunofluorescence microscopy. ‡Cases where fluorescence staining was seen, but the identity of the cell types was not resolved with certainty.

1.2.2 Ezrin localisation

Following the initial discovery of ezrin in the microvilli of intestinal epithelial cells (Bretscher, 1983), the protein has been identified in a number of different cell types. It is found in gastric parietal cells (Hanzel et al, 1989; Urushidani et al, 1989), and in human placental microvilli (Edwards and Booth, 1987), and a wide-ranging study by Berryman et al (1993) revealed that high levels of ezrin are expressed in the intestines, stomach, lung, kidney and, to a lesser extent, the spleen. In each of these organs, the antibody staining was found to be cell type-specific: for example, within the stomach, the surface mucosa, parietal, chief and visceral mesothelial cells all showed either moderate or high relative staining intensities, whereas the endothelial and smooth muscle did not appear to contain ezrin (Berryman et al, 1993). It is concentrated on the apical surface of many types of simple epithelia (Berryman et al, 1993).

1.2.3 Moesin localisation

Moesin has been found to be most abundant in lung, spleen and kidney (Berryman et al, 1993). Again, the distribution within the organs varies according to cell type. In the lung, moesin could not be detected at all in the terminal bronchioles nor in the pleural mesothelial cells, but a relatively high amount of the protein was visualised in alveolar tissue (Berryman et al, 1993). In the same study, moesin was found to be enriched in the endothelia of all the tissues studied, although it was also revealed to be present in certain epithelial cell types. Amieva and Furthmayr (1995) found moesin to be present in fibroblast, epithelial, endothelial, neuronal and bone-marrow derived cells. Although ezrin and moesin are co-expressed in human lymphocytes, monocytes and neutrophils, moesin is the quantatively dominant ERM protein in these cells (Shcherbina et al, 1999). In the multiple cell types that express moesin, it is found

primarily in filopodia and retraction fibres, although in some cells it is also found in microvilli and microspikes (Amieva et al, 1995).

1.2.4 Radixin localisation

Radixin was originally isolated from the adherens junctions of rat liver cells (Tsukita et al, 1989). It has been found highly concentrated at the cleavage furrow at the onset of cytokinesis in chicken intestinal smooth muscle (Sato et al, 1991) and is known to be a component of hepatocyte microvilli (Amieva et al, 1994) and cardiac intercalated discs (Tsukita et al, 1989). Gonzales-Agosti and Solomon (1996) found radixin to be the sole ERM protein in chick sympathetic neuron growth cones. However, the localisation of this ERM protein has been the subject of some controversy. Tsukita et al (1989) claimed that radixin localised to adherens junctions but not focal contacts, whereas Sato et al (1992) claimed that adherens junctions, cleavage furrows and focal contacts were clearly stained by an anti-radixin polyclonal antibody. Franck et al (1993) stated that of the three ERM proteins, only radixin is an authentic component of adherens junctions and focal contacts. Amieva et al (1994) found none of the three ERM proteins to be present in adherens junctions, even though Tsukita et al (1989) originally isolated the protein from rat liver adherens junctions. Bretscher et al (1997) have examined the subcellular distribution of radixin in cultured cells and found that it colocalises to ruffles and microvilli but not focal contacts.

1.2.5 General localisation of ERM proteins

Despite the discrepancies in the published literature with regards to the distribution of the ERM proteins, there is a general consensus that all three proteins localise to actin-rich cell surface projections (figure 1.6) such as microvilli, microspikes, pseudopodia, and lamellopodia (Berryman et al, 1993; Franck et al, 1993; Amieva et al, 1995).

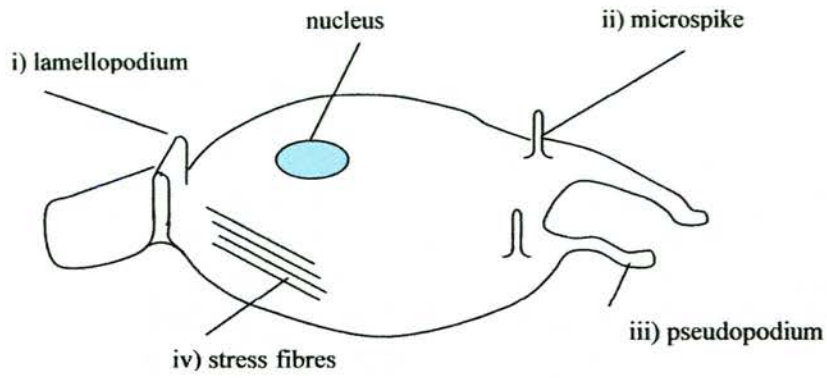

Figure 1.6. Localisation of the ERM proteins to many kinds of actin-containing membrane projections such as i) lamellopodium – a sheet-like projection of the plasma membrane, ii) microspike – a thin, stiff protrusion usually seen at the leading edge of a cell, iii) pseudopodium – temporary projections used by the cell for motion or ingesting iv) stress fibres – structures formed in response to tension across the cell, which are involved in anchoring the cell at focal contacts.

Microvilli have been shown to decrease in number and length, to the point of complete eradication, after exposure to a mixture of ezrin/radixin/moesin antisense oligonucleotides (Takeuchi et al, 1994). Bonhila et al (1999) found a clear correlation between high levels of ezrin expression and the formation of apical microvilli in rat pigmented epithelial cells. Furthermore, the overexpression of ERM binding partners such as CD44, CD43 and ICAM-2 leads to a significant elongation of microvilli in cultures fibroblasts (Yonemura et al, 1999).

1.2.6 Localisation and development

The conflicting results mentioned above as to the whereabouts of the ERM proteins are possibly due to antibodies recognising different activation states of the proteins (reviewed in Bretscher et al, 1997). Additionally, the expression levels and distribution patterns of the ERM proteins can vary according to the stage of development of the host organism. Louvet et al (1996) examined the pattern of ezrin staining during mouse embryo development and found

pronounced differences in the distribution of the protein at the various stages of development. Firstly, the total ezrin content of the cells between the 8-cell to the blastocyst stage decreases by 35%, in comparison to a decrease of only 4% for total protein content, indicating that the pattern of ezrin loss is different to that observed for proteins in total (Louvet et al, 1996).

Secondly, Louvet's group used confocal microscopy to reveal that in the eggs and in early stage embryos, ezrin can be found all around the cell periphery (figure 1.7). However, after compaction - a polarisation event which occurs at the 8-cell stage - ezrin becomes restricted to the apical pole (a microvillus-based structure that forms as part of the compaction process). Following transition from the 8-cell to the 16-cell stage, during which time the cells can divide symmetrically or asymmetrically, ezrin becomes totally segregated to the outer layer of those cells which have undergone asymmetric division (Louvet et al, 1996).

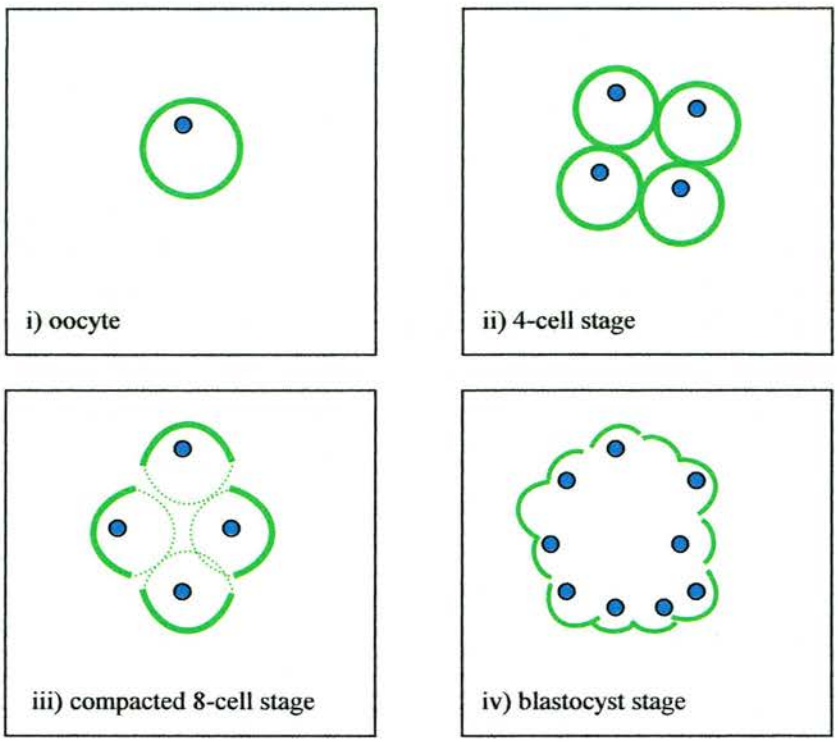

Figure 1.7. Diagrammatical representation of the changes in ezrin distribution during the growth of a mouse embryo. i) and ii) Up to the 4-cell stage, ezrin can be clearly seen around the entire membrane of each individual cell iii) Around the 8-cell stage, ezrin begins to lose the complete cortical distribution that is exhibited up to this point iv) Ezrin is only to be found in the outermost layers of the blastocyst. Adapted from Louvet et al, 1996.

1.3.1 Structure and domains

The ERM proteins can be divided into three domains, shown as a ribbon representation in figure 1.8. The first is the FERM or N-terminal domain, the second is the α-domain, and the third is the C-terminal domain.

1.3.2 The FERM domain

The FERM domain (Chisti et al, 1998) is approximately 300aas long. Pearson et al (2000) crystallised the FERM domain of moesin complexed to a truncated form of the moesin C-terminus. The crystal structure revealed that the FERM domain can itself be divided into three subdomains, F1, F2 and F3, which are arranged in a cloverleaf shape. All three subdomains have homology to other proteins. The F1 subdomain is similar to ubiquitin, the F2 domain is similar to Acyl-Coenzyme A binding protein, and the F3 domain is homologous to the fold of an adaptable ligand-binding module seen in pleckstrin homology domains, in phosphotyrosine binding domains and in Enabled/VASP-1 (vasodilator-stimulated phosphoprotein-1) domains.

Hamada et al (2000) crystallised the radixin FERM domain and found that the overall dimensions of the domain were ~70Å by 70Å, with a thickness of 40Å. The authors proposed from this study that, despite the FERM domain consisting of three separate domains, the FERM domain functions as a single unit: for example, the linker regions between the three domains are very short - between 13 and 18 residues - and their sequences are well conserved throughout the band 4.1 family (Hamada et al, 2000).

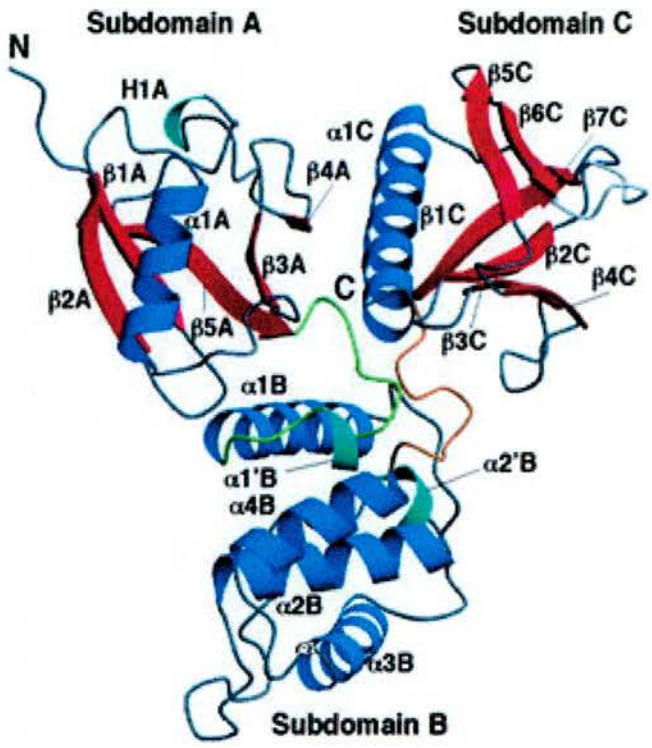

Figure 1.8. Ribbon representation of the crystal structure of the radixin FERM domain. The FERM domain is composed of three subdomains, A, B and C. α-helices are shown in blue, β-strands are shown in red. The linker regions between subdomains A-B and B-C are coloured in green and brown respectively. Adapted from Hamada et al, 2000.

1.3.3 The α-domain

The N-terminal FERM domain is followed by a less conserved coiled coil region called the α-domain, which is ~200aas in length. This region acts as a type of hinge and enables the N-terminus to fold over and engage with the C-terminus of a single protein molecule.

1.3.4 The C-terminal domain

The third domain is the ~80aa hydrophilic C-terminus. In moesin, the C-terminal tail adopts an extended meandering structure that, when complexed to the N-terminus, blocks large surfaces of the interacting domains (Pearson et al, 2000). In radixin, the N-terminus/C-terminus interaction buries 2700Å^2 of the FERM domain surface and 2950 Å^2 of the tail surface (Hamada et al, 2000).

1.3.5 The polyproline stretch

A polyproline stretch of aas is present at residues 470-476 in ezrin, and residues 470-477 in radixin. However, these residues are not present in moesin, nor in willin (figure 1.9).

```
RADIXIN          KAFAAQEDLEKTKEELKTVMSAPPPPPPPPVIPPTENEHDEHDENNAEAS---AELSNEG 504
MOESIN           KAQMVQEDLEKTRAELKTAMSTP------HVAEPAENEQDEQDENGAEAS---ADLRADA 498
EZRIN            RAKEAQDDLVKTKEELHLVMTAPPPPPPPVYEPVSYHVQESLQDEGAEPTGYSAELSSEG 507
WILLIN           EDMLMSRKLNGHSGLIVKEIGSSTSSSSETVVKLRGQSTDSLPQTICRKPKTSTDRHSLS 536
```

Figure 1.9. Sequence alignment of the regions of ezrin and radixin containing a polyproline stretch (underlined) which is not present in moesin or in willin. Colour code = red - small + hydrophobic (incl. aromatic), blue – acidic, magenta – basic, green - hydroxyl + amine + basic

1.3.6 Conformation and ERMADs

Gary and Bretscher (1993) pioneered the investigations into the homo- and heterotypic associations of the ERM proteins via the isolation of a stable ezrin-moesin complex by immunoprecipitation from A431 cells. These researchers also demonstrated the ability of ezrin and moesin to self-associate *in vitro* (Gary and Bretscher, 1993). Ezrin was then found to associate with a 77kDa protein believed to be the gastric form of radixin (Andreoli et al, 1994). Merlin was revealed to have similar self-association regions (Nguyen et al, 2001). The interactions between the ERM proteins occur via regions that have been named N- or C-Ezrin-Radixin-Moesin Association Domains (N- or C-ERMADs) (Gary and Bretscher, 1995) (figure 1.10).

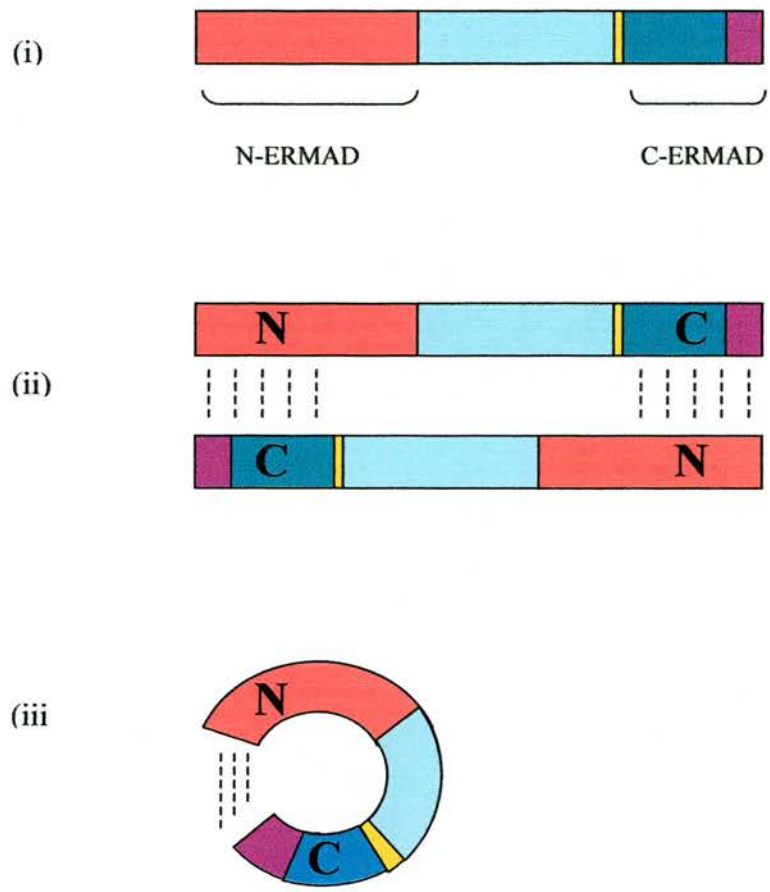

Figure 1.10. (i) The ERM proteins have N- and C- ERM Association Domains or ERMADs. (ii) The ERMADs are involved in the formation of ERM dimers. These dimers may be between one species of protein, such as an ezrin-ezrin interaction, or there may be two different types of protein involved, such as an ezrin-moesin interaction. (iii) The N-ERMAD and C-ERMAD of a single molecule of protein may also interact via an intramolecular head to tail interaction.

FERM α region polyproline

C-terminus, which includes the.... actin binding domain

The ezrin N-ERMAD was mapped to residues 1 - 296, and the C-ERMAD was mapped to the last 107aas of the protein, residues 479 - 585 (Gary and Bretscher, 1995). The N- and C-ERMADs are involved in both intermolecular interactions, e.g. between two ezrin molecules, or between an ezrin and a radixin molecule, and also in intramolecular interactions, whereby the N- and the C-ERMAD of a single molecule of one of the proteins can fold up via a head-to-tail interaction.

Whether the interactions are inter- or intramolecular, the result is the masking of the membrane binding N-ERMAD and the actin binding C-ERMAD regions of the protein(s) (figure 1.11). In this state, the ERM protein is inactive. Once the protein becomes activated, the binding sites are no longer hidden and the protein is then capable of binding to the actin cytoskeleton and the plasma membrane (PM), or to linker proteins in the PM such as EBP50 (Reczek and Bretscher, 1998). A shift of the ezrin oligomeric (binding sites masked, inactive) form to the monomeric (binding sites available, active) form has been shown to coincide with the stimulation of acid secretion by gastric parietal cells (Zhu et al, 2005).

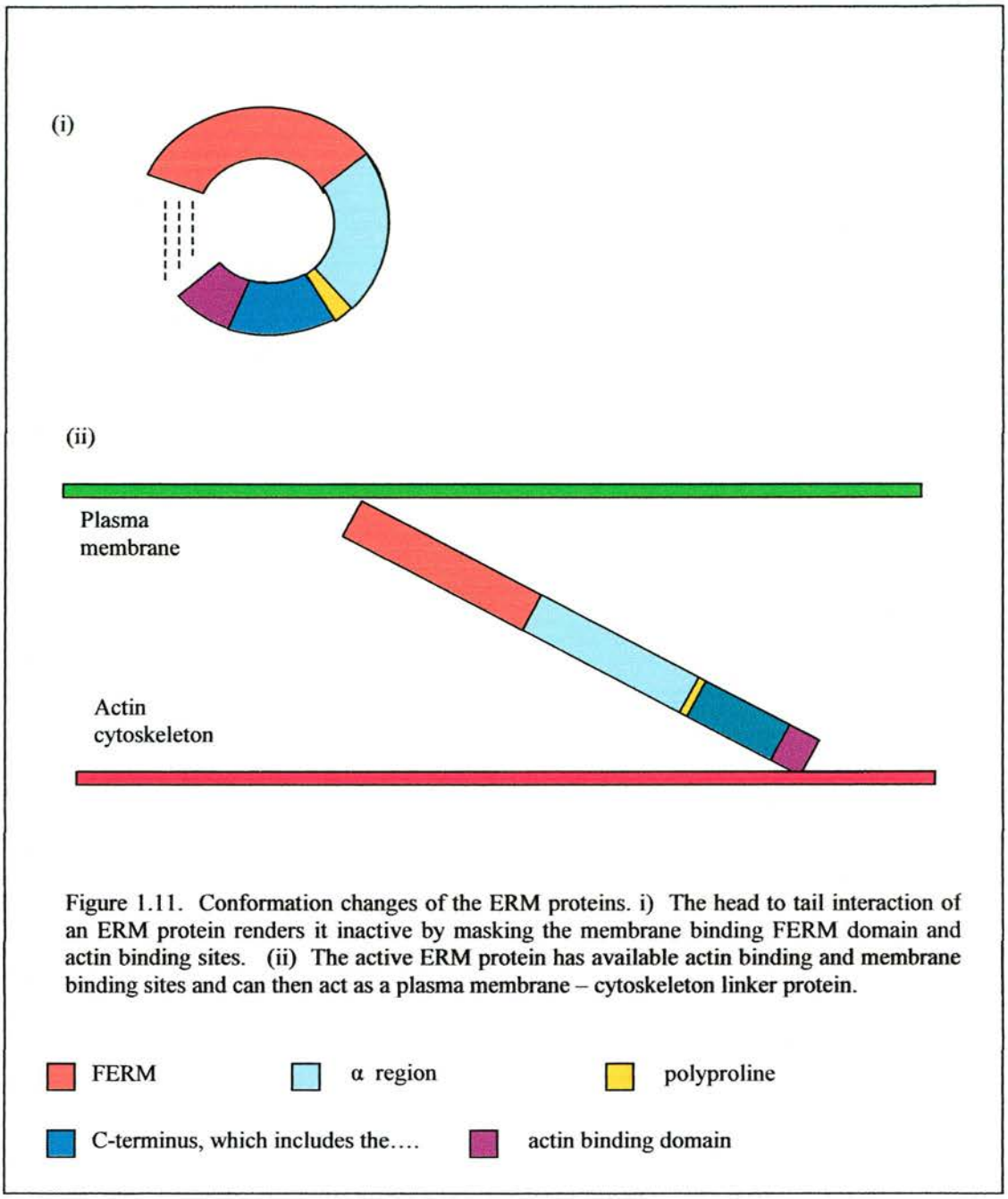

Figure 1.11. Conformation changes of the ERM proteins. i) The head to tail interaction of an ERM protein renders it inactive by masking the membrane binding FERM domain and actin binding sites. (ii) The active ERM protein has available actin binding and membrane binding sites and can then act as a plasma membrane – cytoskeleton linker protein.

Interestingly, the merlin C-terminus has a higher affinity for the ezrin N-terminus than it has for its own C-terminus (Nguyen et al, 2001). The complex resulting from the intramolecular interaction between the N-terminus and C-terminus of human moesin was crystallised in 2000 (Pearson et al, 2000). The data resulting from this crystal structure provided a model that could account for observations such as those of Matsui et al (1998), that the phosphorylation of radixin on T564 markedly suppressed its head-to-tail association. The equivalent residue in moesin, T558, is contained within a positively charged surface which is positioned opposite the negatively charged FERM domain surface; upon phosphorylation of T558, the accompanying negative charge of the phosphoryl group would cause electrostatic interference between the surfaces (Pearson et al, 2000). Furthermore, the side chains surrounding T558 approach it closely enough to implicate the necessity of some structural rearrangement, should a phosphoryl group be introduced (Pearson et al, 2000).

1.3.7 Expression of the ERM N-termini and C-termini

Studies by Martin et al (1995) using insect sf9 (*Spodoptera frugiperda*) cells revealed that the ezrin C-terminus residues 310-586 possesses cell extension promoting activity, an activity which is negatively regulated by the N-terminus residues 1-233 of the protein. Similarly, Henry et al (1995) showed that high levels of expression of the radixin C-terminus domain induces formation of long processes all over the surfaces of Hela (Helen Lane) cells. This group observed that the N- and C-termini and the full length protein could all behave differently according to whether the expression levels were moderate or high. The amino terminus of radixin - when expressed at moderate levels - was diffuse throughout the cell, but when expressed at high levels, the N-terminus polypeptide began to show cortical localisation (Henry et al, 1995). At low levels of expression, full length radixin localised to various cortical structures and to the cleavage furrow of dividing cells, but when only the C-terminus

of the protein was expressed, no localisation to the cleavage furrow was observed (Henry et al, 1995).

Although Henry et al (1995) found that it was the expression of the C-terminus of radixin which caused the production of long processes on cell surfaces, a contrasting result was obtained by Amieva et al (1999), who examined the effect of expression of the N- and C-termini of the ERM proteins in NIH3T3 cells. In this instance, expression of the N-terminus of moesin caused the formation of abnormally long filopodia, whereas expression of the full length or the C-terminus of the protein had no effect upon the appearance of the cells.

1.4.1 Functions of the ERM proteins

Evidence has been obtained in favour of both functional redundancy and non-redundancy of ERM proteins. In support of the former, immunofluorescent staining of NIH3T3 cells revealed that expression of a full length radixin construct largely abolished moesin staining without any apparent changes in phenotype, implying that exogenous radixin can substitute for endogenous moesin without any discernable consequences (Henry et al, 1995). Doi et al (1999) produced knock-out mice that were deficient in moesin, yet no abnormalities at the tissue level could be detected. Since human platelets predominantly express moesin, Doi and his colleagues collected platelets from these moesin deficient mice and, contrary to their expectations, found no disruption to platelet aggregation activity. Takeuchi et al (1994) exposed mouse mammary tumour cells to ezrin, radixin and moesin antisense oligonucleotides. None of the antisense oligonucleotides, either singly or in pairs, induced any morphological change in the cells, whereas exposure of the cells to a mixture of antisense oligonucleotides directed against all three ERM proteins led to a significant change in cell shape.

However, the same study also provided conflicting evidence that the proteins are not actually redundant. Takeuchi and his colleagues proceeded to trypsinize the mouse cells and replated them in the presence of antisense oligonucleotides. The cells treated with radixin-antisense completely lost the ability to reattach to the substratum, those cells treated with ezrin-antisense seemed to partially lose their ability to reattach, and those treated with moesin-antisense attached normally (Takeuchi et al, 1994). In a separate investigation employing antisense technology, alterations in growth cone morphology were observed after double suppression of radixin and moesin, but not after double suppression of ezrin and radixin, nor of ezrin and moesin (Paglini et al, 1998).

Two ERM binding proteins, EBP50 (ERM binding protein 50)and the β2 adrenergic receptor, appear to depend specifically on ezrin for their proper localisation in the apical membrane of airway epithelial cells, as apical moesin cannot substitute for this function (Huang et al, 2003). Furthermore, the ezrin FERM domain binds directly to CD95 (Lozupone et al, 2004) whereas radixin and moesin do not (Lozupone et al, 2004; Parlato et al, 2000), suggesting, according to Lozupone et al (2004), that ezrin has a specific role in linking CD95 to actin. Lozupone's group noted that the region of ezrin involved in binding CD95 was located between ezrin residues 149 - 168, an area which has 60 - 65% homology between ezrin, radixin and moesin, as compared with the 86% homology observed in the whole FERM domain (Lozupone et al, 2004).

1.4.2 Roles in Disease

Merlin is the product of the NF2 gene (Rouleau et al, 1993; Trofatter et al, 1993). It is a tumour suppressor that is defective or absent in Neurofibromatosis Type 2, a rare autosomal dominant disease (1 in 35,000 people) that predisposes affected individuals to meningiomas, schwannomas and astrocytomas (Gutman, 1997). Most schwannomas result from a biallelic inactivating mutation in the NF2 gene, and Bashour et al (2002) were able to reverse the abnormal cytoskeletal phenotype associated with schwannoma cells by the introduction to the cells of merlin isoform 1 (specifically, as merlin isoform 2 did not reverse the phenotype [Bashour et al, 2002]). A model for the role of merlin and the ERM proteins in cancer is shown in figure 1.12.

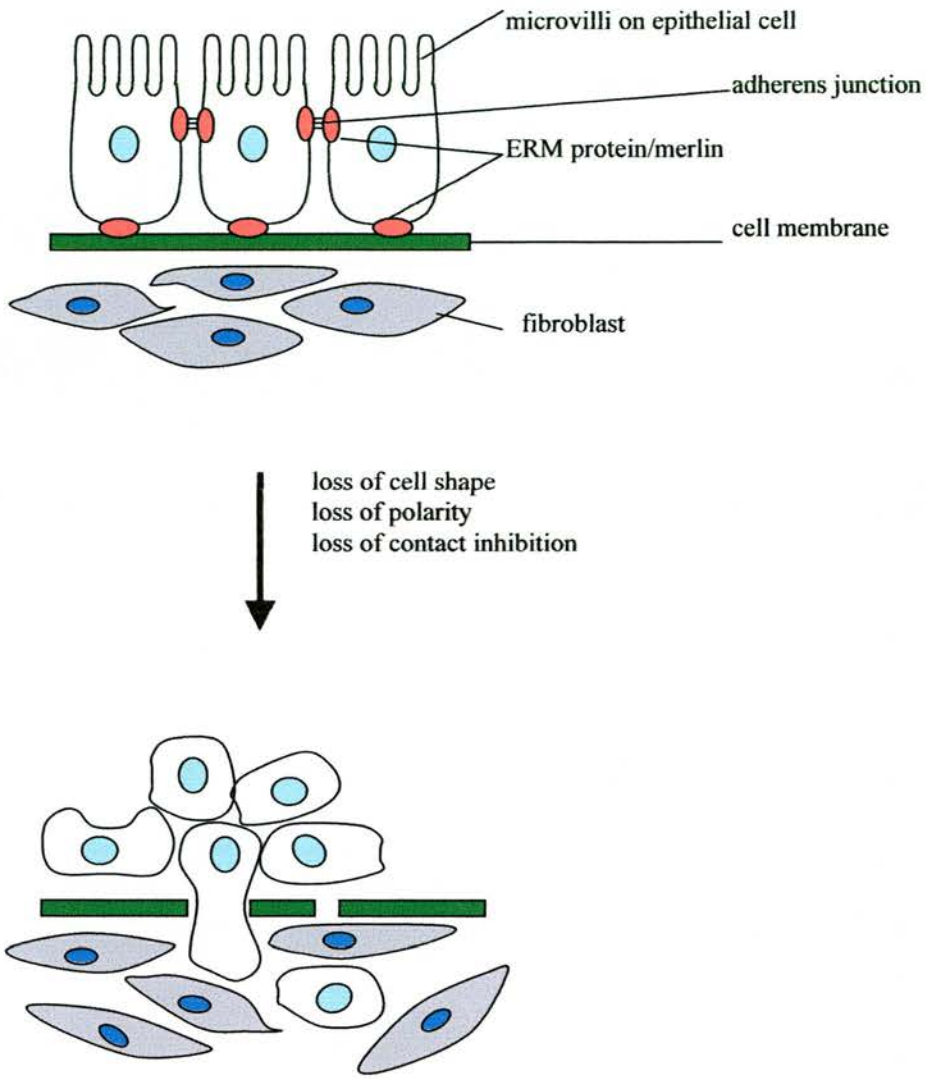

Figure 1.12. Illustration of role of ERM proteins/merlin in cancer. The loss of functional ERM proteins is believed to lead to increased metastasis and invasiveness due to the involvement of these proteins in maintaining cell shape, polarity and contact inhibition. Adapted from McClatchey, 2003.

1.4.3 ERM proteins and cancer

Ezrin also has been shown to have an involvement in the cancerous activity of cells. *In vitro*, high expression of ezrin in cultured cells causes cell transformation and is associated with cell proliferation (Kaul et al, 1996; Jooss and Muller, 1995). Antisense nucleotides to ERM proteins disrupt cell adhesion, possibly contributing to metastasis (Takeuchi et al, 1994). In metastatic rhabdomyosarcoma cells, ezrin has been revealed to be a key regulator of the metastatic process: the introduction of a dominant negative form of ezrin into a highly metastatic cell line caused the cells - normally adept at forming cellular processes and tubules - to remain as cysts, eradicating the usual branching morphogenesis and development of vessel-like networks exhibited by this cell line, both behaviours being associated with a highly invasive phenotype (Yu et al, 2004). Functional ezrin has been shown to be required for metastasis of breast cancer cells (Elliott et al, 2005).

The interaction between the ERM proteins and the CD44 receptor has been implicated as a contributing factor to a variety of cancer phenotypes (reviewed in Martin et al, 2003). Neutral endopeptidase 24.11 (NEP) is a cell surface peptidase known to inhibit prostate cancer cell proliferation and migration, and NEP has been demonstrated to inhibit the CD44-ERM interaction by competitive binding to the ERM proteins (Iwase et al, 2004) (figure 1.13).

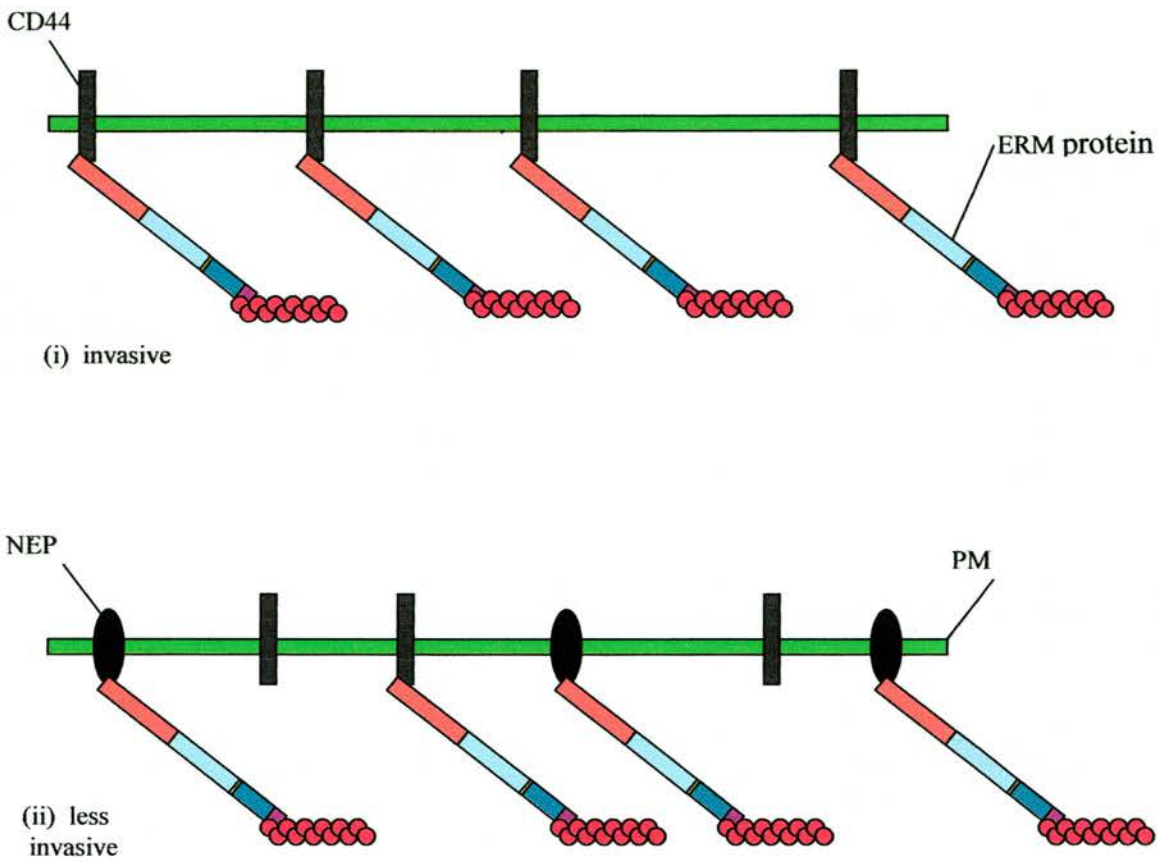

Figure 1.13. Model proposed by Iwase et al (2004) of the role played by the ERM proteins and the CD44 and neutral endopeptidase (NEP) receptors in the metastasis of prostate cancer cells. (i) Cancer cells have a lower expression level of the NEP receptor, allowing any available ERM proteins to be recruited, without competition, to the CD44 receptor, thus promoting cell invasion and migration. (ii) In cells where the NEP receptor is expressed, NEP competes with CD44 for the binding of the ERM proteins so that CD44 does not bind to the ERM proteins, which leads to a less invasive phenotype. PM = plasma membrane.

The involvement of the ERM family in various aspects of the cancer process has led to the use of these proteins as biomarkers and prognostic agents. Kobayashi et al (2004) analysed the cytoplasmic versus membranous distribution of moesin in oral squamous cell carcinomas, and revealed that patients whose cancerous cells showed a predominantly cytoplasmic expression pattern for moesin had a poorer overall survival rate compared to patients with tumour cells showing a membranous bias for moesin expression.

1.4.4 ERM proteins and other diseases

The majority of the current literature on disease associations of the ERM family emphasises their role in carcinogenesis and metastasis. There are publications, however, which reveal a role for these proteins in diseases as diverse as Downs Syndrome, diabetes and bacterial infections. Moesin levels have been shown to be significantly decreased in foetal Downs Syndrome brain (Lubec et al, 2001). The amino terminals of ezrin, radixin and moesin were found to bind to advanced glycation end products (AGEs) in diabetic rat kidney cells (McRobert et al, 2003), and AGEs have been strongly linked to diabetic complications. Fais (2005) has postulated that an ezrin-fas ligand colocalisation may have a role in diseases where apoptosis is a central pathogenic mechanism, such as Acquired Immune Deficiency Syndrome (reviewed in Fais et al, 2005). Geiger et al (2006) found a strict correlation between an increase in ezrin immunoreactivity and Human Immunodeficiency Virus encephalopathy.

The adhesion of Enteropathogenic *E.coli* (EPEC) to cells is known to induce the accumulation of a number of cytoskeletal proteins underneath the bacteria, including ezrin. Although the concentration of ezrin does not change following EPEC infection, threonine phosphorylation of the protein increases, as does tyrosine phosphorylation, and these changes lead to an enhanced association of ezrin with the cytoskeleton in EPEC-infected cells (Simonovic et al,

2001). Ezrin has also been found to play a pivotal role in the cytoskeletal modifications caused by the *Neisseria meningitidis* infective process (Eugene et al, 2002). During this process, cellular protrusions develop that are similar to microvilli in both shape and ezrin content, and these are believed to be responsible for bacterial engulfment and internalisation (Eugene et al, 2002); a representation of such a process is shown in figure 1.14.

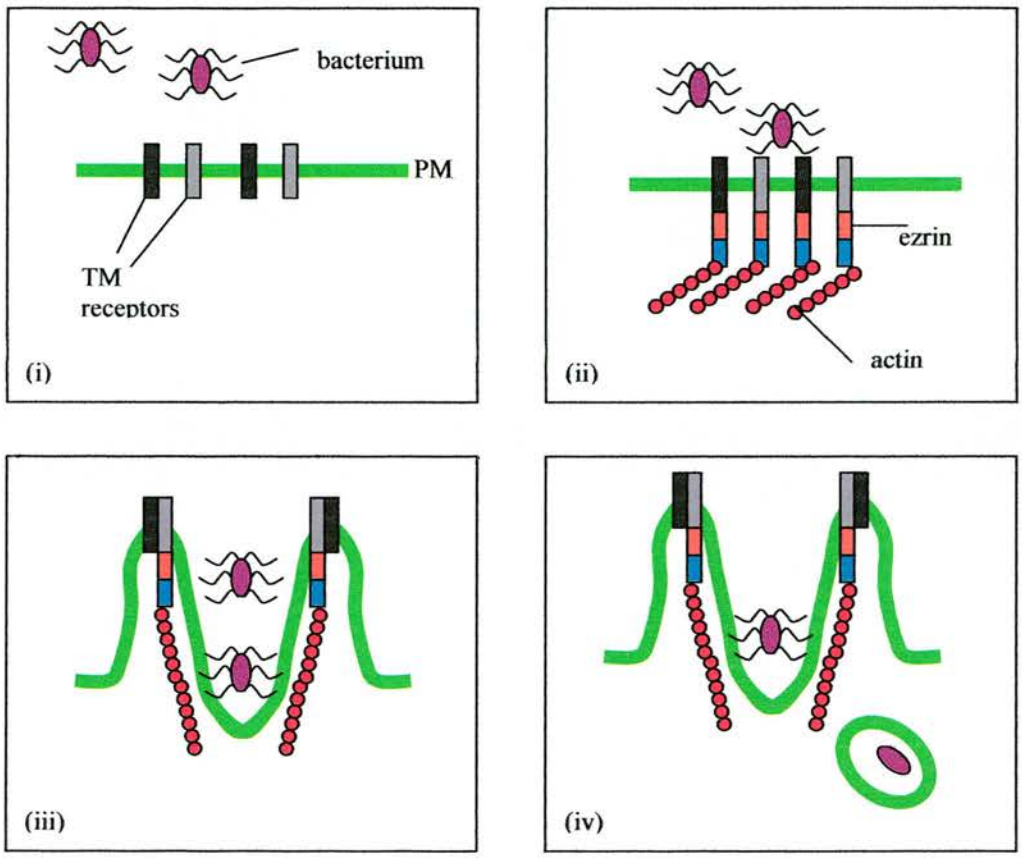

Figure 1.14. Ezrin plays a role in the internalisation of *N. meningitidis* bacteria. (i) The bacterial pili interact with a cellular receptor, possibly CD46. Other receptors involved in the internalisation process include CD44 and ICAM-1. (ii) Ezrin is recruited to the receptors and ezrin in turn recruits actin to the site. (iii) Microvilli are formed at the site of internalisation. (iv) The bacteria become engulfed and are internalised into the cell. Adapted from Nassif et al, 2002. PM = plasma membrane. TM = transmembrane.

1.4.5 Role in cell shape

ERM proteins play a role in cell shape and motility and in cell-cell/cell-substrate adhesion. Bretscher (1989) first observed that ezrin phosphorylation plays a role in the formation of cell surface projections. The exposure of cultured mouse mammary tumour cells to a mixture of ezrin/radixin/moesin antisense oligonucleotides was found to induce a significant change of cell shape (Takeuchi et al, 1994). In normal rat-1 cells, laser ablation of ezrin resulted in a pronounced loss of cell shape and rounding of the cell (Lamb et al, 1997). Overproduction of a truncated form of ezrin was shown to cause delocalisation of ezrin from the microvilli, an event that was concomitant with cell flattening (Crepaldi et al, 1997). In the case of rat RPE (retinal pigmented epithelial) cell microvilli, the structures appear to be strongly dependent on ezrin expression, since the treatment of primary cultures of RPE cells with ezrin antisense caused an almost complete disappearance of microvilli (Bonhila et al, 1999).

1.4.6 Role in cell adhesion

With regards to adhesion, ezrin has been found to enhance cell adhesion of *Spodoptera frugiperda* insect cells in culture (Martin et al, 1995), and overexpression of ezrin in NIH3T3 cells was shown to lead to a loss of contact inhibition (Kaul et al, 1996). Two substitution mutations in the Na-H exchanger isoform 1 (NHE1) plasma membrane exchanger, which caused the specific inhibition of the ERM binding ability of the proteins, led to a loss of cell-cell contacts in fibroblasts (Denker and Barber, 2002). Immunofluorescence microscopy has revealed that the ERM proteins colocalise with CD44 at BHK (baby hamster kidney) cell-cell adhesion sites (Tsukita et al, 1994).

1.4.7 Role in cell motility

There is also a considerable body of evidence to suggest the ERM proteins' involvement in cell movement. Legg et al (2002) showed that dynamic association and disassociation of CD44 and ezrin in response to PKC (protein kinase C) activation is a critical step in the control of directional cell motility. The eradication of ezrin expression via micro-CALI (Chromophore Assisted Laser Inactivation) caused an inhibition of membrane ruffling at the leading edge of fos-transformed fibroblasts, along with a concomitant inhibition of PM extension (Lamb et al, 1997). ERM dephosphorylation plays a role in the resorption of microvilli to enable the process of lymphocyte transendothelial migration (Brown et al, 2003). Using truncated N- and C-terminus-expressing constructs, Martin et al (1995, 1997) determined regions of ezrin capable of inducing an aberrant cell extension phenotype in insect sf9 cells, which is not observed with full length ezrin.

1.4.8 Interaction with the plasma membrane

The cloning and sequencing of ezrin in 1989 (Gould et al, 1989; Turunen et al, 1989) revealed its homology to band 4.1, a protein known to play a key role in linking actin to the transmembrane protein glycophorin C (Anderson and Lovrien, 1984). This led to speculation that ezrin might also function as a membrane-cytoskeleton linker protein and this hypothesis was then confirmed by Algrain et al (1993).

Molecules in the plasma membrane that associate with ERM proteins are termed ERM Binding Membrane Proteins (ERM-BMPs) (Yonemura and Tsukita, 1999). They can be subdivided into two classes: the first class is involved in direct attachment of ERM proteins to the plasma membrane and the second class is involved in indirect attachment (figure 1.15).

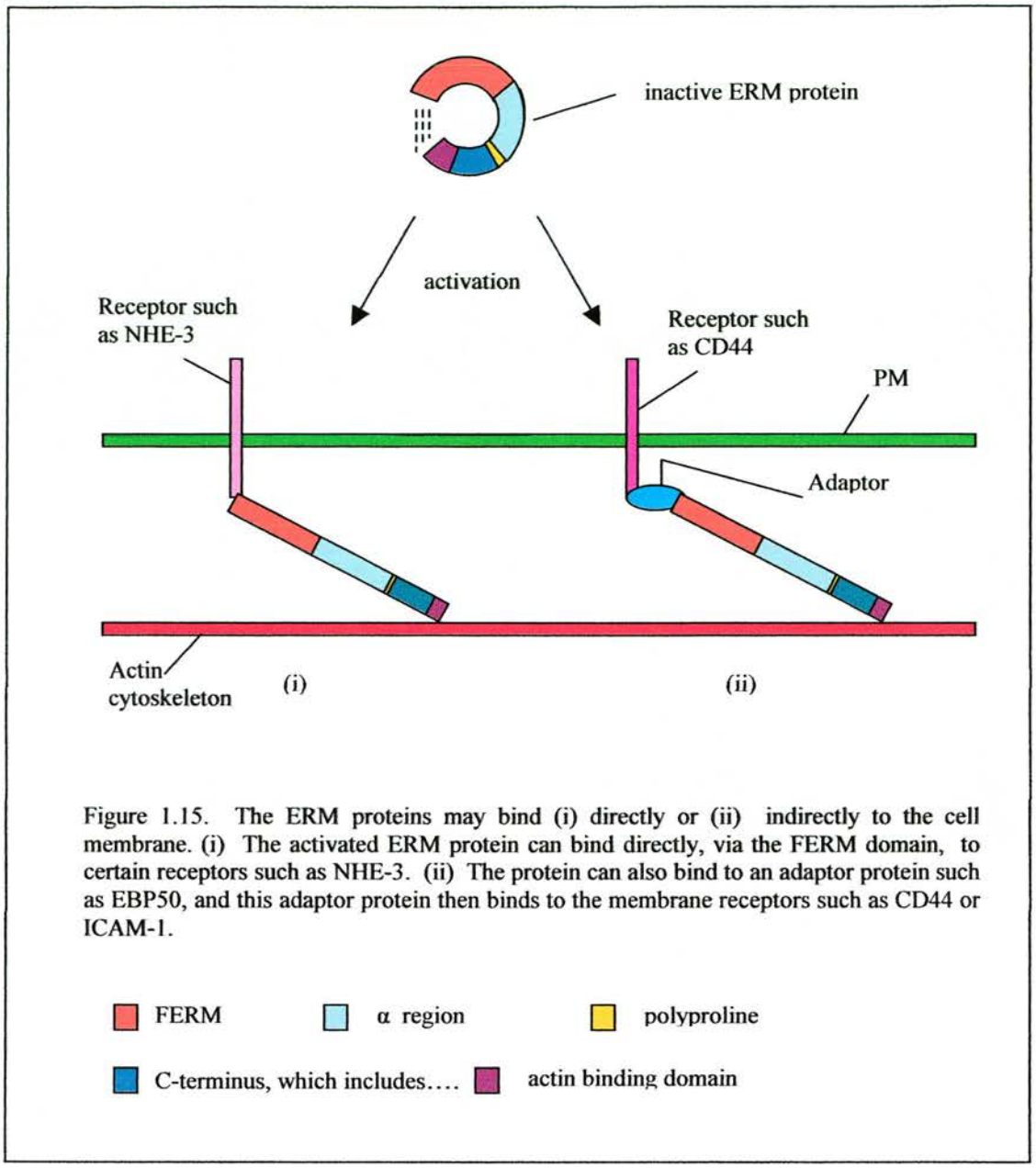

Figure 1.15. The ERM proteins may bind (i) directly or (ii) indirectly to the cell membrane. (i) The activated ERM protein can bind directly, via the FERM domain, to certain receptors such as NHE-3. (ii) The protein can also bind to an adaptor protein such as EBP50, and this adaptor protein then binds to the membrane receptors such as CD44 or ICAM-1.

1.4.9 Direct attachment to plasma membrane

Using an anti-moesin polyclonal antibody, Tsukita et al (1994) co-immunoprecipitated moesin with a 140kDa integral membrane protein revealed to be CD44. At low ionic strength ERM proteins were found to bind directly to the cytoplasmic domain of CD44, but this binding became undetectable at physiological ionic strength (Hirao et al, 1996). The redistribution of

ICAM-1 in response to transient ezrin expression in mouse lymphoma cell uropods revealed ICAM-1 to be another direct binding partner for the ERM proteins (Helander et al, 1996). Moesin was also then shown to bind to CD44 and also to CD43 and ICAM-3 (Serrador et al, 1998). Ezrin also binds to CD43 (Serrador et al, 1998) and to ICAM-1 and ICAM-2 but not ICAM-3 (Heiska et al, 1998).

Using affinity chromatography, Berryman and Bretscher (2000) identified a 32 kDa protein from placental microvilli that specifically associated with the ezrin C-terminus, which they named CLIC5, a member of the Chloride Intracellular Channel gene family. A 78kDa protein named AKAP78 (cAMP-dependent protein kinase [A-kinase] anchoring protein 78) was isolated by Dransfield et al (1997) from gastric parietal cells, and was found to be present in both the soluble and insoluble fractions of the cells. In fact, AKAP78 was was revealed to be ezrin (Dransfield et al, 1997), and the authors also showed in this study that ezrin is a major AKAP in gastric parietal cells, possibly functioning as a tether for type II A-kinases. PA2.26, a small mucin-like transmembrane glycoprotein, colocalises with ERM proteins in actin-containing plasma membrane projections (Scholl et al, 1999). The ERM-binding region of the CD44, CD43 and ICAM-2 has been mapped to a region in the juxta-membrane cytoplasmic domain of these proteins that is rich in positively charged amino acids, mainly lysine and arginine residues (Yonemura et al, 1998) (figure 1.16). Ezrin connects syndecan 2 - a member of the transmembrane heparan sulphate proteoglycan family of receptors implicated in cell-cell and cell-substrate adhesion - to the actin cytoskeleton (Granes et al, 2000). Further studies revealed that this interaction is independent of any other protein (Granes et al, 2003).

CD44 [1]RRRCGQKKKLVINGGNGTV[19]

CD43 [1]RQRQKRRTGALTLSRGGKRNGTVDAWAGPAR[31]

ICAM-2 [1]HWHRRRTGTYGVLAAWRRLPRAFRARPV[28]

Figure 1.16. The ERM proteins bind to regions with a cluster of positively charged residues in the cytoplasmic domains of receptors CD44, CD43 and ICAM-2 (Yonemura et al, 98). The sequences above are for the juxta-membrane cytoplasmic domains of CD43 and CD44 and for the entire cytoplasmic domain of ICAM-2. Positively charged residues are highlighted in blue.

1.4.10 Indirect attachment to plasma membrane

The first evidence of an indirect linkage between ERM proteins and the cell membrane was uncovered by Reczek et al (1997) who examined a group of polypeptides that had been retained on beads containing immobilised ezrin or moesin N-terminal fragments. The retained polypeptides were shown to be differentially phosphorylated species of ERM binding phosphoprotein 50 (EBP50), which was revealed to be the human homologue of rabbit Na^+H^+ Exchanger Regulatory factor (NHE-RF) (Reczek et al, 1997). In addition to binding to ezrin and moesin, as mentioned above, EBP50 was also observed to interact with radixin and moesin (Murthy et al, 1998). Nguyen et al (2001) revealed that the binding of EBP50 to the ezrin N-terminus can be inhibited by the presence of the ezrin C-terminus, but that the binding of EBP50 to the merlin N-terminus is not inhibited by either the merlin C-terminus nor the ezrin C-terminus (Nguyen et al, 2001).

EBP50 has been revealed to be a component of an anchoring complex which serves to bind lipid rafts to the cytoskeleton: the EBP50 PDZ (PSD95 [postsynaptic density protein 95] discs large Zonula occludens) domain binds to a membrane adaptor protein, the EBP50 C-terminus binds to an ERM protein, and the resulting assembly is involved in the negative regulation of immune synapse formation (Brdickova et al, 2001; Itoh et al, 2002). Disruption of the EBP50 gene *in vivo* revealed a pivotal role for EBP50 in maintaining activated ERM proteins in the intestinal microvilli of mice (Morales et al, 2004).

The rabbit homologue of EBP50, NHE-RF, is a protein cofactor necessary for the PKA regulation of the Na^+/H^+ exchanger isoform 3 (NHE3) of the kidney proximal tubule (Weinman et al, 1995), and Yun et al (1997) used a yeast two hybrid screen to look for proteins that interact with NHE3. They recovered a protein with 55% homology to EBP50, which was named NHE3 Kinase A Regulatory Protein (E3KARP). Both EBP50 and E3KARP contain two PDZ domains followed by a carboxy terminal sequence that binds active ERM proteins (Reczek and Bretscher, 2001). However, the two proteins have been found to have mutually exclusive cellular distribution (Ingraffea et al, 2002). Immunofluorescence microscopy performed on a variety of murine tissues revealed that, for example, EBP50 was enriched in kidney proximal tubule cells whereas E3KARP is absent, and E3KARP is found throughout the alveoli (with a distribution similar to that of radixin and moesin), whereas EBP50 is restricted to the terminal bronchioles (with a distribution similar to ezrin) (Ingraffea et al, 02).

1.4.11 Interaction with the actin cytoskeleton

Anderson et al (1984) observed that the founder member of the ERM family, band 4.1, provided the link between the transmembrane protein glycophorin and the actin cytoskeleton.

The homology of ezrin to band 4.1, in terms of both primary and secondary structure, led Algrain et al (1993) to investigate a proposed similar role for ezrin. Experiments using truncated ezrin N-terminal and C-terminal constructs demonstrated that ezrin interacts with membrane associated structures via its N-terminus and with the actin cytoskeleton via its C-terminus. Affinity chromatography experiments enabled the mapping of the actin binding site to the carboxy-terminal 34aas of ezrin (Turunen et al, 1994). A contrasting result was obtained by Shuster and Herman (1995), who found that ezrin preferentially interacted with the β-isoform of actin but that this binding was not direct. However, moesin was then also found to possess a C-terminal actin binding site (Pestonjamasp et al, 1995). A T558D substitution mutation in moesin, believed to mimic phosphorylation of the T558 residue, was proposed to activate the binding of moesin to actin by exposing the actin binding site in the moesin C-terminus (Huang et al, 1999) and Nakamura et al (1999) proposed that a conformational change caused by phosphorylation, and either cationic detergents or polyphosphatidylinositides, was the best explanation for moesin binding to F-actin (filamentous actin).

An alignment of the terminal 34aas of the ERM proteins and willin is shown in figure 1.17.

```
RADIXIN          LHAENVKAGRDKYKTLRQIRQGNTKQRIDEFEAM 583
MOESIN           IHAENMRLGRDKYKTLRQIRQGNTKQRIDEFESM 577
EZRIN            IHNENMRQGRDKYKTLRQIRQGNTKQRIDEFEAL 586
WILLIN           QQCINIQDAFPVKRTSKYFSLDLTHDEVPEFVV- 614
                  :  *:: .    :* : :  . *::.: **
```

Figure 1.17. Sequence alignment of the terminal 34 aas of ezrin, radixin, moesin, where an actin-binding domain was mapped to by Turunen et al (1994). Human willin has been included in the alignment. * - identical residue, : - conserved residue, . – semiconserved residue. Colour code = red - small + hydrophobic (incl. aromatic), blue – acidic, magenta – basic, green - hydroxyl + amine + basic

Blot overlays using ^{125}I-labelled F-actin and G-actin (globular actin) revealed that bovine neutrophil ezrin and moesin bound specifically to F-actin, and that G-actin did not bind to either protein (Pestonjamasp et al, 1995), whereas recombinant ezrin was found to bind both F- and G-actin (Roy et al, 1997). The latter study also revealed the presence of a new actin binding site in ezrin; surprisingly, this site was located in the amino terminus of the protein (Roy et al, 1997) (figure 1.18).

```
RADIXIN          RLRINKRILALCMGNHELYMRRRKPDTIEVQQMKAQAREEKHQKQLERAQLENEKKKREI 332
MOESIN           RLRINKRILALCMGNHELYMRRRKPDTIEVQQMKAQAREEKHQKQMERAMLENEKKKREM 332
EZRIN            RLRINKRILQLCMGNHELYMRRRKPDTIEVQQMKAQAREEKHQKQLERQQLETEKKRRET 332
WILLIN           CPMRSRHLLQLLSNSHRLYMN-LQPVLRHIRKLEENEEKKQYRESYISDNLDLDMDQLEK 356
                     .:::* *  ..*.***.  :*   .::::: : .:::::::.     *: : .: *

RADIXIN          AEKEKERIE-REKEELMERLKQIEEQTIKAQKELEEQTRKALELDQERKRAKEEAERLEK 391
MOESIN           AEKEKEKIE-REKEELMERLKQIEEQTKKAQQELEEQTRRALELEQERKRAQSEAEKLAK 391
EZRIN            VEREKEQMM-REKEELMLRLQDYEEKTKKAERELSEQIQRALQLEEERKRAQEEAERLEA 391
WILLIN           RSRASGSSAGSMKHKRLSRHSTASHSSSHTSGIEADTKPRDTGPEDSYSSSAIHRKLKTC 416
                  .: .       *.: : * .  ...: ::.    :   :    ::. . :  . :
```

Figure 1.18. Sequence alignment of the regions of the ERM proteins encompassing a secondary actin-binding site mapped to ezrin residues 281 – 333 (highlighted in yellow) by Roy et al, 1997. Human willin has been included in the alignment. * - identical residue, : - conserved residue, . – semiconserved residue. Colour code = red - small + hydrophobic (incl. aromatic), blue – acidic, magenta – basic, green - hydroxyl + amine + basic

1.4.12 ERM proteins and the nervous system

As willin was initially identified as a protein of neurological origin, it was a matter of interest to examine the functions of the other ERM proteins within the nervous system. Several studies have shown that the proteins are critical for the normal development of the nervous system. For instance, all three ERM proteins can be found highly concentrated at Nodes of Ranvier (Melendez-Vasquez et al, 2001). Activated ERM proteins have been found in growth cone-like cap structures at the tips of myelinating Schwann cells, structures which are believed to be imperative for the efficient formation of Nodes of Ranvier (Gatto et al, 2003). Dickson

et al (2002) investigated the binding of the ERM proteins to the axonal cell adhesion molecule L1, and found evidence to suggest that the interaction between L1, actin and ezrin may play a role in axonal outgrowth and neuronal differentiation (Dickson et al, 2002).

The ERM proteins appear to be of considerable importance in the normal development of growth cones. Gonzales-Agosti and Solomon (1996) demonstrated that the collapse of growth cones in cultured chick neurones, caused by the withdrawal of NGF (nerve growth factor), led to a pronounced decline in the radixin staining of the growth cones; this phenotype could be rescued by the readdition of NGF, and the re-formation of the growth cones is accompanied by the relocalisation of radixin (Gonzales-Agosti and Solomon, 1996). When micro-CALI of radixin was targeted to the middle of the leading edge of chick dorsal root ganglia growth cones, the growth cones would often split in two (Castelo and Jay,1999). Double suppression of radixin and moesin in embryonic rat hippocampal cells caused a variety of alterations to the growth cones, and also caused an 8-10 times decrease in the rate of advance of the neuritic tips as compared to control growth cones (Paglini et al, 1998).

1.4.13 Role in cell division/cell cycle

The ERM proteins have been shown to be involved in cell cycle dynamics. Immunofluorescence microscopy photographs published by Tsukita et al (1994) showed that the ERM proteins colocalise with CD44 at the cleavage furrow of dividing BHK cells. An anti-radixin polyclonal antibody detected the presence of radixin specifically at the cleavage furrow of dividing rat fibroblasts, whereas no radixin staining could be found in these cells during interphase (Sato et al, 1991). Henry et al (1995) detected only radixin and moesin in cortical structures in nondividing HeLa cells but found all three ERM proteins to be present in the cleavage furrow of dividing cells (figure 1.19).

Kaul et al (1996) isolated a spontaneously immortalised mouse fibroblast cell line which was highly enriched in ezrin; when these researchers microinjected the purified IgG fraction of anti-ezrin antiserum into these cells, it blocked the cells' entry into S phase (Kaul et al, 1996). The nucleocytoplasmic shuttling of merlin, which may be linked to its tumour suppressor function, has been shown to be dependent on the cell cycle (Muranen et al, 2005).

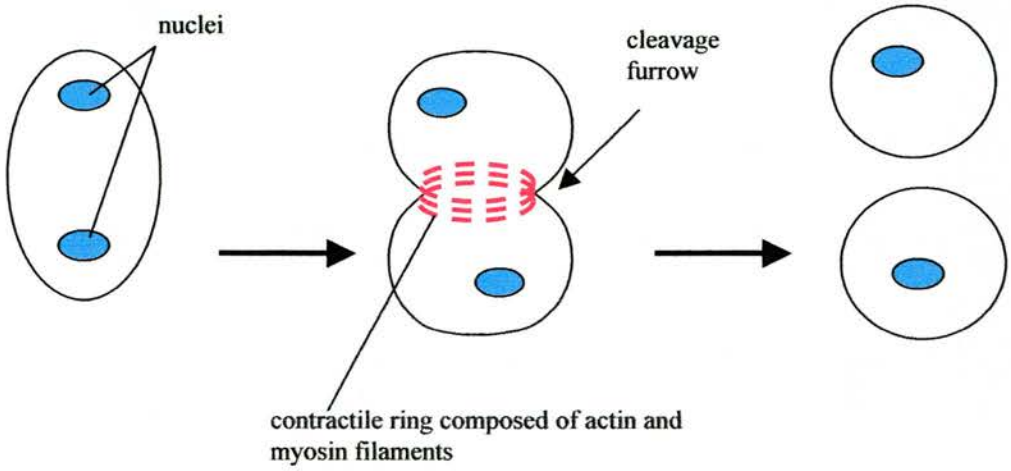

Figure 1.19. Function of the contractile ring in cytokinesis. The ERM proteins have been found to localise to the cleavage furrow during cytokinesis, where they probably play a role in recruiting actin filaments to form the actin-myosin contractile ring which allows the two daughter cells to divide and separate.

1.4.14 Cell polarisation

The ERM family are known to be involved in the polarisation of cells. Paglini et al (1998) have shown that radixin and moesin regulate key aspects of growth cone development and, by the authors' inference, are also involved in the development of neuronal polarity. Transfection of peripheral blood T-lymphocytes with a moesin-T558D mutant was found to inhibit the numbers of polarised cells following chemokine stimulation (Brown et al, 03). Treatment of

T-lymphocytes with agents that induce cell polarisation, such as the chemokine RANTES (regulated upon activation, normal T cell-expressed and -secreted), was shown to cause an increase in the association of moesin with ICAM-3 (Serrador et al, 1997) and pretreatment of RANTES-stimulated cells with butanedione monoxime, a drug which prevents lymphocyte polarisation, then led to a diminution in the association of moesin with ICAM-3 (Serrador et al, 1997). Examination of the imaginal disc epithelial cells of *Drosophila* larvae possessing a mutant moesin gene showed that the cells did not express the usual polarity markers, and the resulting loss of polarity was accompanied by invasive behaviour (Speck et al, 2003). Zhou et al (2005) have amassed data which suggests that T567 phosphorylation of ezrin may direct the protein to activity at the basolateral membrane in gastric parietal cells, and away from apical localisation.

1.4.15 Membrane trafficking

A small amount of evidence has accumulated to suggest involvement of the ERM proteins in membrane trafficking. Cao et al (1999) showed that the proper sorting of internalised β2-adrenergic receptors requires that the receptors interact with EBP50 and the ERM proteins. A study by Defacque et al (2000) found that ezrin and moesin (the authors were unable to distinguish between the two proteins at the time the experiments were conducted) appeared to be essential for actin assembly by phagosomes. Moesin has been found to be involved in the vesicular trafficking of the water channel aquaporin-2 to the PM (Tamma et al, 2005).

1.5.1 Regulation of the ERM proteins

The phosphorylation of ERM proteins has been shown to play a key role in their activation. Krieg and Hunter (1992) noted that extensive tyrosine phosphorylation of ezrin occurred simultaneously with cytoskeletal rearrangement in A431 cells following EGF stimulation. Following site directed mutagenesis, these residues were identified as Y145 and Y353; however, the authors noted that Y145 is not conserved in band 4.1, and Y353 is unique to ezrin (Krieg and Hunter, 1992). A T558 residue, conserved in both ezrin (T567) and radixin (T564), was then identified as being the only phosphorylation site in moesin that is utilised during thrombin activation of platelets (Nakamura et al, 1995). This threonine residue is also present in willin as T596 (figure 1.20).

```
RADIXIN          VMNHRSEEERVTETQKNERVKKQLQALSSELAQARDETKKTQNDVLHAENVKAGRDKYKT 564
MOESIN           MAKDRSEEERTTEAEKNERVQKHLKALTSELANARDESKKTANDMIHAENMRLGRDKYKT 558
EZRIN            IRDDRNEEKRITEAEKNERVQRQLVTLSSELSQARDENKRTHNDIIHNENMRQGRDKYKT 567
WILLIN           LDDIRLYQKDFLRIAGLCQDTAQSYTFGCGHELDEEGLYCNSCLAQQCINIQDAFPVKRT 596
                 : . *  ::   .     :   :  :: .     .:    .     :  *:: .    :*
```

Figure 1.20. Sequence alignment of the ERM proteins' conserved threonine residue (highlighted), which is also conserved in willin. * - identical residue, : - conserved residue, . – semiconserved residue.

The same series of experiments revealed that changes in cell shape accompanied different ERM phosphorylation states: by using staurosporine or calyculin A to cause the complete inhibition or saturation, respectively, of the phosphorylation state of moesin, Nakamura et al (1995) were able to demonstrate that either extreme caused the production of unusually long filopodia in thrombin-stimulated platelets. The link between phosphorylation of ERM proteins and cytoskeletal changes was further confirmed with the discovery that the phosphorylation state of ezrin appeared to increase the protein's association with the

cytoskeleton (Chen et al, 1995). Phosphorylation of moesin was found to play a crucial role in the formation of microvilli-like structures (Oshiro et al, 1998).

1.5.2 Threonine phosphorylation

The T564/T567/T558 residue identified by Nakamura et al (1995) as being critical during thrombin activation was then shown by Matsui et al (1998) to suppress, when phosphorylated, the interaction between the recombinant N- and C-terminus of radixin, indicating that the phosphorylated residue interferes with the intermolecular and/or intramolecular interactions of the ERM proteins. Immunofluorescence studies on a variety of different cell types revealed that C-terminus-phosphorylated ERM proteins were exclusively found close to the PMs of the cells, whereas full length ERMs were found both close to the PM and in the cytoplasm (Hayashi et al, 1999), which again correlated with the hypothesis that phosphorylation of the C-terminus accompanies activation of the proteins; however, the authors did stipulate that they were unsure at this point if ERM C-terminus phosphorylation was the cause or result of activation of the proteins.

Phosphorylation of radixin T564 was found to markedly suppress the head-to-tail interaction of the protein (Matsui et al, 1998). The replacement of T558 with D558 in moesin, to mimic phosphorylation of this residue, was shown to greatly enhance the F-actin-binding ability of moesin, and this step was also shown to be involved in the disruption of the N- and C-terminal interactions of the protein (Huang et al, 1999). More recently, phosphorylation of ezrin was found to play an important role in the remodelling of the apical cytoskeleton in association with increased acid secretion by gastric parietal cells, but the critical residue involved was revealed to be a serine residue, S66 (Zhou et al, 2003).

1.5.3 Phosphorylation by Rho

Whilst there has been little argument that phosphorylation plays a pivotal role in the activation of the ERM proteins, the identity of the phosphorylating agent proved to be a matter of some contention. The appearance of Rho-GDI (Rho-GDP[guanosine diphosphate]-dissociation inhibitor) in an immunoprecipitated complex of CD44 and ERM proteins from BHK cells, along with subsequent experiments using C3 toxin, a specific inhibitor of Rho, gave the first indications that Rho may be involved in the regulatory phosphorylation of the ERM proteins (Hirao et al, 1996). The interaction of Rho-GDI with the ERM proteins was shown to have an involvement in the activation of Rho (Takahashi et al, 1997). In MDCK (Madin-Darby canine kidney) cells, activation of Rho was found to be essential for the association of ERM proteins with the PM (Kotani et al, 1997). Moesin was revealed to be a component of both the Rho and Rac signalling pathways, although without directly interacting with either of these proteins (Mackay et al, 1997), and Rho was found to be necessary - and sufficient - for the phosphorylation of radixin and moesin in NIH3T3 cells (Shaw et al, 1998). Oshiro et al (1998) demonstrated the Rho kinase-dependent phosphorylation of moesin's T558 residue in COS 7 (monkey renal) cells.

However, following their publication regarding the Rho kinase-dependent phosphorylation of the conserved T558/T564/T567 residue of the ERM proteins (Matsui et al, 1998), Matsui et al (1999) then claimed that the phosphorylation of the ERM proteins by a constitutively active mutant of RhoA was not suppressed by Y27632, a specific inhibitor of Rho kinase. These results suggested that although Rho kinase could phosphorylate the ERM proteins, other kinases and other phosphorylation pathways may also be involved. By this time, a sizeable quantity of evidence had accumulated for the role of phosphatidyl inositol-4, 5-bisphosphate (PIP2) in activating the ERM proteins, leading Matsui et al (1999) to propose a model for the

activation of the proteins whereby PIP2, generated by PI-4-P-5K (phosphatidyl inositol 4-phosphate 5-kinse) in response to RhoA activation, initiates the activation of the ERM proteins, a state which is then maintained via threonine phosphorylation by as yet unknown kinases. However, Yonemura et al (2002) discovered that both Rho-dependent and Rho-independent pathways of ERM protein activation exist, and that the proteins can remain active without C-terminal phosphorylation, although both the Rho-dependent and Rho-independent pathways require a local increase in concentration of PIP2 (Yonemura et al, 2002).

1.5.4 Phosphorylation by other kinases

The findings of Matsui et al (1999), that inhibition of Rho kinase does not necessarily inhibit ERM phosphorylation, and those of Yonemura et al (2002), that there are in existence Rho-independent pathways for the phosphorylation of ERM proteins, expedited the research into other kinases as contenders for the role of phosphorylating agent. Both Pietromonaco (1998) and Simons (1998) observed PKCθ-mediated phosphorylation of the ERM proteins. PKCα has been shown to phosphorylate the proteins' conserved threonine residue *in vivo* (Ng et al, 2001). Evidence has been found to suggest that ezrin phosphorylation by PKA is involved in parietal cell cytoskeletal remodelling (Zhou et al, 2003).

1.5.5 Interaction with PIP2

The ERM proteins are now known to bind to PIP2 via their FERM domain (figure 1.21). Niggli et al (1995) first noted that ezrin contained a phospholipid-binding site in its N-terminal domain and that this domain interacts with PIP2 with high affinity. Using an *in vitro* binding assay, Hirao et al (1996) found that the interaction between ERM proteins and CD44 was facilitated by the presence of PIP2. PIP2 was found to induce an interaction between ezrin and ICAM-1 and also to enhance the interaction between ezrin and ICAM-2 (Heiska et al, 1998).

Several methods for enhancing the binding of moesin to F-actin were uncovered by Huang et al (1999), one of which was exposure to PIP2, and Nakamura et al (1999) also found, during actin-moesin binding assays, evidence to suggest that phosphatidyl inositol-4-phosphate and PIP2 promoted the binding of actin to moesin.

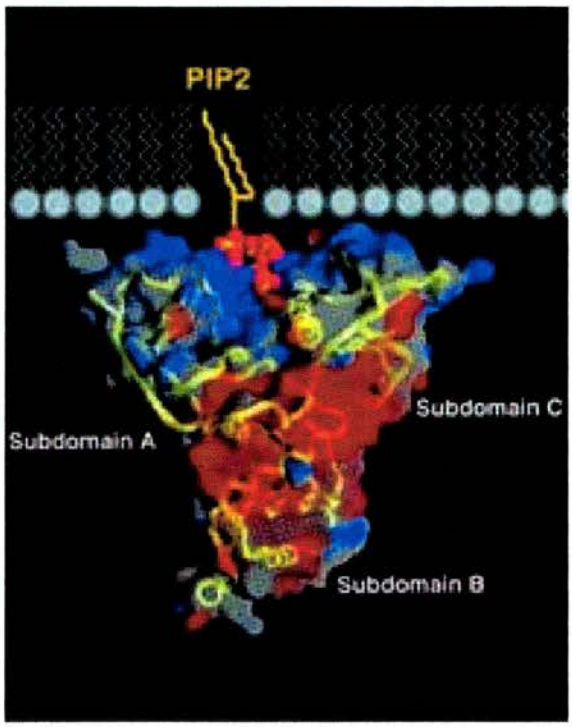

Figure 1.21. Diagram showing the binding of PIP2 to the radixin FERM domain. The FERM domain is shown in terms of surface electrostatic potentials, positive – blue and negative – red, over a yellow ribbon tracing of the main chain. PIP2 is shown as a yellow diacyl glycerol chain attached to a red IP3 headgroup which is bound in between subdomains A and C. Adapted from Hamada et al, 2000.

The early stage investigations into the activation of the ERM proteins were mainly based around phosphorylation studies, but as the role of phosphoinositides became more apparent, an increasing number of publications appeared that examined the role of PIP2 in the ERM

proteins' regulation. Matsui et al (1999) found that the primary agent involved in the RhoA-dependent activation of ERM proteins *in vivo* is PIP2, and not a ROCK (Rho-associated kinase) such as Rho. These findings then appeared to have been supported by the discovery that phosphorylation is not necessary for the activation of the ERM proteins in MDCK cells (Yonemura et al, 2002). Experiments had been performed which revealed that the ERM proteins could become activated in the absence of Rho activation, but that both Rho-dependent and Rho-independent activation of the protein required a local elevation of PIP2 concentration (Yonemura et al, 2002). Furthermore, the crystal structure of radixin complexed to the inositol 1,4,5-trisphosphate (IP3) headgroup of PIP2 had been determined (Hamada et al, 2000) (figure 1.21). Basing their hypothesis on the observed IP3-induced displacements within the crystal structure, the authors postulated a PIP2-mediated unmasking of the FERM domain and, by implication, a PIP2-mediated activation of the ERM proteins (Hamada et al, 2000).

1.5.6 Activation via both PIP2 and phosphorylation

Fievet et al (2004) then proposed a model that allowed for the involvement of both PIP2 and Rho, whereby these two agents acted sequentially. Using cell lines containing either wild type ezrin or ezrin that had no PIP2 binding ability, along with an antibody capable of detecting the phosphorylation state of the critical ezrin T567 residue, they determined that PIP2 binds ezrin in a manner that precedes, and is required for, T567 phosphorylation and subsequent ezrin activation (Fievet et al, 2004).

Two PIP2 binding sites have been identified in ezrin by Barrett et al (2000). The first motif is a $KK(X)_6(K/R)K$ motif at aa residues 63 - 72, and the second is a $KK(X)_3K(X)_3KK$ motif at aa residues 253 - 263. Mutagenesis of these binding sites in ezrin caused the protein to withdraw from the PM (Barrett et al, 2000).

1.5.7 Inactivation

Little has been published about the specifics of the inactivation of the ERM proteins. One early avenue of investigation involved calpain, a Ca^{2+}-dependent protease: an increase in intracellular Ca^{2+} in gastric parietal cells was shown to stimulate the production of a 55kDa ezrin breakdown product (Yao et al, 1993; Shuster and Herman, 1995). However, moesin and radixin have both been found to be insensitive to calpain (Shcherbina et al, 1999). Also, Chen et al (1994) found that inhibition of cellular calpain did not prevent the dissociation of ezrin from the cytoskeleton during anoxia-induced brush border breakdown in rabbit proximal tubule cells.

Kondo et al (1997) observed that, in response to fas ligand-mediated apoptosis, the ERM proteins translocate from the plasma membrane to the cytoplasm and that this event is concomitant with dephosphorylation. Phosphorylation and PIP2 pathways are known to be involved in the activation of the proteins (as mentioned above in 1.5.3 – 1.5.6) and it is possible that in many cases, reversing these pathways would lead to the inactivation of the proteins; Bretscher et al (1999) surmises that dephosphorylation of the critical T558/T564/T567 residue by phosphatases is one of the likely mechanisms of inactivation.

1.5.8 Summary of project aims

The overall aim of this project was to characterise the newly discovered protein, willin. As virtually nothing was known about willin, other than its partial DNA sequence and its point of origin in the mammalian nervous system, many avenues of exploration were open. Due to an anti-willin antibody being available prior to the beginning of this body of research, an examination into the presence of the protein in various cells lines was judged to be a potential starting point. A further line of inquiry, again involving the antibody but also involving the available partial DNA sequence, encompassed protein expression and purification experiments. The availability of microscope apparatus which enabled the visualisation of fluorescent-tagged proteins within individual cells, either as fixed slides or as live cell imaging, invited an exploration of the intracellular localisation and behaviour of the protein.

A brief outline of the aims of this research relating to particular chapters is included at the start of each chapter.

Chapter 2: Experimental

All chemicals are from Sigma unless otherwise stated.

2.1.1 DNA materials and methods

2.1.2 General information

- Working concentrations of antibiotics: ampicillin 100μg/ml, chloramphenicol 34μg/ml and kanamycin 50μg/ml.
- Bacterial strains used:

  1) *E.coli* Dh5α® [Φ80d*lacZ*ΔM15, *recA*1, *endA*1, *gyrA*96, *thi*-1, *hsdR*17 (r_K-, m_K+), *supE*44, *relA*1, *deoR*, Δ (*lacZYA-argF*)U169]

  2) *E.coli* BL21(DE3)pLysS [F-, *ompT*, $hsdS_B$, (r_B-, m_B-), *dcm*, *gal*, λ(DE3), pLysS (Cm^r)]

2.1.3 DNA Reagents

TBE

89mM Tris borate, pH 8.3; 2mM EDTA

6x DNA loading buffer

2x TBE; 50% [v/v] Glycerol; 0.1% [w/v] Bromophenol blue

DNA agarose gels

1% [w/v] Agarose in TBE; 0.05% [w/v] Ethidium bromide

Luria Broth (LB)

1% [w/v] Bacto-tryptone; 0.5% [w/v] Bacto-yeast extract; 1% [w/v] NaCl

LB plates

1% [w/v] Bacto-tryptone; 0.5% [w/v] Bacto-yeast extract; 1% [w/v] NaCl ; 1.6% agar

SOB

2% [w/v] Bacto-tryptone; 0.5% [w/v] Bacto-yeast extract; 0.05% [w/v] NaCl; 0.25M KCl; 10mM $MgCl_2$

$T_{10}E_{0.5}$

10mM Tris, pH 7.4; 0.5.M EDTA

2.1.4 General cloning strategy

Oligonucleotide primers were created to amplify target sequences of DNA via the polymerase chain reaction (PCR) and to allow the addition of novel restriction enzyme sequences to those target sequences. To allow priming from the 5' end of the gene, the forward primer was designed to contain the first 6 codons of the 5' end of the target sequence. If necessary, an initiating methionine codon was added in prior to the first codon of the target sequence. The sequence for the appropriate restriction enzyme was placed immediately upstream of the first codon. Any nucleotides that were deemed helpful for maximising the restriction enzyme cleavage activity (according to the New England Biolab technical section entitled "Cleavage Close to the End of DNA Fragments") were added in, when appropriate, upstream of the

restriction enzyme sequence. When designing primers that would be used in conjunction with expression vectors, extra nucleotides were added into the sequence of the primer where necessary, to maintain the translation frame of the vector. The extra nucleotides were chosen to produce amino acids that would cause minimal disruption to the fusion proteins.

The reverse or 3' primer was designed in a similar manner to the 5' primer. The last 6 codons of the target gene were used and these were followed by the sequence of the required restriction enzyme. If necessary, a stop codon was placed between the end of the last codon and the start of the restriction enzyme sequence. As with the 5' primer, if any nucleotides were required to increase the activity of the restriction enzyme, these were added in downstream of the restriction enzyme sequence. The 3' primer was reversed and complemented to allow priming of the gene from the 3' end.

2.1.5 Agarose gel electrophoresis

Flat bed agarose gels of concentration 1 - 2% were prepared with 1x TBE. Ethidium bromide was added to a final concentration of 0.5µg/ml. The DNA samples were mixed with DNA loading buffer and loaded into the wells. A 1kb DNA molecular weight marker (Promega) was usually run on each gel. Electrophoresis was carried out at 50-100V in 1x TBE containing ethidium bromide at a concentration of 0.5µg/ml. The DNA bands were visualised using a UV transilluminator.

2.1.6 Polymerase Chain Reaction (PCR)

The PCR was used to amplify regions of DNA for cloning. A typical reaction was performed in a 50µl volume and contained the following components: 5µl of a 5µM

solution of the forward primer (oligonucleotides obtained from Invitrogen); 5µl of a 5µM solution of the reverse primer; 5µl of the Taq/Turbo manufacturer's 10x reaction buffer; 0.5µl of a 20µM solution of the four dNTPs; 0.1 – 0.5µg of template DNA; 0.5µl of Taq (Promega) or PfuTurbo® DNA polymerase (Stratagene); MQH_20 to a final volume of 50µl. The reaction mixture was overlaid with 50µl mineral oil and DNA amplification was carried out on a thermal cycler under the following conditions: 1 cycle of 94°C for 5 minutes; 25 cycles of 94°C for 1 minute, 55°C for 1 minute and 72°C for 1.5 minutes; 1 cycle of 72°C for 10 minutes. The annealing temperature of 55°C was modified for each reaction according to the composition of the primers and the strength of DNA band obtained. A 5µl sample of each reaction was mixed with DNA loading buffer and electrophoresed to check that the reaction had produced a band of the desired size.

2.1.7 Purification of PCR products

PCR products were purified using the Wizard ® SV Gel and PCR Clean-Up System. An equal volume of Membrane Binding Solution was added to the PCR reaction mixture. A SV minicolumn was inserted into a collection tube and the PCR mixture was transferred into the minicolumn. The minicolumn was centrifuged at 10,000g for 1 minute. The flow-through was discarded and the minicolumn was reinserted into the collection tube. 700µl of Membrane Wash Solution was added and the minicolumn was centrifuged at 10,000g for 1 minute. The flowthrough was discarded and the minicolumn was reinserted into the collection tube. 500µl of Membrane Wash Solution was added and the minicolumn was centrifuged at 10,000g for 5 minutes. The minicolumn was placed in a fresh 1.5ml microcentrifuge tube and 50µl of nuclease-free dH_2O was added to the minicolumn, which was incubated at

room temperature for 1 minute and then centrifuged at 10,000g for 1 minute to elute the DNA.

2.1.8 Purification of DNA fragments from agarose gels

DNA fragments were purified from agarose using the Wizard ® SV Gel and PCR Clean-Up System. Following electrophoresis, the band containing the required DNA was excised from the agarose gel and placed in a 1.5ml microcentrifuge tube. 10µl of Membrane Binding Solution was added per 10mg of gel slice and the mixture was vortexed then incubated at 65°C until the gel slice had dissolved. A SV minicolumn was inserted into a collection tube and the dissolved gel slice mixture was placed in the minicolumn. All subsequent steps were identical to that described in Purification of PCR products.

2.1.9 Determination of DNA concentration

The concentration of DNA was calculated by monitoring the absorbance levels at 260nm in a spectrophotometer.

2.1.10 Restriction enzyme digests

2µg of plasmid DNA were digested with 2 units of enzyme (restriction enzymes from Promega) and 2.5µl of 10x restriction enzyme buffer in a total volume of 25µl, the remainder of the reaction mixture comprising MilliQ (MQ) H_20. The reaction components were incubated for between three and sixteen hours at the temperature recommended by the manufacturer.

2.1.11 Ligation of PCR products into vector DNA

The vector DNA and PCR DNA were digested with the appropriate restriction enzymes. The PCR products were prepared for ligation using the procedure described in Purification of PCR products. The vector DNA was prepared for ligation using the procedure described in Purification of DNA fragments from agarose gels. The ligation reactions were carried out in a total volume of 20µl. The ligation reaction typically contained the following components: 100ng of vector DNA; an equal quantity, or a two-fold excess, or a five-fold excess of insert DNA; 2µl of the manufacturer's 10x reaction buffer; 1 unit of T4 DNA ligase (Promega); dH_2O to a final concentration of 20µl. The ligation mixture was incubated at 4°C for 16 hours and then transformed into competent *E. coli*.

2.1.12 10ml overnight cultures

Unless otherwise stated, 10 ml overnight cultures were prepared by adding a scraping from a glycerol stock to 10ml of LB into which the appropriate antibiotics had been added. The culture was grown for 12-16 hours at 37°C in an orbital shaker at 200rpm.

2.1.13 Preparation of competent E.coli

500µl of a 10ml overnight culture was used to inoculate 50ml of antibiotic selective LB. The culture was grown at 37°C at 200g until the OD_{600} reached 0.3-0.4. The culture was centrifuged at 3500g for 10 minutes at 4°C. The pellet was resuspended in 20ml ice cold 0.1M $CaCl_2$ and incubated for 30 minutes on ice. The cells were centrifuged at 1500g for 5 minutes at 4°C, resuspended in 1ml ice cold 0.1M $CaCl_2$.

2.1.14 Transformation of E. coli

The two strains of *E.Coli* used were DH5α and BL21/DE3/pLysS. 200µl of competent cells was used per transformation, to which 10µl of the 20µl ligation mix was added. The sample was left on ice for 10 minutes and then heat shocked in a water bath at 42°C for 45 seconds. The sample was placed on ice for 5 minutes. 1ml of SOB without antibiotic was added to each sample and the mixture was grown at 37°C at 200g for one hour. 100µl from each sample was plated out onto antibiotic selective plates. The remaining 900µl was centrifuged at 10,000g for 20 seconds, most of the resulting supernatant was discarded, but a small amount of supernatant was retained to resuspend the cell pellet. The cells were then plated out onto antibiotic selective plates. The selection plates were incubated for 12-16 hours at 37°C.

2.1.15 Screening for recombinant clones using α-complementation

To select for recombinant clones in this manner, the antibiotic selection plates contained IPTG (Cambio) at a concentration of 40mg/ml and X-gal (Melford) at 40mg/ml.

2.1.16 Small scale preparation of plasmid DNA

Small quantities of plasmid DNA were prepared using the Wizard ® Plus Minipreps DNA Purification System. A 10ml overnight culture was centrifuged at 10,000g for 1 minute. The pellet was resuspended in 250µl Cell Resuspension Solution and transferred to a 1.5ml microcentrifuge tube. 250µl of Cell Lysis Solution was added and the tube was inverted 4x to mix the contents. 10µl of Alkaline Protease Solution was added and the sample was inverted 4x then incubated for 5 minutes at room

temperature. 350µl of Neutralisation Solution was added and the tube was inverted 4 times. The sample was centrifuged at maximum speed for 10 minutes at room temperature. A spin column was inserted into a collection tube and the cleared lysate was decanted into the spin column. The spin column was centrifuged at maximum speed for 1 minute at room temperature. The flow-through was discarded and the column was reinserted into the collection tube. 750µl of Wash Solution was added, the column was centrifuged at maximum speed for 1 minute and the flow-through was discarded. The column was reinserted into the collection tube and the wash step was repeated with 250µl of Wash Solution, this time centrifuging for 2 minutes. The spin column was transferred to a fresh microcentrifuge tube and 100µl of nuclease-free dH_2O was added. The spin column was centrifuged at maximum speed for 1 minute to elute the DNA.

2.1.17 Medium scale preparation of plasmid DNA

Medium scale quantities of plasmid DNA were prepared using the Qiagen ® Plasmid Midi Kit. 500µl of a 10ml overnight culture was used to inoculate 50ml of antibiotic selective LB which was then grown for 12 hours at 37°C at 200rpm. The cells were harvested by centrifugation at 6,000g for 15 mins at 4°C. The pellet was resuspended in 4ml of Buffer P1. 4ml of Buffer P2 was added and the mixture was inverted 4 times then incubated at room temperature for 5 minutes. 4ml of chilled Buffer P3 was added, the mixture was inverted 4 times and then incubated on ice for 15 minutes. The sample was centrifuged at 20,000g for 30 minutes at 4°C. The supernatant was removed and re-centrifuged at 20,000g for 15 minutes at 4°C. During the centrifugation, a Qiagen-tip 100 was equilibrated by applying 4ml of Buffer QBT which was allowed to flow through the column. At the end of the

centrifugation, the supernatant was removed, applied to the equilibrated Qiagen-tip and allowed to flow through the column. The Qiagen-tip was washed with 2 x 10ml of Buffer QC. The DNA was then eluted with 5ml of Buffer QF. The DNA was precipitated by the addition of 3.5ml of room temperature isopropanol and the mixture was centrifuged at 15,000g for 30 minutes at 4°C. The DNA pellet was washed with 2ml of room temperature 70% ethanol and centrifuged at 15,000g for 10 minutes. The pellet was air-dried for 10 minutes and then resuspended in 100µl of nuclease-free dH_2O.

2.1.18 Nucleotide dideoxy sequencing of recombinant DNA clones

2µg of DNA and 5µM of sequencing primer (Appendix I) were placed in a tube with MQH_20 to a final volume of 12µl. Alex Houston at the University of St Andrews performed automated sequencing on a Perkin Elmer ABI Prism™ 377 DNA sequencer. The sequencing data were viewed using Chromas.

2.1.19 Glycerol stocks

A single colony from a freshly streaked antibiotic selective plate was grown for 12-16 hours in 5ml antibiotic selective LB at 37°C at 200rpm. 0.85ml of the resulting culture was placed in a sterile 1.5ml microcentrifuge tube, to which was added 0.15ml of sterile glycerol. The mixture was vortexed briefly and then frozen at -70°C. A sterile pipette tip was generally used to remove a scraping from the glycerol stock.

2.2.1 Protein materials and methods

2.2.2 General information

- Antibodies: goat HRP-conjugated anti-rabbit from Upstate. Rabbit anti-rat willin antibody (914[3]) against the sequence KEASKGIDOFGPPMIIH, produced in house. Chicken anti-human willin antibody (CK1) against the sequence KLNFHNNRVMQDRRS and rabbit HRP-conjugated anti-chicken from Davids Biotechnologie. An additional rabbit HRP-conjugated anti-chicken antibody was also obtained from Sigma. CK1 antibody was affinity purified by Davids Biotechnologie via epoxy immobilisation on 1ml of MiniAffi2 matrix with 3mg of immobilised peptide. The buffer used was 100mM phosphate, 100mM Na-acetate, pH6.8.

2.2.3 Protein Reagents

Protein sample buffer (PSB)

10mM Tris, pH 6.8; 2% [v/v] ß-mercaptoethanol; 4% [w/v] SDS; 20% [v/v] glycerol; 0.2% [w/v] bromophenol blue

WCE lysis buffer

1x Complete protease inhibitor cocktail tablets (Roche) in PBS

SDS-PAGE stacking gel – lower

40% Acrylamide – 1.25ml; dH_2O – 2.41ml; 1M Tris pH 8.8 – 1.25ml; 10% SDS – 50µl; 10% APS – 50µl; TEMED – 2µl

SDS-PAGE stacking gel – upper

40% Acrylamide – 190µl; dH_2O – 1.1ml; 1.5M Tris pH 6.8 – 190µl; 10% SDS – 15µl; 10% APS – 15µl; TEMED – 1.5µl

SDS-PAGE running buffer

25mM Tris; 192mM Glycine; 0.1% SDS

Coomassie stain

20% [v/v] Methanol ; 20% [v/v] Glacial acetic acid; 0.2% [w/v] Coomassie brilliant blue R250

Coomassie destain

20% [v/v] Methanol; 10% [v/v] Glacial acetic acid

Phosphate buffered saline (PBS)

0.01M Phosphate buffer, pH 7.4; 2.7mM Potassium chloride; 0.137M Sodium chloride

Enhanced Chemiluminescence ECL) substrates (Pierce®)

50% [v/v] Supersignal® West Pico stable peroxide solution; 50% [v/v] Supersignal® West Pico luminol solution

Developing solution

10% Kodak® LX24 X-ray developer

Fixing Solution

20% Kodak® fixer

STEDS

150mM NaCl; 10mM Tris, pH 9.5; 1mM EDTA; 5mM DTT; 0.3% Sarcosyl

Elution buffer

50mM Tris, pH 9.5; 15mM Glutathione; 10mM DTT

Dialysis buffer

150mM NaCl; 50mM Tris, pH 9.5; 1mM EDTA; 5mM DTT

Protein lipid overlay (PLO) blocking buffer

50mM Tris-HCl, pH 7.5; 150mM NaCl; 0.1% [v/v] Tween 20 ; 2mg/ml fatty acid-free BSA

TBST

50mM Tris-HCl, pH 7.5; 150mM NaCl; 0.1% [v/v] Tween 20

Western blot transfer buffer

25mM Tris, pH 8.3; 192mM Glycine; 20% [v/v] Methanol

Blocking buffer 1

5% [w/v] Skimmed milk powder in PBS

Blocking buffer 2

5% [w/v] Skimmed milk powder in TBS; 0.5% Tween

Incubation buffer 1

0.2% [w/v] Gelatine in PBS; 0.1% [v/v] Tween

Incubation buffer 2

3% [w/v] Skimmed milk powder in TBS; 0.1% [v/v] Tween

Wash buffer 1

As for Incubation buffer 1

Wash buffer 2

0.1% [v/v] Tween in TBS

Immunoprecipitation (IP) Buffer 1

1x Complete protease inhibitor cocktail tablets (Roche); 10mM Tris 7.4; 150mM NaCl

IP Buffer 2

1x Complete protease inhibitor cocktail tablets; 10mM Tris 7.4; 150mM NaCl; 0.1% Triton-X 100

IP Buffer 3

1x Complete protease inhibitor cocktail tablets; 10mM Tris 7.4; 150mM NaCl; 1% Triton-X 100

2.2.4 Bradford Assay

A series of dilutions of known concentrations of bovine serum albumin (Promega) was set up in 500µl aliquots of mqH_20. A sample (between 1-10µl) from each supernatant of unknown protein concentration was placed in a microcentrifuge tube and made up to 500µl with mqH_20. 500µl of Bradford's reagent was added to each tube, mixed briefly and incubated for two minutes at room temperature. The solutions were placed into cuvettes and the A_{595} of the samples with known protein concentration was measured and used to plot a standard curve. The A_{595} of the unknown samples was measured and the standard curve was used to convert the absorbance of the unknown samples into protein concentration.

2.2.5 Denaturing polyacrylamide gel electrophoresis (SDS-PAGE)

For the majority of SDS-PAGE that was performed, a 5% stacking gel and a 10% resolving gel were used. A 6-175kDa protein broad range molecular weight marker (NEB) was usually run on each gel. The gels were run using a Hoefer Mighty Small Mini-Vertical Unit filled with 200ml of 1X tris-glycine running buffer. Electrophoresis was carried out at a constant current of between 40-120mA, depending on the number and thickness of gels, until the bromophenol blue dye front reached the bottom of the gel.

2.2.6 Coomassie brilliant blue staining

The proteins separated by SDS-PAGE were visualized by staining with Coomassie brilliant blue. The gel was soaked in Coomassie brilliant blue staining solution for 15 minutes with agitation, after which the staining solution was discarded. The gel was destained with frequent changes of the destaining solution until the background was clear.

2.2.7 Antibody panning

200µl of a 50% agarose-BSA bead slurry was placed in a microcentrifuge tube and the slurry was washed twice with 1ml PBS. 100µl of antibody was added to the beads and the mixture was placed on a wheel and mixed for 30 minutes at room temperature. The microcentrifuge tube was spun at 10,000g for 15 seconds to pellet the beads and the superntatant containing the panned antibody was then removed to a fresh tube.

2.2.8 Western blotting

The apparatus used was a Hoefer Mighty Small Transphor Tank Transfer Unit. The following components were soaked in transfer buffer and then laid on top of the cassette in the order given: one sponge insert, two pieces of 3mm blotting paper, a piece of nitrocellulose membrane, the SDS-PAGE gel, two more pieces of blotting paper and a second sponge insert. The cassette was closed, the tank was partially filled with transfer buffer and the cassette was placed into the tank. The tank was then filled to the maximum buffer level with transfer buffer and a current of 400mA was applied for 2 hours.

After staining and destaining the gel to check that the proteins had transferred to the membrane, the membrane was placed into blocking buffer 1 or 2 and blocked with gentle agitation for either 1 hour at room temperature or overnight at 4°C. The membrane was washed briefly with wash buffer 1 or 2 and then incubated with the primary antibody in 10ml incubation buffer 1 or 2 for 1 hour. Following three 10 minute washes with 10ml of wash buffer 1 or 2, the secondary antibody was added to 10ml incubation buffer 1 or 2 and the membrane was incubated in this for a further hour. Three washes were performed as before. The bands on the blot were detected using chemiluminescence according to the manufacturer's instructions.

2.2.9 Immunoprecipitation

Two 60mm dishes were washed twice with ice cold PBS. The cells were scraped from the dish using 500µl IP Buffer 3 per pair of 60mm dishes, placed in a microcentrifuge tube, titurated and incubated on ice for 10 mins. The samples were centrifuged at 4°C at high speed for 15 minutes. During this time, 5mg of Preswell Protein A conjugated beads were resuspended in 500µl IP Buffer 1. The bead mixture was incubated on ice for five minutes and washed twice with PBS using a low centrifuge speed for the washes. 50µl of the supernatant from the cell samples was mixed with PSB and boiled for five minutes then frozen at -20°C. The remaining supernatant was added to the washed beads, 5µl of antibody was added to each tube and the samples were tumbled on a wheel for 2 hours at 4°C. After this time each sample was washed firstly with 1ml of IP Buffer 3, then with 1ml of IP Buffer 2, with both washes conducted at 4°C. The beads were mixed with PSB and boiled for five minutes. The samples were frozen at -20°C and, prior to running the samples on an SDS-PAGE gel, each was briefly centrifuged.

2.2.10 Small scale expression of proteins

1ml of a 10ml overnight culture of BL21 cells containing the construct to be induced was used to inoculate 10ml of LB containing the appropriate antibiotics. The culture was grown at 37°C at 200rpm until an OD_{600} of 0.3-0.4 was reached. Prior to induction, a control uninduced sample was prepared as follows: 1ml of the culture was removed and centrifuged at 10,000g for 30 seconds. The pellet was resuspended in 6x PSB and boiled for 3 minutes then frozen at -20°C. IPTG (Cambio) was added to the remaining culture to a final concentration of 1mM and the culture was induced by growing for 3 hours at room temperature. 500µl of the induced culture was removed and centrifuged at 10,000g for 30 seconds. The pellet was resuspended in 6x PSB, boiled for 3 minutes and frozen at -20°C. The uninduced and induced samples were then run on an SDS-PAGE gel and then Coomassie stained and destained to check for the presence of a band representing the induced protein.

2.2.11 Solubilisation using guanidinium hydrochloride

This method was the same as that described in small scale expression of proteins, up to the point where the cells are harvested into a pellet. Following this centrifugation step, the cell pellet was resuspended in 300µl 100mM Tris pH 8.1/100mM EDTA. The suspension was sonicated for 15 seconds and centrifuged at 10,000g for 1 minute. The supernatant was discarded and the pellet was washed 3 times in 100mM Tris pH 8.1/100mM EDTA. 100µl of 6M guanidinium hydrochloride was added to the pellet and the tube was gently rotated at 4°C for 1 hour. The sample was centrifuged at 10,000g for 1 minute and the supernatant was retained for SDS-PAGE analysis.

2.2.12 Small scale purification of proteins – method 1

A 10ml culture of BL21 cells containing the appropriate construct was grown overnight in antibiotic selective LB. The culture was induced via the addition of IPTG to a final concentration of 1mM and then grown at room temperature and at 200rpm until an OD of 1 was reached. The culture was centrifuged at 10,000g for 30 seconds, successively, until all of the culture had been harvested in a microcentrifuge tube. 300µl of PBS [which later, with extra additions, became lysis buffer – section 2.2.13] was added to the pellet which was then sonicated and placed immediately on ice. The tubes were centrifuged at 4°C for 5 mins at 10,000g and the supernatants were transferred to fresh tubes [*pellet here may have been retained for analysis]. 50µl of a 50% GST-sepharose slurry, prepared according to the manufacturer's instructions, was added to the supernatant and then mixed gently by rotation for 5 minutes at room temperature. 1ml of ice cold PBS was added to the tube, the tube was inverted several times to mix and then centrifuged at 10,000g for 15 seconds to harvest the beads. The supernatant was removed and two more washes were performed in a similar manner. An equal quantity of 6x PSB was added to the contents of the tube and the sample was boiled for 3 minutes then analysed by SDS-PAGE.

2.2.13 Small scale purification of proteins - method 2

A 10ml culture of BL21 cells containing the appropriate construct was grown overnight in antibiotic selective LB. The culture was induced via the addition of IPTG to a final concentration of 1mM and then grown at room temperature and at 200rpm until an OD of 1 was reached. The culture was centrifuged at 10,000g for 30 seconds, successively, until all of the culture had been harvested in a microcentrifuge

tube. 300µl of ice cold STEDS buffer was added to the pellet which was then sonicated for 20 seconds and placed immediately on ice. 50µl of a 50% GST-sepharose slurry (Amersham Pharmacia), prepared according to the manufacturer's instructions, was added to the lysed cells and then mixed gently by rotation for 2 hours at 4°C. 1ml of ice cold PBS was added to the tube, the tube was inverted several times to mix and then centrifuged at 10,000g for 15 seconds to harvest the beads. The supernatant was removed and two more washes were performed in a similar manner. An equal quantity of 6x PSB was added to the contents of the tube and the tube was boiled for 3 minutes then analysed by SDS-PAGE.

To check the elution of the protein from the beads, after the third wash 50µl of elution buffer was added to the beads which were again placed in a wheel and mixed for 5 minutes at 4°C to elute the protein. The supernatant was collected in a fresh microcentrifuge tube.

2.2.14 Medium scale purification of proteins

A 10ml overnight culture of BL21 cells containing the construct to be induced was used to inoculate 300ml of LB containing the appropriate antibiotics. The culture was grown at 37°C at 200rpm until an OD_{600} of 0.6-0.8 was reached. The culture was induced by the addition of IPTG to a final concentration of 1mM and grown at room temperature for a further three hours at 200rpm. An OD_{600} reading was taken and used to calculate how much of the culture was required to provide 60 ODUs and how many 60 ODU aliquots were obtainable. For example:

1ml of culture gives an OD of 1.5

For 60 ODU, 60/1.5 = 40mls of culture are required

300/40 = 7.5 therefore 7 aliquots of 60 ODU are obtainable from this batch

The cells from each 60 ODU aliquot were harvested at 3,500rpm for 10 minutes. The pellet was resuspended in 1.2ml of ice cold STEDS and then sonicated for 4 x 20 seconds, with 40 second breaks in between, during which time the tubes were placed on ice. After the fourth sonication, 200µl of a 50% GST-sepharose slurry, prepared according to the manufacturer's instructions, was added to the lysed cells and the mixture was placed in a wheel and left mixing for 2 hours at 4°C. 5ml of ice cold PBS was added to the tube, the tube was inverted several times to mix and then centrifuged at 3,000rpm for 30 seconds to harvest the beads. The supernatant was removed and two more washes were performed in a similar manner. After the third wash, 200µl of elution buffer was added to the beads which were again placed in a rotation wheel and mixed for 5 minutes at 4°C to elute the protein. The supernatant was collected in a fresh microcentrifuge tube.

2.2.15 Dialysis of purified fusion proteins

The purified pGex proteins were placed into a short length of hydrated dialysis tubing which was tightly secured at both ends and placed in a beaker full of dialysis buffer with a magnetic stirrer included. The apparatus was left stirring over a period of 24 hours at 4°C, during which time the buffer was changed twice more. After 24 hours the dialysed proteins were extracted from the dialysis tubing with a needle and syringe. If the yield of the protein was too low following dialysis, the protein would be concentrated by the use of centricons, according to the manufacturer's instructions.

2.2.16 Protein Lipid Overlay Assay

A lipid-spotted membrane (Echelon PIP array™) was incubated in blocking buffer for one hour at room temperature. The membrane was incubated overnight at 4°C with agitation in fresh blocking buffer containing 5nM of fusion protein. The membrane was washed 10 times over 50 minutes in TBST followed by a 1 hour incubation at room temperature with a 1:2000 dilution of anti-GST monoclonal antibody in blocking buffer. The membrane was washed 10 times over 50 minutes in TBST and then incubated for 1 hour with a 1:5000 dilution of HRP-conjugated antimouse secondary antibody. The membrane was washed 12 times over one hour with TBST and then subjected to chemiluminescent detection.

2.2.17 *Protein/peptide competition – method 1*

A western blot was performed in a similar manner to that described in 2.2.8 except that all volumes of reagents were halved, as usually a smaller membrane was being analysed, and at the point of the addition of the primary antibody, either protein solution to a final volume (of 5mls) of up to 10nM, or peptide in PBS to a final volume (of 5 mls) of up to100µg/ml was also added in.

2.2.18 Protein/peptide competition – method 2

5µl of primary antibody was placed in a microcentrifuge tube along with either protein solution to a final volume (of 5mls) of up to 10nM, or peptide in PBS to a final volume (of 5 mls) of up to100µg/ml. PBS was added to the tube to a final volume of 1ml. The samples were placed on a wheel and rotated for 30 mins at room temperature, then centrifuged at 10,000g at 4°C for 15 minutes. Approximately 980µl of supernatant was collected from each tube and added to 4ml blocking buffer 1 or 2

to give a final volume of just under 5mls. The normal western blotting procedure (2.2.8) was carried out from this point on, except that all volumes of reagents were halved.

2.3.1 Tissue culture materials and methods

2.3.2 General information

- Cell culture: All cell lines were kept in a 37°C incubator in the presence of 5% CO_2 in air.

2.3.3 Tissue culture reagents

Culture medium (CHO, COS, HEK and SK-N-SH cell lines)

Dulbecco's modified Eagle's medium ; 10% foetal calf serum (Globepharm); 2mM glutamine; 50μg/ml streptomycin; 50 IU/ml penicillin

Culture medium (RPE, RPEc5 and RPEc5TCL1 cell lines)

Dulbecco's modified Eagle's medium/ Nut Mix F-12 (Gibco); 10% foetal calf serum 30mM $NaHCO_3$; 11μg/ml gentamycin (Gibco); 11μg/ml hygromycin B in PBS (Gibco)

Trypsin-EDTA

0.05% [w/v] Trypsin (Gibco) in 0.01M PBS; 0.5mM EDTA

Lysis buffer

1% [v/v] Triton-X 100 in PBS; 1x complete protease inhibitor cocktail tablets; 1mM PMSF

WCE buffer

1x complete protease inhibitor cocktail tablets in PBS

Fixing cells

4% Paraformaldehyde in PBS, pH 7.4; 200 units/ml Phalloidin (Cambio) in methanol; Gelvatol (Monsanto) supplemented with 0.1% DABCO and 0.1% DAPI

2.3.4 Passaging of cell lines

Each cell line was passaged 2-3 times per week. To passage the cells, the culture medium was removed from the flask and the cell layer was washed once with 1.5ml trypsin/EDTA. The cell layer was then incubated with 1.5ml of trypsin/EDTA for 5 minutes and the cells were collected in 15ml of culture medium and then split as required.

2.3.5 Breaking cells out of -70°C storage

A 5ml tissue culture flask was used for this procedure. 4ml of culture prewarmed culture medium containing an extra 10% FCS was placed in the flask. A cryotube containing 1ml of frozen cell suspension was removed from storage in liquid nitrogen and thawed quickly in a 37°C water bath. The cell mixture was pipetted into the flask and incubated in a 37°C incubator in the presence of 5% CO_2 in air. After 12-16

hours the cells were trypsinised, harvested in normal tissue culture medium and placed in a T75 flask.

2.3.6 Freezing down cells for storage in liquid nitrogen

Three flasks of cells at 100% confluency were trypsinised for five minutes. The trypsin was removed and the cells were harvested in 3.2ml of culture medium. 0.8ml of the cell suspension was aliquoted into each of four cryotubes. 100µl of each of fetal calf serum and DMSO was added to each cryotube and the tubes were put into an isopropanol bath and placed in a -70°C freezer for five hours. The cryotubes were then removed from the isopropanol bath and placed in liquid nitrogen.

2.3.7 Transfection Procedure

Prior to the transfection procedure, 60mm dishes were seeded with a volume of cells estimated to give the appropriate confluency to allow efficient transfection after 24 hours. For each transfection, 600µl of Optimem was placed in a microcentrifuge tube. Lipofectamine was added to the tube at a concentration of 2µg of Lipofectamine per µg of DNA. The amount of DNA added to the mixture was 2µg if the aim of the procedure was to produce slides, or 4µg if the dishes were to be used for a western blot. The tubes were mixed by flicking and then incubated for 30 minutes at room temperature. After 30 minutes, the culture medium was removed from the 60mm dishes and the dishes were washed twice with 3ml Optimem. 2.4ml Optimem was placed in each dish and the transfection mixture was then added. The dishes were placed in the 37°C incubator and left for 6 hours, after which the transfection medium was removed and replaced with 5ml of the usual culture medium.

2.3.8 Fixing cells

All washes were performed with ice cold PBS and the cells were shielded from light as much as possible throughout the fixing process. The culture medium was removed from the 60mm dishes and the coverslips were washed three times with 3ml of PBS, each wash lasting for 5 minutes. 3ml of 4% paraformaldehyde was added to the dishes and left for 20 minutes. The coverslips were then washed as before with one extra wash included. The cells were permeabilised with 3ml of PBS/0.2% Triton for 10 minutes and then washed once with PBS for 5 minutes. One unit of phalloidin diluted in methanol was added to each coverslip and left for 5 minutes. The cells were given one further wash with PBS and then mounted onto slides using 30µl of gelvatol. The slides were left to set for at least 1 hour. Cells were viewed using a DeltaVision® RT Restoration Imaging System.

2.3.9 Lysing cells

The culture medium from a T75 flask or 60mm dish of cells at 100% confluency was removed and the cell layer was washed up to five times with PBS. The amount of lysis buffer used was 150µl per flask or 50µl per dish. The lysis buffer was added to the flask or dish and a cell scraper was used to scrape the cells off the surface of the container. The cell suspension was placed in a microcentrifuge tube and the suspension was pippetted up and down several times to mix and then left on ice for 10 minutes. The lysed cells were then spun at 13,000rpm for 10 minutes at 4°C. The supernatant was removed and placed in a fresh tube. A 100µl (for a flask) or 30µl (for a 60mm dish) sample was removed from the supernatant, mixed with protein sample buffer and boiled for 3 minutes. The cell pellets were resuspended in protein sample buffer and boiled for 3 minutes.

2.3.10 WCE lysis method

The culture medium from a T75 flask or 60mm dish of cells at 100% confluency was removed and the cell layer was washed up to five times with PBS. The amount of WCE buffer buffer used was 150µl per flask or 50µl per dish. The lysis buffer was added to the flask or dish and a cell scraper was used to scrape the cells off the surface of the container into a microcentrifuge tube. Protein sample buffer was added to the tube, which was then boiled for three minutes.

2.4.1 Yeast materials and methods

2.4.2 General information

- Yeast strain used: *Saccharomyces cerevisiae* Y190 (genotype, MATa, *gal4-542*, *gal80-538*, *his3*, *trp1-901*, *ade2-101*, *ura3-52*, *leu2-3, 112*, URA3::GAL1-LacZ, Lys2::GAL1-HIS3cyh^r)

2.4.3 Yeast reagents

Yeast extract-peptone-dextrose + adenine (YPAD) liquid media

1% [w/v] Yeast extract; 2% [w/v] Peptone; 1% [w/v] Glucose; 0.01% [w/v] Adenine hemisulphate

YPAD Plates

1% [w/v] Yeast extract; 2% [w/v] Peptone; 1% [w/v] Glucose; 0.01% [w/v] Adenine hemisulphate; 1.67% [w/v] Bacto-agar

Liquid knockout medium, pH 5.6

0.067% [w/v] Amino acid drop out mixture; 0.67% [w/v] Yeast nitrogen base; 1% [w/v] Glucose

Knockout plates, pH 5.6

0.067% [w/v] Amino acid drop out mixture; 0.67% [w/v] Yeast nitrogen base; 1% [w/v] Glucose; 1.67% [w/v] Bacto-agar

Amino acid drop out mixture: minus Trp

2.0g Adenine hemisulphate; 2.0g Arginine HCl; 2.0g Histidine HCl; 2.0g Isoleucine; 4.0g Leucine; 2.0g Lysine HCl; 2.0g Methionine; 3.0g Phenylalanine; 2.0g Serine; 2.0g Threonine; 2.0g Tyrosine; 1.2g Uracil; 9.0g Valine

Cracking Buffer Stock, pH 6.8

40mM Tris-HCl ; 8M Urea ; 5% [w/v] SDS; 0.1mM EDTA; 0.04% [w/v] Bromophenol blue

Cracking Buffer – Complete

1ml Cracking buffer stock ; 10µl β-mercaptoethanol; 1x PMSF ; 1x complete protease inhibitor cocktail tablets

NaOH/β-Mercaptoethanol (NaOH/ β-ME)

2M NaOH; 8% β-Mercaptoethanol

Z Buffer

0.04M $NaH_2PO_4.H_2O$, pH7; 0.01M KCl; 0.05M $MgSO_4.7H_20$

Yeast autoactivation detection solution

100ml Z-Buffer; 1.67ml of 20mg/ml X-GAL in DMF; 270µl β-mercaptoethanol

2.4.4 Yeast high efficiency transformation

An overnight culture was set up in 5ml YPAD using a scraping of a Y190 glycerol stock. An amount of the 5ml starter culture calculated to give a final concentration of $2x10^7$ cells/ml was used to inoculate 50ml of YPAD. The flask was placed in a 30°C incubator and grown at 200rpm for the required amount of time (usually 3 – 5 hours). The culture was harvested in a sterile 50ml centrifuge tube by centrifugation at 5,000rpm for 5 minutes. The supernatant was poured off and the cells were washed in 25ml sterile water and centrifuged as before. The water was poured off and the cells were resuspended in 1ml 100mM LiAc and the suspension was transferred to a 1.5ml microcentrifuge tube and centrifuged at top speed for 15 seconds. The LiAc was removed and 400µl of 100mM LiAc was used to resuspend the cells. The cell suspension was vortexed and 50µl of cells were aliquoted into a microcentrifuge tube for each transformation required. The transformation mix was added, keeping to the order specified to allow the PEG to shield against the high concentration of LiAc: firstly, 240µl 50% [w/v] PEG, then 36µl 1M LiAc, 50µl of 2mg/ml ssDNA, between 0.1 – 10µg plasmid DNA in *x*µl H_20, and 34-*x* µl dH_20 to give a final total volume of 360µl. Each tube was vortexed vigorously for one minute until the cell pellet was thoroughly resuspended. The tube was incubated for 30 minutes in a 30°C water bath, and then heat shocked in a 42°C water bath for 30 minutes. The mixture was

centrifuged at 7,000rpm and the transformation mix was removed. 1ml of sterile water was placed into each tube and the cell pellet was gently resuspended. Generally, 200µl of transformed cell suspension was plated onto selection plates.

2.4.5 Extraction of yeast proteins – method 1

For each transformed yeast strain to be assayed, a 5ml overnight culture was grown in yeast selective medium using a single colony of 1-2mm diameter and no more than four days old. A 5ml overnight culture of an untransformed control colony was also usually grown alongside the transformed strains. The overnight cultures were vortexed for 1 minute to disperse cell clumps, then all 5mls of the culture was used to inoculate 50ml of YPD medium. The cultures were grown at 250rpm at 30°C until the OD_{600} reached 0.4-0.6. Each culture was quickly chilled by pouring it into a prechilled 100ml centrifuge tube that was half-filled with ice. The tube was then immediately placed in a prechilled rotor and centrifuged at 1000g for 5 mins at 4°C. The supernatant was poured off and the cell pellet was washed by resuspending it in 50ml ice cold dH_20 followed by centrifugation as before. The recovered pellet was immediately frozen in liquid nitrogen and stored at -70°C.

The OD_{600} reading of each of the 1ml samples was multiplied by the culture volume to give a final figure in optical density units (ODUs). For example, OD 0.6 x 55ml = 33 ODUs. This figure was used to calculate the amount of Cracking buffer (Complete) needed for each sample, using 100µl of Cracking buffer (Complete) per 7.5 ODUs of cells.

To aid in the resuspension of the frozen cell pellets, the cracking buffer was prewarmed to 60°C, with the PMSF added immediately before use. Each cell pellet was resuspended in the calculated optimum amount of warmed cracking buffer. The cell suspensions were transferred to microcentrifuge tubes containing 80µl of sterile glass beads per 7.5 ODUs of cells. The samples were heated at 70°C for 10 mins and then vortexed vigorously for 1 minute before being centrifuged at 10,000rpm for 5 mins at 4°C. Each supernatant was transferred to a fresh microcentrifuge tube and placed on ice. Further supernatant was collected by adding 50µl of cracking buffer to each sample, heating the tube to 100°C for 3 mins, vortexing the sample for 1 minute, centrifuging as before and then adding the resulting supernatant to the previously collected supernatant. The samples were boiled briefly and then immediately loaded onto an SDS-PAGE gel.

2.4.6 Extraction of yeast proteins – method 2

An overnight starter culture as described in method 1 was used to inoculate 25ml of YPAD medium which was grown at 200rpm in a 30°C incubator until a cell density of $5x10^6$ cells/ml was reached. The cells were centrifuged at 5,000rpm for five minutes, the supernatant was removed and the cells were washed in 1ml ice cold dH_2O. The suspension was transferred to a microcentrifuge tube and centrifuged at maximum speed for one minute. The cell pellet was resuspended in 1ml ice cold dH_2O containing 100µg/ml PMSF. 150µl of ice cold NaOH/β-ME was added and the tube was inverted several times then incubated on ice for 10 minutes. 150µl of ice cold 50% TCA was added, the tube was inverted several times and incubated on ice for 10 minutes. Each tube was centrifuged for 2 minutes at maximum speed. The cell pellets were washed with 1ml ice cold acetone, centrifuged for 2 minutes at

maximum speed. The supernatant was removed and the pellet was left to air-dry. The pellet was resuspended in 100µl of PSB, heated to 95°C for five minutes and then the samples were loaded onto an SDS-PAGE gel.

2.4.7 Extraction of yeast proteins – method 3

An overnight starter culture as described in method 1 was used to inoculate 10ml of YPAD medium which was grown at 200rpm in a 30°C incubator until a cell density of $1x10^7$ cells/ml was reached. For each transformed strain to be assayed, 1.5ml of cells was harvested by centrifugation at maximum speed for one minute. The cells were washed with 1ml dH_2O and centrifuged as before. Each cell pellet was resuspended in 100µl of PSB and heated at 95°C for 5 minutes, after which the samples were centrifuged for 5 minutes at maximum speed before being loaded onto an SDS-PAGE gel.

2.4.8 Yeast autoactivation detection

Transformation mixtures were plated out in duplicate onto yeast selection plates. When the colonies were four days old, a filter lift assay was performed as follows: a circular piece of Whatman 3MM filter paper was placed on top of the yeast colonies on the plate until the paper was saturated. The paper was removed, taking the colonies with it, and dropped into liquid nitrogen for 10 seconds. The filter paper was removed from the liquid nitrogen and placed colonies-upwards on a flat surface until it had thawed. Another two freeze-thaw cycles were performed and the filter paper was then placed in a fresh petri dish. 5mls of Z Buffer containing freshly added β–mercaptoethanol and X-GAL was poured onto the filter paper and the dish was

incubated at 37°C for 24 hours. The plate was checked for colour changes at regular time intervals.

Chapter 3: Analysis of anti-willin antibodies and examination of the expression of the native willin gene and protein.

3.1 Aims:

- Investigation into the possible presence of the willin gene in rat sciatic nerve and brain libraries.
- Characterisation of the 914[3] anti-willin antibody.
- Characterisation of the CK1 anti-willin antibody.
- The use of these antibodies to determine the possible expression of willin in several different mammalian cell lines.

3.2 Introduction

Two anti-willin antibodies had been obtained by the St Andrews laboratory. The first antibody, known as 914[3] (Appendix II), was produced by immunising a rabbit with an 18-amino acid peptide derived from the N-terminal sequence of the rat willin protein. An affinity purified version of this antibody was also available. The second antibody, CK1 (Appendix II), was produced by immunising a chicken and extracting the antibody from eggs laid by this animal. Again, an affinity purified version of the antibody was also available. Both of the antibodies required characterisation in terms of (i) what dilutions were suitable for use in western blotting, (ii) confirmation that the preimmune sera were unreactive, (iii) the specificity of the antibodies and (iv) the usefulness of the affinity purified versions.

Several mammalian cells lines were available for analysis. Since the other ERM proteins are widely expressed in cultured cell lines (Amieva et al, 1995; Sato et al, 1992) it was hoped that willin also would be detected, via western blotting, in one or more of the cell lines available. If these experiments could successfully provide a preliminary indication of the presence of willin in cultured cells, this would pave the way for further investigations into the expression of the native protein, such as inhibiting the expression of willin via RNAi (RNA interference) which could then be confirmed by the disappearance of a band on a western blot.

The IMAGE clone that had been obtained from the MRC IMAGE Consortium DNA Bank coded for a protein of approximately 70kDa. The identification of a band of this size in the cell lines by one of the antibodies available would suggest that this antibody may detecting natively expressed willin. However, if a band of similar size could be detected by the second antibody also, this would then provide corroborating evidence that willin is expressed in that particular cell line(s).

The search for native willin was initially centred on searching for the willin gene in two rat libraries, a brain library and a sciatic nerve library.

3.3.1 Attempts at detecting the presence of the full length willin gene

A partial fragment of the willin gene had been pulled out of a rat sciatic nerve library during a yeast-two-hybrid screen (Gunn-Moore et al, 2005). Three oligonucleotide primers were designed to enable attempts at finding the full length rat gene, via the PCR, in a sciatic nerve library or in a rat brain library.

During the experiment described in the early part of this chapter, the DNA sequences available were those of a partial rat willin sequence (accession no. AF441249), and a full length willin sequence had also been discovered via bioninformatic searches, which was that of a skin cell-derived human sequence (accession no. AK055545). The intention was to use the final nucleotides of the available partial rat sequence as the basis for a forward primer (figure 3.1, primer 1). Two reverse primers were designed which were based on the human sequence (figure 3.2, primers 2 and 3). The first of these reverse primers, H willin1, was based on the final nucleotides of the human sequence and the second, H willin6, was based on nucleotides lying a few bases outside the stop codon of the human sequence.

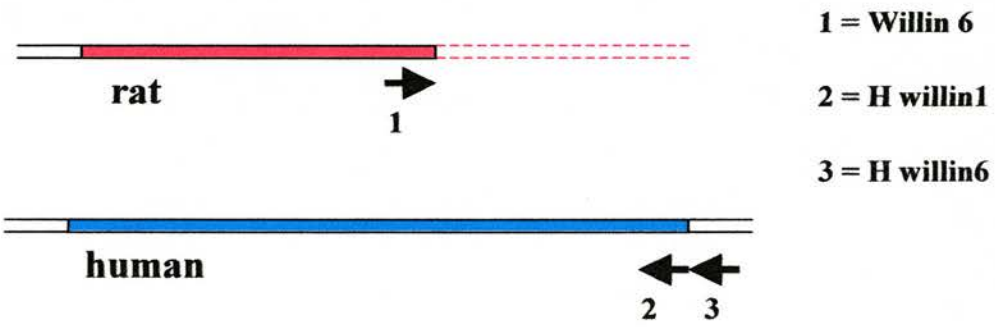

Figure 3.1. Diagram to show the primers that were used in an attempt to discover the remainder of the DNA sequence of a partial rat willin gene.

The PCR was performed using the two sets of primers - Willin 6 + H willlin1 (primers 1 + 2 in figure 3.1) and Willin 6 + H willin 6 (primers 1 + 3 in figure 3.1) - and each set was used to search both a rat sciatic nerve library and a rat brain library. The resulting PCR products were run on an agarose gel alongside a DNA molecular weight marker but none appeared to be of the appropriate size (full length dermal

willin clone, accession no. AK055545, predicted size 1869bp) and instead ranged from ~300 to ~1200bp. As it was believed possible that these products could be isoforms of the rat willin gene, several of the bands were cut out from the gel and cloned into pBlueScript vector. The clones were then analysed by automated DNA sequencing. However, the DNA that was contained within the clones was found to be *E.coli* DNA. The sequences of the primers were examined and were found to have some similarity to certain regions of the *E.coli* chromosome. The attempts at cloning a full length rat cDNA clone by the PCR was abandoned but by this point, the full length clone of human willin had become available for purchase from the MRC UK HGMP Resource Centre (clone derived from human uterine cells, accession no BC020521).

3.3.2 Investigation into the expression of willin with the 914[3] antibody

On each of the western blots shown in this chapter, typically 20 - 25µg of cell lysate, as determined by a Bradford assay, would be loaded in each lane. Supernatants were loaded unless otherwise indicated. Unless otherwise stated, the positive control was induced bacterial cell lysates containing GST-HFL (section 5.3.8).

Preliminary western blot experiments were carried out with the 914[3] antibody using lysed samples from Retinal Pigmented Epithelial (RPE) cells and RPE clone 5 (RPEc5) cells. The latter was a cell line produced via irradiation of normal RPE cells. The cells were harvested and lysed according to the method described in section 2.3.9 and then loaded onto an SDS-PAGE gel. After transfer of the gel to nitrocellulose membrane, a western blot was performed as described in section 2.2.8 using the 914[3] antibody at an initial 1:500 dilution.

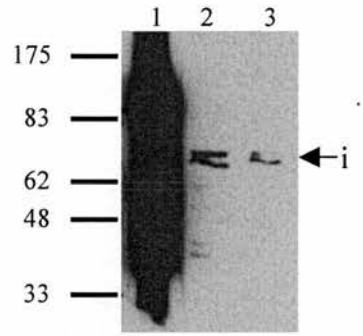

Figure 3.2. Western blot analysis of lysates from RPE and RPEc5 cells using the 914[3] antibody. Lane (1) contains the purified fusion protein GST-HFL as a positive control. Other lanes contain equal amounts of cell extracts from (2) RPE cells and (3) RPEc5 cells

The western blot in figure 3.2 revealed a doublet in both lanes containing cell lysate (figure 3.2, ←i). The doublet migrated to the approximate location that the full length willin protein was predicted to migrate to, which is the 70kDa area. Other ERM proteins had also been seen to migrate as doublets, and even triplets (Alfthan et al, 2004).

The signal from the positive control lane (induced bacterial cell extracts containing GST-HFL [98kDa], which is a gluthathione-S-transferase fusion protein composed of GST and full length human willin – section 5.3.8) was very pronounced, as at this stage the amount of control protein to load onto the SDS-PAGE gels had not yet been optimised. Although the majority of the GST-HFL fusion protein could be observed on Coomassie stained SDS-PAGE gels at the expected location of 98kDa, western blotting frequently also detected a gradient of suspected breakdown products, leading to a smeared effect throughout the length of the lane.

3.3.3 Western blots using 914³ preimmune serum

Serum was available that had been withdrawn prior to the immunisation process from the rabbit that produced the 914³ antibody. This serum was used in a western blot as a control to ensure that the bands that were being detected were due specifically to post-immunisation antibodies. Equal amounts of purified GST-HFL protein were loaded in duplicate onto an SDS-PAGE gel. After transfer of the gel to nitrocellulose membrane, the membrane was divided into two halves. One half of the membrane was incubated with preimmune serum and the other half was incubated with the 914³ antibody. The results are shown in figure 3.3.

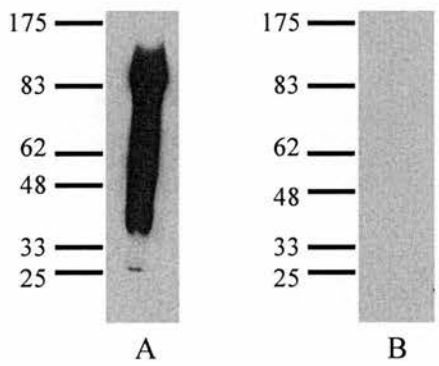

Figure 3.3. Analysis of the 914³ preimmune serum. Western blot A – 1:1000 dilution of 914³ antibody was used. Western blot B – 1:1000 dilution of preimmune serum was used. On both blots, equal amounts of purified GST-HFL protein were loaded.

Figure 3.3 shows that, as before, the 914³ antibody reacted strongly with the positive control. The preimmune serum did not react with the positive control, indicating that there were no anti-willin antibodies present in the rabbit prior to immunisation.

A similar experiment was then performed with extracts from the mammalian cell lines. Equal amounts of protein from RPE, RPEc5 and CHO cell extracts were loaded in duplicate onto SDS-PAGE gels for electrophoresis and then transferred to

nitrocellulose membranes. One set of samples was probed with preimmune serum and the other set was probed with the 914^3 antibody.

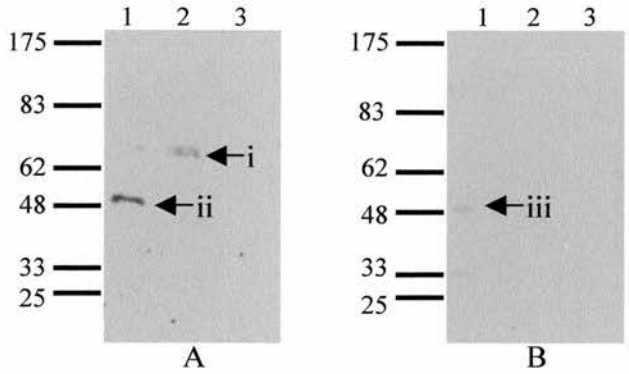

Figure 3.4. Continued analysis of the 914^3 preimmune serum Western blot A – a 1:1000 dilution of 914^3 antibody was used. Western blot B – a 1:1000 dilution of preimmune serum was used. Each blot contained equal amounts of the following: (1) CHO cell lysate (2) RPE cell lysate (3) RPEc5 cell lysate

These western blots in figure 3.4 indicated that the ~70kDa band (figure 3.4, ←i) in the RPE lane and the faint ~70kDa band in the CHO lane did not result from a reaction with any antibody present in the animal before it was immunised with the willin peptide. A ~50kDa band appeared in each of the lanes containing CHO cell extract (figure 3.4, ← ii and ←iii). However, the band resulting from incubation with the preimmune serum (figure 3.4, ←iii) was much weaker than that which appeared following incubation with the 914^3 antibody (figure 3.4, ←ii). This result was of interest as it was an indication that the 914^3 antibody could be picking up a possible smaller isoform of the protein. The existence of a ~50kDa isoform had already been observed in another member of the ERM family by Kaul et al (1999), who described their discovery as a 55kDa N-terminal cleavage form of ezrin.

3.3.4 Cross reaction of the 914³ antibody with Bovine Serum Albumin (BSA)

Seven cell lines were analysed to check for the presence of the ~70kDa and ~50kDa bands. These seven cell lines included lines that had been used previously i.e. RPE, RPEc5 and CHO cells. Additionally, cells from the irradiated RPEc5 line had been injected into a mouse and a tumour had resulted. A cell line had been established from the tumour and this new cell line was named RPEc5 tumour cell line 1 (RPEc5Tcl1). Extracts from the RPEc5Tcl1 line were used in this experiment, along with extracts from COS7, HEK293 and SK-N-SH neuroblastoma cells. A new molecular weight marker, New England Biolabs (NEB) Broad Range 2-212kDa, was loaded onto the SDS-PAGE gel alongside the previously used molecular weight marker, NEB Broad Range 6-175kDa. The SDS-PAGE gel was transferred to nitrocellulose membrane and a western blot was performed in the usual manner using a 1:1000 dilution of the 914³ antibody.

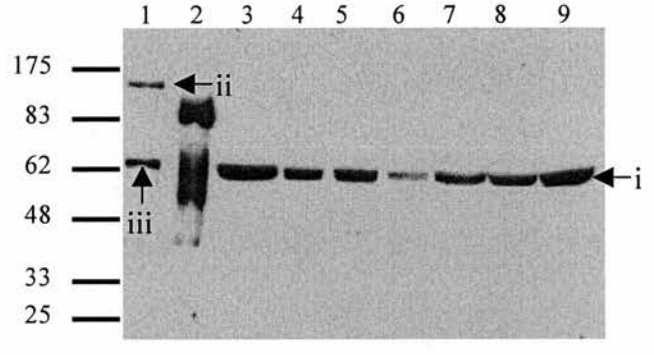

Figure 3.5. Western blot analysis of seven different cell extracts using the 914³ antibody. Lanes contain (1) NEB 2-212kDa molecular weight marker (2) positive control (3) CHO lysate (4) COS lysate (5) HEK lysate (6) SK-N-SH lysate (7) RPE lysate (8) RPEc5 lysate (9) RPEc5Tcl1 lysate.

As shown in figure 3.5, all seven of the cell lines were observed to contain a band at the approximate position corresponding to that expected for the putative native

protein (figure 3.5, ←i). However, it was also noted that the 914[3] antibody was cross-reacting with two bands present in the NEB 2-212kDa molecular weight marker (figure 3.5 , ←ii and ←iii). Although cross-reaction of any kind is undesirable, the cross-reaction of the 66.5 kDa band (figure 3.5, ←iii) posed a particular problem as it was very close to the expected size of the native willin. The manufacturers stated that the 66.5 kDa band was bovine serum albumin (BSA).

BSA is present in the DMEM used for culturing the cell lines. The current protocol for the lysis of the cell lines was to wash the T75 flasks once or twice with PBS to remove the traces of the media. An experiment was designed which would reveal if DMEM-derived BSA was the likely source of the ~70kDa bands in the western blots that had been performed so far. Four equally confluent flasks were used. The substratum of the first flask was washed once prior to harvesting the cells, the second flask was washed three times, the third flask was washed five times and the fourth flask was washed seven times.

If the ~70kDa band was due to contamination of the cell lysates with BSA then an increase in the number of washes to remove the media would correlate with a decrease in the intensity of the band. If, however, the ~70kDa band was due to a protein present inside the cells - the putative native willin - then the number of washes would have no effect on the intensity of the band since the washes were performed prior to the lysis of the cells.

The extracts from the flasks were lysed into supernatant and pellet fractions and then equal amounts of each sample were used in a western blot. The antibody used was 914^3 at a 1:1000 dilution.

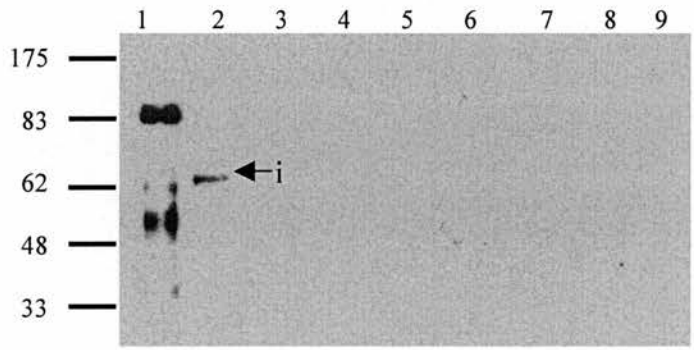

Figure 3.6. Western blot showing results of an experiment where an increasing number of washes were used prior to lysing cells to observe the effect on the ~70kDa band. Lane (1) = positive control. Other lanes contain either supernatant [S] or pellet [P] fractions of CHO cells. Lanes (2) S, 1 wash (3) S, 3 washes (4) S, 5 washes (5) S, 7 washes (6) P, 1 wash (7) P, 3 washes (8) P, 5 washes (9) P, 7 washes.

The only ~70kDa band (figure 3.6, ←i) that appeared was that in the lane containing cells that had been washed only once. Since an increasing number of washes caused the band to disappear, it was assumed that the ~70kDa bands that had been detected in the above western blots were actually BSA. Subsequently, all flasks or dishes of cells were washed four times to ensure the removal of all the media.

3.3.5 Panning of the 914^3 antibody

In addition to using an increased number of washes to prevent the contamination of the cell lysates with BSA, the 914^3 antibody was tumbled with BSA-conjugated agarose beads. It was hoped that this panning process would cause all the antibodies

present that had an affinity for BSA to bind to the agarose beads, hence facilitating their removal from the serum.

To confirm that this approach would prevent any further reaction with BSA, the 914^3 antibody was panned (section 2.2.7) and then both the original unpanned and the panned versions were used in a western blot. The SDS-PAGE gel used for this western blot was loaded with three different types of sample. Firstly, a positive control was included (GST-HFL) to ensure that panning the antibody had no adverse effect on the antibody's ability to recognise the willin protein. Secondly, BSA at a concentration of 1μg and 2μg was loaded onto the gel. Thirdly, the BSA-containing NEB Broad Range 2-212kDa molecular weight marker that had originally signalled the cross-reaction of the 914^3 antibody with BSA was also included on the gel.

All samples were loaded identically and in duplicate to allow comparison of the panned versus the non-panned versions of the 914^3 antibody. The panned and unpanned antibodies were both used at a 1:1000 dilution.

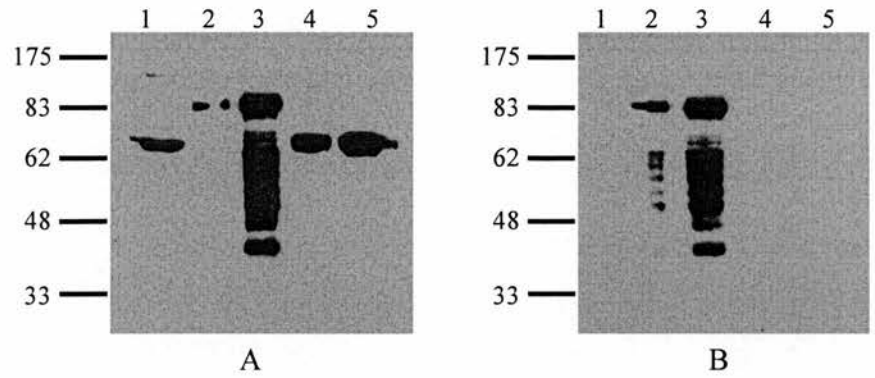

Figure 3.7. Comparison of unpanned and panned versions of the 914^3 antibody. Blot A was probed with a 1:1000 dilution of unpanned 914^3. Blot B was probed with a 1:1000 dilution of panned 914^3. Each blot contained: lane (1) NEB Broad Range 2-212kDa molecular weight markers (2) 1µl positive control (3) 3µl positive control (4) 1µg BSA (5) 2 µg BSA.

Figure 3.7 showed that panning the antibody appeared to eradicate any cross-reaction of the 914^3 antibody with BSA. The panned version of the 914^3 antibody will henceforth be referred to as $p914^3$ (panned 914^3).

3.3.6 Use of the panned 914^3 antibody to detect native willin

Samples of RPE, RPEc5 and RPEc5Tcl1 cell lines were loaded onto SDS-PAGE gels with the intention of attempting to detect willin in these cells lines using the panned 914^3 antibody. The resulting membrane was incubated with the $p914^3$ antibody at a concentration of 1:1000.

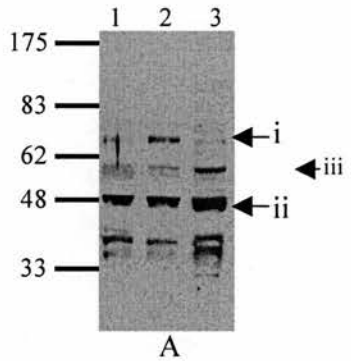

Figure 3.8. Western blot to detect native willin in RPE-derived cell lines. The p914[3] antibody was used at a dilution of 1:1000. The lanes contain equal amounts of protein from: (1) RPE cells (2) RPEc5 cells (3) RPEc5Tcl1 cells.

The p914[3] antibody detected ~70kDa bands in all three cell lines on this blot (figure 3.8, ←i). The non-specific binding was high on this western blot but again a strong band of around ~50kDa was detected by the antibody (figure 3.8, ←ii), as had been previously observed (figure 3.4). [Arrow ←iii is mentioned in section 3.6.2]

3.3.7 Alteration of the lysis protocol to the "Whole Cell Extract" method

Although the desired result of detecting a ~70kDa band had been achieved with the panned 914[3] antibody (figure 3.8), the intensity of this band was not particularly strong.

The time taken from the point of scraping the cells from a dish or flask to the point of boiling them in protein sample buffer was usually 20+ minutes. This included a 10 minute incubation on ice in SDS-containing buffer to lyse the membranes, followed by a 10 minute centrifugation to separate the lysates into soluble and insoluble fractions. This method was intended to determine if the ~70kDa band would be found in the cell membrane fraction or in the cytoskeletal fraction. But even though

protease inhibitors were present in the lysis buffer and the incubation and centrifugation steps were performed on ice and in a 4°C room respectively, the possibility existed that the willin protein was being degraded during the 20 minutes.

An attempt was made to enhance the ~70kDa signal by altering the cell lysis method. A simpler method for lysing the cells was devised whereby the cells were washed as usual and then simply scraped off the dish or flask in a small amount of protease-containing buffer (WCE [whole cell extract] buffer), mixed with protein sample buffer and then immediately boiled for five minutes. It was anticipated that the presence of SDS in the protein sample buffer, combined with boiling, would be sufficient to lyse the cells. Although this method would not permit the determination of whether the detected bands were present in the supernatant or the pellet, it was hoped that the shortened protocol would promote a stronger signal from the ~70kDa band.

This approach was named the "WCE" (whole cell extract) method (2.3.10) and was initially tried with three cell lines: CHO, HEK293 and SK-N-SH. A western blot was performed with these samples using the p914[3] antibody at a 1:1000 dilution.

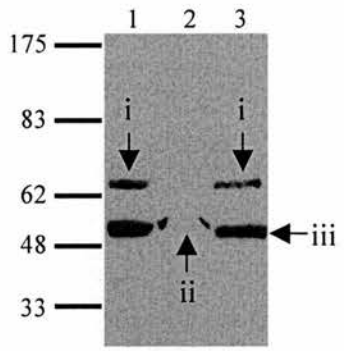

Figure 3.9. Results from using a shortened protocol for cell lysis in an attempt to increase the signal from the ~70kDa band. The p914[3] antibody was used at a concentration of 1:1000. The lanes contain equal amounts of whole cell extracts from (1) CHO cells (2) HEK cells (3) SK-N-SH cells.

The revised protocol appeared to be of assistance in obtaining a stronger signal from the ~70kDa band, as shown in figure 3.9 (← i). The band is absent in the HEK293 cells in this western blot (figure 3.9, ←ii) but the HEK293 lane does not appear to have transferred very well, possibly due to an air bubble between the gel and the membrane during the transfer process. Notably, on this western blot the only two bands that appear are those of ~70kDa (figure 3.9, ← i) and ~50kDa (figure 3.9, ←iii).

3.3.8 Panning and characterisation of the AP 914[3] antibody

Since a strong, reproducible ~70kDa band had been visualised with the panned version of the 914[3] antibody, attention was then turned to the affinity purified version of this antibody. It was hoped that the affinity purified version would detect the same ~70kDa band (and possibly also ~50kDa band) that was detected using the non-affinity purified version.

Since the affinity purified version of the 914^3 antibody (henceforth referred to as the AP 914^3 antibody) was a derivative of the 914^3 antibody, it was deemed necessary to also pan the affinity purified version. The panned version of the AP 914^3 antibody will henceforth be referred to as the pAP 914^3 antibody.

Western blots were performed with cell lysates using both the AP 914^3 and pAP 914^3 antibodies. The purpose of these blots was firstly to determine if the affinity purified version of the 914^3 antibody could detect a ~70kDa band, and secondly to check that if the affinity purified version did recognise a ~70kDa band, the panning of the antibody would not interfere with this process. A positive control of GST-HFL was also loaded onto the SDS-PAGE gels to ensure that both versions of the antibody would recognise the expressed full length willin protein.

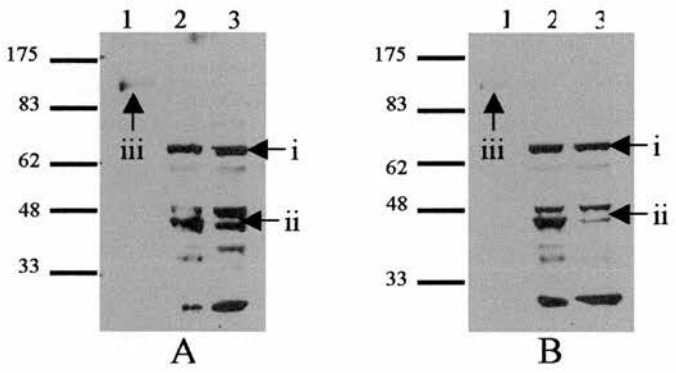

Figure 3.10. Comparison of unpanned and panned affinity purified 914^3 antibody. Blot A was incubated with a 1:1000 dilution of (unpanned) AP 914^3 antibody. Blot B was incubated with a 1:1000 dilution of panned AP 914^3 antibody. Lanes contain: (1) positive control, and equal amounts of (2) CHO cell lysate (3) SK-N-SH cell lysate.

Both the unpanned and panned versions of the AP 914[3] antibody were capable of visualising the ~70kDa band (figure 3.10, ←i). There is again a signal to be seen in the ~50kDa region (figure 3.10, ←ii), although in this western blot there are not one, but two, bands present here. In comparison with previous blots there is only a slight reaction from both antibodies with the GST-HFL positive control (figure 3.10, ←iii). However, this may be due to less positive control being used in all western blots at this stage; in previous blots too much positive control had been loaded, resulting in a very strong signal which covered most of the length of the lane.

3.3.9 Analysis of the presence of willin in soluble and insoluble cell fractions

The WCE method of extracting the cell contents proved helpful in recovering a signal from the ~70kDa band. However, it was still desirable to know if this band would be found in the membrane fraction or the cytoskeletal fraction upon lysis of the cells. The success of the WCE method (~ 5 minutes) (section 2.3.10) over the incubation/centrifugation method (~ 25 minutes) (section 2.3.9)suggested that it was imperative to take the lability of the protein into consideration in order to retain the ~70kDa signal.

In previous western blots, the cell samples had frequently undergone two or more freeze/thaw cycles and it was now believed that this may have contributed to the weakening or loss of the ~70kDa signal. Attempts were once again made to explore which fraction the ~70kDa band localised to, but on this occasion - and on all future occasions where western blots of this kind were performed - the number of freeze/thaw cycles was kept at less than two. The cells used in this experiment were CHO cells.

It was also necessary to confirm that panning the affinity purified version of the 914^3 antibody eliminated any cross-reaction with BSA. To confirm that the pAP 914^3 antibody did not cross-react with BSA, 1µg of BSA was included on the SDS-PAGE gel. The membrane was incubated with the pAP 914^3 antibody at a 1:500 dilution.

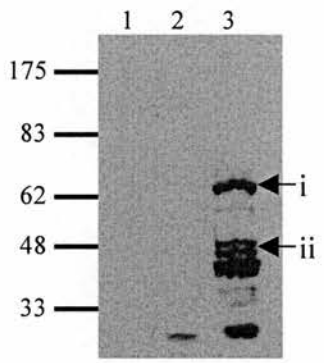

Figure 3.11. Examination of the location of the ~70kDa band in CHO cells after fractionation. The cross-reactivity of the pAP 914^3 antibody with BSA was also analysed. Lanes contain: (1) 1 µg BSA, and equal amounts of protein from (2) CHO cell supernatant (3) CHO cell pellet.

The western blot in figure 3.11 confirmed that the pAP 914^3 antibody does not cross-react with BSA. Also, since equal volumes of both pellet and supernatant were loaded, the implication from this western blot is that the majority of the protein constituting the ~70kDa band (figure 3.11, ←i) is to be found in the insoluble fraction in CHO cells. Three bands are now visible in the ~50kDa region (figure 3.11, ←ii).

A further western blot was performed in a similar manner to the above except that a further three cell lines were used to investigate the distribution of the ~70kDa band in the soluble and insoluble fractions, to see if the pattern of distribution seen in the

CHO cells was evident in other cells lines also. The western blot was performed using the pAP 914^3 antibody, again at a concentration of 1:1000.

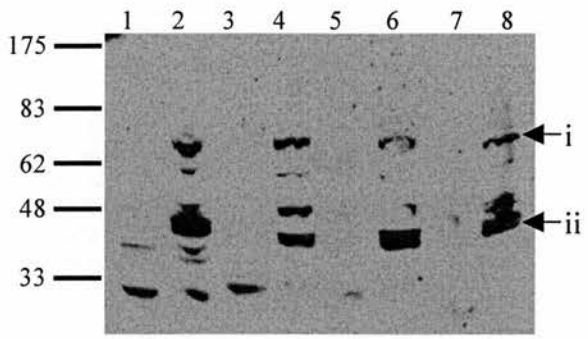

Figure 3.12. Analysis of the location of the ~70kDa band in four different cells lines after fractionation. The lanes were loaded with equal amounts of protein from either the supernatant [S] or the pallet [P] fractions of each cell line. Lanes contain: (1) CHO, S (2) CHO, P (3) COS, S (4) COS, P (5) HEK, S (6) HEK, P (7) SK-N-SH, S (8) SK-N-SH, P

In all four cell lines, all of the ~70kDa protein appears to be in the cytoskeletal fraction (figure 3.12, ←i). As before, although in varying numbers, bands are also obtained in the ~50kDa region and again the majority of these bands only appear in the cytoskeletal fraction (figure 3.12, ←ii).

3.3.10 Confirming the specificity of the bands detected by the 914^3 antibody

It was necessary to confirm that the bands that were being observed with all versions of the 914^3 antibody were due specifically to the primary antibody and not to the secondary antibody. Samples from CHO, HEK293 and COS7 cells were loaded in duplicate onto SDS-PAGE gels, along with a positive control, and transferred to nitrocellulose membrane after electrophoresis. The control membrane was probed with a 1:1000 dilution of the pAP 914^3 antibody followed by incubation with the secondary antibody at the usual concentration of 1:2000. The second membrane was

probed with the secondary antibody only, at a concentration of 1:2000. Both membranes were treated identically and were developed in the same cassette for the same length of time.

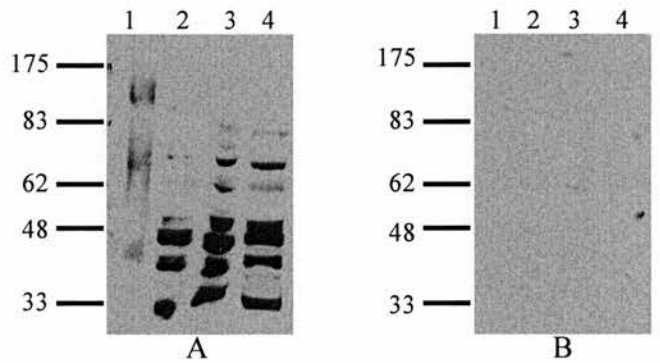

Figure 3.13. Comparison of western blots with and without primary antibody. Blot A was incubated with 1:1000 pAP 914[3] followed by 1:5000 anti-rabbit HRP antibody. Blot B was incubated with 1:5000 anti-rabbit HRP antibody only. Lanes contain (1) positive control, and equal amounts of protein from the pellets of (2) CHO cells (3) HEK cells (4) SK-N-SH cells.

Fig 3.13 shows that no bands were obtained when the secondary antibody alone is used, confirming that all the ~70kDa bands that have been detected in western blots were due specifically to the primary antibodies.

3.3.11 Peptide competition with the pAP 914[3] antibody

To provide further confirmation that the ~70kDa bands that had been observed on the western blots were due to the primary antibody, peptide competition was performed with the pAP 914[3] antibody. The first procedure used is described in section 2.2.17. Several different amounts of peptide were used to determine which peptide concentration would be ideal for saturating all the substrate binding sites of the primary antibody, thereby knocking out the signals obtained on the films. Four lanes on an SDS-PAGE gel were loaded with equal amounts of CHO cell extract and the

gel was transferred to a nitrocellulose membrane. At the stage in the procedure where the primary antibody was added in to each strip for a one hour incubation, the willin peptide was also added into the incubation mixture to a final concentration of 10μg/μl for the first strip, 50μg/μl for the second strip and 100μg/μl for the third strip. A fourth strip was incubated without any peptide as a control. The antibody used for all four membranes was a 1:1000 dilution of the pAP 914[3] antibody.

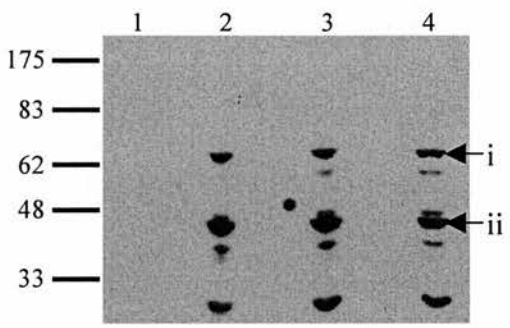

Figure 3.14. Peptide competition with the 18-amino acid willin peptide. Each of the four strips of nitrocellulose membrane contained an equal amount of protein from CHO cell pellets. The strips were incubated with a 1:1000 dilution of the pAP 914[3] antibody and (1) no peptide, and peptide to a final concentration of (2) 10μg/ml (3) 50μg/ml (4) 100μg/ml.

Unexpectedly, the result that was obtained in figure 3.14 was the reverse of what had been predicted. No signal was observed from the control membrane strip, even though this was the only strip where a signal was expected, since no peptide was present to interfere with the binding of the primary antibody. Conversely, all three of the strips that had been incubated in the presence of the willin peptide produced a signal.

Interestingly, the major signals arising from each strip were in the ~70kDa (figure 3.14, ←i) and ~50kDa (figure 3.14, ←ii) regions. The experiment was repeated but the same result was obtained.

Due to the unexpected results obtained when performing peptide competition with the putative native protein, the same experiments were then attempted using a known source of the willin protein i.e. purified GST-HFL fusion protein, as opposed to a speculative source of the willin protein i.e. extracts from the mammalian cells.

Furthermore, two different buffers were used: firstly, the PBS-gelatine-tween buffer (2.2.3 blocking buffer 1) that had been used in all western blots up until this point, and secondly a TBS-tween buffer (2.2.3 blocking buffer 2) that had not been used before. The TBS-based buffer was used as it was thought possible that the presence of the gelatine in the PBS-based buffer was causing the peptide to stick to the membrane.

Four strips of membrane containing identical amounts of purified GST-HFL were treated as follows: two of the strips were subjected to peptide competition in the PBS-based buffer and the other two strips were subjected to peptide competition in the TBS-based buffer. Of each of these pairs of strips, one of the pair was used as a control and was not incubated with any peptide and the other member of the pair was incubated with peptide to a final concentration of 100μg/ml. The results are shown in figure 3.15.

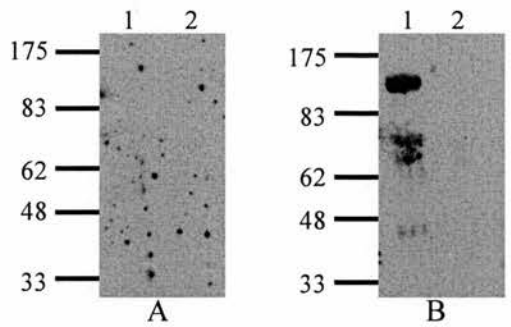

Figure 3.15. Peptide competition using the willin peptide, performed on the GST-HFL fusion protein. Two different buffers were used. Blot A = PBS-gelatine-Tween buffer. Blot B = TBS-Tween buffer. The pAP 914[3] antibody was used at a 1:1000 dilution in all cases. All lanes contain 0.3µg of purified GST-HFL protein. Lane (1) on each membrane was not incubated with any peptide. Lane (2) on each membrane was incubated with willin peptide (100µg/ml).

The film resulting from the peptide competition performed in the PBS-based buffer showed only background signals, indicating the unsuitability of this buffer for these experiments. However, the peptide competition that was performed in the TBS-based buffer was successful: a band corresponding to the purified GST-HFL protein appeared in the control lane but disappeared upon addition of 100µg/ml of willin peptide to the incubation solution. From this point on, all western blots were performed in TBS-based [gelatine-free] buffers.

3.3.12 Peptide and protein competition using the pAP 914[3] antibody

A further attempt was then made to perform peptide competition against the ~70kDa band that was observed in the mammalian cells lines. In addition to switching the buffer from PBS-based to the TBS-based solutions, two other factors were altered. These factors were: (1) alongside attempting to erase the ~70kDa band through peptide competition, an attempt was also made to achieve this outcome using purified full length willin, which should also be capable of saturating the pAP 914[3] antibody recognition sites and thereby prevent the antibody from adhering to the membrane,

and (2) the protocol of the experiment was altered to that of preincubating the primary antibody with the peptide/protein for 30 minutes at room temperature (section 2.2.18) - versus the previous method where no preincubation was used (section 2.2.17) - to allow time for the peptide/protein to saturate the antibody binding sites.

Equal amounts of CHO cell extracts were loaded in triplicate onto an SDS-PAGE gel and, after transfer to a nitrocellulose membrane, the membrane was divided into three pieces. The first piece was the control membrane, which was incubated with primary antibody alone. The second piece was incubated with a primary antibody + willin peptide mixture, where the final concentration of peptide used was 100μg/ml. The third piece was incubated with the primary antibody + willin protein mixture, where the amount of protein used was 20nM. In all three cases the amount of primary antibody used was a 1:1000 dilution of the pAP 914[3] antibody.

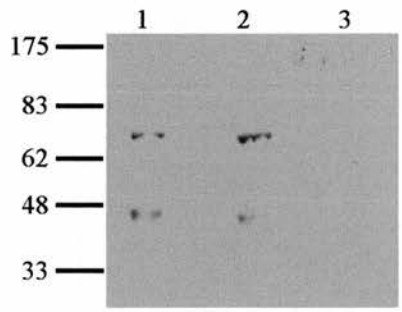

Figure 3.16. Peptide and protein competition with CHO cell extracts using a 1:1000 dilution of the pAP 914[3] antibody. Equal amounts of protein from CHO cell pellets were loaded into each lane. Lane (1) = control (2) pre-incubation with peptide (3) pre-incubation with protein.

Despite the success of the TBS-based buffer in peptide competition to cause the disappearance of the 98kDa GST-HFL band in figure 3.15, the same result was not achieved when mammalian cell extracts were used, as revealed in figure 3.16. However, success was achieved using the purified GST-HFL protein: it can be observed from this western blot that both of the bands that appeared in the control lane were caused to disappear when the primary antibody was pre-incubated with the GST-HFL protein, and so protocol 2.2.18 was used for protein/peptide competition from this point on.

3.3.13 Peptide and protein competition using the p914^3 antibody

Attempts were subsequently made at performing competition experiments using the non-affinity purified version of this antibody i.e. using the p914^3 antibody. It was not anticipated that a successful outcome would be pending from any peptide competition with this version of the antibody due to the failure of previous experiments with the pAP 914^3 antibody, since that antibody was itself a p914^3 derivative. However, it was hoped that the outcome of any experiments performed with the non-affinity purified version might provide some insight into the unexpected results that had been obtained with the affinity purified version. For example, if the affinity purified and the non-affinity purified versions of the antibody behaved in a conflicting manner, then the indication would be that the anomalies seen in figure 3.14 were perhaps somehow due to the process of affinity purification.

Both peptide and protein competition were therefore performed using the p914^3 version of the antibody in an identical manner to that used for the pAP 914^3 antibody. As before, three strips of membrane containing equal quantities of CHO cell extract

were used and the incubation methods were the same as those used for the pAP 914[3] experiments. The results are shown in fig 3.17.

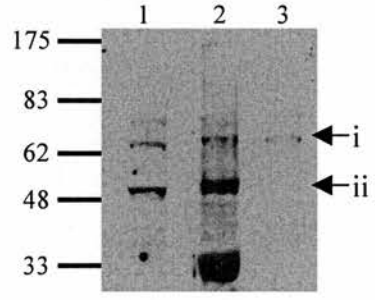

Figure 3.17. Peptide and protein competition with CHO cell extracts. Equal amounts of protein from CHO cell pellets were loaded into each lane. A 1:1000 dilution of the p914[3] antibody was used in each experiment. Lane (1) control (2) pre-incubation with willin peptide (3) pre-incubation with GST-HFL protein.

The results from the peptide competition assay using the p914[3] antibody are similar to those seen using the pAP 914[3] antibody: rather than decreasing the signal, the pre-incubation of antibody with peptide seems to actually cause an increase in the signal from not just that of the ~70kDa band but also that of the background bands contained in the lane. With regards to the protein competition, the ~70kDa band (figure 3.17, ←i) is not completely eradicated by the pre-incubation of the p914[3] antibody with the purified willin protein, although the density of this band has been reduced, whereas the ~50kDa band (figure 3.17, ←ii) does disappear under these conditions.

3.3.14 Protein competition using GST as the competing agent

The conclusion was drawn that whereas the p914[3] antibody could not be considered appropriate for detection of the presence of native willin in mammalian cell lines, the

successful outcome of protein competition experiments using the panned affinity purified version of the antibody (pAP 914[3]) indicated it may have a use for investigations into expression of the native protein. A final experiment was then performed with this antibody. To ensure that the disappearance of the ~70kDa and ~50kDa bands in figure 3.16 was caused by the willin part of the GST-HFL protein, and not by the GST headgroup of this fusion protein, protein competition was performed using purified GST as the sole competing agent.

Two strips of nitrocellulose membrane containing identical amounts of CHO cell lysate were incubated as follows: one of the strips was probed with a mixture of pAP 914[3] antibody + GST protein, a mixture which had been pre-incubated with gentle rotation for 30 minutes at room temperature. The control strip was probed with a solution that had been treated identically to the first mixture except that no GST protein was present. The strips were then subjected to enhanced chemiluminescence in the same cassette for the same length of time.

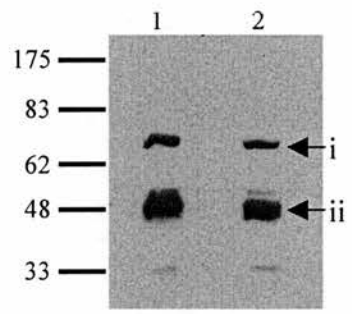

Figure 3.18. Protein competition with CHO cell extracts using purified GST. Equal amounts of protein from CHO cell pellets were loaded into each lane. A 1:1000 dilution of the pAP 914[3] antibody was used in each experiment. Lane (1) = control (2) pre-incubation with purified GST.

This western blot confirmed that pre-incubation of the pAP 914[3] antibody with purified GST had no effect upon the ability of this antibody to detect the ~70kDa (figure 3.18, ←i) and ~50kDa (figure 3.18, ←ii) bands. This indicates that, in the previous protein competition experiments with the GST-HFL protein, the disappearance of the ~70kDa band and other bands was solely due to the interference of the purified willin protein and was not caused by the GST moiety.

3.4.1 Characterisation of the antibody CK1

The second anti-willin antibody available was was named anti-chicken 1 and will henceforth referred to as the CK1 antibody. The CK1 antibody was analysed to ensure that it recognised purified willin protein and to see if it cross-reacted with BSA. Expressed GST-HFL willin and BSA were used in a western blot which was probed with the CK1 antibody at a 1:1000 dilution.

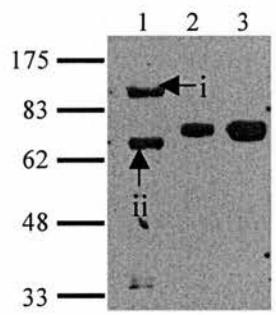

Figure 3.19. Preliminary analysis of the CK1 antibody, used at a dilution of 1:1000. Lanes contain (1) positive control (2) 1µg BSA (3) 2µg BSA.

The western blot in figure 3.19 showed that the CK1 antibody recognised purified willin. In lane 1, the upper band that appears at ~98kDa (figure 3.19, ←i) is the full length fusion protein GST-HFL. The band that appears underneath at ~70kDa (figure

3.19, ←ii) is likely to be the full length protein without the GST moiety, which has perhaps undergone mechanical cleavage.

However, this antibody also cross-reacted with BSA. The CK1 antibody was then panned in a similar manner to that used for the 914[3] antibody and further comparative western blots were performed using unpanned and panned CK1 each at a dilution of 1:1000.

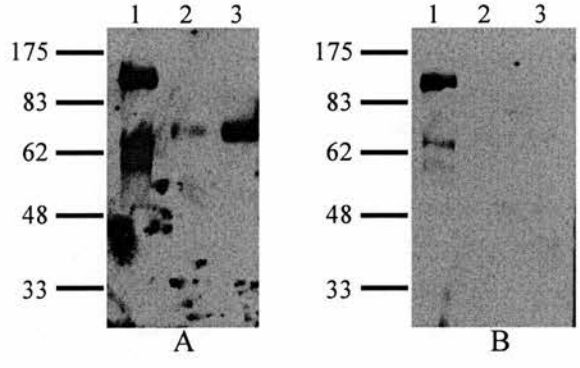

Figure 3.20. Comparison of unpanned and panned versions of the CK1 antibody. Blot A was probed with a 1:1000 dilution of unpanned CK1. Blot B was probed with a 1:1000 dilution of panned CK1 . Each blot contained: lane (1) positive control (2) 1μg BSA (3) 2 μg BSA.

It can be observed from the western blot in figure 3.20 that the panning of the CK1 antibody greatly diminishes the cross-reactivity of this antibody with BSA.

3.4.2 Characterisation of affinity purified CK1

The affinity purified version of the CK1 antibody was also available, and since the cross-reactivity of the panned CK1 antibody with BSA was minimised but not abolished, the affinity purified version of this antibody was then investigated. It was hoped that the additional purification step used in the preparation of affinity purified

antibodies would elicit an increase in the specificity of the antibody. A western blot was performed, again using bacterial lysates containing the expressed GST-HFL protein as a positive control and again BSA was included in the blot. The affinity purified CK1 antibody was used at a 1:500 dilution.

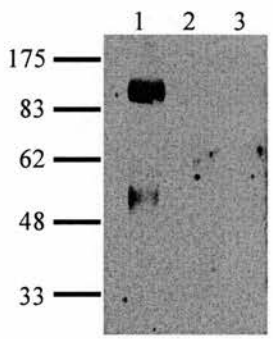

Figure 3.21. Analysis of the affinity purified CK1 antibody, used at a dilution of 1:500. Lanes contain (1) positive control (2) 1µg BSA (3) 2µg BSA.

The affinity purified CK1 antibody did not appear to react with BSA, as shown in figure 3.21, but was nonetheless panned as a precautionary measure. The antibody was panned as described in section 2.2.7 and the resulting antibody was referred to as pAP CK1 (panned Affinity Purified CK1). A western blot was then performed with the pAP CK1 antibody and the result is shown in fig 3.22.

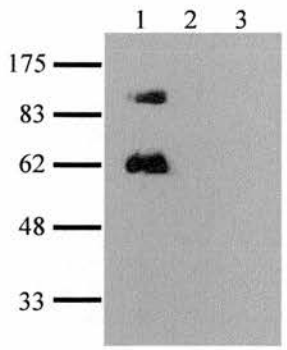

Figure 3.22. Analysis of the panned affinity purified CK1 (pAP CK1) antibody, used at a dilution of 1:500. Lanes contain (1) positive control (2) 1µg BSA (3) 2µg BSA.

No cross-reactivity with BSA was observed in this blot with the pAP CK1 antibody.

An attempt was then made to visualise the ~70kDa band in mammalian cell lines with the pAP CK1 antibody. The WCE protocol for lysing the cells was used. The membrane was incubated with the pAP CK1 antibody at a dilution of 1:1000.

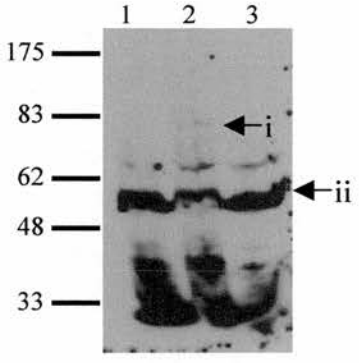

Figure 3.23. An attempt to visualise the ~70kDa band using the pAP CK1 antibody. The antibody was used at a concentration of 1:1000. The lanes contain equal amounts of protein from pellets of: (1) CHO cells (2) HEK cells (3) SK-N-SH cells.

A ~70kDa band is faintly visible in the HEK293 lane of this western blot (figure 3.23, ←i), although there is a much stronger signal from the ~50kDa bands (figure 3.23, ←ii).

3.4.3 Use of a new secondary antibody

To see if changing the anti-chicken secondary antibody that was used with the pAP CK1 antibody would help to produce clearer western blots, a new secondary antibody was tested. The secondary antibody that had previously been used was HRP-conjugated anti-chicken from Davids Biotechnologie and this antibody was now replaced with HRP-conjugated anti-chicken from Sigma.

The WCE method was used to obtain extracts of four different cell lines which were run on an SDS-PAGE gel and then transferred to nitrocellulose membrane. Several western blots were performed using differing concentrations of primary and secondary antibody. The optimal concentrations for this combination of antibodies were revealed to be 1:750 dilution of pAP CK1 antibody followed by a 1:20,000 dilution of the Sigma anti-chicken secondary antibody, as this produced the western blot shown in figure3.24.

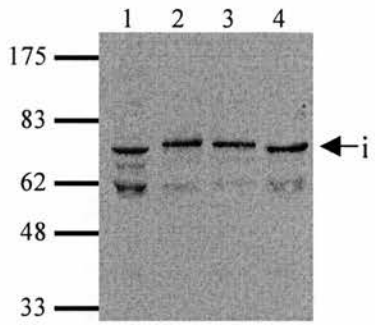

Figure 3.24. An attempt to enhance the signal from the ~70kDa band using the pAP CK1 antibody. A 1:750 dilution of the antibody was used for this western blot and a new secondary antibody was also used. Lanes contain equal amounts of protein from the pellets of (1) CHO cells (2) COS cells (3) HEK cells (4) SK-N-SH cells.

The use of the Sigma secondary antibody did produce a much clearer band in the ~70kDa region (figure 3.24, ←I), with much less background signal than those that had been obtained with the Davids Biotechnologie antibody. Notably, however, there is no visible evidence of the ~50kDa band in any cell extract.

To confirm that the bands visible in figure 3.24 were the result of post-immunisation antibodies, a western blot was performed using the available preimmune serum from the animal that produced the CK1 antibody. A western blot using secondary antibody only was also performed.

Cell lysates were loaded in triplicate onto SDS-PAGE gels and transferred to nitrocellulose membranes following electrophoresis. The first membrane was incubated with a 1:750 dilution of the pAP CK1 antibody, the second membrane was incubated with a 1:750 dilution of the CK1 preimmune serum and the third membrane was incubated with no primary antibody. All three membranes were then incubated with equal amounts of secondary antibody (1:20,000 Sigma HRP-conjugated anti-

chicken). The three membranes were exposed to the same film for the same length of time.

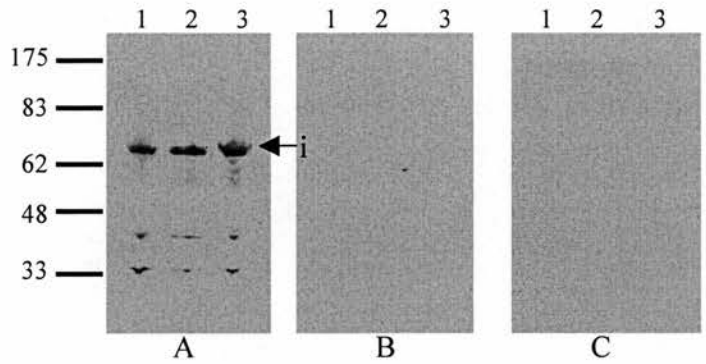

Figure 3.25. Confirmation of the specificity of the pAP CK1 antibody. Blot A was incubated with a 1:750 dilution of pAP CK1, blot B was incubated with a 1:750 dilution of preimmune serum and blot C was incubated with secondary antibody only. Lanes contain equal amounts of protein from the pellets of (1) CHO cells (2) HEK cells (3) SK-N-SH cells.

Figure 3.25 shows that no bands could be seen on the preimmune blot that equated to the ~70kDa bands (figure 3.25, ←i) that appeared on the pAP CK1 blot. Also, no bands could be seen on the blot that was incubated with secondary antibody only. These results indicate that the ~70kDa bands detected by the pAP CK1 antibody were due specifically to antibodies arising from the immunisation process. Time constraints prevented any further analysis of the pAP CK1 antibody such as protein or peptide competition.

3.5 Conclusions

A band corresponding to the predicted size of human willin (~70kDa) has been discovered in several different mammalian cells lines by two independent antibodies, pAP 914^3 and pAP CK1. The ~70kDa band cannot be visualised by either the anti-rabbit nor the anti-chicken secondary antibodies alone. The ~70kDa band does not result from any antibodies present in either of the preimmune sera taken from the animals that produced the antibodies. The band can be observed in CHO, COS7, HEK293 and SK-N-SH cells and is always in the insoluble fraction. Either one or more bands in the size region of ~50kDa also are frequently, but not always, detected with the two aforementioned antibodies.

The antibodies 914^3 and CK1, and all their derivatives, recognise a purified fusion protein that contains human willin. The antibodies 914^3 and CK1 cross-react with BSA. A combination of affinity purification and panning of the antibodies using BSA-conjugated sepharose beads leads to the abolition of detectable cross-reaction with BSA.

Peptide competition with the $p914^3$ and pAP 914^3 antibodies has been unsuccessful for unknown reasons, but better results were obtained with protein competition. A purified protein containing GST fused to human willin was used in protein competition experiments. Of the two bands that were regularly detected by the $p914^3$ antibody, the ~50kDa band was successfully eliminated by protein competition but the ~70kDa band was not. Of the two bands that were regularly detected by the pAP 914^3 antibody, both the ~50kDa and ~70kDa bands were eradicated by protein

competition and the disappearance of the bands was specifically due to the willin sequence of the fusion protein.

The two antibodies that have been identified as the most appropriate for use in detecting native willin are pAP 914[3] and pAP CK1. The recommended dilutions for these antibodies in western blot experiments are approximately 1:750 pAP CK1 (followed by 1:20,000 Sigma HRP-conjugated anti-chicken) and 1:1000 pAP 914[3] (followed by 1:2000 Upstate HRP-conjugated anti-rabbit).

3.6 Chapter 3 Discussion

3.6.1 PCR screening

The initial attempt at finding the native willin protein involved screening a library for the gene using the PCR, which was unsuccessful due to a cross reactivity of the primers used with areas of *E.coli* DNA. However, this does not preclude the possibility that such a method could be successful if different primers were used and could therefore perhaps form the basis of some future work.

3.6.2 Western blots with 914^3-based antibodies

The first western blot that was performed using the 914^3-based antibody (section 3.3.2) revealed a doublet. At the time, this was taken as a indication that the native protein had been perhaps been detected, the doublet possibly corresponding to phosphorylated and unphosphorylated forms of the protein: Alfthan et al (2004) observed, in the case of merlin, the migration of triplet forms of the protein. The authors concluded that these forms were hyperphosphorylated, phosphorylated and hypophosphorylated forms, and demonstrated the loss of the hyperphosphorylated band following treatment with PKA inhibitor H89. In retrospect, however, it is likely that the doublet in figure 3.2 was actually composed of BSA at 66.5kDa and the putative native protein at ~70kDa, because once the BSA problem was eradicated, the doublet in the ~70kDa region changed to a single band.

The emergence of another band, at ~50kDa, in the western blot in figure 3.4 was an interesting result as not only had a 50kDa isoform of ezrin been discovered, but bioinformatics data also indicated that willin itself had several differently sized

isoforms. However, the blot performed with the preimmune serum shown in figure 3.4 also produced a band - albeit a fainter one - in the ~50kDa region. The detection of the ~50kDa band could therefore not be regarded as as valid a result as the detection of the ~70kDa band. So although the ~50kDa band continued to be monitored alongside the ~70kDa band, the primary focus of the experiments remained centred on the ~70kDa band.

The cross-reaction of an antibody with a non-target protein can result from the target and non-target proteins sharing only a very small amount of peptide sequence. An amino acid alignment, shown in Appendix III, revealed that two sequences, each of three amino acids, were identical in both BSA and human willin, which is believed to be the cause of the cross-reactivity. Washing the cells three times or more eliminated the band, believed to be BSA, that appeared when the cells were washed only once (figure 3.6), and panning the antibodies eradicated, as shown in figure 3.7 for example, any detectable ability of the p914[3] antibody to cross-react with 2μg of BSA. Together, these results implied that the chances of BSA continuing to contaminate the Western blots in the ~70kDa region were very low.

The three related cells lines - REP, RPEc5 and RPEc5TCL1 - shown in the western blot in figure 3.8 were analysed to see if there was any evidence that willin was upregulated or downregulated in irradiated or cancerous cells. The blot in figure 3.8 indicates that there may in fact be a downregulation of the ~70kDa band in the tumorous cells compared to the normal cells, which was of interest as research external to this laboratory had shown that willin was downregulated in certain types of head and neck cancers (Prof Mike Prystowsky, Albert Einstein College of

Medicine, New York; pers. comm.). It is unknown whether the other bands that are apparent on this (figure 3.8) and other western blots are just background bands, or breakdown products, or are isoforms of willin (or possibly a mixture of the three); but if other isoforms of the protein are present on these western blots, then figure 3.8 may show not just the downregulation of willin (lane 3 versus lane 1, ←i), but also possibly the upregulation of another isoform (lane 3 versus lane 1, ←iii).

The ability of the WCE lysis method to produce stronger ~70kDa bands than the centrifugation lysis method is believed to be due to the decrease in time taken to lyse the samples. At the time these experiments were performed, evidence for the lability of the protein had not yet accumulated, but there are now many indications that the protein is extremely susceptible to factors such as proteolytic attack or mechanical shearing. Firstly, the strength of the bands obtained by the WCE method usually had an increased intensity compared to those obtained by the centrifugation lysis method, the latter being a method of extraction that took around five times as long as the former to complete. Freeze/thawing the samples, even minimally, was also eventually revealed to be detrimental. Additionally, it was either very difficult or impossible to express the N-terminus of the protein (sections 5.3.5 - 5.3.7) due to, certain evidence suggests, the breakdown of the expressed proteins. When the expression of willin was eventually attained, it was in the form of the full length protein, which is believed to have offered increased protection against, for example, proteolytic attack, yet which still appeared to be quite labile, due to the trail of suspected breakdown products that appeared underneath the full length fusion protein (section 5.3.9, figure 5.8).

The detection of two bands in the ~50kDa region in the western blot shown in figure 3.10, versus only one ~50kDa band in, for example, figure 3.9, is possibly due to an increased resolution on the SDS-PAGE gel (by running it further). Or it may be due to the use of different versions of the antibody: the non-affinity purified version of the antibody was used in figure 3.9 and the affinity purified version was used in figure 3.10.

The appearance of the ~70kDa band in the CHO cell pellet, but not at all in the CHO cell supernatant, in the blot shown in figure 3.11 was somewhat unexpected: although experiments elsewhere in this thesis (section 5.3.10) had shown that an expressed GST fusion protein containing full length willin was almost completely insoluble and was therefore, prior to solubilisation, only to be found in the cell pellet, it was known that the other members of the ERM family exist, when in inactive form, as a soluble pool in the cytoplasm (Gary et al, 1995). However, neither the blot shown in figure 3.10, nor any subsequent blots performed with the pAP 914^3 antibody, gave any indication that the ~70kDa band was present in the cytoplasm. Additionally, western blot analysis of cells transfected with the EGFP-tagged willin N-terminus revealed that in two different cell types, the N-terminus localises to the cell pellet (sections 4.3.7 and 4.5.2); although the ERM proteins' first actin-binding domain was revealed to be in the C-termini of the proteins, an N-terminus binding site has also been identified [Roy et al, 1997]). Also, figure 3.12 showed that the situation was not particular to CHO cells only and that, in four different cell lines, the antibody detected ~70kDa and ~50kDa bands in only the insoluble fractions.

The fact that the other bands that appear on blot 3.12 are also in the cell pellet only, and are therefore behaving in a manner similar to the putative native protein (the ~70kDa band), and to the GST fusion protein containing full length willin, and to the EGFP-tagged N-terminus of the protein, lends some support to the possibility that these extra bands are not just background signals but are possibly isoforms of the protein; however, they could also be breakdown products.

The presence of yet another band in the 50kDa region - three bands in figure 3.11 versus only two bands in figure 3.10 - may be due, as stated previously, to an increased resolution of the SDS-PAGE gel. An additional possibility is that as evidence continued to amass that indicated the lability of the protein, more care was taken in the extraction procedure and it is noted that prior to performing the blot in figure 3.11, the number of freeze/thaw cycles was kept to a minimum. If isoforms of the protein do exist that are equally as labile as the full length protein, keeping the number of freeze/thaw cycles as low as possible may have resulted in an increased number of isoforms being detected.

3.6.3 Peptide and protein competition with 914^3-based antibodies

Several inconsistencies resulted from the peptide and protein competition experiments. For example, using the pAP 914^3 antibody, peptide competition was successful in eradicating a band representing the full length purified GST fusion protein (figure 3.15), but unsuccessful in eradicating the ~70kDa band corresponding to the putative native protein (figure 3.16). And although peptide competition did not eliminate the ~70kDa band, protein competition did (figure 3.16). Furthermore, the peptide actually increased, rather than decreased, the signal from the ~70kDa and

~50kDa areas of the membrane that was being subjected to peptide competition (figure 3.16). And finally, only the ~50kDa band detected by the p914[3] antibody, but not the ~70kDa band detected by this antibody, could be eradicated by protein competition (figure 3.17).

The reason for the ability of the peptide to enable the elimination of the band representing the GST-HFL fusion protein, but not the bands representing the putative native protein, is unknown. The peptide used in these experiments had been synthesised several years previously and it is possible that it was now too old to be used in any experiments.

With regards to the peptide competition experiments that were performed using the purported native protein, it is perhaps significant that the two areas of the membrane that gave the strongest signal - and which conversely should have given the weakest signal - are the ~70kDa and ~50kDa regions (figure 3.14). Other molecular biological techniques rely on the ability of proteins or peptides to adhere to nitrocellulose membrane when used in an incubation buffer. Such a case in point is the protein lipid overlay procedure described in section 5.3.18. In these types of experiments, lipid-spotted membranes are incubated overnight with a protein-containing solution, during which time the protein is expected to bind to the membrane at the positions where any lipid with which the protein has an affinity is spotted.

It seems possible, therefore, that since the ERM proteins are known to have an affinity for themselves via an intramolecular interaction (section 1.3.6), the addition

of a fragment of the willin protein into an incubation buffer which is then used to incubate a membrane containing the putative whole protein could in fact lead to the peptide, and in turn the antibodies, adhering to those positions on the membrane where the putative protein and any of its isoforms are located. A similar event might have occurred when incubating the membrane with the purified fusion protein, but the size of the fusion protein (98kDa) may have caused it to be washed away during the wash steps whereas the smaller size of the peptide allowed it to continue to adhere to the membrane. If the peptide is actually sticking to the ~70kDa and ~50kDa proteins on the membrane and thereby increasing the signal from these bands, it is possible that under different conditions, such as alteration of the constituents of the incubation buffer, the peptide would no longer adhere to the membrane.

The elimination of the ~70kDa band via peptide competition has been achieved by another laboratory (Prof. Mike Prystowsky, Albert Einstein College of Medicine, New York; pers.comm.). The concentration of peptide used to obtain this result was a final concentration of 500µg/ml and it may also be relevant that a new batch of the peptide was synthesised for that experiment. Such a concentration was never used during any of the experiments described in this chapter, which used a maximum of 100µg/ml. This is because several sources were consulted as to how to perform the experiments and no source recommended using more than a final concentration of 100µg/ml because, according to these sources, at concentrations above 100µg/ml, any peptide will begin to affect any antibody.

The possibility also exists that the peptide competition failed because the bands correlating to the putative native protein are not in fact willin. However, bands

corresponding to the putative native protein were successfully eradicated using a purified willin protein preparation and the success of this competition was shown to be unconnected to the GST headgroup of the fusion protein.

However, although protein competition successfully eliminated both the ~70kDa and ~50kDa bands that resulted from the use of the pAP 914^3 antibody, for unknown reasons only the ~50kDa band detected by the $p914^3$ antibody could be eliminated by this method (figure 3.17). Due to this and other incongruities revealed during these protein and peptide competition experiments, further work in this area is warranted. An ideal starting point would be to firstly synthesise a new batch of the peptide and, following this, similar competition experiments to those mentioned in this chapter could be performed with both the pAP 914^3 and pAP CK1 antibodies.

3.6.4 Western blotting with CK1-based antibodies

The pAP CK1 antibody was not examined as extensively as the $p914^3$ antibody. As the experiments in this chapter were performed sequentially, most work was done on the 914^3 antibody since it was the first antibody available. However, the pAP CK1 blots shown in figure 3.22 reveal very little background bands compared to those that frequently resulted from the use of the pAP 914^3 antibody (eg figure 3.10 although, as mentioned previously, these background bands may in fact be isoforms of willin). No bands were detected by the corresponding preimmune serum, nor by the secondary antibody alone, and this antibody may eventually prove to be the superior of the two anti-willin antibodies.

Although a band of ~70kDa could be reproducibly detected by both the pAP 914^3 and pAP CK1 antibodies, the most conspicuous difference between the blots resulting from the two different antibodies was the lack of bands in the ~50kDa region on the pAP CK1 blots, although possibly a band would reappear with slight modifications of antibody concentrations. If the ~50kDa bands are eventually revealed to be willin isoforms then it would perhaps be desirable to have an antibody that could detect these isoforms and so the pAP 914^3 antibody would be favoured in such circumstances; whereas if these bands are simply background signals then the pAP CK1 antibody would be the preferred candidate for future western blots and similar experiments.

Note: Subsequent to the completion of the labwork for this thesis, the SK-N-SK cells were found to be contaminated with other cells. This contamination was traced back to several months before my research with this cell line began; therefore any experiments in this chapter and others which included SK-N-SH cells were potentially performed with contaminated SH-N-SH cells. I accepted these cells in good faith and, having only ever worked with the contaminated form of these cells, was never aware of any differences in morphology, etc., that otherwise might have alerted me to the problem.

Chapter 4: Imaging of the subcellular targeting of willin in mammalian cell lines using enhanced green fluorescent protein (EGFP) fusion proteins.

4.1 Aims:

- Investigation into the subcellular location of willin-EGFP fusion proteins in RPE, CHO, COS7, HEK293 and SK-N-SH cells.
- Comparison of the targeting of the full length protein versus that of the N-terminus and C-terminus of the protein.
- Examination of the effect of the expression of the tagged proteins on cell morphology.

4.2 Introduction

Members of the ERM family are known to play a role in membrane-cytoskeletal interactions (section 1.3.6) and to localise to actin-rich cell surface structures such as microvilli and filopodia (section 1.2.5). It was anticipated that willin may play a similar role and that this hypothesis could be examined with fluorescence microscopy using enhanced green fluorescent protein (EGFP) and phalloidin, a fungal toxin that causes the actin cytoskeleton to fluoresce (reviewed in Cooper et al, 1987). Several plasmids were constructed using the vector pEGFP-N1, which produces fusion proteins that contain EGFP at the C-terminus of the protein of interest. This type of fusion protein was desirable, since if the EGFP was at the N-terminus of the protein, it could interfere with the targeting of the protein of interest.

The first plasmid contained full length human willin fused to EGFP (pHFL-EGFP). The second construct contained the human willin N-terminus alone fused to EGFP (pNW-EGFP) and the third contained the willin C-terminus alone fused to EGFP (pCW-EGFP). The purpose of dividing the protein into its constituent halves for fluorescence imagery was twofold. Firstly, it would be expected that the intact protein would behave in a different manner to the N-terminus or C-terminus alone and a notable difference in the pattern of localisation between the three constructs would serve to validate any results observed with the full length protein. Secondly, any loss of function observed following the transfection of the constructs containing only the N- or C-terminus would indicate a role for the terminus that was absent.

For the construction of each of the plasmids shown below, primer and DNA sequences are contained in Appendices I - III. In each of the fluorescence microscopy pictures shown below, the abbreviations Rc, Gc and Bc will be used to indicate which channels are switched on for that particular image, where Rc is the red channel only, Gc is the green channel only, RGBc is all three channels, RGc is the red and green channels only, and so on. Photographs were taken on 63x magnification.

4.3.1 Construction of the plasmid pHFL-EGFP

Two oligonucleotide primers were designed which would anneal to the 5' and 3' end of the template DNA pIMAGE and enable the amplification of the willin sequence with the addition of novel restriction enzyme sites (figure 4.1). The forward primer was NW GFP F, which added an EcoRI site to the 5' end of the sequence adjacent to the first codon. The reverse primer was CW GFP R, which added a BamHI site to the 3' end of the sequence.

The primers were used to amplify the full length sequence of the human willin gene. The amplified fragment and the pEGFP-N1 vector were digested with the restriction enzymes EcoRI and BamHI, ligated and transformed into competent DH5α *E.coli* cells. Several of the resulting colonies were analysed for their plasmid content. Positive clones were initially identified by analysing the size of the band produced on an agarose gel following restriction enzyme digests.

To check that the plasmid DNA from the positive clones contained the pHFL-EGFP construct, the DNA from one of the positive clones was analysed by automated sequencing. The results from the sequencing confirmed that the full length willin gene had been cloned into the pEGFP-N1 vector.

The primer and DNA sequences used for the construction of each plasmid are contained in Appendices I – III.

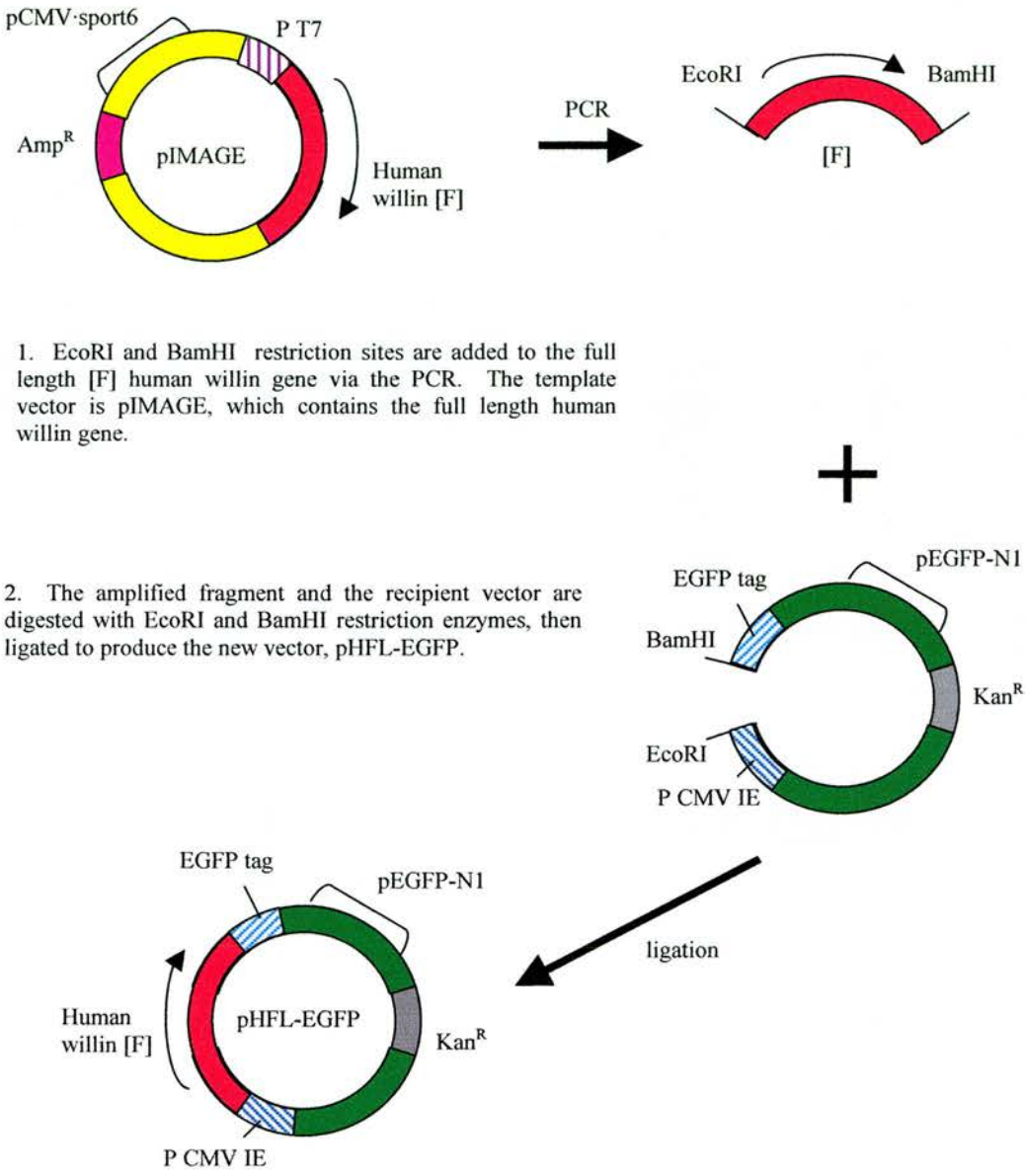

Figure 4.1. Construction of the expression vector pHFL-EGFP, which contains the full length [F] human willin gene. p = plasmid, P = promoter.

4.3.2 Construction of the plasmid pNW-EGFP

Two oligonucleotide primers were designed which would anneal to the N-terminus of the IMAGE clone and enable the amplification of this part of the gene with the addition of novel restriction enzyme sites (figure 4.2). The forward primer was NW GFP F, which added an EcoRI site to the 5' end of the sequence. The reverse primer was NW GFP R, which added a BamHI site to the 3' end of the sequence.

Positive clones were identified by restriction enzyme digests and subsequently confirmed by automated DNA sequencing.

The primer and DNA sequences used for the construction of each plasmid are contained in Appendices I - III.

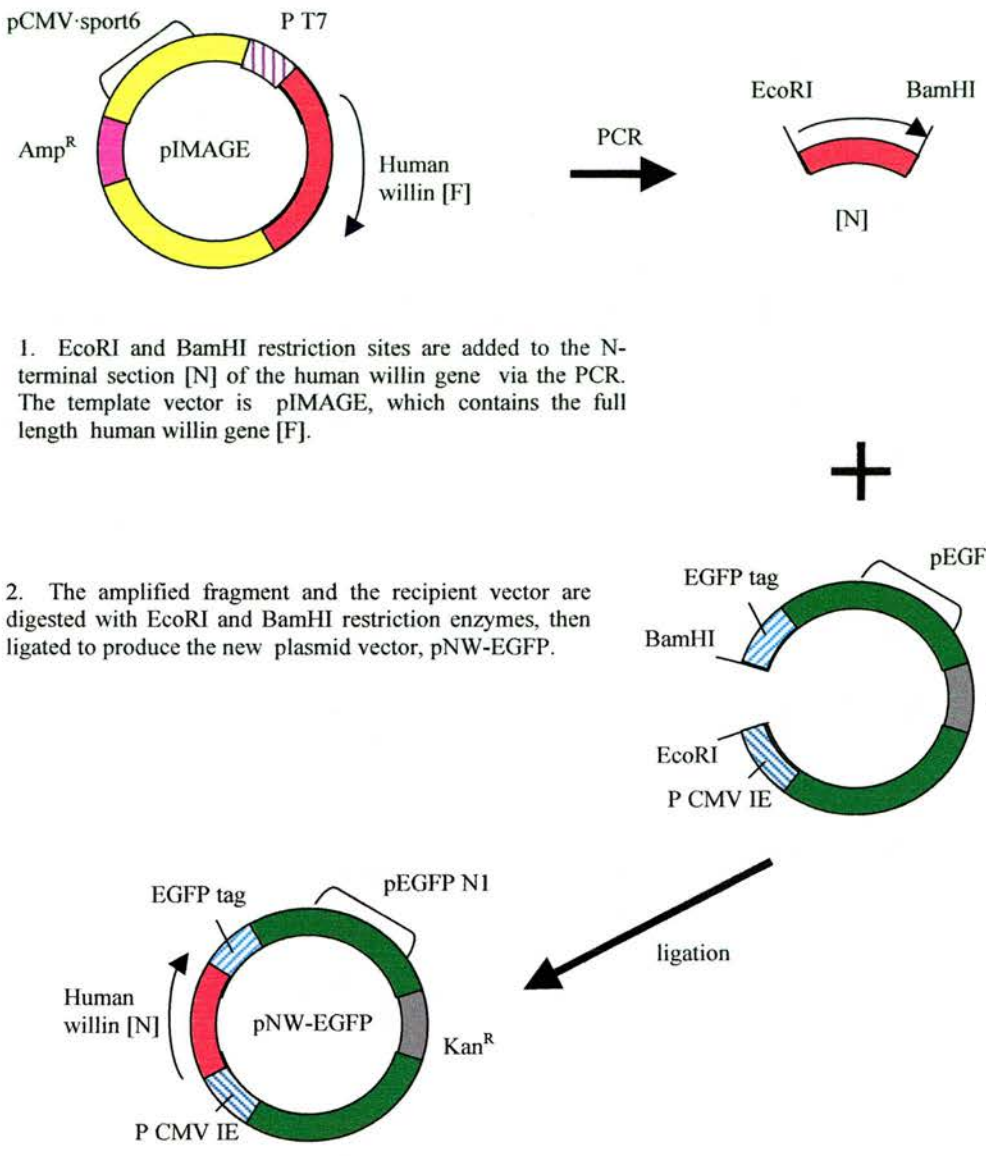

1. EcoRI and BamHI restriction sites are added to the N-terminal section [N] of the human willin gene via the PCR. The template vector is pIMAGE, which contains the full length human willin gene [F].

2. The amplified fragment and the recipient vector are digested with EcoRI and BamHI restriction enzymes, then ligated to produce the new plasmid vector, pNW-EGFP.

Figure 4.2. Construction of the expression vector pNW-EGFP, which contains the N-terminal section [N] of the human willin gene. p = plasmid, P = promoter.

Two oligonucleotide primers were designed which would anneal to the C-terminus of the IMAGE clone and enable the amplification of this part of the gene with the addition of novel restriction enzyme sites (figure 4.3). The forward primer was CW GFP F, which added an EcoRI site to the 5' end of the sequence. The reverse primer was CW GFP R, which added a BamHI site to the 3' end of the sequence.

Positive clones were identified by restriction enzyme digests and subsequently confirmed by automated DNA sequencing.

The primer and DNA sequences used for the construction of each plasmid are contained in Appendices I – III.

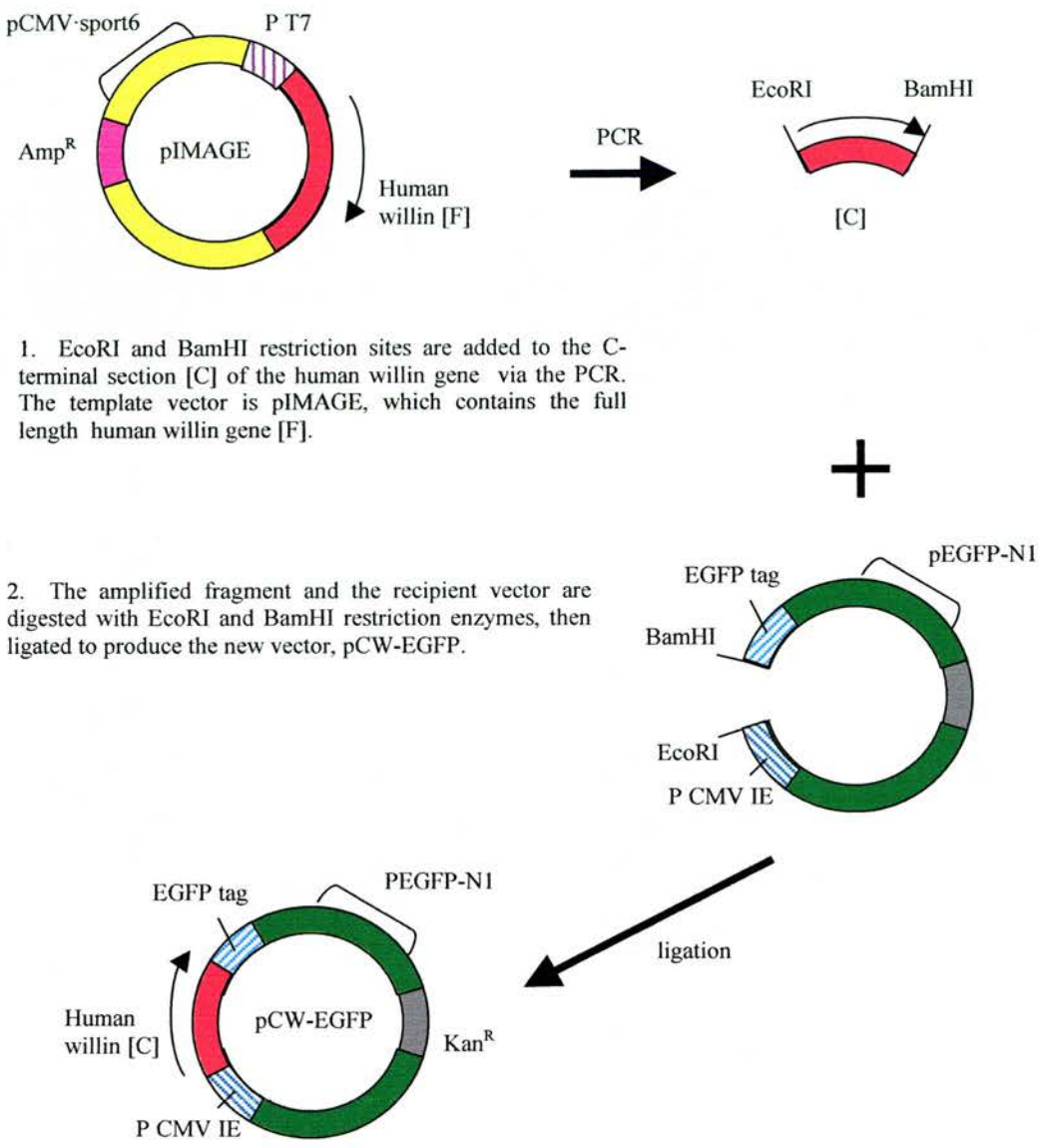

Figure 4.3. Construction of the expression vector pCW-EGFP, which contains the C-terminal section [C] of the human willin gene. p = plasmid, P = promoter.

4.3.4 Transfection of pHFL-EGFP and pEGFP-N1 into SK-N-SH cells

Willin was first isolated from neuronal tissue (cerebellum and sciatic nerve; FGM, pers. comm.), therefore SK-N-SH neuroblastoma cells were judged to be a good starting point to perform preliminary experiments. After transfecting a batch of these cells (section 2.3.7) with the pHFL-EGFP construct containing the full length willin gene, the cells were left for approximately 24 hours and then fixed, during which process the actin cytoskeleton was stained with phalloidin according to the method described in section 2.3.8. A different set of cells was transfected with the pEGFP-N1 vector as a control. The results are shown in figure 4.4.

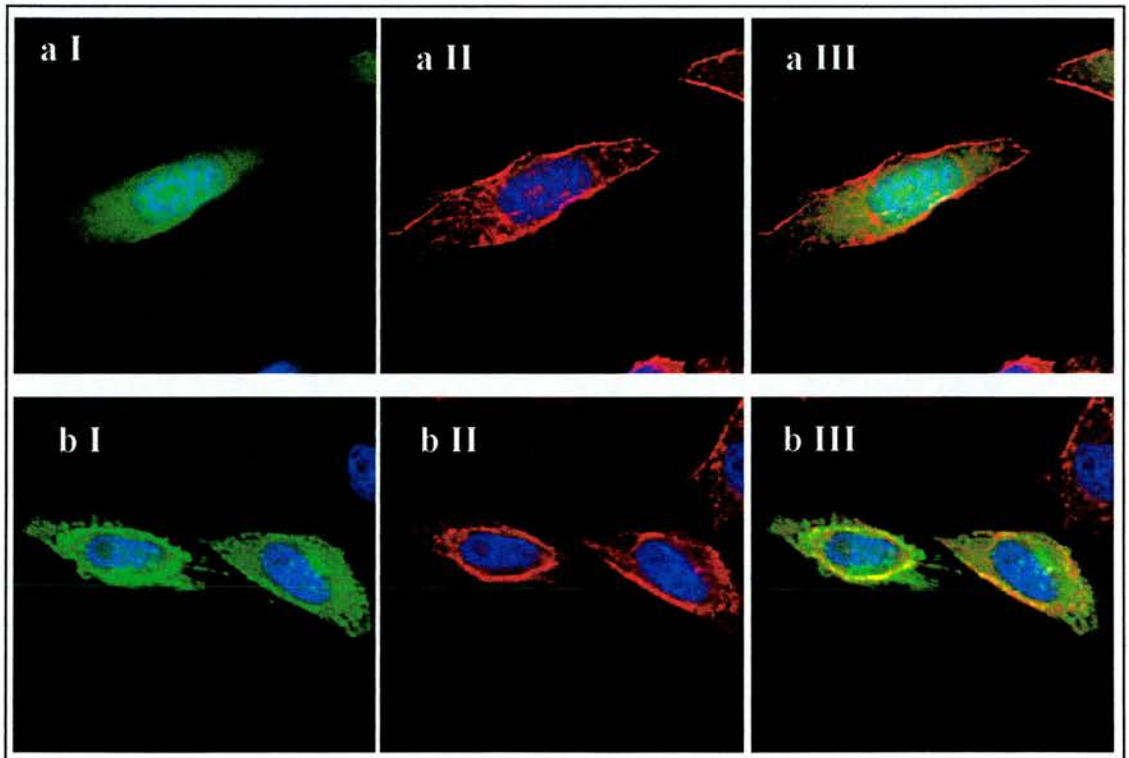

Figure 4.4. Transfection of pEGFP-N1 and pHFL-EGFP into SK-N-SH cells. (a) pEGFP-N1 (b) pHFL-EGFP. I – RGc, II – RBc, III - RGBc. Red – actin, blue – nuclei.

Figure 4.4 shows that the control construct pEGFP-N1 exhibited a different pattern of distribution to the willin-containing construct pHFL-EGFP. The green fluorescence in figure 4.4aI shows a typical random EGFP distribution. There is no thickened boundary of green fluorescence around the outside of the cell to indicate that the EGFP protein localises to the membrane of the cell. This contrasts with the localisation pattern shown in figure 4.4bI, where it can be seen that the willin-EGFP fusion protein localised to the cell membrane and to the cytoplasm, within which discrete points of expression can be observed.

The actin cytoskeleton is also shown in figures 4.4aII and 4.4bII, and, whereas the distribution of willin in the cell pictured in 4.4bI closely mirrors the distribution of actin around the outside of the same cell in shown in figure 4.4bII, there is no corresponding similarity to be seen with the distribution of EGFP 4.4aI and actin 4.4aII. Finally, the colocalisation of green fluorescence with red fluorescence produces an orange/yellow colour; the yellow fluorescence evident in 4.4bIII, but not in 4.4aIII, indicates again that EGFP-tagged willin colocalises with actin but EGFP alone does not.

4.3.5 Transfection of pNW-EGFP and pCW-EGFP into SK-N-SH cells

Another transfection experiment was performed, this time using the constructs pNW-EGFP and pCW-EGFP. The purpose of this experiment was to examine any differences between the distributions of the full length fusion protein versus that of the N- and C-terminus fusion proteins. Each of the three dishes of cells was transfected with the same amount of DNA according to the process described in section 2.3.7 and treated under exactly the same conditions during the fixing process.

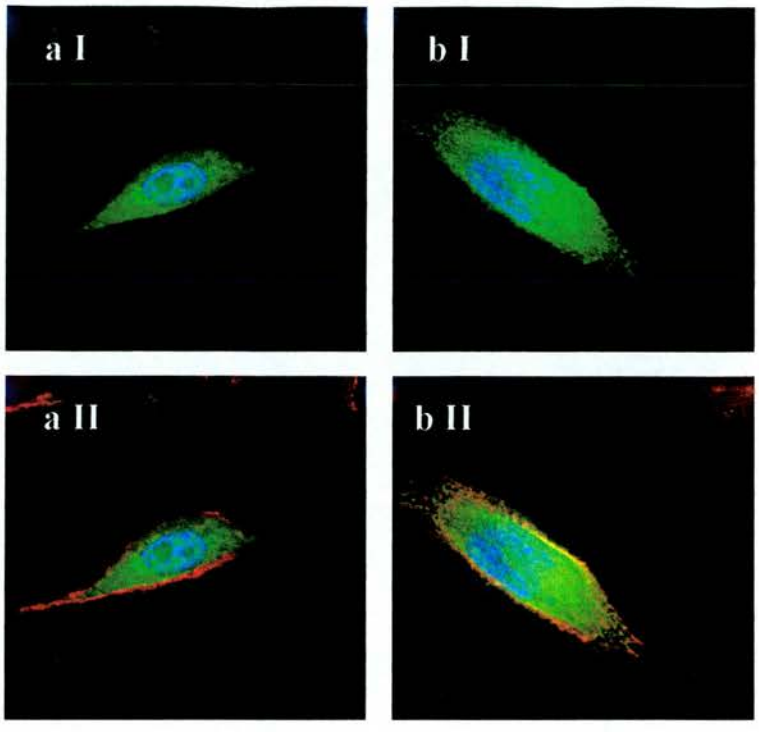

Figure 4.5. Transfection of willin N- and C-termini into SK-N-SH cells. (a) pNW-EGFP (b) pCW-EGFP. I – GBc, II – RGBc. Red – actin, blue – nuclei.

As with the pEGFP-N1 construct, the cells shown in Figures 4.5aI and bI show that the lack of either the N- or the C- terminus results in a pattern of distribution that differs from that seen with the full length protein. The thickened green boundary around the cells transfected with pHFL-EGFP, shown in the previous figure, 4.4bI, is not as strongly evident in figure 4.5aI and bI i.e. the cells transfected with the N- or C-terminus of willin,.

Transfection with the pNW-EGFP construct appeared to abolish the ability of willin to colocalise with actin, as implied by the lack of yellow fluorescence in figure 4.5aII. However, figure 4.5bII shows that transfection with the pCW-EGFP construct, whilst somewhat diminishing the appearance of willin-actin colocalisation, does not appear

to completely eradicate it: a degree of yellow fluorescence is still visible when this construct is expressed.

4.3.6 The effect of cytochalasin D

The chemical cytochalasin D disturbs the structure of the actin cytoskeleton of a cell by inhibiting the polymerisation of actin filaments (reviewed in Cooper et al, 1987). If willin is a membrane-cytoskeletal linker protein, then the perturbation of the actin cytoskeleton of a cell should also result in the disruption of the distribution of willin, possibly in a manner where the distribution of one closely mirrors that of the other. To investigate further the role of willin and actin, several transfections were performed as before, using all three constructs. Immediately prior to the fixing process, cytochalasin D was added to a final concentration of 10mM for 60 minutes. The cells were then fixed and viewed as normal (figure 4.6).

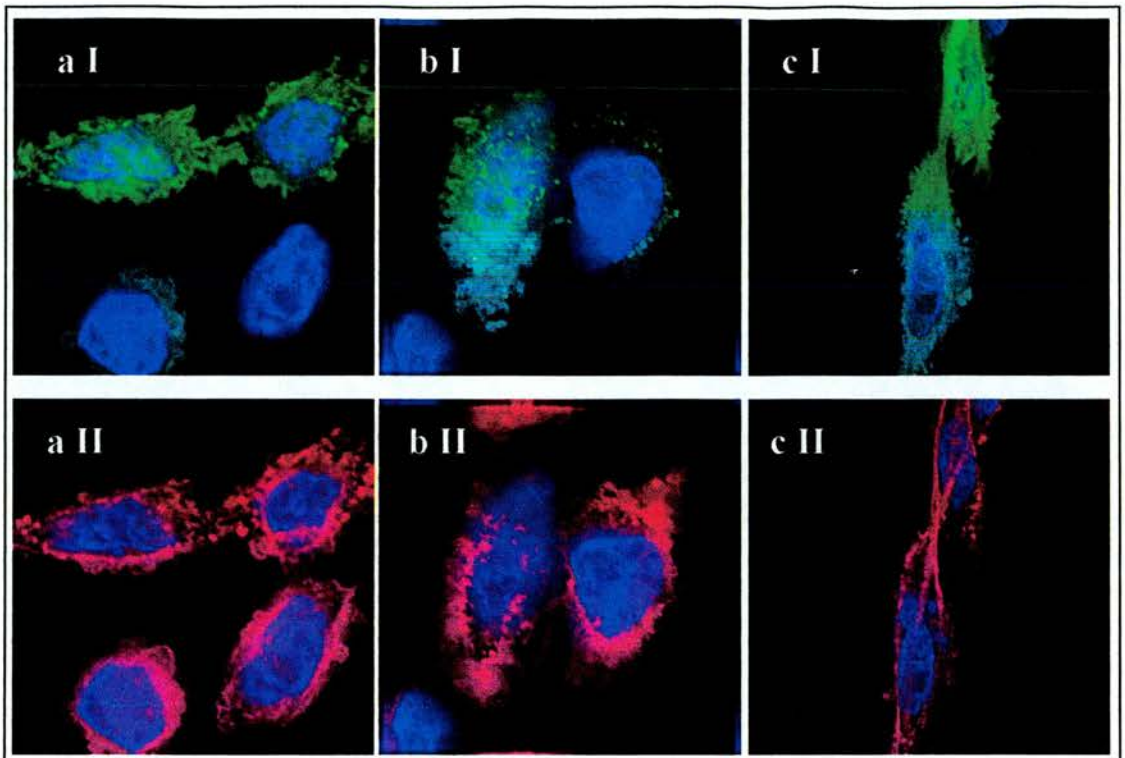

Figure 4.6. Transfection of EGFP tagged full length willin and willin N- and C-termini into SK-N-SH cells which were then treated with cytochalasin D prior to fixing. (a) pHFL-EGFP (b) pNW-EGFP (c) pCW-EGFP. I – GBc, II – RBc. Red – actin, blue – nuclei.

The cytochalasin D experiments gave further indication of willin's ability to colocalise with actin. The pattern of willin localisation shown in 4.6a I is very similar to the pattern of actin localisation evidenced in 4.6a II, which would seem to suggest that, like the other members of the ERM family, full length willin appears to act as a membrane-cytoskeletal linker.

In figures 4.6b I and 4.6b II, and 4.6c I and 4.6c II, which show cells expressing the pNW-EGFP and pCW-EGFP constructs respectively, the distribution of the expressed N- and C-terminals of the protein do not mirror the distribution of the disrupted actin cytoskeleton in the same way as the cells that were transfected with

the full length protein (figure 4.6aI and aII). This would perhaps again indicate that the ability of willin to colocalise with actin is somewhat impeded when the full length protein is not present.

4.3.7 Western blotting of SK-N-SH cells transfected with pCW-EGFP and pNW-EGFP

In an attempt to confirm the results obtained via fluorescence imaging with the three willin-EGFP constructs, western blotting experiments were carried out using fractionated transfected SK-N-SH cells. It was anticipated that the results observed in figures 4.5 and 4.6 could possibly be corroborated by transfecting cells with each of the three constructs and then noting which cellular fraction, membranous or cytoskeletal, the fusion proteins could then be detected in. However, since the only antibodies available initially were to the N-terminus of the willin protein, preliminary western blots were carried out using only the constructs expressing the full length and N-terminus of the willin protein.

SK-N-SH cells were transfected with the pHFL-EGFP and pNW-EGFP constructs. A control group of cells was left untransfected. The cells were left for approximately 24 hours before being lysed and centrifuged to split the cells into soluble and insoluble fractions (section 2.3.9). To allow accurate comparison of which cellular fraction the fusion proteins were to be found in, equal amounts of both the cell pellets and the cell supernatants were loaded. A western blot was performed as described in section 2.2.8 and the resulting membrane was probed with the p914[3] antibody at a 1:1000 dilution.

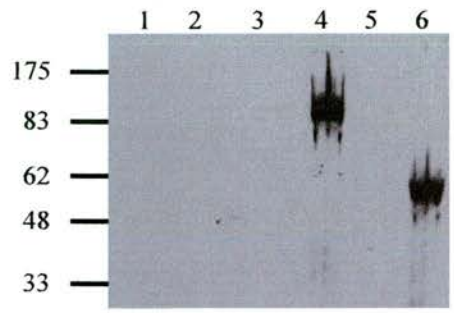

Figure 4.7. Western blot to show the localisation of the pHFL-EGFP and pNW-EGFP fusion proteins following transfection into SK-N-SH cells. The p914[3] antibody was used at a 1:1000 dilution. Lanes contain equal amounts of supernatant [S] or pellet [P] fractions of (1) untransfected [S] (2) untransfected [P] (3) pHFL-EGFP transfected [S] (4) pHFL-EGFP transfected [P] (5) pNW-EGFP transfected [S] (6) pNW-EGFP transfected [P]. Expected sizes: pHFL-EGFP – 98kDa, pNW-EGFP – 56kDa.

In the western blot in figure 4.7, both the control supernatant lane and control pellet lane were blank, indicating that the two bands that appeared on the film represent the two fusion proteins of interest. Both bands are the correct predicted size: the pHFL-EGFP fusion protein has been calculated to be 98kDa and the pNW-EGFP fusion protein to be 56kDa. There was no indication of either of the fusion proteins in the soluble fractions and both appear only in the insoluble fraction.

Attempts were then made to duplicate the results obtained in the western blots in figure 4.7 by using an anti-GFP antibody. Using this antibody would have the advantage of the detection of the pCW-EGFP construct. However, the results obtained using the anti-GFP antibody were indecipherable as the resulting films contained a large number of bands in every lane, which negated the possibility of identifying bands representing the fusion proteins.

4.4.1 Localisation of pHFL-EGFP to membranous structures

From the preliminary studies in SK-N-SH cells it was apparent that the distribution of willin is complex. Therefore the pHFL-EGFP construct was transfected into a series of different cell-lines, including CHO, COS7, HEK293, RPE and RPEc5TCL1 cells. In many cases willin could be located in the plasma membrane of transfected cells, and to membranous structures, examples of which are shown in the following figures.

Figure 4.8 shows the appearance of a COS7 cell that is expressing the full length protein. Colocalisation of willin with actin occurs in certain areas of the cell (4.8c, ←i) but not others. Interestingly, willin also appeared to colocalise with some of the COS7 cell projections but not others: two projections (4.8c, ←ii and ←iii) did not seem to colocalise with actin, whereas another projection does (4.8c, ←iv), including at a small concentrated patch of willin appearing at the end of this projection where there is also a corresponding small concentrated patch of actin (4.8c, ←iv).

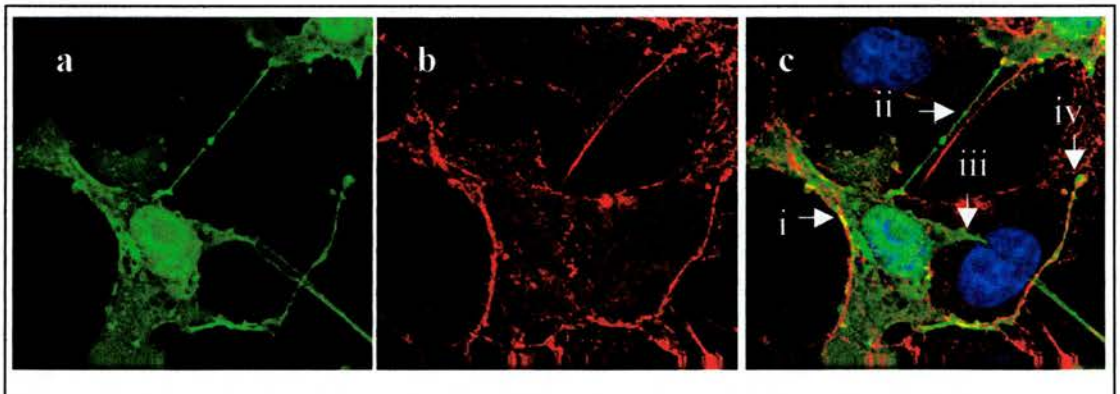

Figure 4.8. Transfection of pHFL-EGFP into COS7 cells. (a) Gc (b) Rc (c) RGBc. Red – actin, blue – nucleus.

Figures 4.9 and 4.10 show normal RPE cells and tumorous RPE cells (RPEc5TCL1) respectively. The actin around the outside of the normal cells (fig 4.9) can be seen to

be much thicker than that of the cancerous cells (fig 4.10). It is notable that in the normal cells there is a clear colocalisation of willin and actin around the circumference of the cell whereas this is no longer apparent in the tumour cells. Additionally, the actin in the tumour cells appears to be more dense throughout the cytoplasm than in the normal cells and the abnormal distribution of actin in the tumour cells is matched by the denser distribution of willin in these cells. An area of precise colocalisation of willin and actin in the tumour cells can be seen between the two transfected cells (arrow, 4.10c).

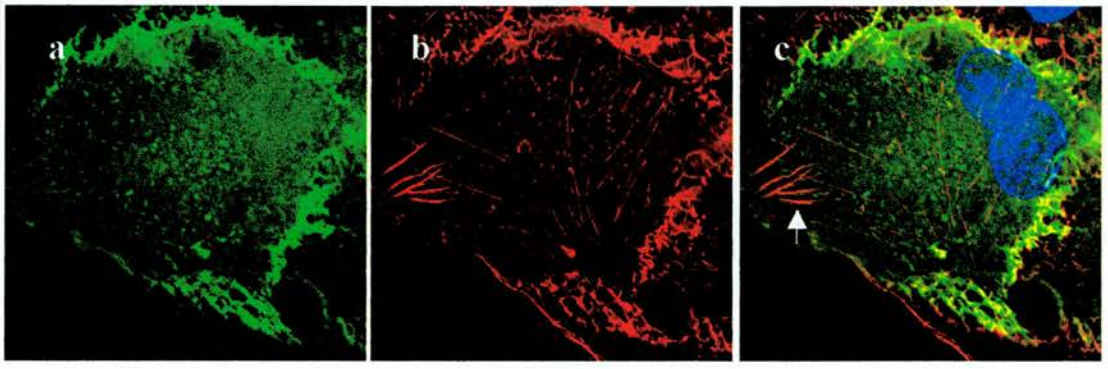

Figure 4.9. Transfection of pHFL-EGFP into RPE cells. (a) Gc (b) Rc (c) RGBc. Red – actin, blue – nucleus. Arrow in (c) shows localisation with stress fibres, mentioned below.

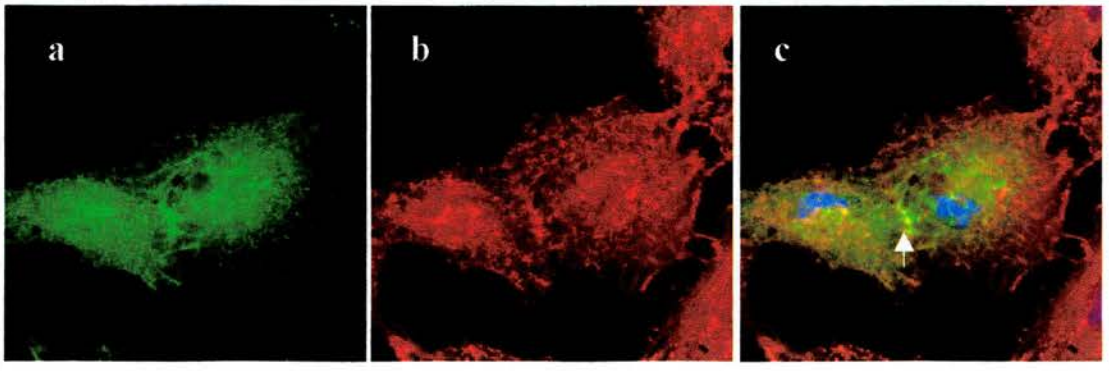

Figure 4.10. Transfection of pHFL-EGFP into RPEc5TCL1 cells. (a) Gc (b) Rc (c) RGBc. Red – actin, blue – nucleus.

Figure 4.11. shows that CHO cells also could also display membranous staining of the full-length willin-EGFP. In both the RPE cell in figure 4.9 (arrow), and the CHO cells in figure 4.11, co-localisation of willin-EGFP with actin stress fibres was evident.

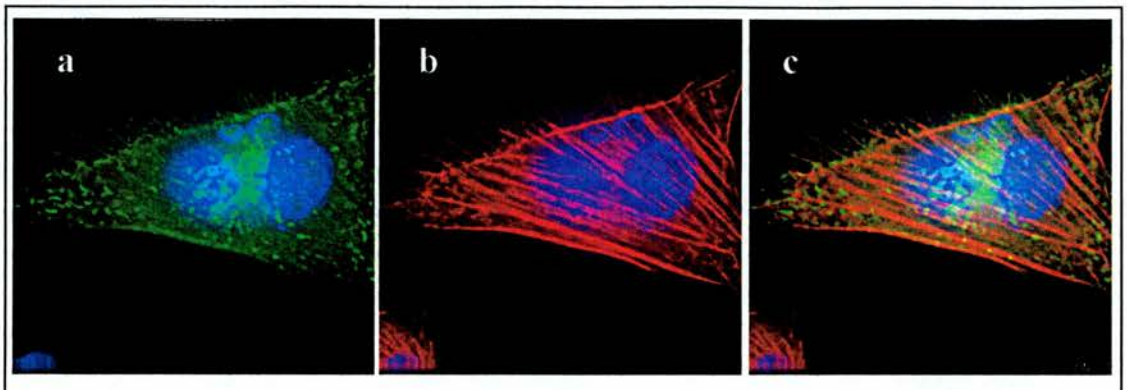

Figure 4.11. Transfection of pHFL-EGFP into CHO cells. EGFP-tagged full length willin localises to stress fibres in these cells. (a) GBc (b) RBc (c) RGBc. Red – actin, blue – nuclei.

Willin has also been seen to localise to membrane projections in HEK293 cells (figure 4.12 and figure 4.13).

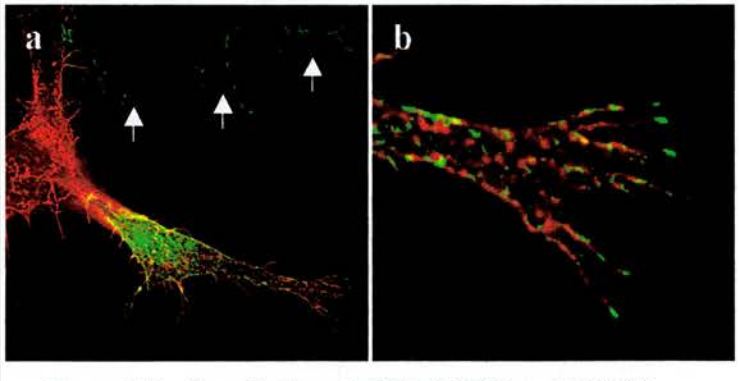

Figure 4.12. Transfection of pHFL-EGFP into HEK293 cells. (a), (b) – RGc. Red – actin. (a) shows the entire cell [arrows are mentioned in Discussion], (b) shows localisation of the protein to the tips of projections

Figure 4.12a shows a HEK293 cell which has been transfected with full length willin [arrows are mentioned in Discussion]. The area where the most intense yellow fluorescence is to be found is the area of the transfected cell that is in contact with a neighbouring cell. Figure 4.12b shows a close up of this cell, where it can be seen that the full length protein is to be found particularly concentrated at the tips of the projections of the "tail" of this cell.

In figure 4.13, it can be seen that willin colocalises closely with actin in the main body of the projection and to the base of each of the projections emanating from it, whereas further outwards from the base of the projections, willin and actin assume an alternating pattern of localisation. The arrows in figure 4.13d indicate how it is frequently - although not always - the case that when a segment of the projection deviates from linear growth, a small concentrated patch of willin can be seen at the point where the direction changes.

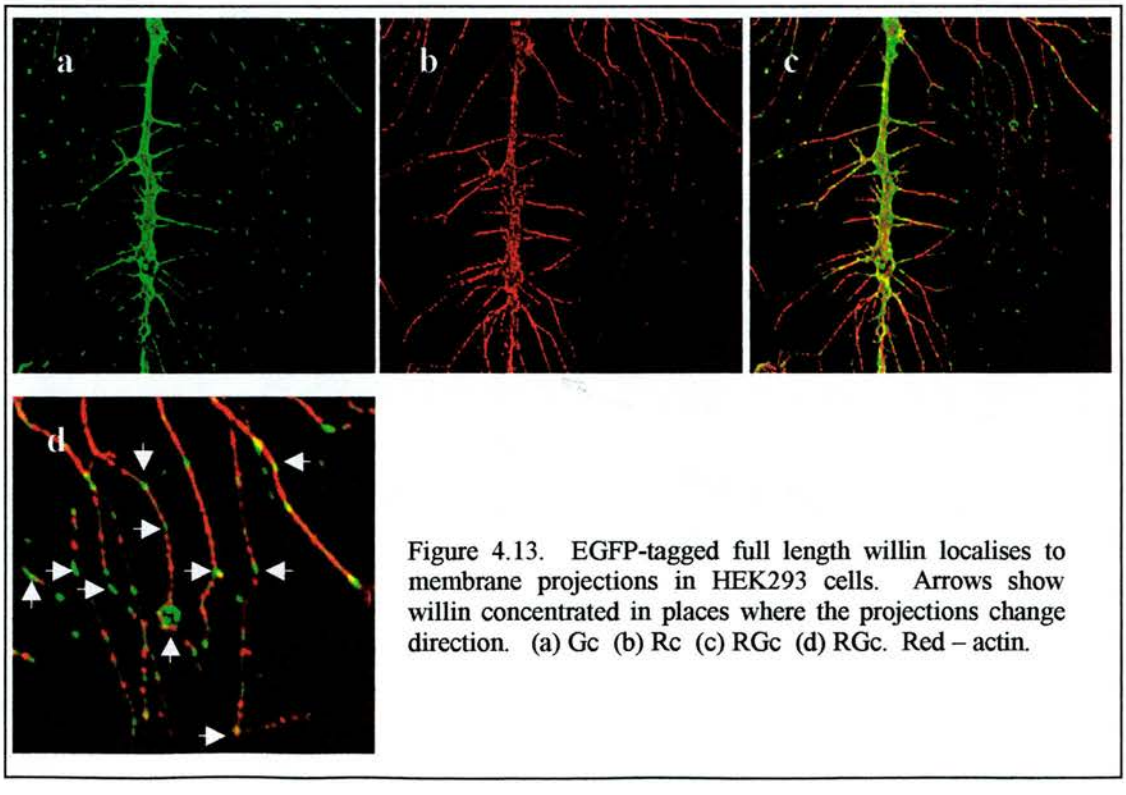

Figure 4.13. EGFP-tagged full length willin localises to membrane projections in HEK293 cells. Arrows show willin concentrated in places where the projections change direction. (a) Gc (b) Rc (c) RGc (d) RGc. Red – actin.

Expression of willin-EGFP in membrane projections is also observed in transfected RPE cells. Figure 4.14a-c shows several different sections through an RPE cell that was transfected with the pHFL-EGFP construct. The first section, figure 4.14a, shows the hollow bases of several projections on the surface of the cell (arrows). Sections taken further up through the same cell show how the full length protein concentrates in the core of these projections (figure 4.14 b and c, arrows).

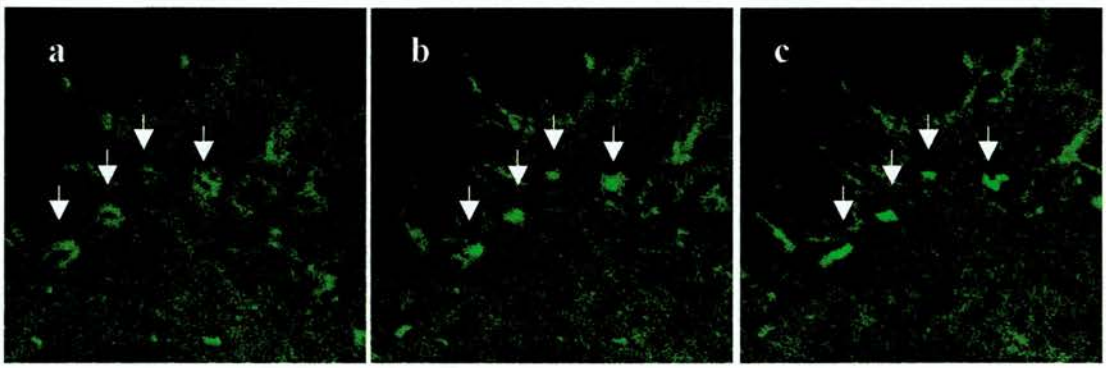

Figure 4.14. EGFP–tagged full length willin localises to membrane projections (arrows) in RPE cells. (a), (b), (c) – Gc.

4.4.2 Localisation of willin to the mammalian cell midbody/contractile ring

To allow one cell to divide into two, a contractile ring forms between the cells which forms the cleavage furrow, and later the midbody (reviewed in Alberts et al, 1994a). Willin has been found to localise to the midbody or the cleavage furrow in four cell lines examined.

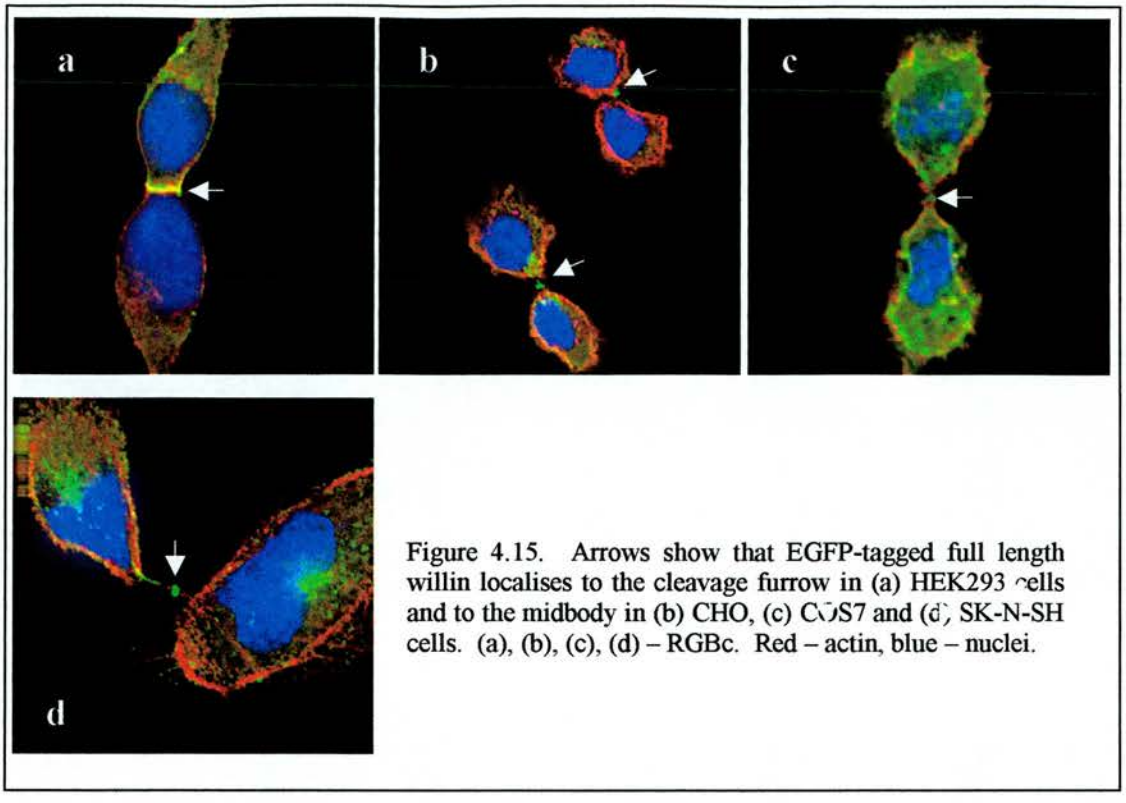

Figure 4.15. Arrows show that EGFP-tagged full length willin localises to the cleavage furrow in (a) HEK293 cells and to the midbody in (b) CHO, (c) COS7 and (d) SK-N-SH cells. (a), (b), (c), (d) – RGBc. Red – actin, blue – nuclei.

Figure 4.15 shows that full length willin localises to the cleavage furrow in HEK293 cells (4.15a, arrow) and to the midbody in CHO (4.15b, arrow), COS7 (4.15c, arrow) and SK-N-SH cells (4.15d, arrow). The full length protein may also possibly localise to the midbody in HEK293 cells but this was not captured in the photographs.

Figure 4.16a and b shows enlarged pictures of the contractile ring of the HEK293 cells and demonstrates the specific colocalisation of willin with the actin in the contractile ring. The enlarged picture of the midbody of the COS7 cells shown in figure 4.16c and d shows how each of the dividing cells projects a "V" shaped actin structure (4.16d, arrows), between which the midbody structure that willin localises to can be seen to sit (4.16c, arrow).

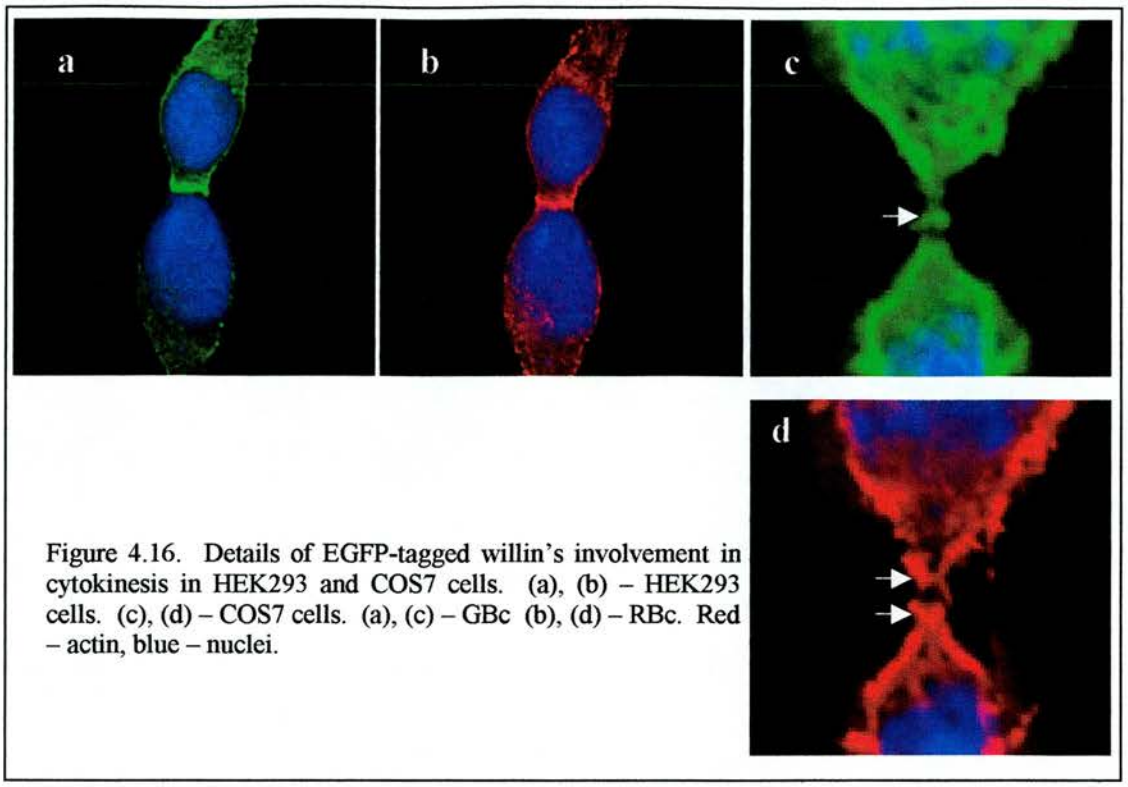

Figure 4.16. Details of EGFP-tagged willin's involvement in cytokinesis in HEK293 and COS7 cells. (a), (b) – HEK293 cells. (c), (d) – COS7 cells. (a), (c) – GBc (b), (d) – RBc. Red – actin, blue – nuclei.

4.4.3 Localisation of willin to the cell nucleus

Full length willin has also been revealed to localise to the nucleus in COS7, CHO, HEK293 and SK-N-SH cells, as shown in figure 4.17.

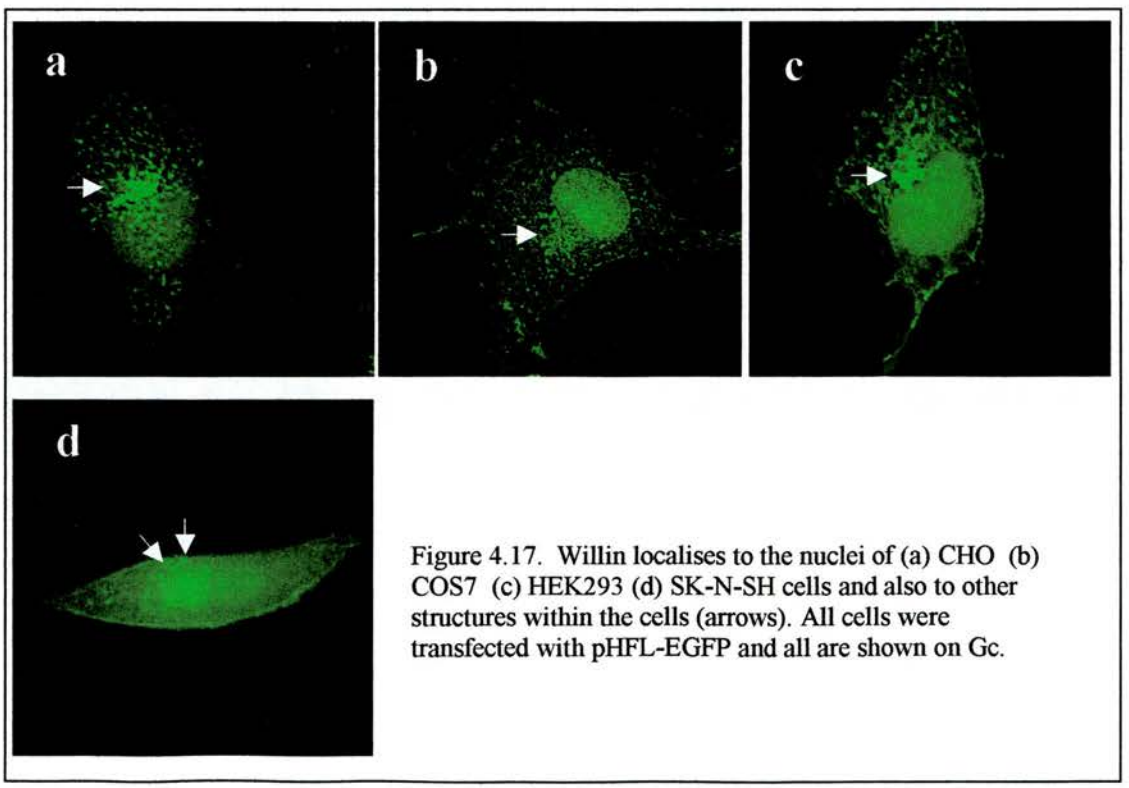

Figure 4.17. Willin localises to the nuclei of (a) CHO (b) COS7 (c) HEK293 (d) SK-N-SH cells and also to other structures within the cells (arrows). All cells were transfected with pHFL-EGFP and all are shown on Gc.

In the above pictures the SK-N-SH cell (4.17d) appears as though it is about to enter mitosis, due to the presence of two nuclei inside the cell. However, the two nuclei are not identical: the nucleus on the left is brighter than that on the right and also has several peripheral regions (arrows) that willin localises to but which do not appear to be present (or visible) on the nucleus on the right.

In the first three cells shown in figure 4.17, willin also localises to a structure next to each of the nuclei (arrows), possibly an organelle.

It is unclear from the SK-N-SH cells shown in figure 4.17d whether willin also localises to a similar structure in this cell type. However, figure 4.18 shows the protein does localise to a bright perinuclear pool in the SK-N-SH cells.

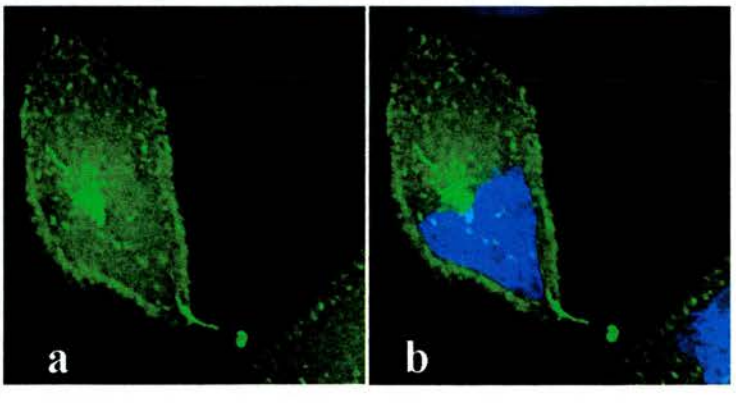

Figure 4.18. Willin concentrates in a perinuclear pool (arrow) in SK-N-SH cells. Cells were transfected with pHFL-EGFP. (a) Gc (b) BGc. Blue – nuclei.

Although the protein does not appear to localise to the nucleus in the SK-N-SH cells in figure 4.18 as it does in figure 4.17, this is possibly due to a difference in the distribution of the protein that is cell cycle-dependent, since the cell shown in figure 4.18 is one half of a pair of cells that had presumably just undergone mitosis.

4.5.1 Interference in cell division in HEK293 cells

HEK293 cells were also each transfected with the pNW-EGFP and pCW-EGFP constructs. The transfection of either the pNW-EGFP or pCW-EGFP constructs into HEK293s was discovered to have quite a profound effect on the appearance of the cells, as shown in figure 4.19.

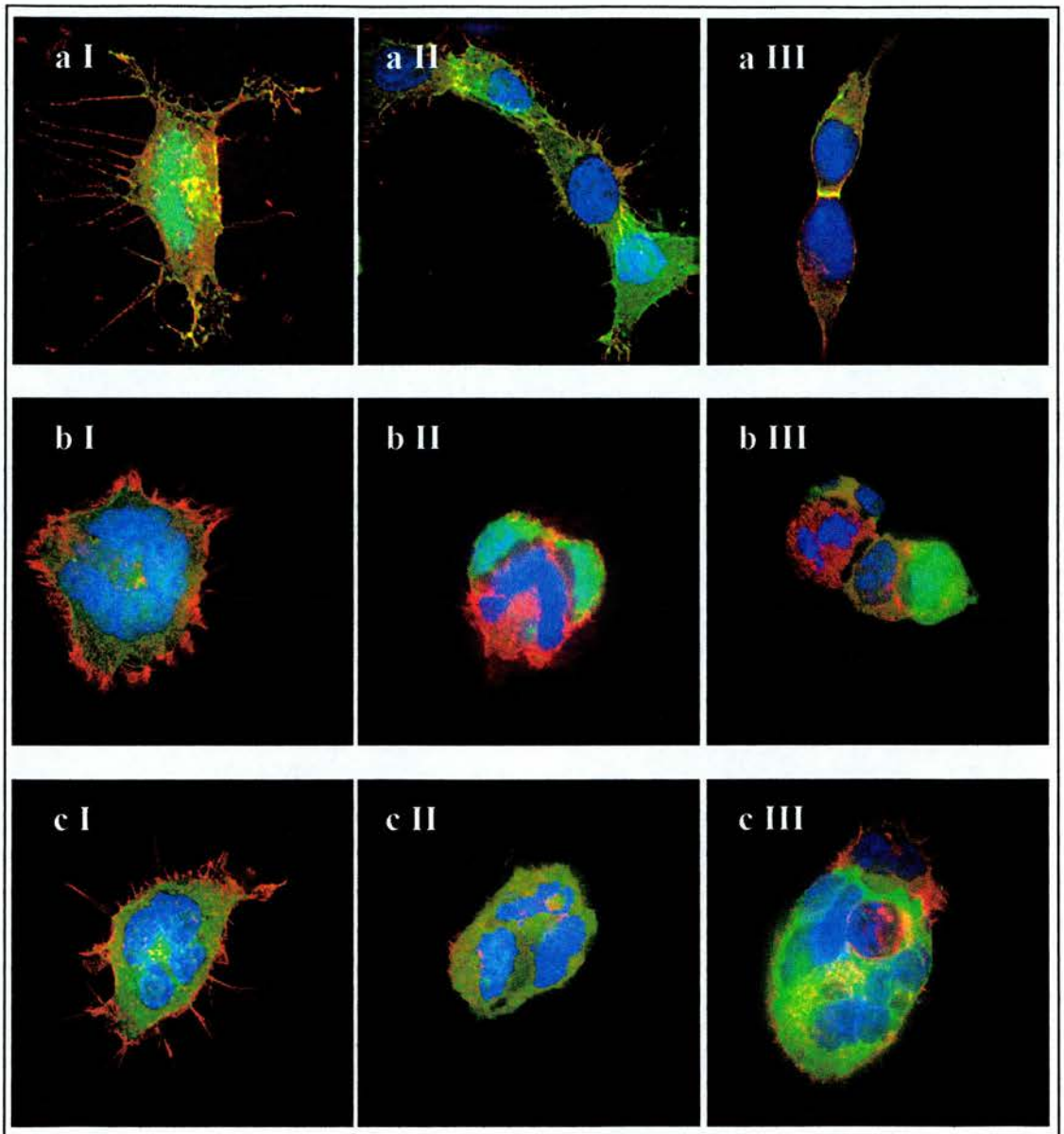

Figure 4.19. Aberrant cell morphology results from the transfection of either the willin N- or C-terminus into HEK293 cells. Cells were transfected with (a) pHFL-EGFP (b) pNW-EGFP (c) pCW-EGFP. All cells are shown on RGBc. Red – actin, blue – nuclei.

Figure 4.19aI - III shows a selection of HEK293 cells that have been transfected with full length willin, figure 4.19bI - III shows HEK293 cells that have been transfected with the N-terminus of willin and figure 4.19cI - III shows HEK293 cells that have been transfected with the C-terminus of willin.

The HEK293 cells transfected with either the N- or C-terminus of willin also generally appeared to have a much thicker cytoskeleton, as shown in figure 4.20b and 4.20c versus 4.20a. A further point of difference evident in the cells in figure 4.20 is in the cell nuclei. Figure 4.20 shows how the nuclei of cells transfected with full length willin (4.20a) vary considerably from the appearance of cells transfected with the N-terminus (4.20b) or C-terminus (4.20c) of the protein, in that there are more of them.

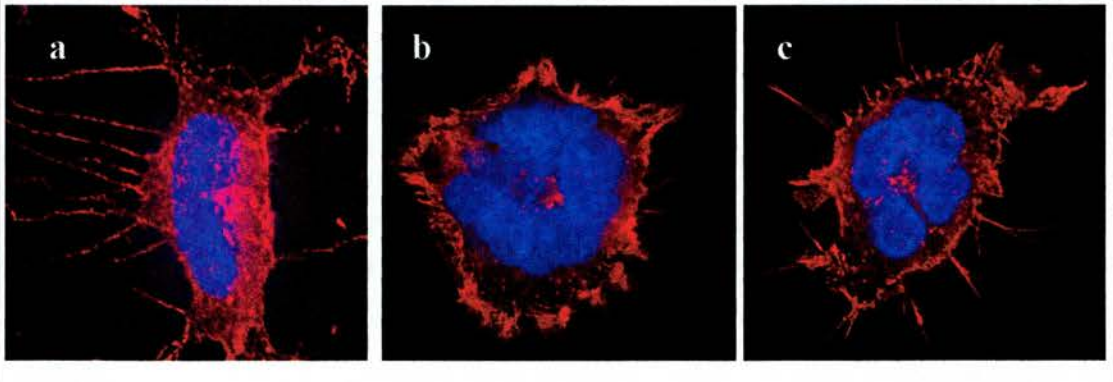

Figure 4.20. Abnormal appearance of nuclei and cytoskeleton in HEK293 cells transfected with the EGFP-tagged N- or C-terminus of willin. Cells were transfected with (a) pHFL-EGFP (b) pNW-EGFP (c) pCW-EGFP. (a), (b), (c) – RBc. Red – actin, blue – nuclei. [A view of each of these cells on the RGB channel is seen in figure 4.19a, b and c.]

4.5.2 "Conjoined" HEK293 cells

A further irregularity seen in the HEK293 cells transfected with the pNW-EGFP or pCW-EGFP constructs was the frequent appearance of small, conjoined pairs of cells as shown in figure 4.21.

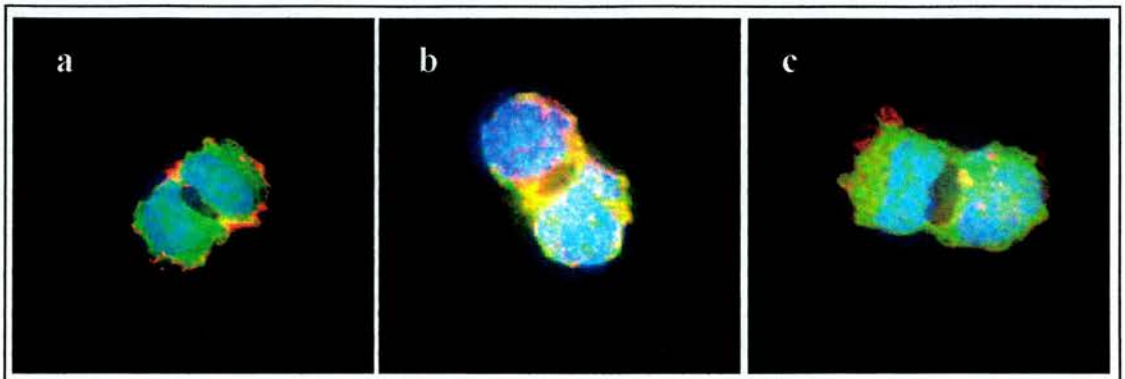

Figure 4.21. Small conjoined pairs of cells frequently appeared in HEK293 cells that had been transfected with the EGFP-tagged N- or C-terminus of willin. Cells were transfected with (a) and (b) pNW-EGFP (c) pCW-EGFP. (a), (b), (c) – RGBc. Red – actin, blue – nuclei.

Pairs of cells with an appearance similar to these were never observed in cells transfected with the full length protein and were therefore examined to see if they could help provide an explanation for the aberrant cell morphology seen in figures 4.19. Each of these conjoined pairs of cells appears to have completed telophase but was then unable to progress completely through cytokinesis.

Although the pairs of conjoined cells resulting from transfection with the pNW-EGFP and pCW-EGFP constructs appeared similar, closer inspection revealed differences between cells expressing one or the other of the plasmids. It was regularly observed, for example, that the doublets expressing the N-terminus of the protein had a region of thickened actin on either side of the centre of the pair of cells, in the area where

one would have expected to see a contractile ring: figures 4.22aIII and bIII shows how willin colocalises with actin in these areas.

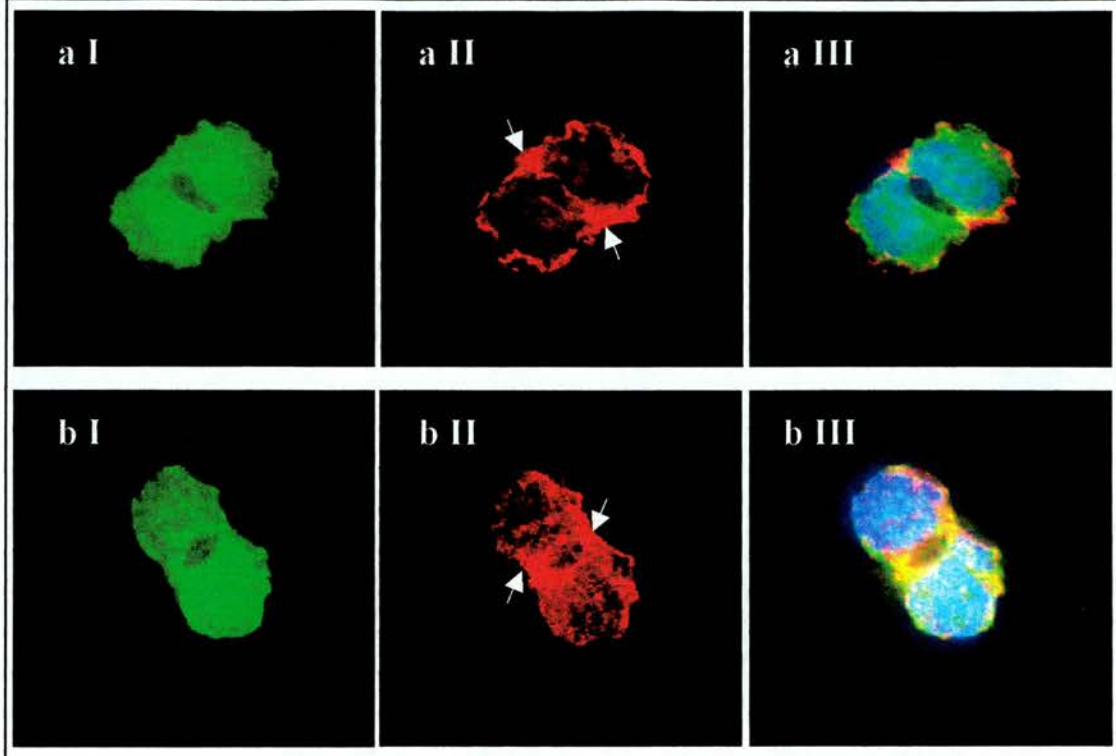

Figure 4.22. The conjoined pairs of cells that resulted from transfection with the willin N-terminus led to a thickening of the actin cytoskeleton (arrows) where the contractile ring would normally have been. Both cells shown were transfected with pNW-EGFP. I – Gc, II – Rc, III – RGBc. Red – actin, blue – nuclei.

The cells that had been transfected with the C-terminus of the protein (figure 4.23) also tended to have a region of thickened actin on either side of centre of the two cells, but it was not as pronounced as that seen in cells transfected with the N-terminus (figure 4.22). Furthermore, a different kind of anomaly was frequently observed in cells that had been transfected with the C-terminus of the protein. Figure 4.23 shows some of these cells and how they each contain a ring of actin at one end of the conjoined pair of cells. These rings are conspicuous in that they do not colocalise with willin (arrows).

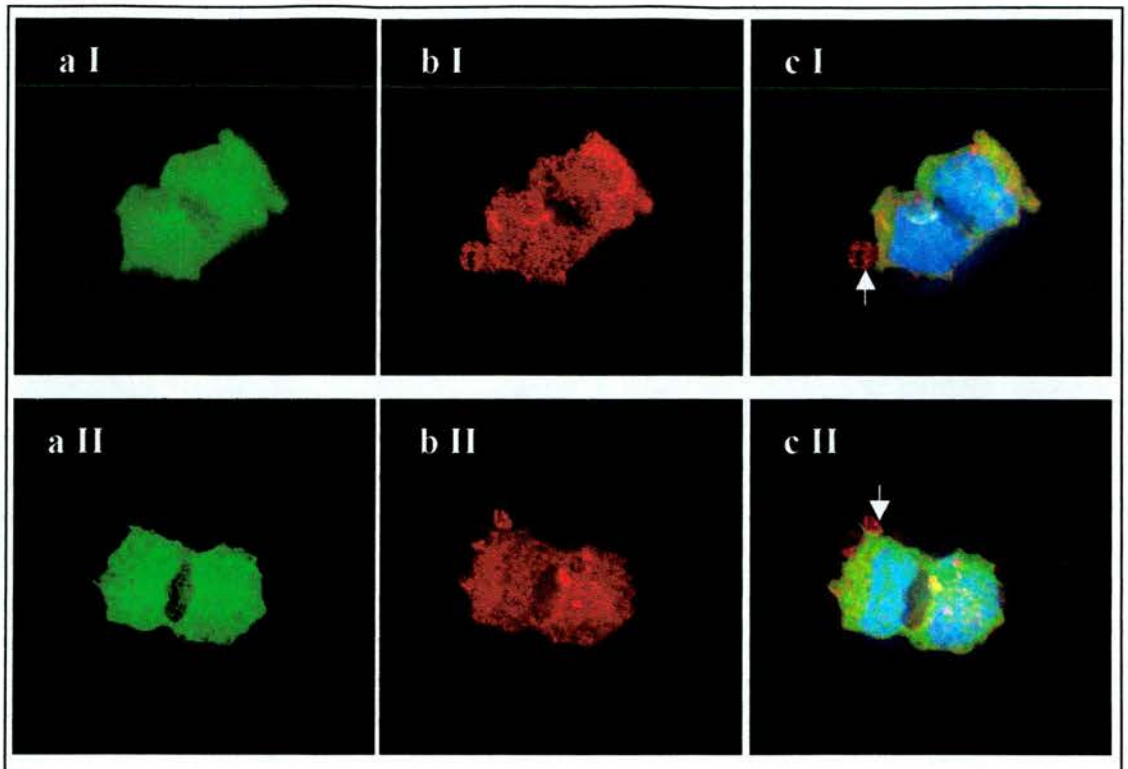

Figure 4.23. The conjoined pairs of cells that resulted from transfection with the willin C-terminus often possessed a ring of actin that did not colocalise with willin (arrows). Both cells shown were transfected with pCW-EGFP. I – Gc, II – Rc, III – RGBc. Red – actin, blue – nuclei.

4.5.3 Western blotting of HEK293 cells using pHFL-EGFP and pNW-EGFP

Due to the actin anomalies seen in the HEK293 cells following transfection with the N- and C-termini of willin, it was decided to perform a western blot similar to that performed using the SK-N-SK cells (figure 4.7). A control batch of cells was left untransfected and two other batches of cells were transfected with the pNW-EGFP and pHFL-EGFP constructs. The cells were harvested and lysed into soluble and insoluble fractions, as described in section 2.3.9, to examine which fraction the full length protein and the N-terminus of the protein would be found in. The membrane was probed with a 1:1000 dilution of the panned 914[3] antibody and the result is shown in figure 4.24.

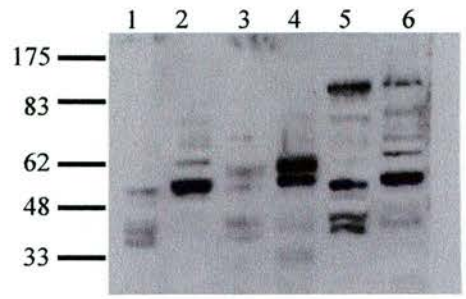

Figure 4.24. Western blot to show the localisation of the pHFL-EGFP and pNW-EGFP fusion proteins following transfection into HEK293 cells. The p914[3] antibody was used at a 1:1000 dilution. Lanes contain equal amounts of supernatant [S] or pellet [P] fractions of (1) untransfected [S] (2) untransfected [P] (3) pNW-EGFP transfected [S] (4) pNW-EGFP transfected [P] (5) pHFL-EGFP transfected [S] (6) pHFL-EGFP transfected [P]. Expected sizes: pHFL-EGFP – 98kDa, pNW-EGFP – 56kDa.

The western blot in figure 4.24 indicates that the full length protein can be found in both the soluble and insoluble fractions but most is present in the soluble fraction, whereas the N-terminus of the protein is also to be found in both the soluble and insoluble fractions but most is to be found in the insoluble fraction. As was the case with the SK-N-SH western blot (section 4.3.7), the presence of the N-terminus in the cytoskeletal fraction was an unexpected find as it was anticipated that this part of the protein would be found in the membranous fraction.

4.6 Conclusions

EGFP-tagged full length human willin shows a different distribution pattern than EGFP alone. The full length protein is targeted to the cell membrane in SK-N-SK cells and also colocalises with actin in these cells, according to immunofluorescence photographs. In SK-N-SH cells, western blot experiments indicate that the full length protein localises to the cytoskeletal fraction only, upon lysis of the cells. In HEK293 cells, western blot experiments show that the full length protein localises to both the soluble and insoluble fractions upon lysis of the cells. Immunofluorescence experiments indicate that the C-terminus of the protein, when expressed as an EGFP fusion protein, also colocalises with actin. The N-terminus of the protein, when expressed as an EGFP fusion protein, does not appear to colocalise strongly with actin according to immunofluorescence experiments. However, western blot experiments indicate that the N-terminus of the protein may in fact colocalise with actin, as it can found in the insoluble fraction of lysed extracts from two different cell lines.

EGFP-tagged full length human willin shows a different pattern of distribution according to which cell lines it is expressed in. In SK-N-SH, CHO, HEK293 and RPE cells the protein can be seen to localise to the membrane and cytoskeleton to a larger degree than is evident in COS7 cells and RPEc5TCL1 cells.

Willin localises to membranous structures such as stress fibres in CHO and RPE cells and to areas of cell-cell adhesion in HEK293 cells. It concentrates strongly at the

base of long projections in HEK293 cells and can be seen to concentrate in areas of a projection prior to a change of direction.

The protein possibly plays a role in cytokinesis. In HEK293 cells, willin localises to the contractile ring. In COS7, CHO and SK-N-SH cells willin localises to the midbody.

The expression of either the N- or C- terminus of the protein causes a slightly different distribution pattern in CHO, COS7 and SK-N-SH cells but has a pronounced detrimental effect on cell morphology in HEK293 cells: the nuclei of these cells frequently occupy a large proportion of the cell.

Small pairs of cells that had failed to complete cytokinesis were regularly observed when cells were transfected with the N- or C-terminus of the protein but were never observed when the cells were transfected with the full length protein. Pairs of these cells that were expressing the N-terminus of the protein often had regions of thickened actin on either side of the cells where the contractile ring should have formed. Pairs of these cells that were expressing the C-terminus frequently possessed a small ring of actin at one end of the conjoined pair, and this ring did not colocalise with willin.

4.7 Chapter 4 Discussion

4.7.1 Localisation of willin in SK-N-SH cells

Other members of the ERM family are known to act as membrane-cytoskeleton linker proteins (section 1.3.6) and the purpose of the experiments in this chapter was to gain insight into whether or not willin had similar functions. The experiments at the beginning of this chapter gave results that were for the most part expected, namely that the full length protein would be found in the cell membrane and would co-localise with actin (section 4.3.4), and that the expression of half of the protein would lead to a distribution that was different from that of the full length protein (section 4.3.5).

In figure 4.6, which illustrates the cytochalasin D experiment, the cytoskeletons in each of the three pictures appear to have been disrupted to varying degrees. The cells in figure 4.6aII (full-length transfected) appear to have the least disrupted cytoskeletons, the cells in 4.6cII (C-terminal transfected) appear to have the next least disrupted cytoskeletons, and the cells in figure 4.6bII (N-terminal transfected) appear to have the most disrupted cytoskeletons. This may imply that the full length protein, in its proposed role as membrane-cytoskeleton linker protein, could serve to protect the cytoskeleton from the kind of cytochalasin-induced disarray seen in the N-terminal transfected cells (figure 4.6b), with the C-terminus of the protein showing a slight degree of similar protection (figure 4.6c). Unfortunately, no experiments could be carried out to confirm - or otherwise - the presence of the C-terminus of the protein in the insoluble fraction, since no antibody was available to the C-terminus sequence, and an anti-EGFP western blot was unsuccessful (section 4.3.7).

A somewhat unexpected result was that the N-terminal half of the protein is found in the insoluble fraction of SK-N-SH cells and not in the soluble fraction, as revealed by the western blot in figure 4.7. It had been considered likely that, being without the C-terminal half of the protein and therefore without the expected actin binding site, the N-terminus would localise to the cell membrane and would be found in the soluble fraction upon lysis of the cells.

However, there may actually be an actin binding site in the N-terminus of the protein since an N-terminal actin binding site is known to exist in ezrin (Roy et al, 1997). If this is the case, then the protein would probably be found in the cytoskeletal fraction of lysed cells regardless of whether it is the whole protein, or the C-terminus, or the N-terminus.

4.7.2 Localisation of willin in other cell lines

The varying distribution of the protein following transfection into other cell lines (figures 4.8 onwards) indicates that willin plays different roles in different cells. An interesting observation is the disparity between the localisation of the protein in RPE (a normal cell line) (figure 4.9) and RPEc5TCL1 (a tumorogenic cell line) (figure 4.10) cells. In RPEc5TCL1 cells, willin no longer colocalises with actin at the perimeter of the cells and instead colocalises with actin in the cytoplasm of the cells. The fact that a difference can be seen between the localisation of the protein in cancerous and non-cancerous cells merits further investigation, particularly since other experiments had shown that the protein is down-regulated in certain types of head and neck cancers (Prof Mike Prystowsky, Albert Einstein College of Medicine, New York; pers. comm.)

The other members of the ERM family are know to localise to membranous structures (section 1.2.5) and the presence of willin in structures such as these, as shown in figures 4.11 – 4.14, indicates that willin also behaves in a similar manner.

Less easy to observe from these pictures is whether or not the protein plays a role in cell-cell and cell-substrate adhesion, as do ezrin, radixin and moesin (section 1.4.6). However, there are a few indications that these roles are shared by willin also. If the fragments of green fluorescence marked by the arrows in figure 4.12a are the remains of HEK293 cells, the fact that these fragments are still attached to the coverslip when the cell has been washed away would suggest that willin does have a part to play in cell-substrate adhesion. Furthermore, if the architecture of the projection shown in figure 4.13 is examined, it would appear that willin can often be seen in many areas of the projection that change direction. To enable a change of direction in a projection that is growing in a liquid medium, a point of adhesion would be of assistance immediately prior to each change of direction and it is therefore possible that willin is localising to points of adhesion in the cell in figure 4.13; this implies a role for the protein in cell-substrate adhesion.

With regard to cell-cell adhesion, the area of strongest willin-actin colocalisation in the RPEc5TCL1 and HEK293 cells (figures 4.10 and 4.12 respectively), is in the region where the cells are contacting each other. This would indicate a role for willin in cell-cell adhesion.

Willin also appears to play a part in cytokinesis, as shown by the pictures showing willin colocalising to the contractile ring and midbody in figure 4.15. This is again a

function shared by other members of the ERM family: ezrin, radixin and moesin have all been shown to localise to the cleavage furrow of dividing cells (section 1.4.14). It is possible that willin does colocalise to the midbody in HEK293 cells also (i.e. not just to the HEK293 contractile ring) and that this occurrence was simply not captured during the microscopy sessions. The HEK293 cells formed considerably more clumps than the other cell lines, and in fact the majority of the HEK293 cells on each slide were to be found clumped together. It was impossible to investigate cells clustered in such a manner as the borders of individual cells were not clearly distinguishable. This greatly reduced the number of HEK293 cells that could be examined.

The two nuclei in the SK-N-SH cell shown in figure 4.17d are clearly stained by green fluorescence, implying that willin localises to the nucleus in this cell type. However, in the SK-N–SH cell shown in figure 4.18, the nucleus is not so clearly demarcated, which then suggests that willin does not colocalise with the nuclei in these cells. Due to the evidence which has accumulated to indicate the ERM family's role in the cell cycle (section 1.4.14), a possible reason for the apparent discrepancy mentioned above is that the localisation of willin may be cell cycle dependent. A similar event is shown in the COS7 cells below in figure 4.25. The protein localises to the nucleus in the mature cells (4.25aI and aII) but this colocalisation is not so evident in the dividing cells (4.25bI and bII).

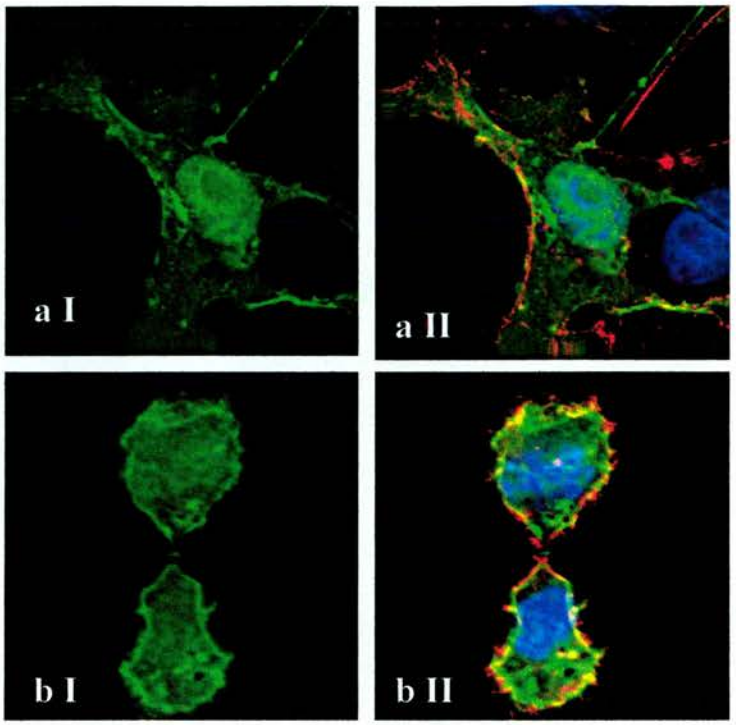

Figure 4.25. The distribution of willin may be cell cycle-dependent. COS7 cells were transfected with pHFL-EGFP.

(a) shows mature cells

(b) shows dividing cells.

I – Gc, II – RGBc.
Red – actin, blue –

Furthermore, the mature COS7 cells in figure 4.25a do not have a thickened boundary of willin around the entire circumference of the cell, whereas the dividing cells shown in figure 4.25b do exhibit such a distribution of the protein; and since the boundary fluorescence in figure 4.25bII is yellow and not green, it would appear that the protein is colocalising with actin around the perimeter of the immature cells, but not to the same extent in the mature cells.

4.7.3 Cellular anomalies following transfection of HEK293 cells

The reason for the willin N- and C-terminus inducing the anomalies in the HEK293 cells (figure 4.19) is unknown. It would appear that transfection with the N- or C-terminus of willin may interfere with mitosis in HEK293 cells, but it is not known at exactly what step in the process.

Due to the amount of the "conjoined" doublets of cells that were observed in cells expressing the willin N- or C-termini (figure 4.21), it appears likely that cytokinesis is not completed in many cases. This is further endorsed by the diminished number and/or length of projections emerging from the cells seen in figure 4.19, which is something that would be expected if the cells could not complete cytokinesis. The normal cells undergoing division, as seen in figure 4.19aIII, are completely smooth, which indicates that projections are only to be found on mature cells. But if cells do not complete cytokinesis satisfactorily then they never reach maturity and so one would anticipate a detrimental effect on the growth of projections.

The fact that high numbers of nuclei appear to be present in one cell would also imply the inability of these cells to complete cytokinesis (figure 4.20). If the cells are reaching telophase, with nuclear division complete, but then cannot proceed onwards to cytokinesis, this would result in one cell with two nuclei. If the cell then attempts another cycle of division, either one or both of the nuclei inside the cell will divide, which, if the cell again cannot complete the attempt at division, will result in three or four nuclei inside one cell. However, the appearance of so many nuclei in the cells expressing the willin N- or C-terminus is conducive towards a hypothesis of interference at an even earlier stage in cell division: the nuclei in many cases do not appear to be fully separated (figure 4.20), which would actually indicate problems prior to, or during, the telophase stage of mitosis.

The thickening of the actin cytoskeleton, as seen in figure 4.20, could also be accounted for by interrupted cytokinesis. A new cytoskeleton must be assembled for the daughter cells during each round of normal cell division, but if the parent cell is

not dividing into two daughter cells and is merely expanding to hold more and more nuclei, then a new cytoskeleton would possibly be distributed onto the same original cell during each attempt at cytokinesis, which would then result in an increasingly thicker cytoskeleton.

Figure 4.17d and 4.18 both show SK-N-SH cells with either willin-nucleus colocalisation (4.17d), or a lack thereof (figure 4.18), implying that the protein varies its nuclear localisation pattern at different times. These observations, coupled with the distortion of the nuclei seen in cells transfected with the pNW-EGFP and pCW-EGFP constructs (figures 4.19 and 4.20), may imply that the protein has a role to play in maintaining normal nuclear function in certain cell types.

It is possible that the multinucleate cells shown in figure 4.19 and 4.20 all started off as the type of doublets seen in figure 4.21. Further work to perhaps address this issue might involve timepoint analysis of HEK293 slides, with the fixing process beginning, say, 60 minutes after transfection and continuing at intervals over a period of maybe 24 to 30 hours.

4.7.4 Actin distribution in the abnormal HEK293 cells

The conjoined pairs of cells that resulted from the transfection of the HEK293 cells with the N- or C-terminus of willin (figures 4.22 and 4.23) may provide a more specific indication as to the nature of the interference in cytokinesis. The anomaly that seemed particular to N-terminus-transfected cells was the areas of thickened actin seen on either side of the centres of the conjoined pairs of cells, as shown in figure 4.22. These channels of actin would provide an obvious impediment to cytokinesis,

since it is in precisely this region that a pair of dividing cells needs to be able to contract and allow the membrane between the cells to pinch off and separate. Having a reinforcement of actin there instead would conceivably interfere with the separation process.

Although the cells shown in figure 4.6 imply that the willin N-terminus does not colocalise with actin, western blot experiments have indicated that the N-terminus of the protein does possibly colocalise with actin (figure 4.24), since the N-terminus is to be found in the insoluble fraction of the lysed cells. These results may at first seem conflicting but might be explained by degrees of possible actin binding, rather than an all-or-nothing theory. As mentioned previously, the first actin binding site for the ERM proteins was discovered in the proteins' C-terminus (Turunen et al, 1994) but then a second binding site was discovered in the N-terminus (Roy et al, 1997). Possibly, therefore, the presence of the complete protein leads to a lot of potential actin binding, seen as the strong regions of colocalisation in the immunofluorescence images, due to the presence of two possible actin binding sites. Then, when only the N-terminus of the protein is present, and therefore only one potential actin binding site is present, the result is less actin binding, exhibited as weaker colocalisation in the photographs.

It is therefore possible that, in the cells transfected with the willin N-terminus that exhibit thickened channels of actin on either side of the midpoint of the dividing cells (figure 4.22), the N-terminus of the protein may itself be recruiting the actin to these positions. The willin N-terminus does appear to colocalise with the actin in these areas, as suggested by the yellow fluorescence seen in figure 4.22. Figure 1.19

(section 1.4.13) shows how the contractile ring of dividing cells is composed of actin and myosin filaments, and the ERM proteins are known to localise to this area (section 1.4.13). It seems possible that when full length willin localises to the cleavage furrow in HEK293 cells, it can carry out any actin-related duties normally, whereas the N-terminus of the protein, when expressed in these cells, is still targeted to the region, but its potential actin-binding or actin-recruiting functions are manifestly affected by the lack of the C-terminus.

In the C-terminal-transfected cells, a small ring-shaped structure showed up repeatedly, as exemplified in figure 4.23. Similar structures could sometimes be seen in the N-terminus-transfected cells, although not as frequently as with the C-terminus-transfected cells. The possibility exists that this structure is in fact the midbody that should have formed between the two cells during cytokinesis. The ERM proteins are known to be involved in defining the polarity of a cell (section 1.4.14). It is therefore not inconceivable that willin also is involved in cell polarity and that when the midbody forms in cells transfected with only the N- or C-terminus of the protein, the polarity of the cell can no longer be signalled correctly, so the midbody no longer forms between the dividing cells but instead forms at one end of the duo, as seen in figure 4.23.

Although the pictures shown in figure 4.23 imply that the EGFP-tagged C-terminus of willin does not colocalise with this actin-containing structure, it is not known whether this is simply due to the orientation of the structure in the sections that were captured. In general, only one section was taken through each cell and possibly if a few more sections had been taken higher or lower through the cell, a ring of willin

would have appeared. Future investigations could therefore encompass an increased number of sections through the cell to clarify this point.

It is perhaps a matter of some interest that the cells expressing the N- and C-termini, with their accompanying abnormal morphology, actually manage to survive at all. It would not be unreasonable to surmise that cells that contain the ratio of nuclear material to cytoplasmic material similar those shown in, for example, figure 4.19, should have undergone apoptosis, which leads to conjecture about the possibility that if the cells should not have survived, the reason for their ability to do so may lie in inappropriate survival signalling. As mentioned in section 4.7.2, willin has already been linked to cancer, and the abnormal appearance of the N- or C-terminus-expressing HEK293 cells in this chapter elicits the question of what happens *in vivo* when the native protein undergoes a functional mutation of some sort.

A final point of note regarding the HEK293 transfections relates to the photographs in figure 4.26, which shows the similarities between the localisation of willin in a HEK293 cell, and that of a protein named dDia2 in a *Dictylostelium* cell.

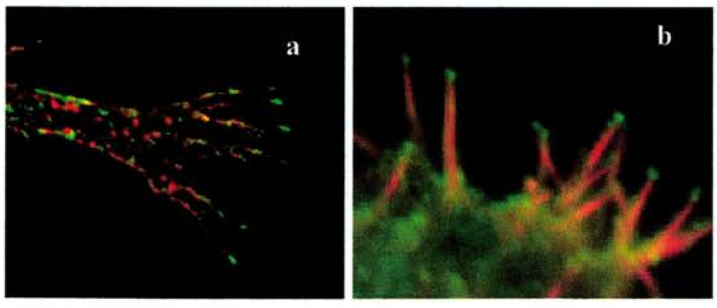

Figure 4.26
(a) Willin localises to cell projection tips in a manner similar to dDia2 (b).

(b) Localisation of dDia2, a proposed actin nucleator, to the filopodial tips of a *Dictylostelium* cell. Photograph taken from Schirenbeck et al, 2005.

Schirenbeck et al (2005) have suggested that dDia2, a formin protein of importance in cell migration and adhesion [which are also functions performed by the ERM family (sections 1.4.6 and 1.4.7)], is an actin nucleator. Actin nucleation is the formation of new actin filaments from actin monomers (reviewed in Alberts et al, 1994b). Mutants lacking dDia2 have significantly fewer and shorter filopodia (Schirenbeck et al, 2005), and figure 4.20 shows that cells transfected with the willin N- or C-terminus also have fewer and shorter projections than cells transfected with the full length protein.

The proteins and pathways that are involved in the process of actin nucleation have yet to be clearly elucidated; willin may perhaps emerge as having a role to play in this process. In addition, radixin was originally isolated by Tsukita et al (1989) in a publication that identified the protein as an actin end-capping protein, involved in the production of actin filaments. It is therefore possible that the proposed role of willin in actin-based activities involves more than simply linking the cytoskeleton to the plasma membrane.

Chapter 5: Investigation into willin's binding partners using protein lipid overlays and live cell imaging.

5.1 Aims:

- Expression of the willin protein
- Purification of the willin protein
- Investigation into willin's interactions with phospholipids via protein lipid overlays and live cell imaging
- Investigation into willin's protein-based interactions via a yeast two hybrid screen

5.2 Introduction

The ability of the ERM proteins to interact, via their FERM domain, with both proteins and lipids (sections 1.4.9, 1.4.10, 1.5.5) led to the design of a set of experiments that would allow the exploration of any similar ability possessed by the willin FERM domain.

The other members of the ERM family are known to bind to, and be regulated by, PIP2 (section 1.5.5). It was unknown if willin would also bind to PIP2 or perhaps some other members of the phosphoinositide family. The initial stages of the investigation involved the expression of the willin protein as a GST fusion protein, which would permit its purification. The purified protein could then be used to observe willin's involvement in protein-lipid interactions.

Willin's phospholipid binding partners were investigated initially via a protein lipid overlay (PLO) procedure (Dowler et al, 2002). This involves the incubation of the purified protein with membranes containing phospholipids that are spotted onto the membrane in a concentration gradient. Interactions of the protein with the phospholipids can then be determined via signals from bound antibodies in a manner similar to that used in western blotting. Following on from the protein lipid overlay experiments, additional information on phospholipid interactions would be gleaned from the *in vivo* dynamics of full length willin tagged with enhanced green fluorescent protein (EGFP) when membrane phospholipid levels were chemically altered.

Since the willin FERM domain can also interact with proteins, preparations were made for a yeast two hybrid library screen. It was hoped that the use of such a screen would enable the identification of other proteins that bound to willin, which would then help to provide more information as to the function of the protein.

For the construction of each of the plasmids shown below, primer and DNA sequences are contained in Appendices I - III.

5.3.1 Construction of the plasmid pGex-Rat

The construct p163scII contained the original fragment of the rat willin gene that had been isolated from a sciatic nerve library during a yeast-two-hybrid screen. The fragment of the DNA that was present in the plasmid encompassed the N-terminus of the gene, which contained the FERM domain. To enable the expression of the N-

terminus of the protein as a GST fusion protein, the gene fragment was cloned into the pGEX-KG vector (figure 5.1).

Two oligonucleotide primers were designed which would anneal to the 5' and 3' end of the target DNA in the p163scII construct and enable the amplification of the sequence of interest with the addition of novel restriction enzyme sites. The forward primer was Willin4, which added an EcoRI site to the 5' end of the sequence adjacent to the first codon. The reverse primer was Willin5, which added a XhoI site to the 3' end of the sequence and a stop codon.

The primers were used to amplify the available N-terminal sequence of the rat willin gene. The amplified fragment and the pGexKG vector were digested with the restriction enzymes EcoRI and XhoI, ligated and transformed into competent DH5α *E.coli* cells. Several of the resulting colonies were analysed for their plasmid content. Positive clones were initially identified by analysing the size of the band produced on an agarose gel following restriction enzyme digests.

To check that the plasmid DNA from the positive clones contained the pGex-Rat construct, the DNA from one of the positive clones was analysed by automated sequencing. The results from the sequencing confirmed that the 163scII fragment, minus the upstream sequence prior to the gene's first codon, had been cloned into the pGex-KG vector.

The primer and DNA sequences used for the construction of each plasmid are contained in Appendices I - III.

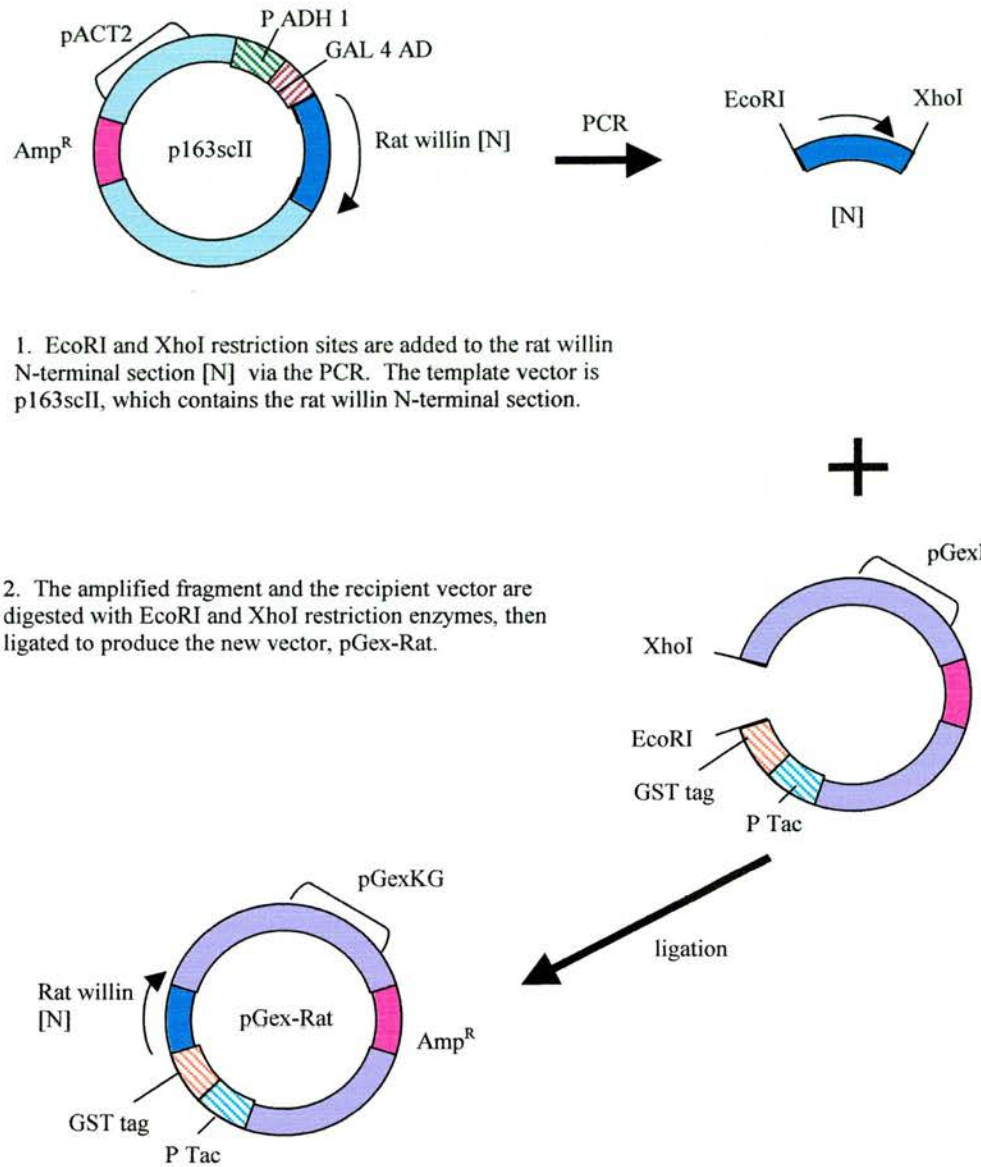

Figure 5.1. Construction of the expression vector pGex-Rat, which contains the N-terminal section [N] of the rat willin gene. AD = activation domain, p = plasmid, P = promoter.

5.3.2 Expression of the plasmid pGex-Rat

The pGex-Rat clone was transformed into competent BL21(DE3)pLysS *E.coli* cells, as described in section 2.1.14, and the transformed cells were plated onto antibiotic selective agar plates. One of the resulting colonies was picked and grown in the appropriate media, then induced as described in small scale expression of proteins (section 2.2.10). The uninduced and induced samples were analysed by SDS-PAGE (figure 5.2).

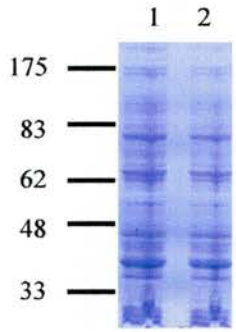

Figure 5.2. Coomassie-stained SDS-PAGE gel showing bacterial lysates that contained (1) uninduced pGex-Rat and (2) induced pGex-Rat.

The predicted size of the fusion protein is 66.5kDa. No band of this size could be seen in the induced lane.

5.3.3 Construction of the plasmid pR-ET

In an attempt to circumvent the problem of lack of expression from the pGex-Rat construct, the same gene fragment was cloned into a different expression vector, pET15b (figure 5.3), which produces fusion proteins with a C-terminal His tag. Two oligonucleotide primers were designed to allow the amplification of the DNA sequence from the template vector, p163scII. The forward primer was RWiletF,

initiating methionine codon. The reverse primer was RWilasR, which added a BamHI site to the 3' end of the sequence and a stop codon.

Positive clones were identified by restriction enzyme digests and automated sequencing. The results from the sequencing confirmed that the rat willin fragment had been successfully cloned into the pET15b vector.

The primer and DNA sequences used for the construction of each plasmid are contained in Appendices I - III.

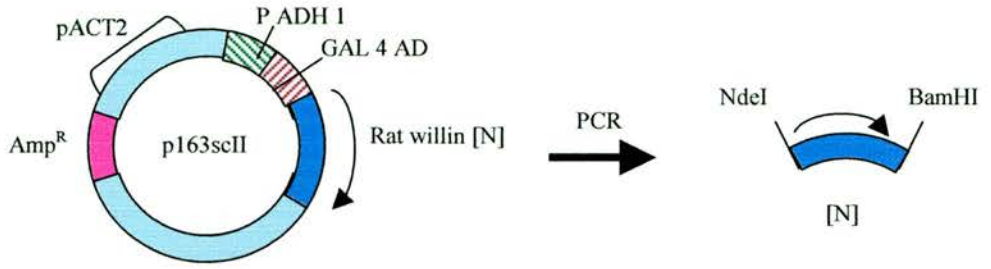

1. NdeI and BamHI restriction sites are added to the N-terminal section [N] of the rat willin gene via the PCR. The template vector is p163scII, which contains the rat willin N-terminal section.

+

2. The amplified fragment and the recipient vector are digested with NdeI and BamHI restriction enzymes, then ligated to produce the new vector, pR-ET.

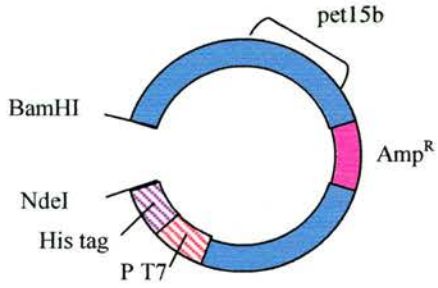

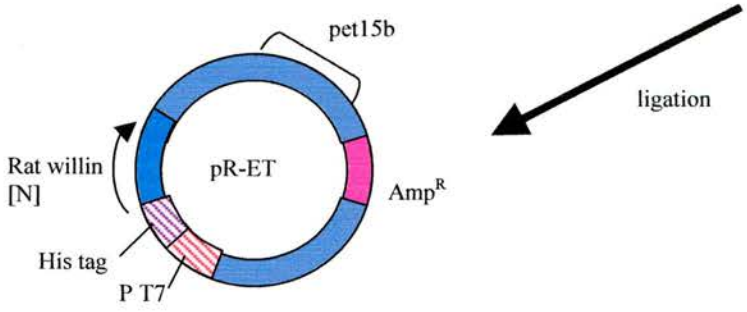

Figure 5.3. Construction of the expression vector pR-ET, which contains the N-terminal section [N] of the rat willin gene. AD = activation domain, p = plasmid, P = promoter.

5.3.4 Construction of the plasmid pH-ET

Shortly after the construction of and expression attempts with the pGex-Rat construct, the first full length willin gene had become available. This full length IMAGE clone, containing the willin sequence from uterine cells, was purchased by our laboratory from the MRC UK HGMP Resource Centre. Oligonucleotide primers were designed to enable the N-terminus of the human willin gene, equivalent to the section of the rat isoform present in the pR-ET construct, to be cloned into the pET15b expression vector (figure 5.4).

The forward oligonucleotide primer used to amplify the sequence was HWiletF, which added an NdeI site to the 5' end of the sequence and which incorporated the initiating methionine codon. The reverse primer was HWilasR, which added a BamHI site to the 3' end of the sequence and a stop codon.

DNA sequencing confirmed that the human N-terminal fragment had been successfully cloned into the pET15b vector.

The primer and DNA sequences used for the construction of each plasmid are contained in Appendices I - III.

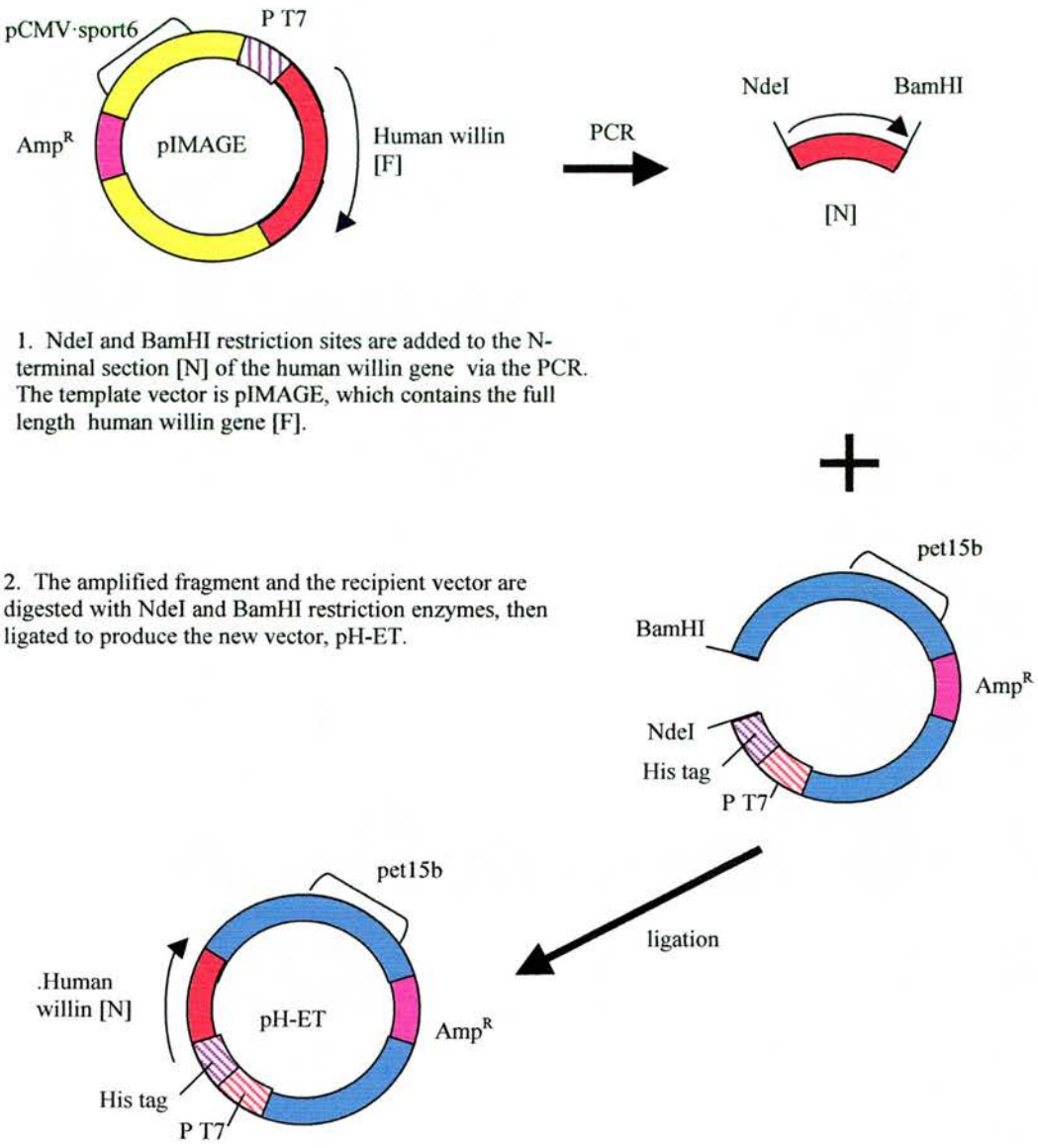

Figure 5.4. Construction of the expression vector pH-ET, which contains the N-terminal section [N] of the human willin gene. p = plasmid, P = promoter.

5.3.5 SDS-PAGE analysis of the plasmids pGex-Rat, pR-ET and pH-ET

The constructs pR-ET and pH-ET were transformed into competent BL21(DE3)pLysS *E.coli* cells (section 2.1.14). The transformed cells were used to inoculate mini-cultures which were then induced and prepared for electrophoresis, as described in section 2.2.10. Another attempt was also made at this time to induce the expression of the pGex-Rat protein.

Uninduced and induced samples of pGex-Rat, pR-ET and pH-ET were analysed via an SDS-PAGE gel (figure 5.5).

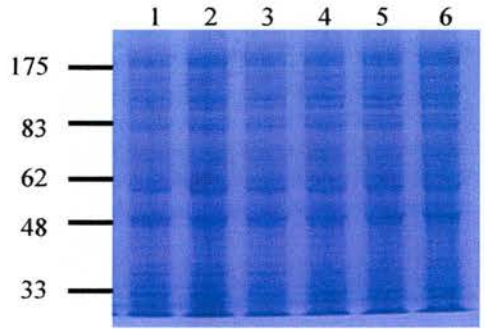

Figure 5.5. Coomassie-stained SDS-PAGE gel showing bacterial lysates containing (1) uninduced pGex-Rat (2) induced pGex-Rat (3) uninduced pR-ET (4) induced pR-ET (5) uninduced pH-ET (6) induced pH-ET. Expected sizes: pGex-Rat – 66.5kDa, pR-ET – 39kDa, pH-ET – 38kDa.

However, as shown in figure 5.5, none of the constructs appeared to be expressing, at least not at a level discernible via Coomassie staining; no lane containing lysates from cells that had been induced appeared to have any band present that was not present in the uninduced lane.

5.3.6 Western blot analysis of pGex-Rat

Since no expression could be observed from any of the three constructs using Coomassie staining, a more sensitive method of detecting protein expression levels was then used, which was western blotting.

The pGex-Rat construct was analysed first. As it is sometimes the case that fusion proteins, for various reasons, are degraded by the cell shortly after they are produced, a time point analysis of the pGex-Rat construct was set up. This entailed sampling the culture at set times after the beginning of the induction. If the fusion protein was being produced but was not remaining intact for very long, the timepoints would give an indication of the best time, if any, to catch the fusion protein when the majority of it was in its intact form.

The timepoints used were 30 mins, 50 mins and 70 mins post-induction. At each of these timepoints, 1ml of the sample was removed and resuspended in protein sample buffer (section 2.2.10). An aliquot of uninduced cells was removed prior to induction for use as a negative control. The samples were applied to an SDS-PAGE gel and electrophoresed then transferred to nitrocelluose membrane which was blocked overnight (section 2.2.8). The membrane was incubated in a 1:2000 dilution of 914[3] antibody followed by a 1:2000 dilution of anti-rabbit HRP antibody (Figure 5.6).

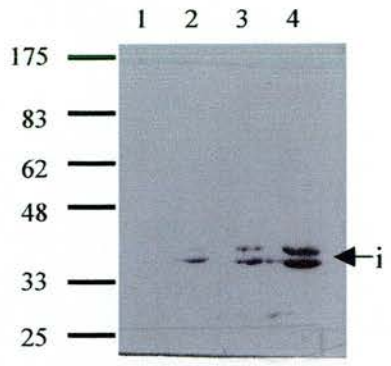

Figure 5.6. Western blot analysis of expression from pGex-Rat, expected size 66.5kDa. Times given are post-induction. (1) uninduced control (2) 30 mins (3) 50 mins (4) 70 mins.

The western blot in figure 5.6 implied that the GST-Rat fusion protein was being degraded since at no point, even relatively early in the induction, is there a band present that could represent the intact fusion protein present. The bands between the 33 and 48kDa marks of the ladder (figure 5.6, ←i) were likely to be the breakdown products of the fusion protein, as they increase in intensity over time.

5.3.7 Western blotting with pR-ET and pH-ET

The experiments that were performed with the pGex-Rat construct revealed that it would not be possible to purify the expressed protein in its intact form no matter how long or short the induction time was. Attention was then focussed on the pR-ET and pH-ET constructs. Western blots were again performed but despite several attempts at producing fusion proteins from these two constructs, no expression at all could be detected from either of them, either as intact fusion proteins or otherwise.

Induced bacterial samples containing the pGex-Rat construct were included on the SDS-PAGE gels used in the analysis of these two constructs in order to confirm that the problem lay with the expression levels from the vectors and not with the western

blot procedure itself, but whilst a signal was always obtained (albeit from the suspected degraded products) from the induced pGex-Rat lanes, no expression was observed in the induced pHET and pRET lanes.

Several strategies were used to try to effect expression from the two constructs, such as transforming them into a fresh batch of cells, selecting several different colonies for analysis and adding glucose to the growth media. Glucose is used to repress the background "leaky" expression from a vector prior to induction, since the products of the expression may be toxic to the host, causing an inhibition of cell growth (Doherty et al, 1993). However, none of these remedial steps caused the pRET nor pHET constructs to express any detectable levels of the fusion proteins they coded for.

5.3.8 Construction of the plasmid pGex-HFL

As the pGex-Rat fusion protein was not detectable in its intact form, and there was no expression of any kind from the pR-ET and pH-ET constructs, a further attempt was made at producing an intact fusion protein. This next construct was based on the pGexKG vector and the full length sequence of human willin was used (Figure 5.7).

Two oligonucleotide primers were designed which would anneal to the 5' and 3' end of the IMAGE clone and enable the amplification of the whole sequence with the addition of novel restriction enzyme sites. The forward primer was HGexF, which added a BamHI site to the 5' end of the sequence. The reverse primer was HWilacR, which added an EcoRI site to the 3' end of the sequence and a stop codon.

Positive clones were identified by restriction enzyme digests and subsequently confirmed by automated DNA sequencing.

The primer and DNA sequences used for the construction of each plasmid are contained in Appendices I - III.

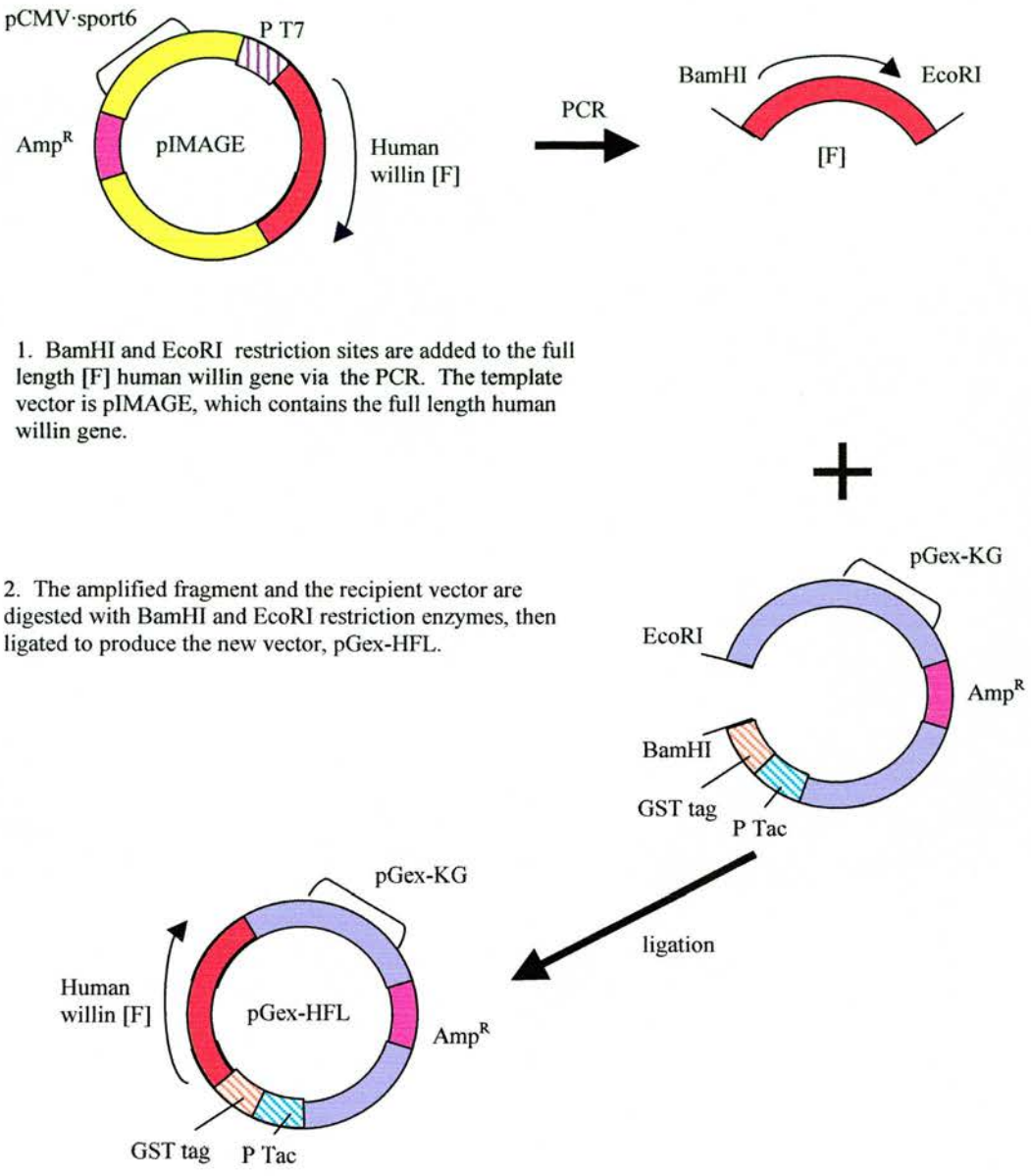

Figure 5.7. Construction of the expression vector pGex-HFL, which contains the full length[F] human willin gene. P = promoter, p = plasmid.

5.3.9 Expression and western blotting of pGex-HFL

The pGex-HFL plasmid was transformed into competent BL21(DE3)pLysS *E.coli* cells. Two different post-induction timepoints were used for the preliminary western blot with pGex-HFL, due to the problems that had occurred with the pGex-Rat plasmid. The timepoints used were 45 and 90 mins (section 2.2.10). Also, four different colonies were selected from the transformation plate (section 2.1.14). An aliquot of uninduced cells was removed prior to induction for use as a negative control. A western blot was performed in the usual manner (section 2.2.8). The membrane was incubated in a 1:2000 dilution of 914[3] antibody followed by a 1:2000 dilution of anti-rabbit HRP antibody (Figure 5.8).

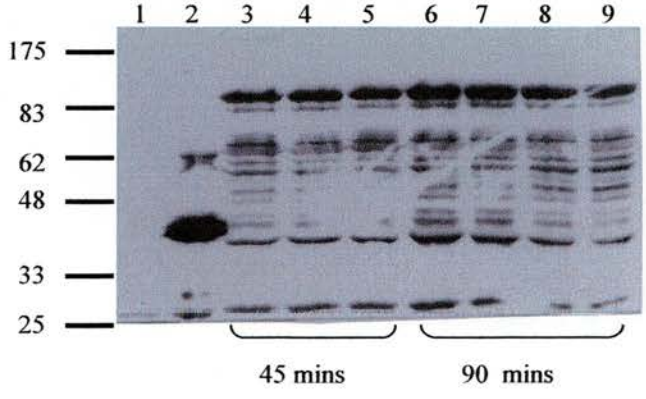

Figure 5.8. Western blot timepoint analysis of pGex-HFL. (1) uninduced colony 1 (2) positive control [induced pGex-Rat] *All the following samples were induced, times given are post-induction, c = colony* (3) C2, 45 mins (4) c3, 45 mins (5) c4, 45 mins (6) c1, 90 mins (7) c2, 90 mins (8) c3, 90 mins (9) c4, 90 mins. Expected size pGex-HFL – 98kDa.

This western blot, figure 5.8, reveals a band of the correct size (98 kDa) appearing in all the lanes carrying induced samples. No corresponding band appeared in the uninduced sample. As would be expected, most of the samples that were induced for

90 minutes had a band of increased density compared to those that were induced for 45 minutes, indicating that the band does indeed represent the fusion protein. A considerable amount of the protein also appears beneath the 98kDa band as breakdown products, but the 98kDa band was deemed strong enough to allow purification.

5.3.10 Small scale purification of pGex-HFL

A small scale purification of the pGex-HFL fusion protein was attempted using glutathione-sepharose beads (section 2.2.12). After boiling the supernatant/beads mixture in protein sample buffer, the sample was loaded onto an SDS-PAGE gel which was then Coomassie blue stained and destained. No band of the expected size could be seen in the lane that should have contained the purified protein. As this indicated a possible problem with the solubility of the protein, the procedure was repeated but this time the pellet that resulted after the lysis and centrifugation of the induced cells (this point is indicated in section 2.2.12) was included on the SDS-PAGE gel. The gel was transferred to nitrocellulose membrane to allow a western blot to be performed, as this would allow the detection of any bands that might not be visible from Coomassie staining. The membrane was incubated with a 1:2000 dilution of 914[3] antibody and a 1:2000 dilution of anti-rabbit HRP antibody (Figure 5.9).

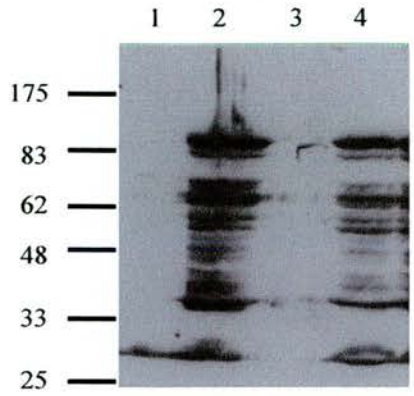

Figure 5.9. Analysis of fractionated lysates containing the pGex-HFL construct. (1) Uninduced pGex-HFL (2) Induced pGex-HFL, pellet fraction (3) Induced pGex-HFL, supernatant fraction (4) Induced pGex-HFL, whole cell extract. Expected size pGex-HFL – 98kDa.

The western blot in figure 5.9 revealed that the pGex-HFL fusion protein was almost entirely insoluble. Most of the fusion protein is visible in the lane that contains the cell pellet, with only a very small amount appearing in the lane that corresponding to the soluble fraction. To allow the protein to be purified, it would first have to be solubilised.

5.3.11 Solubilisation of pGex-HFL

To find the best method for solubilising the GST-HFL fusion protein, various different chemicals and conditions were used. Each chemical or condition was usually tested over a range; for example, the inclusion of sorbitol in the growing media at concentrations of 02.% - 5% v/v. The samples were all processed according to the method described in small scale purification of proteins (section 2.2.12) except that the protein was not eluted from the beads, since at this stage it was sufficient to know whether enough protein was being solubilised so as to promote its presence in the supernatant and hence allow binding to the beads. Therefore, after each sample was mixed with the beads, protein sample buffer was added to the bead/lysate

mixture, the tube was boiled for three minutes and then equal amounts of the samples were loaded onto an SDS-PAGE gel. The chemical or condition that, upon Coomassie blue staining of the gel (section 2.2.6), gave the strongest band when compared to a control was noted. Then the next chemical or condition would be examined until finally a protocol was devised that, via a combination of the most successful conditions and chemicals tested, enabled the purification of the fusion protein.

Each chemical or condition listed below was analysed separately.

5.3.12 Alterations to the induction conditions

Molecular chaperones have been found to assist in the solubilisation of some insoluble proteins (reviewed in Dobson, 2004). Since the possibility existed that the GST-HFL protein was insoluble due to incorrect folding during the induction process, an attempt was made to correct this by heat shocking the cultures for a few minutes prior to induction, to enhance the activity of heat shock proteins and thereby encourage the correct folding of the protein. Two different heat shock temperatures were used, 42°C and 50°C, over timepoints ranging between 30 secs to 5 mins. In other experiments, the amount of IPTG used to induce the protein was lowered by 5x and 10x to produce less of the protein over a given time period. This modification was intended to produce much less of the fusion protein during any given time period and hence not overwhelm the cell's capacity to fold the protein correctly. However, none of these approaches appeared to aid in the solubility of the protein.

5.3.13 Alterations to the growing media

The solubility of a protein can sometimes be enhanced by the addition of sorbitol or sucrose to the bacterial growth media (Blackwell and Horgan, 1991). The addition of these compounds leads to an increase in osmotic pressure, which in turn leads to the accumulation of osmoprotectants in the cell. These osmoprotectants stabilise the native protein structure. Mini-cultures were grown with the inclusion of sorbitol in the LB at a final concentration of between 02.% - 5% v/v. However, the presence of the sorbitol had no effect on the fusion protein's solubility.

A further attempt was made at enhancing the solubility of the protein at the production stage rather than at the purification stage, which was the use of Yeast Terrific (YT) broth - a rich media containing extra nutrients - to grow the cultures in. Two mini-cultures were set up to test this condition (section 2.1.12). Both were inoculated with identical amounts of BL21(DE3)pLysS *E.coli* cells containing the pGex-HFL construct, but the control culture was grown in the usual LB media and the other culture was grown in YT broth. A slightly stronger band from the YT broth sample on the resulting SDS-PAGE gel revealed that YT broth did enhance the solubility of the protein to a small extent.

5.3.14 Varying the pH of the buffer

The proximity of a protein to its isoelectric point (pI) value affects its solubility. The zero net charge carried by a protein when it reaches its pI results in the protein being at its least soluble at this point (reviewed in Turner et al, 2000). This can cause the protein to fall out of solution. Therefore, altering the pH of the buffer that the cell extracts are lysed in can help improve solubility. The control buffer used was

500mM Tris pH7. Several different buffers were made with an increasing pH so that the solubilisation of the protein was examined at 500mM Tris pH7.5, pH8, pH8.5, pH9 and pH9.5. The lysate from the 500mM Tris pH9.5 sample revealed that the solubility of the protein had been slightly increased by the use of this buffer.

5.3.15 Solubilisation via guanidinium salts

Chaotropic agents such as urea or guanidinium compounds may be used in the solubilisation of proteins, since chaotropes destroy the structure of water, thereby decreasing the hydrophobic effect and encouraging proteins to unfold and dissociate (reviewed in Matthews and van Holde, 1996). Solubilisation of the protein using 6M guanidinium hydrochloride (section 2.2.11) was examined concurrently with the sarkosyl method (section 5.3.16 below), and both methods showed a much enhanced solubilisation of the protein compared to a control. The use of guanidinium hydrochloride actually produced stronger bands on SDS-PAGE gels than the use of sarkosyl, indicating guanidinium's stronger ability as a solubilising agent. However, the sarkosyl method produced adequate amounts of the solubilised protein and since guanidinium salts are very strong denaturants, proteins can be irreparably damaged by the use of these compounds. For this reason, the sarkosyl method was chosen over the guanidinium method.

5.3.16 Use of detergents

Detergents are also widely used to solubilise proteins (reviewed in Garavito et al, 2001). Several detergents were used in preliminary trials to see what effect, if any, they would have on the solubility of the protein. Detergents such as the non-ionic detergent Triton X-100 and the alkyl glucoside n-octyl-β-D-glucopyranoside were

added at various concentrations to cell lysates immediately post-sonication (section 2.2.12) but no improvement could be seen in the solubility of the GST fusion protein. Sarkosyl (n-lauroyl sarcosine) is another detergent which is frequently used to solubilise proteins (Frangioni et al, 1993), and when this detergent was tested in the lysis buffer (section 2.2.12), a increased degree of solubilisation was evident on subsequent SDS-PAGE gels.

However, sometimes the presence of the detergent in the final protein preparation is undesirable. Dialysis can remove detergents but this depends on certain factors such as the detergent's critical micelle concentration (CMC), above which a detergent aggregates into micelles (reviewed in Kalipatnapu et al, 2005). To be dialyzable, the concentration of the sarkosyl had to be kept below 0.42%, and so a small scale purification (section 2.2.12) was attempted using sarkosyl at a concentration of 0.3% v/v. The use of sarkosyl this concentration in the lysis buffer resulted in a successful small scale purification which was followed by 24 hours of dialysis (section 2.2.15) to remove the sarkosyl from the purified protein. The protein did not precipitate upon the removal of sarkosyl via dialysis. Furthermore, the post-dialysis protein sample was then reincubated with gluthatione-sepharose beads to ensure that the purified protein would still bind to the beads, which it did.

5.3.17 Medium scale purification of the pGex-HFL protein

The quantities of purified protein that were obtained from the small scale purification method were not sufficient for the protein lipid overlay experiments that were intended to follow. Therefore the small scale protocol was scaled up and then

optimised in as many ways as was deemed necessary, including, for example, the observation of the most advantageous:

- volume of glutathione-sepharose beads to bacterial pellet
- sonication times
- temperature and length of time for incubation of beads with bacterial lysates
- volume and constituents of lysis buffer
- volume and constituents of elution buffer
- temperature and length of time for eluting the protein from the beads

The final protocol that was developed is that given in section 2.2.13 (small scale/2.2.14 (medium scale).

To illustrate the difference between the original protocol and the new protocol, two mini-cultures containing the pGEX-HFL construct were induced and harvested and then one culture was treated according to the description given in 2.2.12 (a generalised protocol for small scale preparation of proteins) whilst the other was treated according to the description given in 2.2.13 (the specific protocol developed as a result of the research above). Equal amounts of the two resulting purified protein preparations were loaded onto an SDS-PAGE gel which was Coomassie-stained after electrophoresis. The gel is shown in figure 5.10.

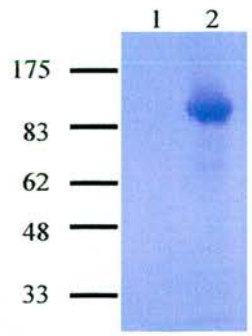

Figure 5.10. Comparison of the old and new purification protocols for the pGex-HFL fusion protein. Both lanes contain equal amounts of eluant. Lane (1) contains a protein solution prepared according to the method described in 2.2.12. Lane (2) contains a protein solution prepared according to the method described in 2.2.13. Expected size pGex-HFL – 98kDa.

It can be seen from the SDS-PAGE gel in figure 5.10 that the former protocol (section 2.2.12) did not enable any visible quantity of the pGex-HFL protein to be purified, whereas the new protocol (section 2.2.13) resulted in detectable amounts of the fusion protein.

5.3.18 Protein Lipid Overlay

The purification of the GST-HFL protein enabled the investigation into the possibility of whether or not willin, like the other members of the ERM family, can bind to phospholipids (section 1.5.5). Commercially available strips of membrane (Echelon) containing phospholipids that were spotted onto them in seven different concentrations had been purchased by this laboratory. The aim of the experiment was to determine if willin interacts with any of the phospholipids. Any positive interactions would result in the GST-HFL protein adhering to an immobilised phospholipid, thereby becoming itself immobilised, and a signal should therefore result, via anti-GST antibody, at the place on the membrane where that particular phospholipid had been spotted.

Dowler et al (2002) recommend using 1-10nM of purified protein for the PLO assay. A mid-range quantity was selected and the experiment was performed using 5nM of the purified, dialysed GST-HFL (section 2.2.16). The antibody used was anti-GST at a 1:2000 dilution. The result is shown in fig 5.11.

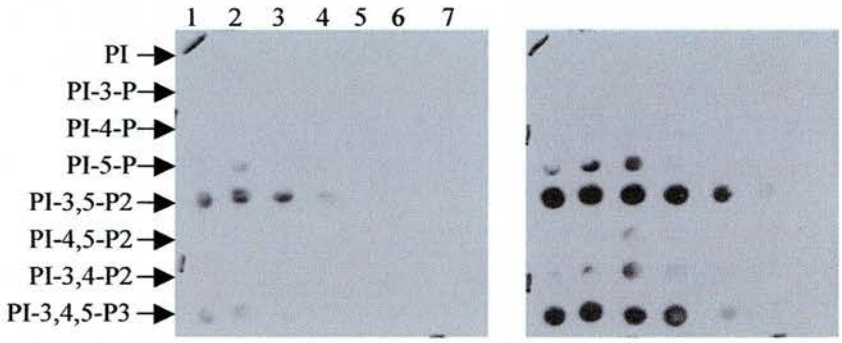

Figure 5.11. Protein lipid overlay using 5nM GST-HFL. Left hand side: 30 second exposure, right hand side: 5 minute exposure. PI = phosphatidyl inositol PI-3-P = phosphatidyl inositol-3-phosphate PI-4-P = phosphatidyl inositol-4-phosphate PI-5-P = phosphatidyl inositol-5-phosphate PI-3,5-P2 = phosphatidyl inositol-3,5-bisphosphate PI-4,5-P2 = phosphatidyl inositol-4,5-bisphosphate PI-3,4-P2 = phosphatidyl inositol-3,4-bisphosphate PI-3,4,5-P2 = phosphatidyl inositol-3,4,5-triphosphate Concentration of phospholipids per spot: lane (1) 100pmol (2) 50pmol (3) 25pmol (4) 12.5pmol (5) 6.3pmol (6) 3.2pmol (7) 1.6pmol.

The film on the left in figure 5.11 shows that the strongest affinity of the GST-HFL is apparently for PI-3,5-P2. The film on the right in figure 5.11 reveals that the second strongest affinity is for PI-3,4,5-P3. Some degree of binding can also be observed with PI-5-P and PI-3,4-P2. These results were unexpected as the other members of the ERM family are primarily known to bind to PI-4,5-P2, whereas the results above suggest that willin binds to PI-4,5-P2 with only the fifth highest affinity out of the eight phospholipids. The PLO was repeated using the same quantity of the fusion protein and the same result ensued.

A construct containing a control fusion protein had been kindly donated by Dr Maria Deak, University of Dundee. This protein is known as DAPP [dual adaptor for phosphotyrosine and 3-phosphoinositides] 1 and it is known to bind to both PI-3,4,5-P3 and PI-3,4-P2 (Dowler et al, 1999). The GST-DAPP1 construct was transformed into competent BL21(DE3)pLysS *E.coli* and one of the resulting colonies was used to inoculate a mini-culture. An uninduced sample of the culture was removed as a control and the mini-culture was then induced and prepared for electrophoresis. The uninduced and induced samples were analysed by SDS-PAGE and the resulting gel showed a band of the correct size in the induced lane. No band of a similar size could be seen in the uninduced lane.

A medium scale purification and dialysis of the GST-DAPP1 protein was then performed, with all conditions being kept identical to those used to produce the GST-HFL protein (sections 2.2.14 and 2.2.15). The purified GST-DAPP1 protein was then used in a PLO experiment at 5nM (figure 5.12).

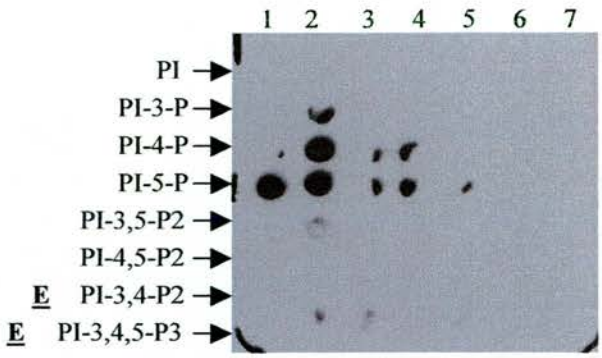

Figure 5.12. Control protein lipid overlay using 5nM GST-DAPP 1. **E** = expected binding sites. PI = phosphatidyl inositol PI-3-P = phosphatidyl inositol-3-phosphate PI-4-P = phosphatidyl inositol-4-phosphate PI-5-P = phosphatidyl inositol-5-phosphate PI-3,5-P2 = phosphatidyl inositol-3,5-bisphosphate PI-4,5-P2 = phosphatidyl inositol-4,5-bisphosphate PI-3,4-P2 = phosphatidyl inositol-3,4-bisphosphate PI-3,4,5-P2 = phosphatidyl inositol-3,4,5-triphosphate Concentration of phospholipids per spot: lane (1) 100pmol (2) 50pmol (3) 25pmol (4) 12.5pmol (5) 6.3pmol (6) 3.2pmol (7) 1.6pmol.

The results were again unexpected. The GST-DAPP 1 protein was observed to bind mainly to PI-4-P and PI-5-P instead of PI-3,4-P2 and PI-3,4,5-P3.

Since the fusion protein was not involved in any kind of targeting experiments where the presence of a protein at the N-terminus would be undesirable, it had not been deemed necessary to cleave the GST moiety from the fusion protein prior to the PLO assays. A final control PLO was therefore performed to ensure that the observed binding was not due to interference by the GST headgroup of the fusion proteins. The control PLO was performed using GST that was extracted and dialysed under identical conditions to those used for the purification of the GST-HFL and the GST-DAPP proteins (sections 2.2.14 and 2.2.15). No binding of GST alone was observed with any of the phospholipids.

5.4.1 Live cell imaging using EGFP-tagged willin

A plasmid had been constructed, as described in section 4.3.1, which contained the full length willin gene in the vector pEGFP-N1. This vector allows the expression of the protein of interest along with EGFP fused to the C-terminus of the protein. The resulting construct was named pHFL-EGFP.

As it was known that other members of the ERM family interacted with PIP2 (section 1.5.5), and evidence had been obtained that willin could also bind to phospholipids (section 5.3.18), live cell imaging was then used to try and capture any movement of the protein when the phospholipid levels of a transfected cell were altered.

An attempt at live imaging had been made at the University of St Andrews using the DeltaVision® RT Restoration Imaging System but the results were inconclusive. The cells had been imaged at timepoints of 1, 2, 8 and 16 minutes after stimulation and it was thought that the movements of the protein may have occurred too rapidly to be captured over this timescale. The Wallac UltraVIEW confocal microscopes at the University of Bristol are capable of imaging over a scale of seconds, rather than minutes, and it was hoped that imaging the cells over this narrower time scale would prove more productive. Experiments were then carried out at the University of Bristol, with the generous assistance of Professor Jeremy Tavaré, Dr Gavin Welsh and the other members of the Tavaré lab.

ARNO (ARF nucleotide-binding-site opener) is a protein that is known to bind to PIP3 via its C-terminal pleckstrin homology domain (Venkateswarlu et al, 1998a). EGF causes an elevation in PIP3 levels via the activation of PI3K (reviewed in

Carpenter and Cohen, 1990), and members of the family of guanine nucleotide exchange factors for ARFs (ADP ribosylation factors), of which ARNO is one, have been found to translocate rapidly to the PM of PC12 cells following EGF stimulation (Venkateswarlu et al, 1998b; Venkateswarlu et al, 1999).

Since a construct containing ARNO-GFP had been kindly donated by Dr Kanamarlapudi Venkateswarlu, University of Bristol, a control was therefore available to ensure that the transfection and imaging conditions during the experiments at the University of Bristol were not at fault should the distribution of the willin-EGFP protein fail to change. However, as stated previously (section 5.3.18), it was not known exactly which phospholipids willin interacted with. Therefore the aim of the live imaging experiments was not to investigate if willin-EGFP moved in a manner similar to ARNO-EGFP, but was instead to investigate if willin-EGFP moved at all.

5.4.2 EGF stimulation of pARNO-GFP-transfected PC12 cells

To check if the ARNO-GFP protein could be made to move to the plasma membrane, PC12 cells were transfected (as described in Gunn-Moore et al, 2005) with the pARNO-GFP construct and left for 24 hours. The cells were then serum starved for 3 hours before being placed under the microscope. EGF was added to the cells to a final concentration of 100ng/ml and then the first image was immediately taken, which is referred to as the time = 0 image. Images were then taken every ten seconds for a total of approximately ten minutes. The results of this experiment are shown in figure 5.13.

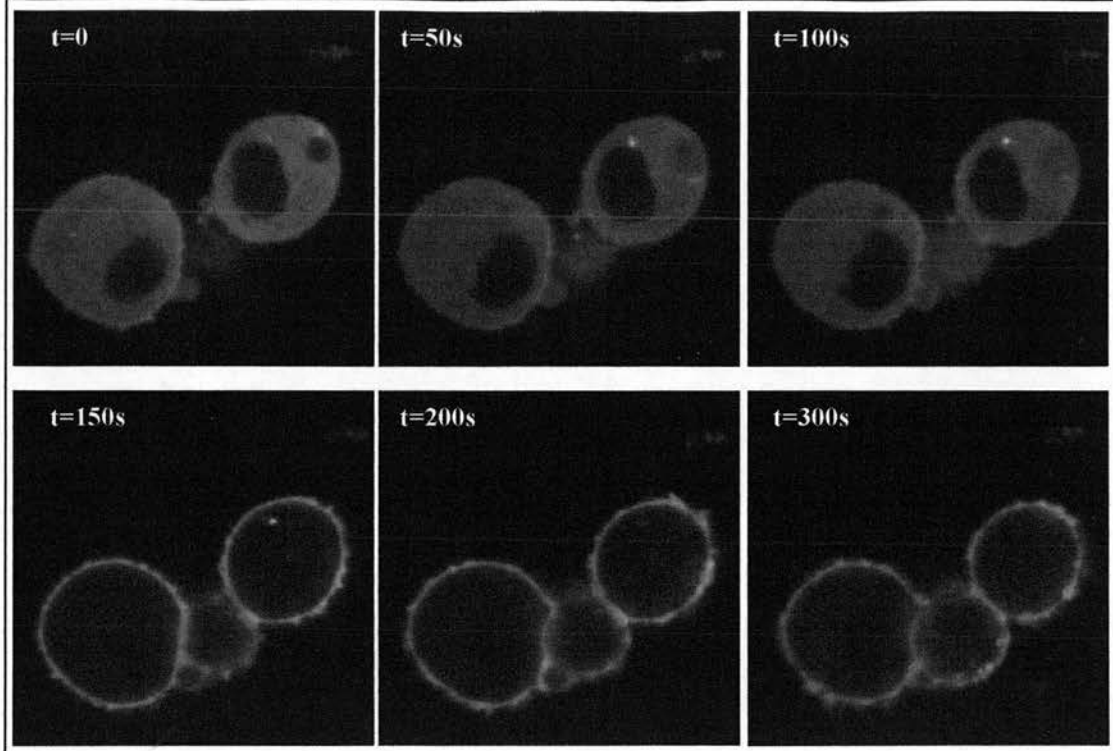

Figure 5.13. Time lapse imaging of PC12 cells transfected with ARNO-GFP. All times are given in seconds (s). At t=0, EGF was added to the cells.

The images in figure 5.13 confirmed that ARNO-GFP was recruited to the PC12 cell membranes in response to EGF.

5.4.3 EGF stimulation of pHFL-EGFP-transfected PC12 cells

PC12 cells were then transfected with the pHFL-EGFP construct. The cells were treated in exactly the same manner as those transfected with the pARNO-GFP cells. Again, EGF was added to a final concentration of 100ng/ml and the cells were imaged every ten seconds for up to ten minutes (figure 5.14).

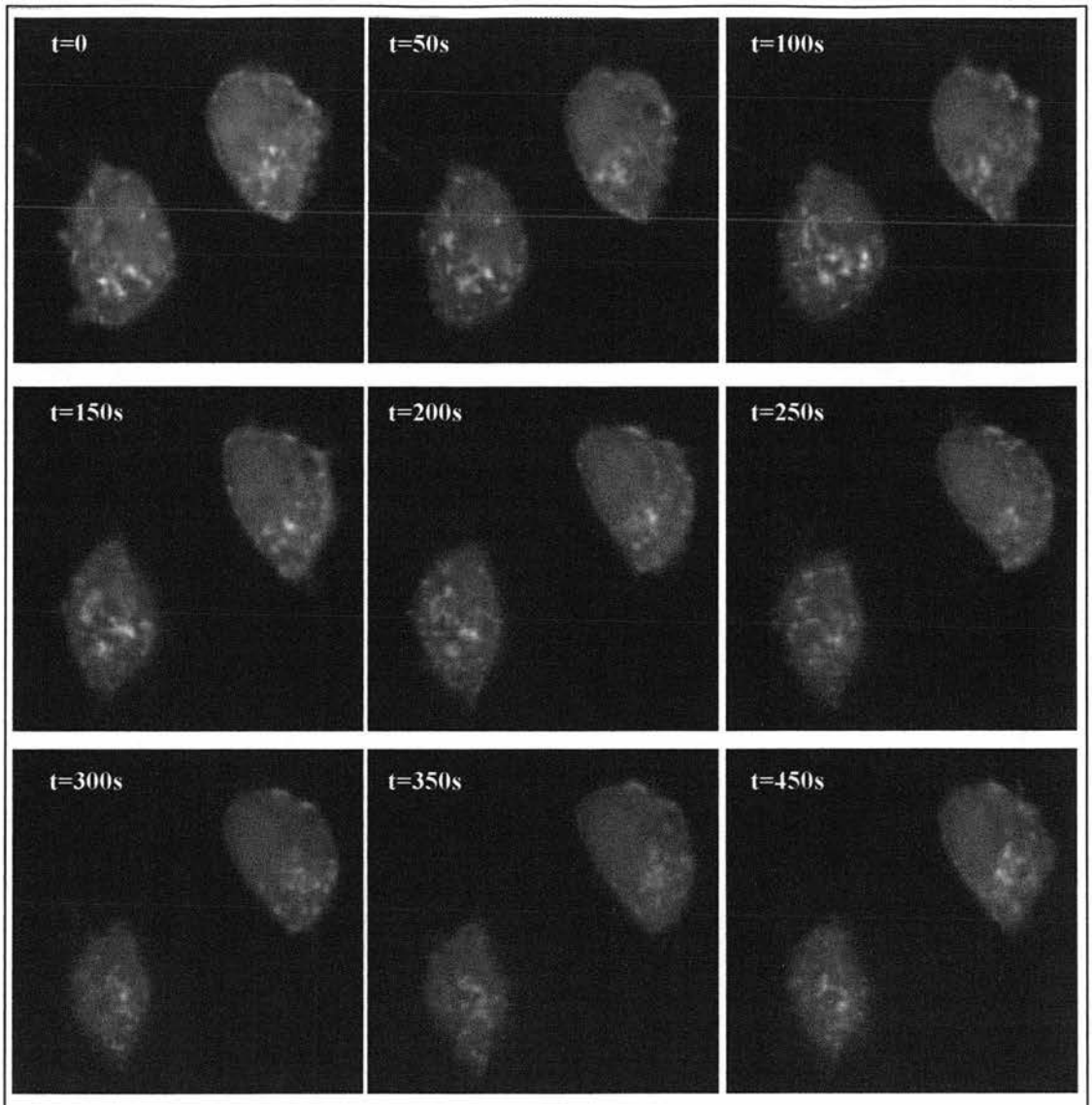

Figure 5.14. Time lapse imaging of PC12 cells, batch 1, transfected with pHFL-EGFP. All times are given in seconds (s). At t=0, EGF was added to the cells.

Although the lower cell drifted slightly, it appeared that in both of the PC12 cells shown in figure 5.14, there was no movement of willin. However, the experiment was repeated with several different dishes of PC12 cells and in some of these cells there was an alteration in their appearance. Figure 5.15 shows an example of this.

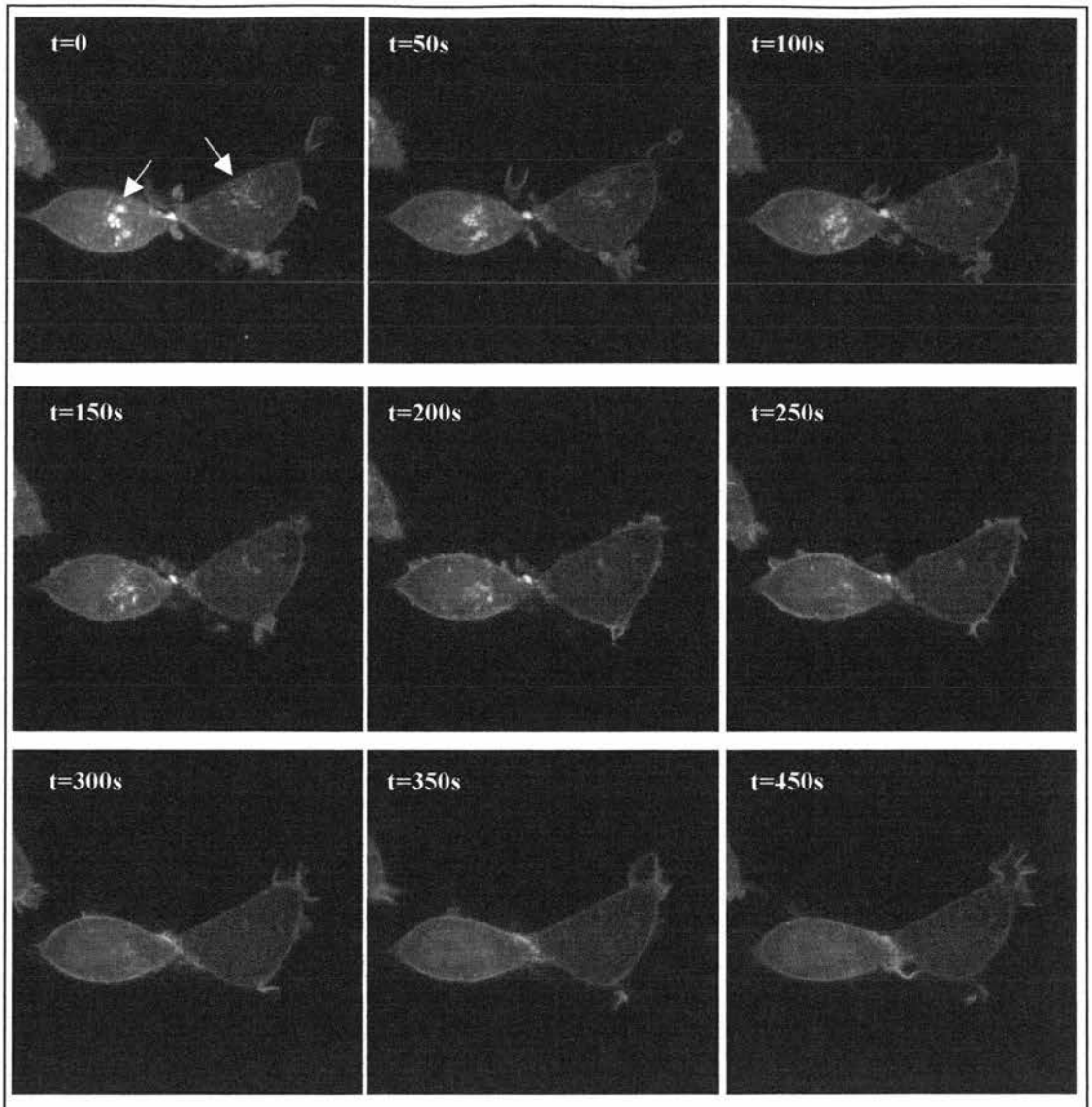

Figure 5.15. Time lapse imaging of PC12 cells, batch 2, transfected with pHFL-EGFP. All times are given in seconds (s). At t=0, EGF was added to the cells.

The cells in figure 5.15 show that willin seemed to move out of cytoplasm of these cells following the addition of EGF. Any recruitment to the PM of the cells was not overly obvious, possibly since the cells already had a ring of willin around the PM to begin with. It was also apparent in these images that the particularly bright area of each of the cells (Figure 5.15(t=0), arrows) became noticeably fainter as time progresses. Additionally, in contrast to the dulling of the aforementioned bright patch

of the cell as time progresses, the nucleus of the cell on the left appeared to become brighter as time progresses; although possibly the nucleus is simply more visible because willin had cleared from the cytoplasm.

Another cell, shown in figure 5.16, again indicated that willin leaves the cytoplasm, and again leaves the bright perinuclear pool (figure 5.16(t=0), arrow). It also seems from these images that the protein had been recruited to the PM after the addition of EGF.

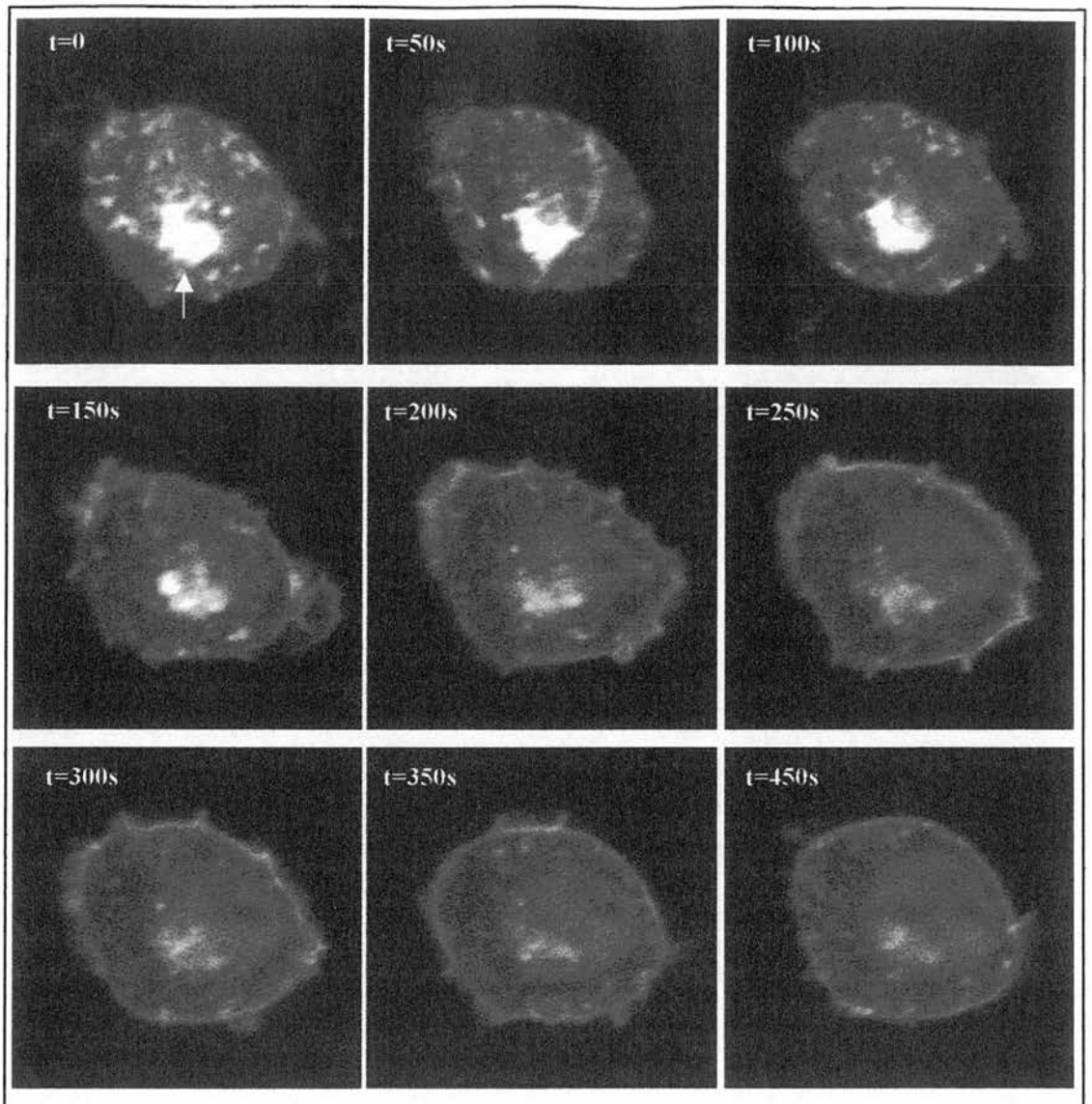

Figure 5.16. Time lapse imaging of PC12 cells, batch 3, transfected with pHFL-EGFP. All times are given in seconds (s). At t=0, EGF was added to the cells.

5.4.4 EGF stimulation of pHFL-EGFP-transfected SK-N-SH cells

To see if either the clearing of the protein from the cytoplasm and/or the recruitment of the protein to the plasma membrane could be duplicated in other cell types, several batches of SK-N-SH cells were transfected with the same construct and imaged in the same manner as the PC12 cells (figure 5.17).

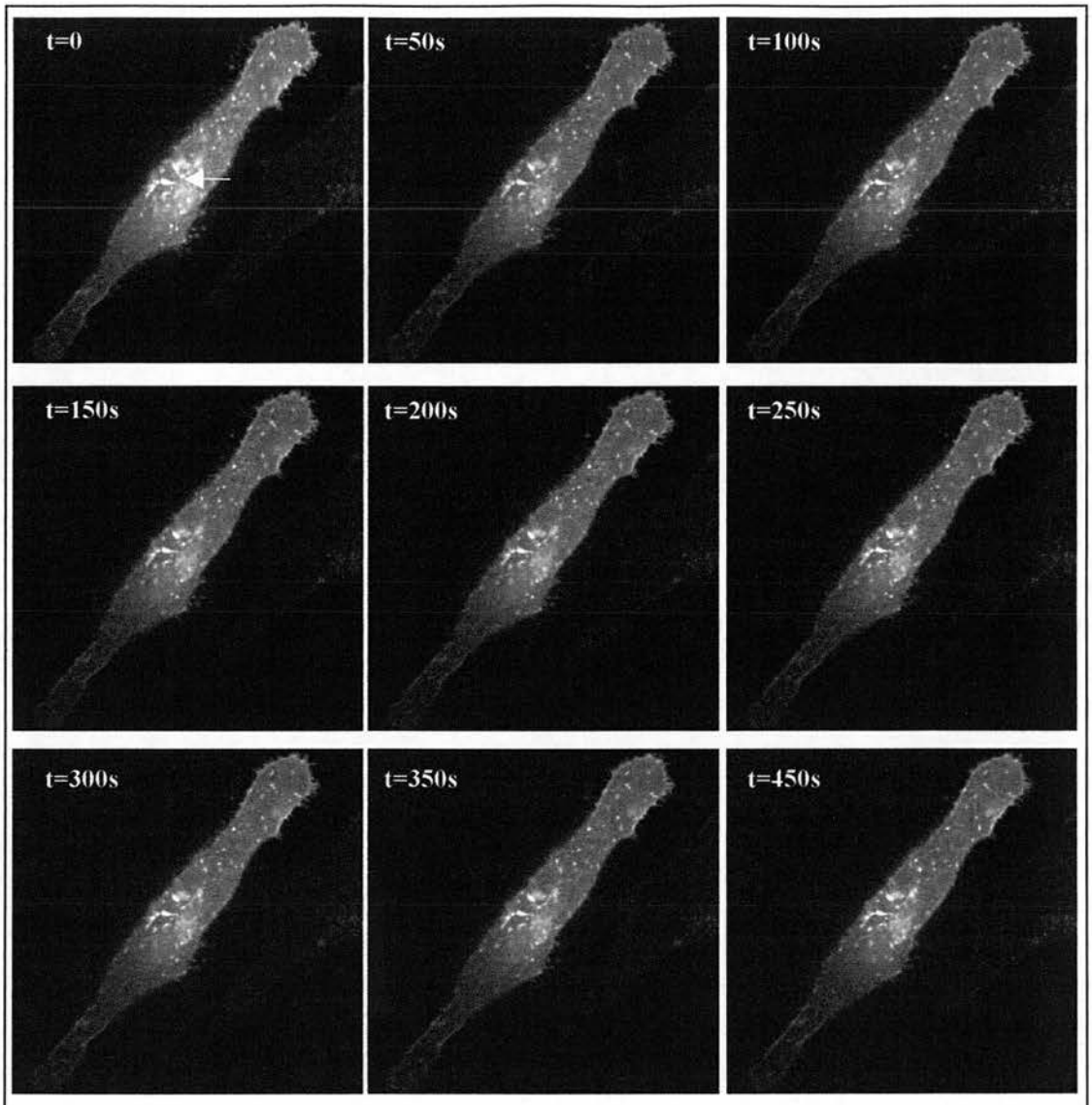

Figure 5.17. Time lapse imaging of SK-N-SH cells transfected with pHFL-EGFP: EGF added. All times are given in seconds (s). At t=0, EGF was added to the cells.

In figure 5.17, although this cell has, in common with the PC12 cells where willin could be seen to move, a region of particular brightness in the cytoplasm (figure 5.17(t=0), arrow), the protein did not seem to respond to EGF in the SK-N-SH cells.

5.4.5 Ionomycin stimulation of pHFL-EGFP-transfected SK-N-SH cells

In addition to EGF, another chemical, ionomycin, was available and this compound is an ionophore known to stimulate PLC (phospholipase C) (reviewed in Varnai et al, 1998). PLC is a multi-isoform enzyme which hydrolyses PIP2 into DAG and IP3, thereby lowering the concentrations of the PIP2 (reviewed in Rhee et al, 1997). Since there were no obvious results following EGF stimulation of the SK-N-SH cells, ionomycin was added instead to the remaining batches of transfected cells at a final concentration of 10μM. The results from one of these experiments are shown in figure 5.18.

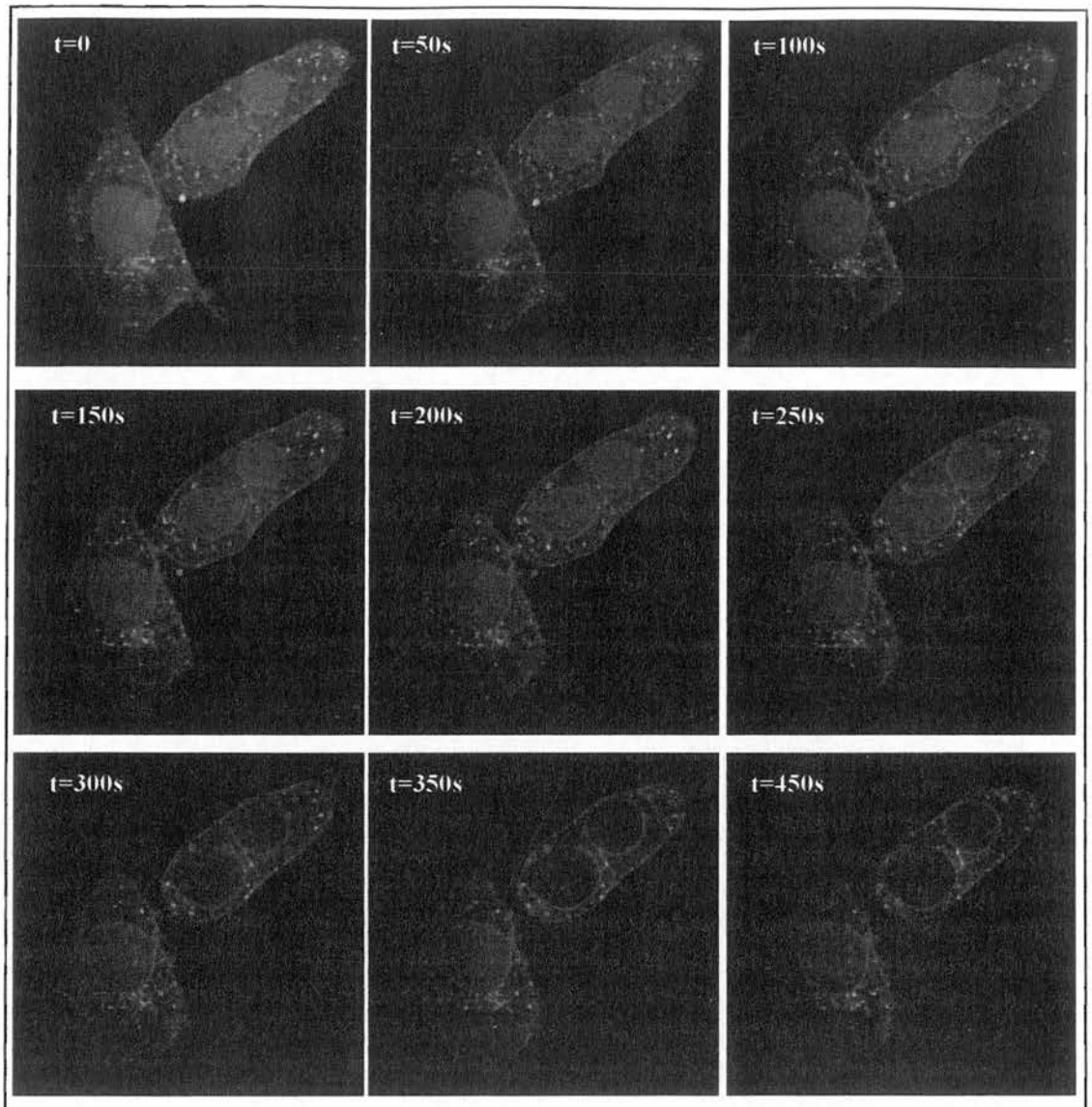

Figure 5.18. Time lapse imaging of SK-N-SH cells transfected with pHFL-EGFP. All times are given in seconds (s). At t=0, ionomycin was added to the cells.

Figure 5.18 reveals that again willin seemed to clear from the cytoplasm of the cells. There also appeared to be an evacuation of willin from the nuclei of the imaged cells with a simultaneous recruitment of the protein to the nuclear membranes and perhaps also the plasma membrane.

5.4.6 Ionomycin stimulation of pHFL-EGFP-transfected CHO-T cells

As was the case with the movement of willin in the PC12 cells following EGF stimulation, the movement of the protein following the addition of ionomycin treatment of the SK-N-SH cells seemed again to be specific to a certain cell type. Figure 5.19 shows that there was no observable movement of willin when ionomycin was used on pHFL-EGFP transfected CHO-T cells.

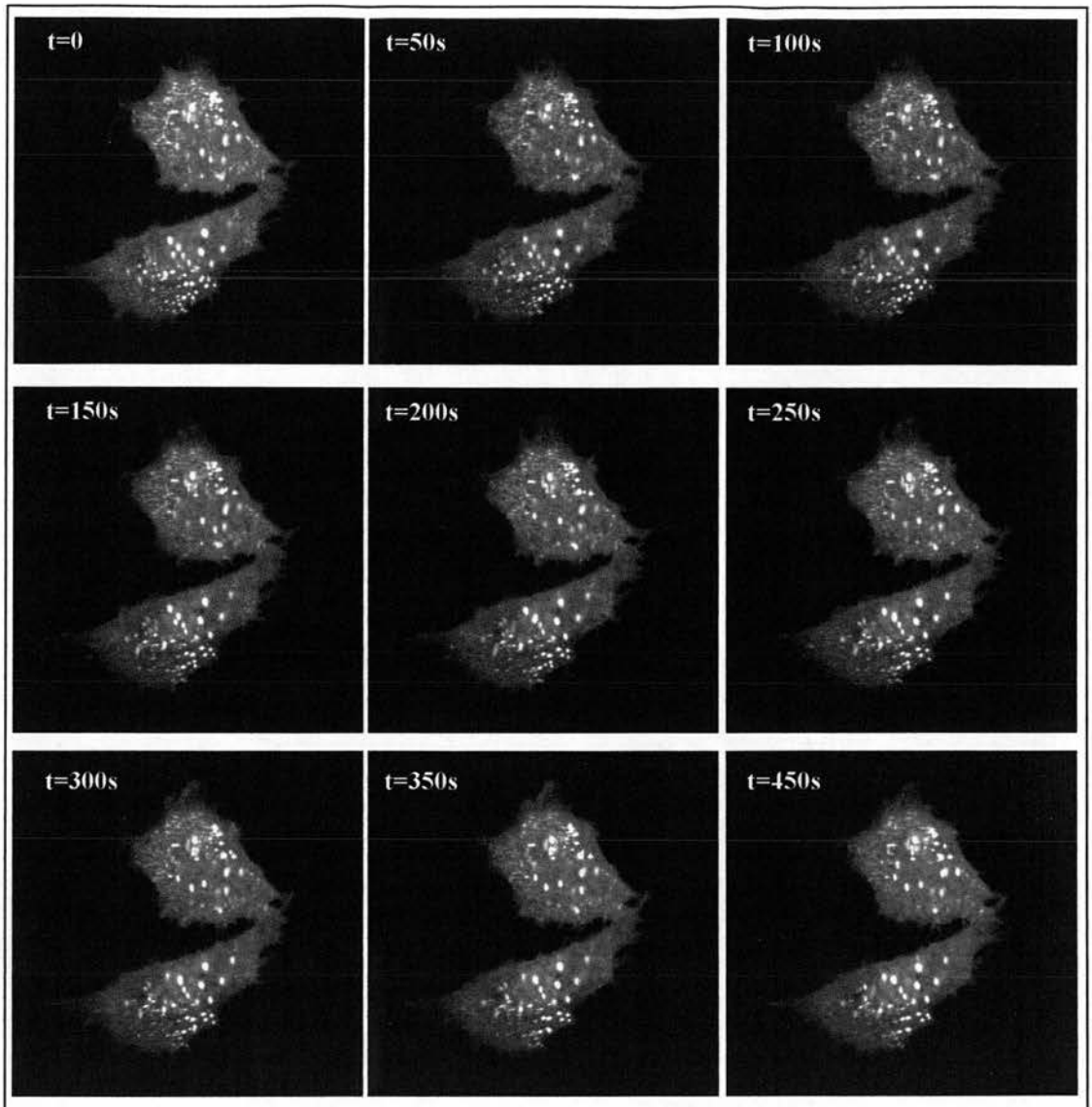

Figure 5.19. Time lapse imaging of CHO-T cells transfected with pHFL-EGFP. All times are given in seconds (s). At t=0, ionomycin was added to the cells.

5.4.7 Video clips of live cell imaging of PC12 and SK-N-SH cells

The movement of the EGFP-tagged protein in the PC12 and SK-N-SH cells can be seen as video clips in the compact disc that accompanies this thesis. The movies show:

Movie 5.20 and movie 5.21 - PC12 cells after EGF stimulation

Movie 5.22 and movie 5.23 - SK-N-SH cells after ionomycin stimulation.

5.5.1 Yeast two hybrid library screen preparations

The yeast two hybrid screen is based around the properties of the yeast GAL4 protein (Chien et al, 1991). This protein can be split, reversibly, into two domains, each of which can be fused to another protein. Domain 1, the DNA-binding domain, is fused to protein X. Domain 2, the activation domain, is fused to protein Y. When the separated GAL4 protein becomes united again, via an interaction between protein X and protein Y, a GAL4-dependent reporter gene is activated. To perform a library screen, a known protein "bait", such as willin, is fused to the GAL4 binding domain, and this construct is then transformed into yeast along with unknown protein sequences which are fused to the GAL4 activation domain. Interactions between willin and any of the unknown proteins are signalled, via the reporter gene, by the yeast colony in which the interaction is occurring.

In an attempt to investigate willin's protein-protein interactions, a construct was designed, based on the vector pAS2-1,which would contain the N-terminus of human willin. The pAS-21 vector is a yeast expression vector which produces proteins fused to a binding domain. A rat brain and rat sciatic nerve library were available which contained fragments of DNA in a complementary vector, pACT-2, which would produce proteins fused to an activation domain. If a pACT-2-based protein and a pAS2-1 - based protein interacted, the binding domain and the activation domains of the fusion proteins would merge and this would indicate a positive interaction. Positive interactions would be signalled by a blue colour from the yeast transformants that contained the two interacting proteins. The construct to be used in the library screen was named pHAS.

5.5.2 Construction of pHAS

Two oligonucleotide primers were designed which would anneal to the IMAGE clone and enable the amplification of the N-terminal human willin sequence with the addition of novel restriction enzyme sites (figure 5.24). The forward primer was HwilasF, which added an EcoRI site to the 5' end of the sequence. The reverse primer was HWilasR, which added a BamHI site to the 3' end of the sequence and a stop codon.

Positive clones were identified by restriction enzyme digests and subsequently confirmed by automated DNA sequencing.

The primer and DNA sequences used for the construction of each plasmid are contained in Appendices I – III.

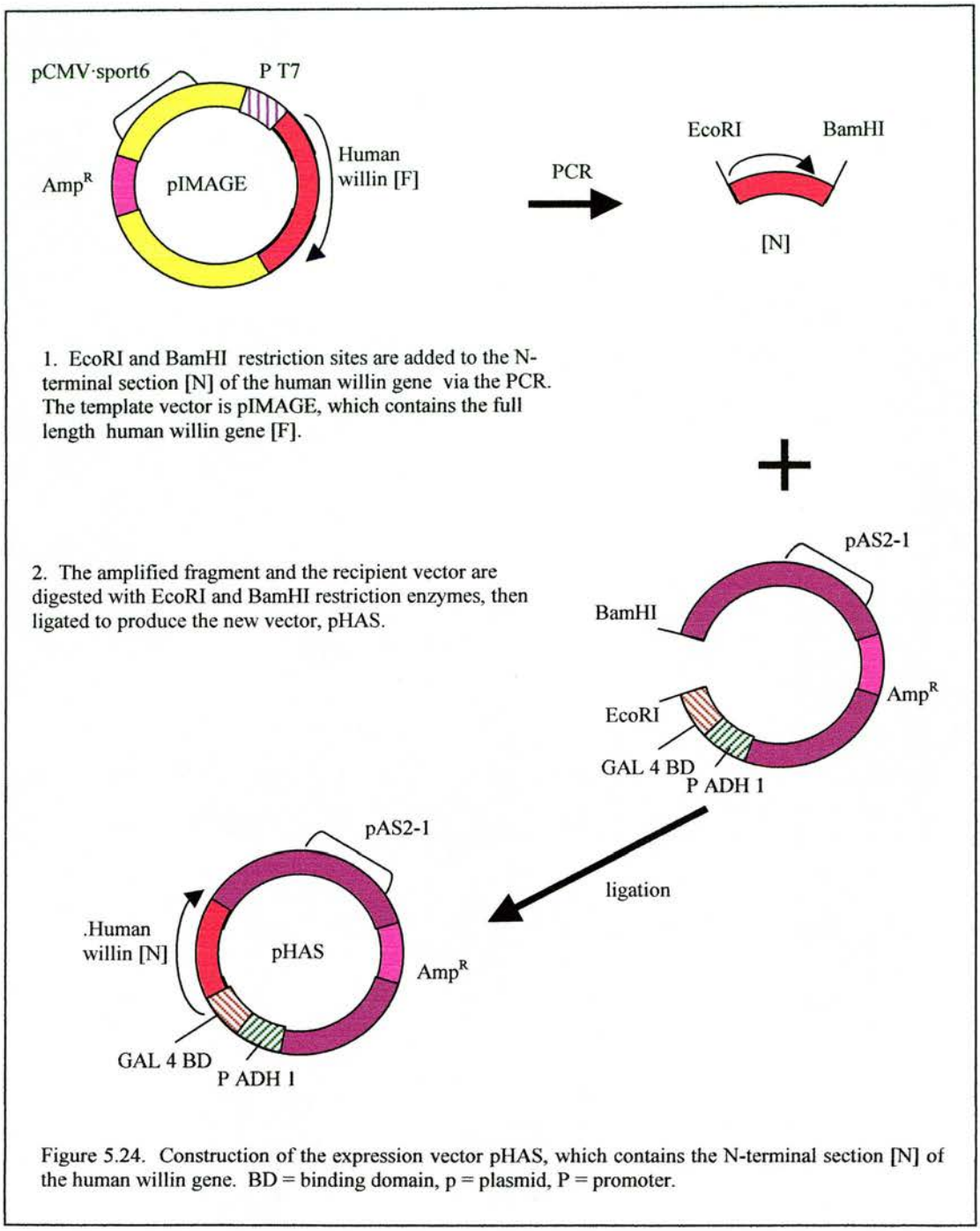

Figure 5.24. Construction of the expression vector pHAS, which contains the N-terminal section [N] of the human willin gene. BD = binding domain, p = plasmid, P = promoter.

5.5.3 Examining pHAS for autoactivation

The success of a yeast two hybrid assay is dependent on a chromogenic assay that signals the interaction of the activation domain of one fusion protein with the binding domain of another by yeast colonies which contain the interacting proteins turning

blue. It is essential to ensure that the bait protein, which contains the binding domain, does not by itself cause yeast colonies to turn blue, a result which is known as autoactivation. To perform this assay, the pHAS construct was transformed into yeast (section 2.4.4) and then plated out onto yeast selective plates that would select those colonies that contained the construct. A filter lift assay was then performed, as described in section 2.4.8, and no autoactivation of the pHAS construct was observed.

5.5.4 Expression of pHAS

Attempts were then made to ensure that the plasmid was expressing the required protein. Using yeast selective media, colonies were isolated that were believed to contain the pHAS plasmid. These colonies were cultured and the cells were lysed using the method described in section 2.4.5, Extraction of yeast proteins – method 1. A western blot was performed with the resulting lysates and using the 914[3] antibody. However, there were no bands present in any of the lanes containing the yeast extracts to indicate that the fusion protein was being expressed. The appearance of a band representing a positive control (cell extracts expressing the GST-HFL fusion protein) indicated that the problem was not related to the western blot protocol.

Further attempts were made with yeast method 1 (section 2.4.5). Usually between 3-6 different colonies were picked and cultured after each transformation, yet no band of the correct size could be seen on any of the western blots. A second protocol was then used, Extraction of yeast proteins – method 2, section 2.4.6, which was based on the use of trichloroacetic acid. However, this method also proved unsuccessful. A third method was then used, Extraction of yeast proteins – method 3, section 2.4.7,

which involved simply pelleting the cultures and then boiling them for several minutes. Using this extraction method tended to produce bands of the correct size on western blots, albeit very faint bands, in maybe 20-30% of colonies assayed. A typical result is shown in figure 5.25.

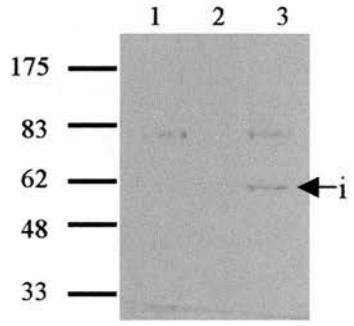

Figure 5.25. Analysis of expression levels of the pHAS construct in yeast via western blotting. (1) colony 1 (2) colony 2 (3) colony 3. Expected size pHAS – 55kDa. [Upper bands are mentioned in Discussion.]

The predicted size of the pHAS construct was 55kDa and is possibly represented by the band indicated in lane 3 in figure 5.25 (←i). However, the band is not very dense and indicates a very low expression from the pHAS construct. The reason for the poor expression is unknown. The sequence of the clone was checked and no mutations were found. Due to the difficulties encountered in obtaining reproducible expression from the pHAS construct, and the additional problem that the expression that did occur was very weak, it was decided that a yeast two hybrid screen should not be performed with this construct.

5.6 Conclusions

Attempts to express the intact N-terminus of the rat or human willin proteins in bacteria were unsuccessful due to either lack of expression from the vector used or to protein degradation. Attempts to express the intact N-terminus of the human willin protein in yeast was partially successful, but the expression levels were not strong enough to permit a yeast two hybrid library screen. However, expression of the intact full length human protein in bacteria was achievable.

The GST-HFL fusion protein is very insoluble, which correlates with the ERM family's actin-binding function. The most potent agents for solubilising this fusion protein are guanidinium hydrochloride and sarkosyl. The solubility of the GST-HFL protein is directly dependent on the amount of sarkosyl present. A sarkosyl-based protocol has been successfully developed for the purification of the full length human protein. This protocol maintains the structural integrity of the GST-HFL protein since the purified version of the protein can be observed to rebind to glutathione-sepharose beads.

Preliminary experiments reveal that willin binds phospholipids. Experiments in this chapter using commercially available phospholipid-containing membranes indicate that willin binds PI-3,5-P2 and PI-3,4,5-P3. However, a control construct did not bind to the expected sites on these membranes. The conclusion must therefore be drawn that the data from these lipid-binding experiments may not be reliable. The unexpected results from the lipid-binding assays are not attributable to the presence of the GST moiety at the N-terminus of the purified protein.

The main conclusion to be drawn from the live imagining experiments is that willin can be observed to move around inside certain cells following stimulus with a growth factor or chemical, and that this movement is dependent on (1) the cell type, (2) the growth factor or chemical used, and (3) other unknown factors.

It is difficult to draw firm conclusions from the live imaging experiments because although in, for example, certain PC12 cells, willin was observed to (a) delocalise from a bright perinuclear pool, (b) delocalise from the cytoplasm, and (c) become recruited to the cell membrane, this did not happen in other PC12 cells. Movement of willin could also be detected in SK-N-SH cells, but only when ionomycin was added; EGF treatment had no observable effect on this cell type.

In another cell line expressing willin-EGFP, namely CHO-T cells, the protein did not visibly respond to any stimulus.

5.7 Chapter 5 Discussion

5.7.1 Expression of full length or partial segments of willin

Considerable difficulties were encountered throughout the process of attempting to stably express willin, either as a partial or full length protein, rat or human, in different vectors and in different microorganisms.

The reason for the lack of expression from the pET15b constructs (section 5.3.5, 5.3.7) could not be established. The western blots that were performed using induced bacterial samples containing the pHET and pRET constructs did not show any induction products at all, intact or otherwise, in the induced lanes. This implied that, unlike the pGex-Rat construct, where the induction products were detected but were the incorrect size for the full length fusion protein (figure 5.6), it would appear that in the case of the pHET and pRET constructs there was simply no synthesis occurring. A similar problem also occurred when attempting to express the N-terminus of the human protein in yeast, which was also described in this chapter (section 5.5.4): expression could only be detected in about 20-30% of the colonies assayed (even though they had been plated on selective media) and when the expression did occur it was at a very low level (figure 5.25).

In summary, the expression of the N-terminus of the rat protein did not produce an intact fusion protein using the bacterial pGEX-KG vector (section 5.3.6), the expression of the N-terminus of the human protein could only be detected 20-30% of the time, and at a very low level, in the yeast pAS2-1 vector (section 5.5.4), and no expression at all could be detected when the N-termini of both the human and rat

proteins were expressed using the bacterial pET15b vector (section 5.3.7). Since the expression problems of the willin N-terminus encompassed three different vectors and two different versions of the protein (human and rat), and occurred in both bacteria and yeast, and the full length protein could be satisfactorily expressed in the pGEX system, the conclusion may be drawn that the problems were more than likely due to the attempted expression of only the N-terminus of the protein.

The expression of the full length fusion protein (section 5.3.9) was believed to be successful because of the ability of the full length protein to fold into its proper conformation during the induction process, which would shield it from intracellular proteases. The N-terminus of the protein would not have been able to fold properly, since half the protein was missing, and therefore whatever the conformation adopted by this fusion protein during synthesis, it would likely have remained exposed to potential proteolytic attack.

Since the GST-HFL fusion protein was almost totally insoluble, a solubilisation procedure had to be devised. If a slightly stronger band of the full length protein had appeared in the supernatant lane on western blots such as that shown in figure 5.9, the investigative work that was needed to solubilise the protein would have been bypassed and instead the original purification procedure (2.2.12) would simply have been scaled up. However, since virtually none of the full length fusion protein appeared to be soluble, the step-by-step analysis of various solubilising methods and conditions was regarded as the quickest way to obtaining the necessary quantities of the protein.

The discussion to accompany each of the methods or chemicals tested for the purification of the full length human protein was placed in the results section, alongside the description of how the condition was tested, rather than here in the discussion section. Therefore no further discussion of these processes is warranted here. Following the elucidation of the new purification protocol, a typical yield after using the method described in section 2.2.14 followed by dialysis and the use of a centricon (according to the manufacturer's instructions) was ~0.6mg/ml, which was ample for the lipid binding experiments that were to follow.

5.7.2 Protein lipid overlay experiments

It cannot be concluded from the protein lipid overlay experiments that willin binds to any particular phospholipids. It appears, however, that willin does bind to some phospholipids, since GST alone does not bind to any phospholipids whereas GST-willin binds to several (section 5.3.18). But since the control fusion protein did not bind to the predicted phospholipids on the membrane, the possibility must be considered that the lipids were not spotted on to the membrane in the order that the manufacturer stated. The identity of the phospholipids that willin did bind to is therefore called into question. It is possible to buy the membranes and phospholipids separately and then spot them on and this would be an appropriate area of further work for the experiments in this chapter. Subsequently, it has been shown by our collaborator, Dr Kanamarlapudi Venkateswarlu, University of Bristol , that the GST-tagged full-length protein, as described in section 5.3.8, is capable of binding to the same phospholipids profile as moesin (Gunn-Moore et al, 2005).

5.7.3 Live cell imaging experiments

However, the indications that willin had an affinity for phospholipids, even unidentified ones, paved the way for the live imaging work at the University of Bristol. The experiments results shown in this chapter did give an indication that willin may be regulated by phospholipid interactions in a manner similar to that of the other members of the ERM family (section 1.5.5, 1.5.6). The experiments were successful in that they achieved the desired outcome, which, due to rigid time constraints, was simply to cause the protein to move in response to a stimulus.

The chemicals used to stimulate the cells were EGF and ionomycin. Within the PC12 cells, in response to EGF stimulation, willin appeared either to 1) not move, or 2) move from the cytoplasm, or 3) move from the cytoplasm to the plasma membrane (figures 5.14, 5.15 and 5.16). It is possible that in all these cells, the protein behaves in exactly the same manner but that the movement is more conspicuous in some cells than others. The protein may be behaving differently within a cell line due to either expression levels that vary from cell to cell, or to cell cycle considerations. Precedents exist for both of these hypotheses: Martin et al (1995) noted different patterns of localisation according to whether the ERM protein constructs were expressed at medium or high levels and in, for example, section 4.7.2, figure 4.25, COS7 cells appear to show a different localisation pattern of the full length EGFP-tagged willin according to whether they are dividing or not.

The cells in which the movements of the protein were perceptible shared a common feature, which was that one particular area inside the cell was brighter than the rest of the cytoplasm (figure 5.15, 5.16). It is possible that this bright area of the cell is

maybe the rough endoplasmic reticulum (RER), since it is always adjacent to the nucleus (this can be seen both in the pictures above and also in those in chapter 4, such as figure 4.17). The bright perinuclear pool may therefore be due to synthesis or modification of the willin-EGFP fusion protein occurring in the RER.

Unlike the control protein ARNO, when willin has been observed to move, not all of it leaves the cytoplasm. It is possible that not all of the protein responds to a signal to leave the cytoplasm and/or go to the plasma membrane. If the bright perinuclear pool (figure 5.15, 5.16) does represent the synthesis/modification of a forthcoming batch of the protein in the RER, this batch may yet have a certain amount of latitude as to where it can localise to. It may then be the case that once a signal does arrive in the cell, via EGF for example, to direct willin to the plasma membrane, the untargeted batch is free to follow these instructions whereas the protein that is in the cytoplasm may already have been modified in some way that precludes it from following suit without some additional signal. The perinuclear pool could also possibly be the Golgi.

Additionally, the cells were serum-starved before the addition of the stimuli but this does not necessarily mean that the physiology of the cell during serum-starving would be exactly the opposite of that seen upon the re-addition of serum or specific growth factors. If all the membrane-cytoskeleton linker proteins in the cell were to leave the membrane upon the removal of serum, the cells would collapse. It is therefore conceivable that it is difficult to observe the EGF-mediated recruitment of the willin to the plasma membrane of every cell imaged because not all of it actually

leaves the membrane in the first place. This seems to be the case in the cells shown in figure 5.15 for example, where, even though the cell has been serum starved, a ring of willin can be seen to surround the cells.

Both the PC12 cells and the SK-N-SH cells showed similarities in their response to EGF and ionomycin respectively, in that willin appeared to move out of the cytoplasm and to the plasma membrane. However, two notable differences occurred with the SK-N-SH cells upon stimulation with ionomycin that did not occur with the PC12 cells following treatment with EGF. When ionomycin was added to the SK-N-SH cells, willin also seems to both leave the nucleus and be recruited to the nuclear membrane (figure 5.18). This is, if anything, the opposite of what happens in the PC12 cells, where the cell on the left in figure 5.15 and the cell in figure 5.16 both have a nucleus that appears to become increasingly brighter after the addition of the EGF.

Both EGF and ionomycin cause a decrease in the PIP2 levels of a cell: EGF and ionomycin stimulate PLC activity, which causes PIP2 to be hydrolysed into IP3 and DAG (reviewed in Varnai et al, 1998). Both of these compounds cause the lowering of cellular PIP2 levels but it is unclear whether they have an entirely similar effect on the movement of willin-EGFP or not.

5.7.4 Video clips: PC12 and SK-N-SH cells

Figures 5.15 and 5.16 and movie clips 5.20 and 5.21 show that when EGF is added to PC12 cells, willin appears to leave the cytoplasm and also leave an area of particular

brightness in the cytoplasm. In addition, the protein may be recruited to the nuclear membrane, since the nuclei in these cells grow brighter following stimulation. Figure 5.18 and movie clips 5.22 and 5.23 show that when ionomycin is added to SK-N-SH cells, willin again leaves the cytoplasm but it is unclear whether the protein is targeted to the PM or not. It does seem as though willin is targeted to the nuclear membrane in these cells and there may also be a simultaneous evacuation of the protein from the nucleus.

These results generally indicate, along with the variations in the distribution of the protein in different cell types (as shown in various immunofluorescence photographs in Chapter 4), that the protein behaves differently according to which type of cell it is expressed in; and also that the localisation of willin may be cell cycle dependent. Willin was originally isolated from a sciatic nerve library (Gunn-Moore et al, 2005) and it is interesting to note that the two cell lines used in these movie clips in which movement of the protein was evident – SK-N-SH and PC12 – were both cell lines derived from neurological tissue. In other cells lines tested, the protein showed no apparent response to EGF or ionomycin stimulation (CHO-T cells, shown in figure 5.19, and HeLa cells – results not shown).

5.7.5 Expression of willin in yeast

It had been the intention to perform for this thesis a yeast two hybrid screen using willin as bait. As mentioned above in section 5.7.1, problems were encountered when trying to express the N-terminus of either the rat or human protein in two different vectors in bacteria. Had this bacterial work preceded the construction of the yeast-based plasmid that was intended for use in a yeast two hybrid assay, then a yeast

construct would not have been attempted using the N-terminus of the protein (pHAS). However, the bacterial and yeast experiments were conducted more or less simultaneously and there were therefore no indications during the construction of the yeast plasmid that expression problems would be forthcoming.

Although the sequence of the full length protein was available for cloning prior to the construction of the pHAS plasmid, the full length sequence was not used for two reasons. Firstly, the N-terminal section of the protein that was cloned into the pHAS vector was 957bp, which was roughly half the size of the 1845bp full length protein; although Pfu Turbo® DNA polymerase, a proof reading enzyme, was used for cloning, there was still a possibility of mutations occurring in the gene during the PCR and the use of only half the sequence decreased this risk. Secondly, the area of interest in terms of investigating novel interactions was the FERM domain which is located in the N-terminus of the protein. It was anticipated that the C-terminus of the protein would bind actin, which meant that if the C-terminus of the protein was also included in the construct, it is very likely that a lot of the positive interactions that would be detected would be just actin.

Therefore using only the N-terminus of the protein was believed to be the most appropriate bait, but figure 5.25 shows the typical expression levels that were obtained using the pHAS construct. The expression from this construct was not reproducible throughout several western blots and so plans for the yeast two hybrid screen were abandoned. The work described in this chapter has revealed that even if other yeast plasmids are used for cloning, there may be expression problems if the N-

terminus only of the protein is used in the vector and it may therefore be prudent to perform any future yeast two hybrid screens with the full length protein.

The appearance of a band of possibly ~70kDa in the yeast cell lysates in figure 5.25 led to the question of what the antibody could be detecting in yeast. As the antibody used was to the N-terminus of willin, the protein sequence of the willin N-terminus was blasted into the *Saccharomyces cerevisiae (S. cerevisiae)* database. The particular database selected was: ORF [open reading frame] Proteins and Translations of Defined ORFS. Four hits emerged, one of which was described as a "dubious ORF". The other three results were as follows:

YGR080W Verified ORF Twinfilin - highly conserved actin monomer-sequestering protein involved in regulation of the cortical actin cytoskeleton, composed of two cofilin-like regions, localizes actin monomers to sites of rapid filament assembly.
YDR296W Verified ORF Protein involved in homologous recombination in mitochondria and in transcription regulation in nucleus; binds to activation domains of acidic activators; required for recombination-dependent mtDNA partitioning.
YER105C Verified ORF Abundant subunit of the nuclear pore complex (NPC), present on both sides of the NPC.

These sequences show that there are in existence yeast proteins which may be being detected by the anti-willin antibody, and the functions of these proteins seem to correlate with some of the proposed functions of willin; in, for example, figure 4.20, the effects of transfecting only the N-/C-terminus of the protein into HEK293 cells can be seen to have a clear effect on the nuclei and cytoskeletons of the cells.

Chapter 6: Final summary and future work

6.1 Summary of work

A band corresponding to a ~70kDa protein, which is possibly native willin, has been detected in several mammaliann cell lines. The band can be visualised by two separate and distinct antibodies against the willin N-terminus, and it is always found in the insoluble fraction of cell lysates. A ~50kDa band, possibly a smaller isoform of the protein, was also repeatedly detected by the two different antibodies.

Both antibodies recognise a purified form of human willin. Protein competition experiments using this purified protein eliminates the ~70kDa and ~50kDa bands as visualised by the panned affinity purified version of one of the antibodies, 914[3].

In several mammalian cell lines, EGFP-tagged willin localises to cell membranes, and to membranous structures such as stress fibres and membrane projections. Expressing only the N- or C-terminus of willin as EGFP-tagged proteins causes an alteration in the distribution of the protein. Willin also colocalises with actin in several cell lines examined. The distribution of willin is cell type-specific, according to both immunofluorescence microscopy photographs and western blotting experiments, with variations in localisation also noted between cancerous (RPEc5Tcl1) and non-cancerous (RPE) versions of the same cell line.

In some cell types, willin localises to the midbody and contractile ring, and to the cell nucleus. Preliminary indications are that the localisation to the nucleus (and possibly other structures) is cell-cycle dependent, and evidence has also been

presented that willin may play a role in cytokinesis. The expression of the EGFP-tagged N- or C-terminus of the protein in HEK293 cells causes marked alterations to cell morphology. The cells develop thickened cytoskeletons, have fewer projections and become packed with nuclear material. Small "conjoined" doublets of HEK293 cells also appeared following transfection with these constructs. These doublets frequently possessed regions of thickened actin in the area where the cleavage furrow should have formed. A small ring of actin was sometimes observed in these doublets, possibly reprenting the midbody but, if so, was incorrectly localised to one end of the doublet instead of to the centre of the dividing cells.

Several areas of investigation indicated that the proeins is both extremely labile and very insoluble. Difficulties were incurred whilst trying to express the N-terminus of the protein, either human or rat, in bacteria or yeast, and via several different expression vectors. Full length willin, when expressed as a GST-fusion protein, proved to be almost entirely insoluble. However, a protocol was successfully developed to enable the solubilisation and purification of the full length protein.

Stimulation of certain cell types with substances that cause alterations in phospholipid levels produced alterations in the distribution of the EGFP-tagged protein. This effect again is cell type-specific and appears to be also dependent on other factors, as yet unknown, but possibly relating to the cell cycle; for example, movement of the protein could be observed in one group of PC12 cells but not in another group of PC12 cells that had been treated under exactly the same conditions.

6.2 Suggestions for further work

To continue the study of the expression of the native protein, as described in Chapter 3, protein/peptide competition experiments could be carried out with the CK1 antibody derivatives. Due to the ambiguous results obtained with peptide competition with the 914[3]-based antibodies, peptide competition could be repeated with these antibodies but using freshly synthesised peptide, since the batch of peptide synthesised for the Chapter 3 work was several years old.

Attempts could be made to sequence and identify the ~70kDa and ~50kDa bands. RNAi (RNA interference) is one such possibility, whereby the mRNA corresponding to that of the full length protein could be silenced to see if this would effect any changes to the visibility of the aforementioned bands on SDS-PAGE gels. Matrix-Assisted Laser Desorption/Ionisation - Time of Flight (MALDI-TOF) mass spectrometry is a facility available at the University of St Andrews: if the bands on an SDS-PAGE gel could be made to disappear by inhibition of mRNA against the willin sequence, then analysing the identity of these bands via MALDI-TOF could help to answer the questions that remain with regards to the ~70kDa and ~50kDa bands.

Other methods of assaying for the presence of the native protein could again involve looking at willin at the RNA level, perhaps via RT-PCR (reverse transcription PCR), to monitor the mRNA levels of the protein in different cells, at different stages of development and at different stages of the cell cycle.

The incongruities relating to the localisation of the N-terminus of the protein could provide an absorbing topic to study. The willin N-terminus appears, via

immumofluorescence experiments, to not colocalise with actin, yet it is to be found in the insoluble fraction of lysed cells. Since an N-terminal actin-binding site has been identified in ezrin (Roy et al, 1997), the possibility of a similar site in willin could be explored. Confirmation of the protein's ability to actually bind actin, be it the full length protein, the C-terminus or even the N-terminus - as opposed to just colocalise with actin - would also be a necessity. This could be addressed via deletion mutagenesis and GST pulldown assays.

The peculiar appearance of the HEK293 cells in response to transfection with the N- or C-terminus of the protein could pave the way for many avenues of investigation. Among the questions waiting to be answered are: what is the exact nature, if any, of the role played by the protein in mitosis in HEK293 (and other) cells? Why do the cells possess such an anomalous ratio of nuclear to cytoplasmic content? Regarding the conjoined doublets, at what point in the cell cycle do the abnormalities begin to manifest? Why don't the cells undergo apoptosis long before they become so densely packed with nuclear material? Answers to these questions might be found via cell cycle studies, using drugs that arrest the cell during various stages of the cell cycle, such as inhibitors of cyclin-dependent kinases.

The development of the protocol to solubilise the full length protein could prove to be advantageous in many different experiments involving the analysis of protein-protein interactions, such as GST pulldown assays.

An attempt could be made to clarify the PLO results, whereupon it would perhaps be advisable to eschew the commercially available phospholipid-spotted membranes,

and instead to purchase the phospholipids individually and spot them on to the membrane oneself.

Further live imaging work along the same lines as that described in Chapter 5 could perhaps provide answers to some of the questions raised by these experiments, namely the reasons behind the vagaries displayed by the protein in localisation between different cell types, and even within the same cell type. Making use of the array of stimulants and inhibitors available for phosphorylation and phospholipid studies could help provide an insight into the signalling pathways involved in the regulation of willin.

To investigate potential binding partners for willin via a yeast two hybrid screen, the use of the full length protein would be a judicious decision; although this may result in a lot of positive signals that turn out to be actin (which in itself would be a confirmative result), results presented in this thesis strongly suggest that the use of the N-terminus of willin is unsuitable for this type of study.

Finally, willin has emerged from the proteome as a neurological protein. Its original detection in cerebellar granular cells and sciatic nerve cells engenders the question of what exactly its function is in these cell types. If such cells could be obtained and cultured, initial experiments might involve the transfection of the EGFP-based constructs into these cells also, as the immunofluorescence studies performed for this thesis have proved to be most intriguing.

Appendix I: Table of primers used

Name of primer	Sequence of primer
T7	TAATACGACTCACTATAGGG
BDF	TCATCGGAAGAGAGTAG
NFAS-AC-F	CGG GAT CCT TAA GAG GAG TCG TGG CGG CAA G
NFAS-AC-R	GGA ATT CTC AGG CCA GGG AAT AGA TGG C
Willin 4	GGA ATT CTG ATG AAC AAA CTG ACC TTC C
Willin 5	CCG CTC GAG CTA GCG GAG GTG GCG CAG GAC GGG
N-AC-F	CGG GAT CCT TAT GAA CAA ATT GAA TTT TC
N-AC-R	GGA ATT CCT ACA GAT TCA TAT AGA GGC GGT G
C-AS-F	GGA ATT CCA GCC TGT CCT GCG CC
C-AS-R	CGG GAT CCT TAC ACA ACA AAC TCT GGA AC
NFAS-AS-F	GGA ATT CAA GAG GAG TCG TGG CGG CAA G
NFAS-AS-R	CGG GAT CCT CAG GCC AGG GAA TAG ATG GC
Willin 6	TCT CCT GCA GCT GCT GAG C
Hwill 1	TTA CAC AAC AAA CTC TGG AAC
Hwill 6	CCT GTA CAG CTG CAC ACA GAC
Rwilas F	GGA ATT CAT GAA CAA ACT GAC CTT CC
RwiletF	GGA ATT CCA TAT GAA CAA ACT GAC CTT CC
Rwil300	ATC CAT TTC CGG GTG CAG
Rwil600	GCA CTG ACA GCC TCC GAG
RwilasR	CGG GAT CCT AGC GGA GGT GGC GCA GGA CGG G
Hwil300	GAC CAA TTT GGG CCT CCT
Hwil600-2	TGG ATG ACG TCG CTG TTC
Hwil900	ATA TAC TAC ACG GGG TGC
Hwil 1200	ACC AAG CCC CGG GAC ACG
Hwil 1500	TGT GAA AGA AAT TGG GTC
HwilasF	GGA ATT CAT GAA CAA ATT GAA TTT TC
HwilacF	CAT GCC ATG GGA CAG CCT GTC CTG CGC C
HwilacR	GGA ATT CTT ACA CAA CAA ACT CTG GAA C
HwilasR	CGG GAT CCC TAC AGA TTC ATA TAG AGG CGG TG
HwiletF	GGA ATT CCA TAT GAA CAA ATT GAA TTT TC
NWGFPF	GGA ATT CGC CAT GAA CAA ATT GAA TTT TC
NWGFPR	CGG GAT CCA GCG ATG CTT CAA TTT CCC
CWGFPF	CGG GAT CCA CAA CAA ACT CTG GAA CTT C
CWGFPR	GGA ATT CAC CAT GGA TAA AAG GGA AAT TGA AGC
HwilacF-2	CGG GAT CCT TCA GCC TGT CCT GCG CC
HGexF	CGG GAT CCA TGA ACA AAT TGA ATT TTC
HW-CT-ASR	CGG GAT CCT TAC ACA ACA AAC TCT GGA AC

Appendix II: Construction of plasmids/ Antibody sequences

Clones based around the rat willin sequence contained all of the available sequence (shown in Appendix III). Shown below is the total sequence of the human willin DNA sequence (Accession no BC020521).

The first three bases used for the construction of plasmid pNW-EGFP are shown in blue, as are the last three bases used for this construct. The first three bases used for the construction of plasmid pCW-EGFP are shown in red, as are the last three bases used for this construct. All clones carrying the N-terminus of the protein began at the first codon listed here, which is the ATG codon shown in blue, and ended at the codon shown in pink.

ATGAACAAATTGAATTTTCATAACAACAGAGTCATGCAAGACCGCCGCAGTGTGTGCATTTT
CCTTCCCAACGATGAATCTCTGAACATCATCATAAATGTTAAGATTCTGTGTCACCAGTTGC
TGGTCCAGGTTTGTGACCTGCTCAGGCTAAAGGACTGCCACCTCTTTGGACTCAGTGTTATA
CAAAATAATGAACATGTGTATATGGAGTTGTCACAAAAGCTTTACAAATATTGTCCAAAAGA
ATGGAAGAAAGAGGCCAGCAAGGGTATCGACCAATTTGGGCCTCCTATGATCATCCACTTCC
GTGTGCAGTACTATGTGGAAAATGGCAGATTGATCAGTGACAGAGCAGCAAGATACTATTAT
TACTGGCACCTGAGAAAACAAGTTCTTCATTCTCAGTGTGTGCTCCGAGAGGAGGCCTACTT
CCTGCTGGCAGCCTTTGCCCTGCAGGCTGATCTTGGGAACTTCAAAAGGAATAAGCACTATG
GAAAATACTTCGAGCCAGAGGCTTACTTCCCATCTTGGGTTGTTTCCAAGAGGGGGAAGGAC
TACATCCTGAAGCACATTCCAAACATGCACAAAGATCAGTTTGCACTAACAGCTTCCGAAGC
TCATCTTAAATATATCAAAGAGGCTGTCCGACTGGATGACGTCGCTGTTCATTACTACAGAT
TGTATAAGGATAAAAGGGAAATTGAAGCATCGCTGACTCTTGGATTGACCATGAGGGGAATA
CAGATTTTTCAGAATTTAGATGAAGAGAAACAATTACTTTATGATTTCCCCTGGACAAATGT
TGGAAAATTGGTGTTTGTGGGTAAGAAATTTGAGATTTTGCCAGATGGCTTGCCTTCTGCCC
GGAAGCTCATATACTACACGGGGTGCCCCATGCGCTCCAGACACCTCCTGCAACTTCTGAGC
AACAGCCACCGCCTCTATATGAATCTGCAGCCTGTCCTGCGCCATATCCGGAAGCTGGAGGA
AAACGAAGAGAAGAAGCAGTACCGGGAATCTTACATCAGTGACAACCTGGACCTCGACATGG
ACCAGCTGGAAAAACGGTCGCGGGCCAGCGGGAGCAGTGCGGGCAGCATGAAACACAAGCGC
CTGTCCCGTCATTCCACCGCCAGCCACAGCAGTTCCCACACCTCGGGCATTGAGGCAGACAC
CAAGCCCCGGGACACGGGGCCAGAAGACAGCTACTCCAGCAGTGCCATCCACCGCAAGCTGA
AAACCTGCAGCTCAATGACCAGTCATGGCAGCTCCCACACCTCAGGGGTGGAGAGTGGCGGC
AAAGACCGGCTGGAAGAGGACTTACAGGACGATGAAATAGAGATGTTGGTTGATGACCCCCG
GGATCTGGAGCAGATGAATGAAGAGTCTCTGGAAGTCAGCCCAGACATGTGCATCTACATCA
CAGAGGACATGCTCATGTCGCGGAAGCTGAATGGACACTCTGGGTTGATTGTGAAAGAAATT
GGGTCTTCCACCTCGAGCTCTTCAGAAACAGTTGTTAAGCTTCGTGGCCAGAGTACTGATTC
TCTTCCACAGACTATATGTCGGAAACCAAAGACCTCCACTGATCGACACAGCTTGAGCCTCG
ATGACATCAGACTTTACCAGAAAGACTTCCTGCGCATTGCAGGTCTGTGTCAGGACACTGCT
CAGAGTTACACCTTTGGATGTGGCCATGAACTGGATGAGGAAGGCCTCTATTGCAACAGTTG
CTTGGCCCAGCAGTGCATCAACATCCAAGATGCTTTTCCAGTCAAAAGAACCAGCAAATACT
TTTCTCTGGATCTCACTCATGATGAAGTTCCAGAGTTTGTTGTGTAA

Sequence in purple= anti-CK1 antibody; sequence in yellow=914[3] antibody

The first M shown below is the initiating methionine of the IMAGE clone, accession BC020521 (full protein sequence is in Appendix III)

MNKLNFHNNRVMQDRRSVCIFLPNDESLNIIINVKILCHQLLVQVCDLLRLKDCHLFGLSVI
QNNEHVYMELSQKLYKYCPKEWKKEASKGIDQFGPPMIIHFRVQYYVEN.....

Appendix III: Accession numbers, DNA and protein sequences

Human willin DNA sequence
Accession no BC020521

ATGAACAAATTGAATTTTCATAACAACAGAGTCATGCAAGACCGCCGCAGTGTGTGCATT
TTCCTTCCCAACGATGAATCTCTGAACATCATCATAAATGTTAAGATTCTGTGTCACCAG
TTGCTGGTCCAGGTTTGTGACCTGCTCAGGCTAAAGGACTGCCACCTCTTTGGACTCAGT
GTTATACAAAATAATGAACATGTGTATATGGAGTTGTCACAAAAGCTTTACAAATATTGT
CCAAAAGAATGGAAGAAAGAGGCCAGCAAGGGTATCGACCAATTTGGGCCTCCTATGATC
ATCCACTTCCGTGTGCAGTACTATGTGGAAAATGGCAGATTGATCAGTGACAGAGCAGCA
AGATACTATTATTACTGGCACCTGAGAAAACAAGTTCTTCATTCTCAGTGTGTGCTCCGA
GAGGAGGCCTACTTCCTGCTGGCAGCCTTTGCCCTGCAGGCTGATCTTGGGAACTTCAAA
AGGAATAAGCACTATGGAAAATACTTCGAGCCAGAGGCTTACTTCCCATCTTGGGTTGTT
TCCAAGAGGGGGAAGGACTACATCCTGAAGCACATTCCAAACATGCACAAAGATCAGTTT
GCACTAACAGCTTCCGAAGCTCATCTTAAATATATCAAAGAGGCTGTCCGACTGGATGAC
GTCGCTGTTCATTACTACAGATTGTATAAGGATAAAAGGGAAATTGAAGCATCGCTGACT
CTTGGATTGACCATGAGGGGAATACAGATTTTTCAGAATTTAGATGAAGAGAAACAATTA
CTTTATGATTTCCCCTGGACAAATGTTGGAAAATTGGTGTTTGTGGGTAAGAAATTTGAG
ATTTTGCCAGATGGCTTGCCTTCTGCCCGGAAGCTCATATACTACACGGGGTGCCCCATG
CGCTCCAGACACCTCCTGCAACTTCTGAGCAACAGCCACCGCCTCTATATGAATCTGCAG
CCTGTCCTGCGCCATATCCGGAAGCTGGAGGAAAACGAAGAGAAGAAGCAGTACCGGGAA
TCTTACATCAGTGACAACCTGGACCTCGACATGGACCAGCTGGAAAAACGGTCGCGGGCC
AGCGGGAGCAGTGCGGGCAGCATGAAACACAAGCGCCTGTCCCGTCATTCCACCGCCAGC
CACAGCAGTTCCCACACCTCGGGCATTGAGGCAGACACCAAGCCCCGGGACACGGGGCCA
GAAGACAGCTACTCCAGCAGTGCCATCCACCGCAAGCTGAAAACCTGCAGCTCAATGACC
AGTCATGGCAGCTCCCACACCTCAGGGGTGGAGAGTGGCGGCAAAGACCGGCTGGAAGAG
GACTTACAGGACGATGAAATAGAGATGTTGGTTGATGACCCCCGGGATCTGGAGCAGATG
AATGAAGAGTCTCTGGAAGTCAGCCCAGACATGTGCATCTACATCACAGAGGACATGCTC
ATGTCGCGGAAGCTGAATGGACACTCTGGGTTGATTGTGAAAGAAATTGGGTCTTCCACC
TCGAGCTCTTCAGAAACAGTTGTTAAGCTTCGTGGCCAGAGTACTGATTCTCTTCCACAG
ACTATATGTCGGAAACCAAAGACCTCCACTGATCGACACAGCTTGAGCCTCGATGACATC
AGACTTTACCAGAAAGACTTCCTGCGCATTGCAGGTCTGTGTCAGGACACTGCTCAGAGT
TACACCTTTGGATGTGGCCATGAACTGGATGAGGAAGGCCTCTATTGCAACAGTTGCTTG
GCCCAGCAGTGCATCAACATCCAAGATGCTTTTCCAGTCAAAAGAACCAGCAAATACTTT
TCTCTGGATCTCACTCATGATGAAGTTCCAGAGTTTGTTGTGTAA

Human willin protein sequence

MNKLNFHNNRVMQDRRSVCIFLPNDESLNIIINVKILCHQLLVQVCDLLRLKDCHLFGLSVI
QNNEHVYMELSQKLYKYCPKEWKKEASKGIDQFGPPMIIHFRVQYYVENGRLISDRAARYYY
YWHLRKQVLHSQCVLREEAYFLLAAFALQADLGNFKRNKHYGKYFEPEAYFPSWVVSKRGKD
YILKHIPNMHKDQFALTASEAHLKYIKEAVRLDDVAVHYYRLYKDKREIEASLTLGLTMRGI
QIFQNLDEEKQLLYDFPWTNVGKLVFVGKKFEILPDGLPSARKLIYYTGCPMRSRHLLQLLS
NSHRLYMNLQPVLRHIRKLEENEEKKQYRESYISDNLDLDMDQLEKRSRASGSSAGSMKHKR
LSRHSTASHSSSHTSGIEADTKPRDTGPEDSYSSSAIHRKLKTCSSMTSHGSSHTSGVESGG
KDRLEEDLQDDEIEMLVDDPRDLEQMNEESLEVSPDMCIYITEDMLMSRKLNGHSGLIVKEI
GSSTSSSSETVVKLRGQSTDSLPQTICRKPKTSTDRHSLSLDDIRLYQKDFLRIAGLCQDTA
QSYTFGCGHELDEEGLYCNSCLAQQCINIQDAFPVKRTSKYFSLDLTHDEVPEFVV

Rat willin (partial) DNA sequence
Accession no AF441249

```
ATGAACAAACTGACCTTCCATAACAACAAAGTCATGCAGGACCGCCGCAGAGTGTGTATTTTCCTCCCC
AATGACAAGTCTGTGAGCATCATCATAAATGTTAAAATTCTGTGTCACCAGTTGCTGGTCCAGGTGTGT
GACCTGCTCAGGTTGAAGGATAGTCACCTCTTTGGTCTCAGTGTTATACAAAATAATGAACACGTATAT
ATGGAATTGTCACAAAAGCTCTATAAGTATTGTCCAAAAGAATGGAAAAAGGAGGCCAGCAAGGGCATC
GACCAGTTTGGGCCTCCCATGATCATCCATTTCCGGGTGCAGTACTATGTGGAGAACGGGAAGCTGATC
AGTGACCGGATTGCGAGATACTATTATTACTGGCACCTAAGGAAACAGGTGCTGCACTCTCAGTGTGTG
CTCAGAGAGGAGGCCTACTTCCTGCTGGCAGCCTTTGCACTGCAGGCTGACCTCGGGAACTTCAAAAGG
AAAGTGCACCATGGAGACTACTTTGAGCCAGAGGCTTACTTCCCAGCATGGGTGGTTTCCAAGCGGGGG
AAGGACTACATCCTGAAACACATTCCAAACATGCACAGAGACCAGTTTGCACTGACAGCCTCCGAGGCA
TATCTAAAGTACATCAAAGAGGCCGTCCGACTGGATGACGTCGCCATCCATTACTACAGACTGTACAAG
GATAAAAGAGAGGTTGAAGGTTCACTGACCCTGGGACTGACCATGCGAGGGATACAGATCTTTCAGAAT
CTAGAAGAAGAGAAACAGTTGCTGTATGATTTCCCCTGGACAAATGTTGGGAAGTTGGTGTTTGTGGGC
AAGAAGTTTGAGATTTTGCCCGATGGCCTCCCCTCCGCCAGGAAGCTGGTCTACTACACCGGGTGCCCC
ACACGCTCCCGGCATCTCCTGCAGCTGCTGAGCAACAGCCACCGGCTCTACATGAACCTGCAGCCCGTC
CTGCGCCACCTCCGC
```

Rat willin (partial) protein sequence

```
MNKLTFHNNKVMQDRRRVCIFLPNDKSVSIIINVKILCHQLLVQVCDLLRLKDSHLFGLSVIQNNEHVY
MELSQKLYKYCPKEWKKEASKGIDQFGPPMIIHFRVQYYVENGKLISDRIARYYYYWHLRKQVLHSQCV
LREEAYFLLAAFALQADLGNFKRKVHHGDYFEPEAYFPAWVVSKRGKDYILKHIPNMHRDQFALTASEA
YLKYIKEAVRLDDVAIHYYRLYKDKREVEGSLTLGLTMRGIQIFQNLEEEKQLLYDFPWTNVGKLVFVG
KKFEILPDGLPSARKLVYYTGCPTRSRHLLQLLSNSHRLYMNLQPVLRHLR
```

AMINO ACID ALIGNMENTS OF WILLIN AND BSA

The two regions of willin that share a three-residue homology with BSA are shown highlighted in blue below.

```
BSA             DCCEKQEPERNECFLSHKDDSPDLPKLKPDPNTLCDEFKADEKKFWGKYLYEIARRHPYF 172
WILLIN          ARYYYYWHLRKQVLHSQCVLREEAYFLLAAFALQADLGNFKRNKHYGKYFEPEAYFPSWV 179
                        *:: : *:     :   * .     .*  : ..:*.:***:   *   .:.


BSA             RMPCTEDYLSLILNRLCVLHEKTPVSEKVTKCCTESLVNRRPCFSALTPDETYVPKAFDE 527
WILLIN          CIYITEDMLMSRKLNGHSGLIVKEIGSSTSSSSETVVKLRGQSTDSLPQTICRKPKTSTD 531
                 :  *** *     .       . :....:...   :  *  . .:*.      **:  :
```

BIBLIOGRAPHY

ALBERTS, B; BRAY, D; LEWIS, J; RAFF, M; ROBERTS, K; WATSON, J. 1994a THE MECHANICS OF CELL DIVISION in *MOLECULAR BIOLOGY OF THE CELL, 3RD ED.* GARLAND PUBLISHING INC. pp911–946

ALBERTS, B; BRAY, D; LEWIS, J; RAFF, M; ROBERTS, K; WATSON, J. 1994b THE CYTOSKELETON in *MOLECULAR BIOLOGY OF THE CELL, 3RD ED.* GARLAND PUBLISHING INC. pp786–861

ALFTHAN, K; HEISKA, L; GRONHOLM, M; RENKEMA, GH; CARPEN, O. 2004. CYCLIC AMP-DEPENDENT PROTEIN KINASE PHOSPHORYLATES MERLIN AT SERINE 518 INDEPENDENTLY OF P21-ACTIVATED KINASE AND PROMOTES MERLIN-EZRIN HETERODIMERIZATION. *JOURNAL OF BIOLOGICAL CHEMISTRY* 279 (18): 18559-18566.

ALGRAIN, M; TURUNEN, O; VAHERI, A; LOUVARD, D; ARPIN, M. 1993. EZRIN CONTAINS CYTOSKELETON AND MEMBRANE-BINDING DOMAINS ACCOUNTING FOR ITS PROPOSED ROLE AS A MEMBRANE-CYTOSKELETAL LINKER. *JOURNAL OF CELL BIOLOGY* 120 (1): 129-139.

AMIEVA, MR; FURTHMAYR, H. 1995. SUBCELLULAR-LOCALIZATION OF MOESIN IN DYNAMIC FILOPODIA, RETRACTION FIBERS, AND OTHER STRUCTURES INVOLVED IN SUBSTRATE EXPLORATION, ATTACHMENT, AND CELL-CELL CONTACTS. *EXPERIMENTAL CELL RESEARCH* 219 (1): 180-196.

AMIEVA, MR; LITMAN, P; HUANG, LQ; ICHIMARU, E; FURTHMAYR, H. 1999. DISRUPTION OF DYNAMIC CELL SURFACE ARCHITECTURE OF NIH3T3 FIBROBLASTS BY THE N-TERMINAL DOMAINS OF MOESIN AND EZRIN: IN VIVO IMAGING WITH GFP FUSION PROTEINS. *JOURNAL OF CELL SCIENCE* 112 (1): 111-125.

AMIEVA, MR; WILGENBUS, KK; FURTHMAYR, H. 1994. RADIXIN IS A COMPONENT OF HEPATOCYTE MICROVILLI IN-SITU. *EXPERIMENTAL CELL RESEARCH* 210 (1): 140-144.

ANDERSON, RA; LOVRIEN, RE. 1984. GLYCOPHORIN IS LINKED BY BAND-4.1 PROTEIN TO THE HUMAN-ERYTHROCYTE MEMBRANE SKELETON. *NATURE* 307 (5952): 655-658.

ANDREOLI, C; MARTIN, M; LEBORGNE, R; REGGIO, H; MANGEAT, P. 1994. EZRIN HAS PROPERTIES TO SELF-ASSOCIATE AT THE PLASMA-MEMBRANE. *JOURNAL OF CELL SCIENCE* 107: 2509-2521, PART 9.

BARRET, C; ROY, C; MONTCOURRIER, P; MANGEAT, P; NIGGLI, V. 2000. MUTAGENESIS OF THE PHOSPHATIDYLINOSITOL 4,5-BISPHOSPHATE (PIP2) BINDING SITE IN THE NH2-TERMINAL DOMAIN OF EZRIN CORRELATES WITH ITS ALTERED CELLULAR DISTRIBUTION. *JOURNAL OF CELL BIOLOGY* 151 (5): 1067-1079.

BASHOUR, AM; MENG, JJ; IP, W; MACCOLLIN, M; RATNER, N. 2002. THE NEUROFIBROMATOSIS TYPE 2 GENE PRODUCT, MERLIN, REVERSES THE F-ACTIN CYTOSKELETAL DEFECTS IN PRIMARY HUMAN SCHWANNOMA CELLS. *MOLECULAR AND CELLULAR BIOLOGY* 22 (4): 1150-1157.

BERRYMAN, M; BRETSCHER, A. 2000. IDENTIFICATION OF A NOVEL MEMBER OF THE CHLORIDE INTRACELLULAR CHANNEL GENE FAMILY (CLIC5) THAT ASSOCIATES WITH THE ACTIN CYTOSKELETON OF PLACENTAL MICROVILLI. *MOLECULAR BIOLOGY OF THE CELL* 11 (5): 1509-1521.

BERRYMAN, M; FRANCK, Z; BRETSCHER, A. 1993. EZRIN IS CONCENTRATED IN THE APICAL MICROVILLI OF A WIDE VARIETY OF EPITHELIAL-CELLS WHEREAS MOESIN IS FOUND PRIMARILY IN ENDOTHELIAL-CELLS. *JOURNAL OF CELL SCIENCE* 105: 1025-1043, PART 4.

BLACKWELL, JR; HORGAN, R. 1991. A NOVEL STRATEGY FOR PRODUCTION OF A HIGHLY EXPRESSED RECOMBINANT PROTEIN IN AN ACTIVE FORM. *FEBS LETTERS* 295 (1-3): 10-12.

BONILHA, VL; FINNEMANN, SC; RODRIGUEZ-BOULAN, E. 1999. EZRIN PROMOTES MORPHOGENESIS OF APICAL MICROVILLI AND BASAL INFOLDINGS IN RETINAL PIGMENT EPITHELIUM. *JOURNAL OF CELL BIOLOGY* 147 (7): 1533-1547.

BRETSCHER, A. 1983. PURIFICATION OF AN 80,000-DALTON PROTEIN THAT IS A COMPONENT OF THE ISOLATED MICROVILLUS CYTOSKELETON, AND ITS LOCALIZATION IN NON-MUSCLE CELLS. *JOURNAL OF CELL BIOLOGY* 97 (2): 425-432.

BRETSCHER, A. 1989. RAPID PHOSPHORYLATION AND REORGANIZATION OF EZRIN AND SPECTRIN ACCOMPANY MORPHOLOGICAL-CHANGES INDUCED IN A-431 CELLS BY EPIDERMAL GROWTH-FACTOR. *JOURNAL OF CELL BIOLOGY* 108 (3): 921-930.

BRETSCHER, A. 1999. REGULATION OF CORTICAL STRUCTURE BY THE EZRIN-RADIXIN-MOESIN PROTEIN FAMILY. *CURRENT OPINION IN CELL BIOLOGY* 11 (1): 109-116.

BRETSCHER, A; EDWARDS, K; FEHON, RG. 2002. ERM PROTEINS AND MERLIN: INTEGRATORS AT THE CELL CORTEX. *NATURE REVIEWS MOLECULAR CELL BIOLOGY* 3 (8): 586-599.

BRETSCHER, A; RECZEK, D; BERRYMAN, M. 1997. EZRIN: A PROTEIN REQUIRING CONFORMATIONAL ACTIVATION TO LINK MICROFILAMENTS TO THE PLASMA MEMBRANE IN THE ASSEMBLY OF CELL SURFACE STRUCTURES. *JOURNAL OF CELL SCIENCE* 110: 3011-3018, PART 24.

BROWN, MJ; NIJHARA, R; HALLAM, JA; GIGNAC, M; YAMADA, KM; ERLANDSEN, SL; DELON, J; KRUHLAK, M; SHAW, S. 2003. CHEMOKINE STIMULATION OF HUMAN PERIPHERAL BLOOD T LYMPHOCYTES INDUCES RAPID DEPHOSPHORYLATION OF ERM PROTEINS, WHICH FACILITATES LOSS OF MICROVILLI AND POLARIZATION. *BLOOD* 102 (12): 3890-3899.

CAO, TT; DEACON, HW; RECZEK, D; BRETSCHER, A; VON ZASTROW, M. 1999. A KINASE-REGULATED PDZ-DOMAIN INTERACTION CONTROLS ENDOCYTIC SORTING OF THE BETA 2-ADRENERGIC RECEPTOR. *NATURE* 401 (6750): 286-290.

CARPENTER, G; COHEN, S. 1990. EPIDERMAL GROWTH-FACTOR. *JOURNAL OF BIOLOGICAL CHEMISTRY* 265 (14): 7709-7712.

CASTELO, L; JAY, DG. 1999. RADIXIN IS INVOLVED IN LAMELLIPODIAL STABILITY DURING NERVE GROWTH CONE MOTILITY. *MOLECULAR BIOLOGY OF THE CELL* 10 (5): 1511-1520.

CHEN, J; COHN, JA; MANDEL, LJ. 1995. DEPHOSPHORYLATION OF EZRIN AS AN EARLY EVENT IN RENAL MICROVILLAR BREAKDOWN AND ANOXIC INJURY. *PROCEEDINGS OF THE NATIONAL ACADEMY OF SCIENCES OF THE UNITED STATES OF AMERICA* 92 (16): 7495-7499.

CHEN, J; DOCTOR, RB; MANDEL, LJ. 1994. CYTOSKELETAL DISSOCIATION OF EZRIN DURING RENAL ANOXIA - ROLE IN MICROVILLAR INJURY. *AMERICAN JOURNAL OF PHYSIOLOGY* 267 (3): C784-C795, PART 1.

CHIEN, CT; BARTEL, PL; STERNGLANZ, R; FIELDS, S. 1991. THE 2-HYBRID SYSTEM - A METHOD TO IDENTIFY AND CLONE GENES FOR PROTEINS THAT INTERACT WITH A PROTEIN OF INTEREST. *PROCEEDINGS OF THE NATIONAL ACADEMY OF SCIENCES OF THE UNITED STATES OF AMERICA* 88 (21): 9578-9582.

CHISHTI, AH; KIM, AC; MARFATIA, SM; LUTCHMAN, M; HANSPAL, M; JINDAL, H; LIU, SC; LOW, PS; ROULEAU, GA; MOHANDAS, N; CHASIS, JA; CONBOY, JG; GASCARD, P; TAKAKUWA, Y; HUANG, SC; BENZ, EJ; BRETSCHER, A; FEHON, RG; GUSELLA, AF; RAMESH, V; SOLOMON, F; MARCHESI, VT; TSUKITA, S; TSUKITA, S; ARPIN, M; LOUVARD, D; TONKS, NK; ANDERSON, JM; FANNING, AS; BRYANT, PJ; WOODS, DF; HOOVER, KB. 1998. THE FERM DOMAIN: A UNIQUE MODULE INVOLVED IN THE LINKAGE OF CYTOPLASMIC PROTEINS TO THE MEMBRANE. *TRENDS IN BIOCHEMICAL SCIENCES* 23 (8): 281-282.

COOPER, JA. 1987. EFFECTS OF CYTOCHALASIN AND PHALLOIDIN ON ACTIN. *JOURNAL OF CELL BIOLOGY* 105 (4): 1473-1478.

CREPALDI, T; GAUTREAU, A; COMOGLIO, PM; LOUVARD, D; ARPIN, M. 1997. EZRIN IS AN EFFECTOR OF HEPATOCYTE GROWTH FACTOR-MEDIATED MIGRATION AND MORPHOGENESIS IN EPITHELIAL CELLS. *JOURNAL OF CELL BIOLOGY* 138 (2): 423-434.

DEFACQUE, H; EGEBERG, M; HABERMANN, A; DIAKONOVA, M; ROY, C; MANGEAT, P; VOELTER, W; MARRIOTT, G; PFANNSTIEL, J; FAULSTICH, H; GRIFFITHS, G. 2000. INVOLVEMENT OF EZRIN/MOESIN IN DE NOVO ACTIN ASSEMBLY ON PHAGOSOMAL MEMBRANES. *EMBO JOURNAL* 19 (2): 199-212.

DENKER, SP; BARBER, DL. 2002. CELL MIGRATION REQUIRES BOTH ION TRANSLOCATION AND CYTOSKELETAL ANCHORING BY THE NA-H EXCHANGER NHE1. *JOURNAL OF CELL BIOLOGY* 159 (6): 1087-1096.

DICKSON, TC; MINTZ, CD; BENSON, DL; SALTON, SRJ. 2002. FUNCTIONAL BINDING INTERACTION IDENTIFIED BETWEEN THE AXONAL CAM L1 AND MEMBERS OF THE ERM FAMILY. *JOURNAL OF CELL BIOLOGY* 157 (7): 1105-1112.

DOBSON, CM. 2004. PRINCIPLES OF PROTEIN FOLDING, MISFOLDING AND AGGREGATION. *SEMINARS IN CELL & DEVELOPMENTAL BIOLOGY* 15 (1): 3-16.

DOHERTY, AJ; CONNOLLY, BA; WORRALL, AF. 1993. OVERPRODUCTION OF THE TOXIC PROTEIN, BOVINE PANCREATIC DNASEI, IN ESCHERICHIA-COLI USING A TIGHTLY CONTROLLED T7-PROMOTER-BASED VECTOR. *GENE* 136 (1-2): 337-340.

DOI, Y; ITOH, M; YONEMURA, S; ISHIHARA, S; TAKANO, H; NODA, T; TSUKITA, S; TSUKITA, S. 1999. NORMAL DEVELOPMENT OF MICE AND UNIMPAIRED CELL ADHESION CELL MOTILITY ACTIN-BASED CYTOSKELETON WITHOUT COMPENSATORY UP-REGULATION OF EZRIN OR RADIXIN IN MOESIN GENE KNOCKOUT. *JOURNAL OF BIOLOGICAL CHEMISTRY* 274 (4): 2315-2321.

DOWLER, S; CURRIE, RA; DOWNES, CP; ALESSI, DR. 1999. DAPP1: A DUAL ADAPTOR FOR PHOSPHOTYROSINE AND 3-PHOSPHOINOSITIDES. *BIOCHEMICAL JOURNAL* 342: 7-12, PART 1.

DOWLER, S; KULAR, G; ALESSI, D. 2002. PROTEIN LIPID OVERLAY ASSAY – PROTOCOL. SCIENCE'S STKE 23 APRIL 2002: 6

DRANSFIELD, DT; BRADFORD, AJ; SMITH, J; MARTIN, M; ROY, C; MANGEAT, PH; GOLDENRING, JR. 1997. EZRIN IS A CYCLIC AMP-DEPENDENT PROTEIN KINASE ANCHORING PROTEIN. *EMBO JOURNAL* 16 (1): 35-43.

EDWARDS, HC; BOOTH, AG. 1987. CALCIUM-SENSITIVE, LIPID-BINDING CYTOSKELETAL PROTEINS OF THE HUMAN PLACENTAL MICROVILLAR REGION. *JOURNAL OF CELL BIOLOGY* 105 (1): 303-311.

ELLIOTT, BE; MEENS, JA; SENGUPTA, SK; LOUVARD, D; ARPIN, M. 2005. THE MEMBRANE CYTOSKELETAL CROSSLINKER EZRIN IS REQUIRED FOR METASTASIS OF BREAST CARCINOMA CELLS. *BREAST CANCER RESEARCH* 7 (3): R365-R373.

EUGENE, E; HOFFMANN, I; PUJOL, C; COURAUD, PO; BOURDOULOUS, S; NASSIF, X. 2002. MICROVILLI-LIKE STRUCTURES ARE ASSOCIATED WITH THE INTERNALIZATION OF VIRULENT CAPSULATED NEISSERIA MENINGITIDIS INTO VASCULAR ENDOTHELIAL CELLS. *JOURNAL OF CELL SCIENCE* 115 (6): 1231-1241.

FAIS, S; DE MILITO, A; LOZUPONE, F. 2005. THE ROLE OF FAS TO EZRIN ASSOCIATION IN FAS-MEDIATED APOPTOSIS. *APOPTOSIS* 10 (5): 941-947.

FIEVET, BT; GAUTREAU, A; ROY, C; DEL MAESTRO, L; MANGEAT, P; LOUVARD, D; ARPIN, M. 2004. PHOSPHOINOSITIDE BINDING AND PHOSPHORYLATION ACT SEQUENTIALLY IN THE ACTIVATION MECHANISM OF EZRIN. *JOURNAL OF CELL BIOLOGY* 164 (5): 653-659.

FRANCK, Z; GARY, R; BRETSCHER, A. 1993. MOESIN, LIKE EZRIN, COLOCALIZES WITH ACTIN IN THE CORTICAL CYTOSKELETON IN CULTURED-CELLS, BUT ITS EXPRESSION IS MORE VARIABLE. *JOURNAL OF CELL SCIENCE* 105: 219-231, PART 1.

FRANGIONI, JV; NEEL, BG. 1993. SOLUBILIZATION AND PURIFICATION OF ENZYMATICALLY ACTIVE GLUTATHIONE-S-TRANSFERASE (PGEX) FUSION PROTEINS. *ANALYTICAL BIOCHEMISTRY* 210 (1): 179-187.

FUNAYAMA, N; NAGAFUCHI, A; SATO, N; TSUKITA, S; TSUKITA, S. 1991. RADIXIN IS A NOVEL MEMBER OF THE BAND-4.1 FAMILY. *JOURNAL OF CELL BIOLOGY* 115 (4): 1039-1048.

GARAVITO, RM; FERGUSON-MILLER, S. 2001. DETERGENTS AS TOOLS IN MEMBRANE BIOCHEMISTRY. *JOURNAL OF BIOLOGICAL CHEMISTRY* 276 (35): 32403-32406.

GARY, R; BRETSCHER, A. 1993. HETEROTYPIC AND HOMOTYPIC ASSOCIATIONS BETWEEN EZRIN AND MOESIN, 2 PUTATIVE MEMBRANE CYTOSKELETAL LINKING PROTEINS. *PROCEEDINGS OF THE NATIONAL ACADEMY OF SCIENCES OF THE UNITED STATES OF AMERICA* 90 (22): 10846-10850.

GARY, R; BRETSCHER, A. 1995. EZRIN SELF-ASSOCIATION INVOLVES BINDING OF AN N-TERMINAL DOMAIN TO A NORMALLY MASKED C-TERMINAL DOMAIN THAT INCLUDES THE F-ACTIN BINDING-SITE. *MOLECULAR BIOLOGY OF THE CELL* 6 (8): 1061-1075.

GATTO, CL; WALKER, BJ; LAMBERT, S. 2003. LOCAL ERM ACTIVATION AND DYNAMIC GROWTH CONES AT SCHWANN CELL TIPS IMPLICATED IN EFFICIENT FORMATION OF NODES OF RANVIER. *JOURNAL OF CELL BIOLOGY* 162 (3): 489-498.

GEIGER, KD; STOLDT, P; SCHLOTE, W; DEROUICHE, A. 2006. EZRIN IMMUNOREACTIVITY REVEALS SPECIFIC ASTROCYTE ACTIVATION IN CEREBRAL HIV. *JOURNAL OF NEUROPATHOLOGY AND EXPERIMENTAL NEUROLOGY* 65 (1): 87-96.

GIRAULT, JA; LABESSE, G; MORNON, JP; CALLEBAUT, I. 1998. JANUS KINASES AND FOCAL ADHESION KINASES PLAY IN THE 4.1 BAND: A SUPERFAMILY OF BAND 4.1 DOMAINS IMPORTANT FOR CELL STRUCTURE AND SIGNAL TRANSDUCTION. *MOLECULAR MEDICINE* 4 (12): 751-769.

GONZALEZAGOSTI, C; SOLOMON, F. 1996. RESPONSE OF RADIXIN TO PERTURBATIONS OF GROWTH CONE MORPHOLOGY AND MOTILITY IN CHICK SYMPATHETIC NEURONS IN VITRO. *CELL MOTILITY AND THE CYTOSKELETON* 34 (2): 122-136.

GOULD, KL; BRETSCHER, A; ESCH, FS; HUNTER, T. 1989. CDNA CLONING AND SEQUENCING OF THE PROTEIN-TYROSINE KINASE SUBSTRATE, EZRIN, REVEALS HOMOLOGY TO BAND-4.1. *EMBO JOURNAL* 8 (13): 4133-4142.

GRANES, F; BERNDT, C; ROY, C; MANGEAT, P; REINA, M; VILARO, S. 2003. IDENTIFICATION OF A NOVEL EZRIN-BINDING SITE IN SYNDECAN-2 CYTOPLASMIC DOMAIN. *FEBS LETTERS* 547 (1-3): 212-216.

GRANES, F; URENA, JM; ROCAMORA, N; VILARO, S. 2000. EZRIN LINKS SYNDECAN-2 TO THE CYTOSKELETON. *JOURNAL OF CELL SCIENCE* 113 (7): 1267-1276.

GUNN-MOORE, FJ; WELSH, GI; HERRON, LR; BRANNIGAN, F; VENKATESWARLU, K; GILLESPIE, S; BRANDWEIN-GENSLER, M; MADAN, R; TAVARE, JM; BROPHY, PJ; PRYSTOWSKY, MB; GUILD, S. 2005. A NOVEL 4.1 EZRIN RADIXIN MOESIN (FERM)-CONTAINING PROTEIN, 'WILLIN'. *FEBS LETTERS* 579 (22): 5089-5094

GUTMANN, DH. 1997. MOLECULAR INSIGHTS INTO NEUROFIBROMATOSIS 2. *NEUROBIOLOGY OF DISEASE* 3 (4): 247-261.

HAMADA, K; SHIMIZU, T; MATSUI, T; TSUKITA, S; TSUKITA, S; HAKOSHIMA, T. 2000. STRUCTURAL BASIS OF THE MEMBRANE-TARGETING AND UNMASKING MECHANISMS OF THE RADIXIN FERM DOMAIN. *EMBO JOURNAL* 19 (17): 4449-4462.

HANZEL, DK; URUSHIDANI, T; USINGER, WR; SMOLKA, A; FORTE, JG. 1989. IMMUNOLOGICAL LOCALIZATION OF AN 80-KDA PHOSPHOPROTEIN TO THE APICAL MEMBRANE OF GASTRIC PARIETAL-CELLS. *AMERICAN JOURNAL OF PHYSIOLOGY* 256 (6): G1082-G1089, PART 1.

HARA, T; BIANCHI, AB; SEIZINGER, BR; KLEY, N. 1994. MOLECULAR-CLONING AND CHARACTERIZATION OF ALTERNATIVELY SPLICED TRANSCRIPTS OF THE MOUSE NEUROFIBROMATOSIS-2 GENE. *CANCER RESEARCH* 54 (2): 330-335.

HAYASHI, K; YONEMURA, S; MATSUI, T; TSUKITA, S; TSUKITA, S. 1999. IMMUNOFLUORESCENCE DETECTION OF EZRIN/RADIXIN/MOESIN (ERM) PROTEINS WITH THEIR CARBOXYL-TERMINAL THREONINE PHOSPHORYLATED IN CULTURED CELLS AND TISSUES - APPLICATION OF A NOVEL FIXATION PROTOCOL USING TRICHLOROACETIC ACID (TCA) AS A FIXATIVE. *JOURNAL OF CELL SCIENCE* 112 (8): 1149-1158.

HEISKA, L; ALFTHAN, K; GRONHOLM, M; VILJA, P; VAHERI, A; CARPEN, O. 1998. ASSOCIATION OF EZRIN WITH INTERCELLULAR ADHESION MOLECULE-1 AND -2 (ICAM-1 AND ICAM-2) - REGULATION BY PHOSPHATIDYLINOSITOL 4,5-BISPHOSPHATE. *JOURNAL OF BIOLOGICAL CHEMISTRY* 273 (34): 21893-21900.

HELANDER, TS; CARPEN, O; TURUNEN, O; KOVANEN, PE; VAHERI, A; TIMONEN, T. 1996. ICAM-2 REDISTRIBUTED BY EZRIN AS A TARGET FOR KILLER CELLS. *NATURE* 382 (6588): 265-268.

HENRY, MD; AGOSTI, CG; SOLOMON, F. 1995. MOLECULAR DISSECTION OF RADIXIN - DISTINCT AND INTERDEPENDENT FUNCTIONS OF THE AMINO-TERMINAL AND CARBOXY-TERMINAL DOMAINS. *JOURNAL OF CELL BIOLOGY* 129 (4): 1007-1022.

HIRAO, M; SATO, N; KONDO, T; YONEMURA, S; MONDEN, M; SASAKI, T; TAKAI, Y; TSUKITA, S; TSUKITA, S. 1996. REGULATION MECHANISM OF ERM (EZRIN/RADIXIN/MOESIN) PROTEIN/PLASMA MEMBRANE ASSOCIATION: POSSIBLE INVOLVEMENT OF PHOSPHATIDYLINOSITOL TURNOVER AND RHO-DEPENDENT SIGNALING PATHWAY. *JOURNAL OF CELL BIOLOGY* 135 (1): 37-51.

HUANG, LQ; WONG, TYW; LIN, RCC; FURTHMAYR, H. 1999. REPLACEMENT OF THREONINE 558, A CRITICAL SITE OF PHOSPHORYLATION OF MOESIN IN VIVO, WITH ASPARTATE ACTIVATES F-ACTIN BINDING OF MOESIN - REGULATION BY CONFORMATIONAL CHANGE. *JOURNAL OF BIOLOGICAL CHEMISTRY* 274 (18): 12803-12810.

HUANG, T; YOU, Y; SPOOR, MS; RICHER, EJ; KUDVA, VV; PAIGE, RC; SEILER, MP; LIEBLER, JM; ZABNER, J; PLOPPER, CG; BRODY, SL. 2003. FOXJ1 IS REQUIRED FOR APICAL LOCALIZATION OF EZRIN IN AIRWAY EPITHELIAL CELLS. *JOURNAL OF CELL SCIENCE* 116 (24): 4935-4945.

HUNTER, T; COOPER, JA. 1981. EPIDERMAL GROWTH-FACTOR INDUCES RAPID TYROSINE PHOSPHORYLATION OF PROTEINS IN A431 HUMAN-TUMOR CELLS. *CELL* 24 (3): 741-752.

ITOH, K; SAKAKIBARA, M; YAMASAKI, S; TAKEUCHI, A; ARASE, H; MIYAZAKI, M; NAKAJIMA, N; OKADA, M; SAITO, T. 2002. CUTTING EDGE: NEGATIVE REGULATION OF IMMUNE SYNAPSE FORMATION BY ANCHORING LIPID RAFT TO CYTOSKELETON THROUGH CBP-EBP50-ERM ASSEMBLY. *JOURNAL OF IMMUNOLOGY* 168 (2): 541-544.

IWASE, A; SHEN, RQ; NAVARRO, D; NANUS, DM. 2004. DIRECT BINDING OF NEUTRAL ENDOPEPTIDASE 24.11 TO EZRIN/RADIXIN/MOESIN (ERM) PROTEINS COMPETES WITH THE INTERACTION OF CD44 WITH ERM PROTEINS. *JOURNAL OF BIOLOGICAL CHEMISTRY* 279 (12): 11898-11905.

JOOSS, KU; MULLER, R. 1995. DEREGULATION OF GENES ENCODING MICROFILAMENT-ASSOCIATED PROTEINS DURING FOS-INDUCED MORPHOLOGICAL TRANSFORMATION. *ONCOGENE* 10 (3): 603-608.

KALIPATNATU, S; CHATTOPADHYAY, A. 2005. MEMBRANE PROTEIN SOLUBILIZATION: RECENT ADVANCES AND CHALLENGES IN SOLUBILIZATION OF SEROTONIN$_{1A}$ RECEPTORS. *IUBMB LIFE* 57(7):505-512

KAUL, SC; KAWAI, R; NOMURA, H; MITSUI, Y; REDDEL, RR; WADHWA, R. 1999. IDENTIFICATION OF A 55-KDA EZRIN-RELATED PROTEIN THAT INDUCES CYTOSKELETAL CHANGES AND LOCALIZES TO THE NUCLEOLUS. *EXPERIMENTAL CELL RESEARCH* 250 (1): 51-61.

KAUL, SC; MITSUI, Y; KOMATSU, Y; REDDEL, RR; WADHWA, R. 1996. A HIGHLY EXPRESSED 81 KDA PROTEIN IN IMMORTALIZED MOUSE FIBROBLASTS: ITS PROLIFERATIVE FUNCTION AND IDENTITY WITH EZRIN. *ONCOGENE* 13 (6): 1231-1237.

KOBAYASHI, H; SAGARA, J; KURITA, H; MORIFUJI, M; OHISHI, M; KURASHINA, K; TANIGUCHI, S. 2004. CLINICAL SIGNIFICANCE OF CELLULAR DISTRIBUTION OF MOESIN IN PATIENTS WITH ORAL SQUAMOUS CELL CARCINOMA. *CLINICAL CANCER RESEARCH* 10 (2): 572-580.

KONDO, T; TAKEUCHI, K; DOI, Y; YONEMURA, S; NAGATA, S; TSUKITA, S; TSUKITA, S. 1997. ERM (EZRIN/RADIXIN/MOESIN)-BASED MOLECULAR MECHANISM OF MICROVILLAR BREAKDOWN AT AN EARLY STAGE OF APOPTOSIS. *JOURNAL OF CELL BIOLOGY* 139 (3): 749-758.

KOTANI, H; TAKAISHI, K; SASAKI, T; TAKAI, Y. 1997. RHO REGULATES ASSOCIATION OF BOTH THE ERM FAMILY AND VINCULIN WITH THE PLASMA MEMBRANE IN MDCK CELLS. *ONCOGENE* 14 (14): 1705-1713.

KRIEG, J; HUNTER, T. 1992. IDENTIFICATION OF THE 2 MAJOR EPIDERMAL GROWTH FACTOR-INDUCED TYROSINE PHOSPHORYLATION SITES IN THE MICROVILLAR CORE PROTEIN EZRIN. *JOURNAL OF BIOLOGICAL CHEMISTRY* 267 (27): 19258-19265.

LAMB, RF; OZANNE, BW; ROY, C; MCGARRY, L; STIPP, C; MANGEAT, P; JAY, DG. 1997. ESSENTIAL FUNCTIONS OF EZRIN IN MAINTENANCE OF CELL SHAPE AND LAMELLIPODIAL EXTENSION IN NORMAL AND TRANSFORMED FIBROBLASTS. *CURRENT BIOLOGY* 7 (9): 682-688.

LANKES, W; GRIESMACHER, A; GRUNWALD, J; SCHWARTZALBIEZ, R; KELLER, R. 1988. A HEPARIN-BINDING PROTEIN INVOLVED IN INHIBITION OF SMOOTH-MUSCLE CELL-PROLIFERATION. *BIOCHEMICAL JOURNAL* 251 (3): 831-842.

LEGG, JW; LEWIS, CA; PARSONS, M; NG, T; ISACKE, CM. 2002. A NOVEL PKC-REGULATED MECHANISM CONTROLS CD44-EZRIN ASSOCIATION AND DIRECTIONAL CELL MOTILITY. *NATURE CELL BIOLOGY* 4 (6): 399-407.

LOUVET, S; AGHION, J; SANTAMARIA, A; MANGEAT, P; MARO, B. 1996. EZRIN BECOMES RESTRICTED TO OUTER CELLS FOLLOWING ASYMMETRICAL DIVISION IN THE PREIMPLANTATION MOUSE EMBRYO. *DEVELOPMENTAL BIOLOGY* 177 (2): 568-579.

LOZUPONE, F; LUGINI, L; MATARRESE, P; LUCIANI, F; FEDERICI, C; IESSI, E; MARGUTTI, P; STASSI, G; MALORNI, W; FAIS, S. 2004. IDENTIFICATION AND RELEVANCE OF THE CD95-BINDING DOMAIN IN THE N-TERMINAL REGION OF EZRIN. *JOURNAL OF BIOLOGICAL CHEMISTRY* 279 (10): 9199-9207.

LUBEC, B; WEITZDOERFER, R; FOUNTOULAKIS, M. 2001. MANIFOLD REDUCTION OF MOESIN IN FETAL DOWN SYNDROME BRAIN. *BIOCHEMICAL AND BIOPHYSICAL RESEARCH COMMUNICATIONS* 286 (5): 1191-1194.

MACKAY, DJG; ESCH, F; FURTHMAYR, H; HALL, A. 1997. RHO- AND RAC-DEPENDENT ASSEMBLY OF FOCAL ADHESION COMPLEXES AND ACTIN FILAMENTS IN PERMEABILIZED FIBROBLASTS: AN ESSENTIAL ROLE FOR EZRIN/RADIXIN/MOESIN PROTEINS. *JOURNAL OF CELL BIOLOGY* 138 (4): 927-938.

MARTIN, M; ANDREOLI, C; SAHUQUET, A; MONTCOURRIER, P; ALGRAIN, M; MANGEAT, P. 1995. EZRIN NH2-TERMINAL DOMAIN INHIBITS THE CELL EXTENSION ACTIVITY OF THE COOH-TERMINAL DOMAIN. *JOURNAL OF CELL BIOLOGY* 128 (6): 1081-1093.

MARTIN, M; ROY, C; MONTCOURRIER, P; SAHUQUET, A; MANGEAT, P. 1997. THREE DETERMINANTS IN EZRIN ARE RESPONSIBLE FOR CELL EXTENSION ACTIVITY. *MOLECULAR BIOLOGY OF THE CELL* 8 (8): 1543-1557.

MARTIN, TA; HARRISON, G; MANSEL, RE; JIANG, WG. 2003. THE ROLE OF THE CD44/EZRIN COMPLEX IN CANCER METASTASIS. *CRITICAL REVIEWS IN ONCOLOGY HEMATOLOGY* 46 (2): 165-186.

MATSUI, T; MAEDA, M; DOI, Y; YONEMURA, S; AMANO, M; KAIBUCHI, K; TSUKITA, S; TSUKITA, S. 1998. RHO-KINASE PHOSPHORYLATES COOH-TERMINAL THREONINES OF EZRIN/RADIXIN/MOESIN (ERM) PROTEINS AND REGULATES THEIR HEAD-TO-TAIL ASSOCIATION. *JOURNAL OF CELL BIOLOGY* 140 (3): 647-657.

MATSUI, T; YONEMURA, S; TSUKITA, S; TSUKITA, S. 1999. ACTIVATION OF ERM PROTEINS IN VIVO BY RHO INVOLVES PHOSPHATIDYLINOSITOL 4-PHOSPHATE 5-KINASE AND NOT ROCK KINASES. *CURRENT BIOLOGY* 9 (21): 1259-1262.

MATTHEWS, C; VAN HOLDE, K.1996 THE THREE DIMENSIONAL STRUCTURE OF PROTEINS in *BIOCHEMISTRY, 2ND ED.* THE BENJAMIN/CUMMINGS PUBLISHING COMPANY INC. pp165-213

MCCLATCHEY, AI. 2003. OPINION - MERLIN AND ERM PROTEINS: UNAPPRECIATED ROLES IN CANCER DEVELOPMENT?. *NATURE REVIEWS CANCER* 3 (11): 877-883.

MCROBERT, EA; GALLICCHIO, M; JERUMS, G; COOPER, ME; BACH, LA. 2003. THE AMINO-TERMINAL DOMAINS OF THE EZRIN, RADIXIN, AND MOESIN (ERM) PROTEINS BIND ADVANCED GLYCATION END PRODUCTS, AN INTERACTION THAT MAY PLAY A ROLE IN THE DEVELOPMENT OF DIABETIC COMPLICATIONS. *JOURNAL OF BIOLOGICAL CHEMISTRY* 278 (28): 25783-25789.

MELENDEZ-VASQUEZ, CV; RIOS, JC; ZANAZZI, G; LAMBERT, S; BRETSCHER, A; SALZER, JL. 2001. NODES OF RANVIER FORM IN ASSOCIATION WITH EZRIN-RADIXIN-MOESIN (ERM)-POSITIVE SCHWANN CELL PROCESSES. *PROCEEDINGS OF THE NATIONAL ACADEMY OF SCIENCES OF THE UNITED STATES OF AMERICA* 98 (3): 1235-1240.

MENG, JJ; LOWRIE, DJ; SUN, H; DORSEY, E; PELTON, PD; BASHOUR, AM; GRODEN, J; RATNER, N; IP, W. 2000. INTERACTION BETWEEN TWO ISOFORMS OF THE NF2 TUMOR SUPPRESSOR PROTEIN, MERLIN, AND BETWEEN MERLIN AND EZRIN, SUGGESTS MODULATION OF ERM PROTEINS BY MERLIN. *JOURNAL OF NEUROSCIENCE RESEARCH* 62 (4): 491-502.

MORALES, FC; TAKAHASHI, Y; KREIMANN, EL; GEORGESCU, MM. 2004. EZRIN-RADIXIN-MOESIN (ERM)-BINDING PHOSPHOPROTEIN 50 ORGANIZES ERM PROTEINS AT THE APICAL MEMBRANE OF POLARIZED EPITHELIA. *PROCEEDINGS OF THE NATIONAL ACADEMY OF SCIENCES OF THE UNITED STATES OF AMERICA* 101 (51): 17705-17710.

MURANEN, T; GRONHOLM, MG; RENKEMA, GH; CARPEN, O. 2005. CELL CYCLE-DEPENDENT NUCLEOCYTOPLASMIC SHUTTLING OF THE NEUROFIBROMATOSIS 2

TUMOUR SUPPRESSOR MERLIN. *ONCOGENE* 24 (7): 1150-1158.

MURTHY, A; GONZALEZ-AGOSTI, C; CORDERO, E; PINNEY, D; CANDIA, C; SOLOMON, F; GUSELLA, J; RAMESH, V. 1998. NHE-RF, A REGULATORY COFACTOR FOR NA+-H+ EXCHANGE, IS A COMMON INTERACTOR FOR MERLIN AND ERM (MERM) PROTEINS. *JOURNAL OF BIOLOGICAL CHEMISTRY* 273 (3): 1273-1276.

NAKAMURA, F; AMIEVA, MR; FURTHMAYR, H. 1995. PHOSPHORYLATION OF THREONINE 558 IN THE CARBOXYL-TERMINAL ACTIN-BINDING DOMAIN OF MOESIN BY THROMBIN ACTIVATION OF HUMAN PLATELETS. *JOURNAL OF BIOLOGICAL CHEMISTRY* 270 (52): 31377-31385.

NAKAMURA, F; HUANG, LQ; PESTONJAMASP, K; LUNA, E; FURTHMAYR, H. 1999. REGULATION OF F-ACTIN BINDING TO PLATELET MOESIN IN VITRO BY BOTH PHOSPHORYLATION OF THREONINE558 AND POLYPHOSPHOINOSITIDES. *MOLECULAR BIOLOGY OF THE CELL* 10: 154A-154A, SUPPL. S.

NASSIF, X; BOURDOULOUS, S; EUGENE, E; COURAUD, PO. 2002. HOW DO EXTRACELLULAR PATHOGENS CROSS THE BLOOD-BRAIN BARRIER?. *TRENDS IN MICROBIOLOGY* 10 (5): 227-232.

NG, T; PARSONS, M; HUGHES, WE; MONYPENNY, J; ZICHA, D; GAUTREAU, A; ARPIN, M; GSCHMEISSNER, S; VERVEER, PJ; BASTIAENS, PIH; PARKER, PJ. 2001. EZRIN IS A DOWNSTREAM EFFECTOR OF TRAFFICKING PKC-INTEGRIN COMPLEXES INVOLVED IN THE CONTROL OF CELL MOTILITY. *EMBO JOURNAL* 20 (11): 2723-2741.

NGUYEN, R; RECZEK, D; BRETSCHER, A. 2001. HIERARCHY OF MERLIN AND EZRIN N- AND C-TERMINAL DOMAIN INTERACTIONS IN HOMO- AND HETEROTYPIC ASSOCIATIONS AND THEIR RELATIONSHIP TO BINDING OF SCAFFOLDING PROTEINS EBP50 AND E3KARP. *JOURNAL OF BIOLOGICAL CHEMISTRY* 276 (10): 7621-7629.

NIGGLI, V; ANDREOLI, C; ROY, C; MANGEAT, P. 1995. IDENTIFICATION OF A PHOSPHATIDYLINOSITOL-4,5-BISPHOSPHATE-BINDING DOMAIN IN THE N-TERMINAL REGION OF EZRIN. *FEBS LETTERS* 376 (3): 172-176.

OSHIRO, N; FUKATA, Y; KAIBUCHI, K. 1998. PHOSPHORYLATION OF MOESIN BY RHO-ASSOCIATED KINASE (RHO-KINASE) PLAYS A CRUCIAL ROLE IN THE FORMATION OF MICROVILLI-LIKE STRUCTURES. *JOURNAL OF BIOLOGICAL CHEMISTRY* 273 (52): 34663-34666.

PAGLINI, G; KUNDA, P; QUIROGA, S; KOSIK, K; CACERES, A. 1998. SUPPRESSION OF RADIXIN AND MOESIN ALTERS GROWTH CONE MORPHOLOGY, MOTILITY, AND PROCESS FORMATION IN PRIMARY CULTURED NEURONS. *JOURNAL OF CELL BIOLOGY* 143 (2): 443-455.

PAKKANEN, R. 1988. IMMUNOFLUORESCENT AND IMMUNOCHEMICAL EVIDENCE FOR THE EXPRESSION OF CYTOVILLIN IN THE MICROVILLI OF A WIDE-RANGE OF CULTURED HUMAN-CELLS. *JOURNAL OF CELLULAR BIOCHEMISTRY* 38 (1): 65-75.

PAKKANEN, R; HEDMAN, K; TURUNEN, O; WAHLSTROM, T; VAHERI, A. 1987. MICROVILLUS-SPECIFIC MR 75,000 PLASMA-MEMBRANE PROTEIN OF HUMAN CHORIOCARCINOMA CELLS. *JOURNAL OF HISTOCHEMISTRY & CYTOCHEMISTRY* 35 (8): 809-816.

PARLATO, S; GIAMMARIOLI, AM; LOGOZZI, M; LOZUPONE, F; MATARRESE, P; LUCIANI, F; FALCHI, M; MALORNI, W; FAIS, S. 2000. CD95 (APO-1/FAS) LINKAGE TO THE ACTIN CYTOSKELETON THROUGH EZRIN IN HUMAN T LYMPHOCYTES: A NOVEL REGULATORY MECHANISM OF THE CD95 APOPTOTIC PATHWAY. *EMBO JOURNAL* 19 (19): 5123-5134.

PEARSON, MA; RECZEK, D; BRETSCHER, A; KARPLUS, PA. 2000. STRUCTURE OF THE ERM PROTEIN MOESIN REVEALS THE FERM DOMAIN FOLD MASKED BY AN EXTENDED ACTIN BINDING TAIL DOMAIN. *CELL* 101 (3): 259-270.

PESTONJAMASP, K; AMIEVA, MR; STRASSEL, CP; NAUSEEF, WM; FURTHMAYR, H; LUNA, EJ. 1995. MOESIN, EZRIN, AND P205 ARE ACTIN-BINDING PROTEINS ASSOCIATED WITH NEUTROPHIL PLASMA-MEMBRANES. *MOLECULAR BIOLOGY OF THE CELL* 6 (3): 247-259.

PIETROMONACO, SF; SIMONS, PC; ALTMAN, A; ELIAS, L. 1998. PROTEIN KINASE C-THETA PHOSPHORYLATION OF MOESIN IN THE ACTIN-BINDING SEQUENCE. *JOURNAL OF BIOLOGICAL CHEMISTRY* 273 (13): 7594-7603.

RECZEK, D; BERRYMAN, M; BRETSCHER, A. 1997. IDENTIFICATION OF EBP50: A PDZ-CONTAINING PHOSPHOPROTEIN THAT ASSOCIATES WITH MEMBERS OF THE

ERM FAMILY.. *MOLECULAR BIOLOGY OF THE CELL* 8: 1024-1024, SUPPL. S.

RECZEK, D; BRETSCHER, A. 1998. THE CARBOXYL-TERMINAL REGION OF EBP50 BINDS TO A SITE IN THE AMINO-TERMINAL DOMAIN OF EZRIN THAT IS MASKED IN THE DORMANT MOLECULE. *JOURNAL OF BIOLOGICAL CHEMISTRY* 273 (29): 18452-18458.

RECZEK, D; BRETSCHER, A. 2001. IDENTIFICATION OF EPI64, A TBC/RABGAP DOMAIN-CONTAINING MICROVILLAR PROTEIN THAT BINDS TO THE FIRST PDZ DOMAIN OF EBP50 AND E3KARP. *JOURNAL OF CELL BIOLOGY* 153 (1): 191-205.

RHEE, SG; BAE, YS. 1997. REGULATION OF PHOSPHOINOSITIDE-SPECIFIC PHOSPHOLIPASE C ISOZYMES. *JOURNAL OF BIOLOGICAL CHEMISTRY* 272 (24): 15045-15048.

ROULEAU, GA; MEREL, P; LUTCHMAN, M; SANSON, M; ZUCMAN, J; MARINEAU, C; HOANGXUAN, K; DEMCZUK, S; DESMAZE, C; PLOUGASTEL, B; PULST, SM; LENOIR, G; BIJLSMA, E; FASHOLD, R; DUMANSKI, J; DEJONG, P; PARRY, D; ELDRIGE, R; AURIAS, A; DELATTRE, O; THOMAS, G. 1993. ALTERATION IN A NEW GENE ENCODING A PUTATIVE MEMBRANE-ORGANIZING PROTEIN CAUSES NEUROFIBROMATOSIS TYPE-2. *NATURE* 363 (6429): 515-521.

ROY, C; MARTIN, M; MANGEAT, P. 1997. A DUAL INVOLVEMENT OF THE AMINO-TERMINAL DOMAIN OF EZRIN IN F- AND G-ACTIN BINDING. *JOURNAL OF BIOLOGICAL CHEMISTRY* 272 (32): 20088-20095.

SATO, N; YONEMURA, S; OBINATA, T; TSUKITA, S; TSUKITA, S. 1991. RADIXIN, A BARBED END-CAPPING ACTIN-MODULATING PROTEIN, IS CONCENTRATED AT THE CLEAVAGE FURROW DURING CYTOKINESIS. *JOURNAL OF CELL BIOLOGY* 113 (2): 321-330.

SCHIRENBECK, A; BRETSCHNEIDER, T; ARASADA, R; SCHLEICHER, M; FAIX, J. 2005. THE DIAPHANOUS-RELATED FORMIN DDIA2 IS REQUIRED FOR THE FORMATION AND MAINTENANCE OF FILOPODIA. *NATURE CELL BIOLOGY* 7 (6): 619-U24.

SCHOLL, FG; GAMALLO, C; VILARO, S; QUINTANILLA, M. 1999. IDENTIFICATION OF PA2.26 ANTIGEN AS A NOVEL CELL-SURFACE MUCIN-TYPE GLYCOPROTEIN THAT INDUCES PLASMA MEMBRANE EXTENSIONS AND INCREASED MOTILITY IN KERATINOCYTES. *JOURNAL OF CELL SCIENCE* 112 (24): 4601-4613.

SERRADOR, JM; ALONSOLEBRERO, JL; DELPOZO, MA; FURTHMAYR, H; SCHWARTZALBIEZ, R; CALVO, J; LOZANO, F; SANCHEZMADRID, F. 1997. MOESIN INTERACTS WITH THE CYTOPLASMIC REGION OF INTERCELLULAR ADHESION MOLECULE-3 AND IS REDISTRIBUTED TO THE UROPOD OF T LYMPHOCYTES DURING CELL POLARIZATION. *JOURNAL OF CELL BIOLOGY* 138 (6): 1409-1423.

SERRADOR, JM; NIETO, M; ALONSO-LEBRERO, JL; DEL POZO, MA; CALVO, J; FURTHMAYR, H; SCHWARTZ-ALBIEZ, R; LOZANO, F; GONZALEZ-AMARO, R; SANCHEZ-MATEOS, P; SANCHEZ-MADRID, F. 1998. CD43 INTERACTS WITH MOESIN AND EZRIN AND REGULATES ITS REDISTRIBUTION TO THE UROPODS OF T LYMPHOCYTES AT THE CELL-CELL CONTACTS. *BLOOD* 91 (12): 4632-4644.

SHAW, RJ; HENRY, M; SOLOMON, F; JACKS, T. 1998. RHOA-DEPENDENT PHOSPHORYLATION AND RELOCALIZATION OF ERM PROTEINS INTO APICAL MEMBRANE/ACTIN PROTRUSIONS IN FIBROBLASTS. *MOLECULAR BIOLOGY OF THE CELL* 9 (2): 403-419.

SHCHERBINA, A; BRETSCHER, A; KENNEY, DM; REMOLD-O'DONNELL, E. 1999. MOESIN, THE MAJOR ERM PROTEIN OF LYMPHOCYTES AND PLATELETS, DIFFERS FROM EZRIN IN ITS INSENSITIVITY TO CALPAIN. *FEBS LETTERS* 443 (1): 31-36.

SHUSTER, CB; HERMAN, IM. 1995. INDIRECT ASSOCIATION OF EZRIN WITH F-ACTIN - ISOFORM SPECIFICITY AND CALCIUM SENSITIVITY. *JOURNAL OF CELL BIOLOGY* 128 (5): 837-848.

SIMONOVIC, I; ARPIN, M; KOUTSOURIS, A; FALK-KRZESINSKI, HJ; HECHT, G. 2001. ENTEROPATHOGENIC ESCHERICHIA COLI ACTIVATES EZRIN, WHICH PARTICIPATES IN DISRUPTION OF TIGHT JUNCTION BARRIER FUNCTION. *INFECTION AND IMMUNITY* 69 (9): 5679-5688.

SIMONS, PC; PIETROMONACO, SF; RECZEK, D; BRETSCHER, A; ELIAS, L. 1998. C-TERMINAL THREONINE PHOSPHORYLATION ACTIVATES ERM PROTEINS TO LINK THE CELL'S CORTICAL LIPID BILAYER TO THE CYTOSKELETON. *BIOCHEMICAL AND BIOPHYSICAL RESEARCH COMMUNICATIONS* 253 (3): 561-565.

SPECK, O; HUGHES, SC; NOREN, NK; KULIKAUSKAS, RM; FEHON, RG. 2003. MOESIN FUNCTIONS ANTAGONISTICALLY TO THE RHO PATHWAY TO MAINTAIN EPITHELIAL INTEGRITY. *NATURE* 421 (6918): 83-87.

SUNI, J; NARVANEN, A; WAHLSTROM, T; AHO, M; PAKKANEN, R; VAHERI, A; COPELAND, T; COHEN, M; OROSZLAN, S. 1984. HUMAN PLACENTAL SYNCYTIOTROPHOBLASTIC MR-75,000 POLYPEPTIDE DEFINED BY ANTIBODIES TO A SYNTHETIC PEPTIDE BASED ON A CLONED HUMAN ENDOGENOUS RETROVIRAL DNA-SEQUENCE. *PROCEEDINGS OF THE NATIONAL ACADEMY OF SCIENCES OF THE UNITED STATES OF AMERICA-BIOLOGICAL SCIENCES* 81 (19): 6197-6201.

TAKAHASHI, K; SASAKI, T; MAMMOTO, A; TAKAISHI, K; KAMEYAMA, T; TSUKITA, S; TSUKITA, S; TAKAI, Y. 1997. DIRECT INTERACTION OF THE RHO GDP DISSOCIATION INHIBITOR WITH EZRIN/RADIXIN/MOESIN INITIATES THE ACTIVATION OF THE RHO SMALL G PROTEIN. *JOURNAL OF BIOLOGICAL CHEMISTRY* 272 (37): 23371-23375.

TAKEUCHI, K; SATO, N; KASAHARA, H; FUNAYAMA, N; NAGAFUCHI, A; YONEMURA, S; TSUKITA, S; TSUKITA, S. 1994. PERTURBATION OF CELL-ADHESION AND MICROVILLI FORMATION BY ANTISENSE OLIGONUCLEOTIDES TO ERM FAMILY MEMBERS. *JOURNAL OF CELL BIOLOGY* 125 (6): 1371-1384.

TAMMA, G; KLUSSMANN, E; OEHLKE, J; KRAUSE, E; ROSENTHAL, W; SVELTO, M; VALENTI, G. 2005. ACTIN REMODELING REQUIRES ERM FUNCTION TO FACILITATE AQP2 APICAL TARGETING. *JOURNAL OF CELL SCIENCE* 118 (16): 3623-3630.

TROFATTER, JA; MACCOLLIN, MM; RUTTER, JL; MURRELL, JR; DUYAO, MP; PARRY, DM; ELDRIDGE, R; KLEY, N; MENON, AG; PULASKI, K; HAASE, VH; AMBROSE, CM; MUNROE, D; BOVE, C; HAINES, JL; MARTUZA, RL; MACDONALD, ME; SEIZINGER, BR; SHORT, MP; BUCKLER, AJ; GUSELLA, JF. 1993. A NOVEL MOESIN-LIKE, EZRIN-LIKE, RADIXIN-LIKE GENE IS A CANDIDATE FOR THE NEUROFIBROMATOSIS-2 TUMOR SUPPRESSOR. *CELL* 72 (5): 791-800.

TSUKITA, S; HIEDA, Y; TSUKITA, S. 1989. A NEW 82-KD BARBED END-CAPPING PROTEIN (RADIXIN) LOCALIZED IN THE CELL-TO-CELL ADHERENS JUNCTION - PURIFICATION AND CHARACTERIZATION. *JOURNAL OF CELL BIOLOGY* 108 (6): 2369-2382.

TSUKITA, S; OISHI, K; SATO, N; SAGARA, J; KAWAI, A; TSUKITA, S. 1994. ERM FAMILY MEMBERS AS MOLECULAR LINKERS BETWEEN THE CELL-SURFACE GLYCOPROTEIN CD44 AND ACTIN-BASED CYTOSKELETONS. *JOURNAL OF CELL BIOLOGY* 126 (2): 391-401.

TURNER, P; MCLENNAN, A; BATES, A; WHITE, M. 2000 PROTEIN STRUCTURE in *INSTANT NOTES IN MOLECULAR BIOLOGY, 2ND ED.* BIOS SCIENTIFIC PUBLISHERS LTD. pp15-30

TURUNEN, O; WAHLSTROM, T; VAHERI, A. 1994. EZRIN HAS A COOH-TERMINAL ACTIN-BINDING SITE THAT IS CONSERVED IN THE EZRIN PROTEIN FAMILY. *JOURNAL OF CELL BIOLOGY* 126 (6): 1445-1453.

TURUNEN, O; WINQVIST, R; PAKKANEN, R; GRZESCHIK, KH; WAHLSTROM, T; VAHERI, A. 1989. CYTOVILLIN, A MICROVILLAR MR 75,000 PROTEIN - CDNA SEQUENCE, PROKARYOTIC EXPRESSION, AND CHROMOSOMAL LOCALIZATION. *JOURNAL OF BIOLOGICAL CHEMISTRY* 264 (28): 16727-16732.

URUSHIDANI, T; HANZEL, DK; FORTE, JG. 1989. CHARACTERIZATION OF AN 80-KDA PHOSPHOPROTEIN INVOLVED IN PARIETAL-CELL STIMULATION. *AMERICAN JOURNAL OF PHYSIOLOGY* 256 (6): G1070-G1081, PART 1.

VARNAI, P; BALLA, T. 1998. VISUALIZATION OF PHOSPHOINOSITIDES THAT BIND PLECKSTRIN HOMOLOGY DOMAINS. *MOLECULAR BIOLOGY OF THE CELL* 9: 120A-120A, SUPPL. S.

VENKATESWARLU, K; GUNN-MOORE, F; OATEY, PB; TAVARE, JM; CULLEN, PJ. 1998A. NERVE GROWTH FACTOR- AND EPIDERMAL GROWTH FACTOR-STIMULATED TRANSLOCATION OF THE ADP RIBOSYLATION FACTOR EXCHANGE FACTOR GRP1 TO THE PLASMA MEMBRANE OF PC12 CELLS REQUIRES ACTIVATION OF PHOSPHATIDYLINOSITOL 3-KINASE AND THE GRP1 PLECKSTRIN HOMOLOGY DOMAIN. *BIOCHEMICAL JOURNAL* 335: 139-146, PART 1.

VENKATESWARLU, K; GUNN-MOORE, F; TAVARE, JM; CULLEN, PJ. 1999. EGF- AND NGF-STIMULATED TRANSLOCATION OF CYTOHESIN-1 TO THE PLASMA MEMBRANE OF PC12 CELLS REQUIRES PI 3-KINASE ACTIVATION AND A FUNCTIONAL

CYTOHESIN-1 PH DOMAIN. *JOURNAL OF CELL SCIENCE* 112 (12): 1957-1965.

VENKATESWARLU, K; OATEY, PB; TAVARE, JM; CULLEN, PJ. 1998B. INSULIN-DEPENDENT TRANSLOCATION OF ARNO TO THE PLASMA MEMBRANE OF ADIPOCYTES REQUIRES PHOSPHATIDYLINOSITOL 3-KINASE. *CURRENT BIOLOGY* 8 (8): 463-466.

WEINMAN, EJ; STEPLOCK, D; WANG, YP; SHENOLIKAR, S. 1995. CHARACTERIZATION OF A PROTEIN COFACTOR THAT MEDIATES PROTEIN-KINASE-A REGULATION OF THE RENAL BRUSH-BORDER MEMBRANE NA+-H+ EXCHANGER. *JOURNAL OF CLINICAL INVESTIGATION* 95 (5): 2143-2149.

YONEMURA, S; HIRAO, M; DOI, Y; TAKAHASHI, N; KONDO, T; TSUKITA, S; TSUKITA, S. 1998. EZRIN/RADIXIN/MOESIN (ERM) PROTEINS BIND TO A POSITIVELY CHARGED AMINO ACID CLUSTER IN THE JUXTA-MEMBRANE CYTOPLASMIC DOMAIN OF CD44, CD43, AND ICAM-2. *JOURNAL OF CELL BIOLOGY* 140 (4): 885-895.

YONEMURA, S; MATSUI, T; TSUKITA, S; TSUKITA, S. 2002. RHO-DEPENDENT AND -INDEPENDENT ACTIVATION MECHANISMS OF EZRIN/RADIXIN/MOESIN PROTEINS: AN ESSENTIAL ROLE FOR POLYPHOSPHOINOSITIDES IN VIVO. *JOURNAL OF CELL SCIENCE* 115 (12): 2569-2580.

YONEMURA, S; TSUKITA, S; TSUKITA, S. 1999. DIRECT INVOLVEMENT OF EZRIN/RADIXIN/MOESIN (ERM)-BINDING MEMBRANE PROTEINS IN THE ORGANIZATION OF MICROVILLI IN COLLABORATION WITH ACTIVATED ERM PROTEINS. *JOURNAL OF CELL BIOLOGY* 145 (7): 1497-1509.

YU, YL; KHAN, J; KHANNA, C; HELMAN, L; MELTZER, PS; MERLINO, G. 2004. EXPRESSION PROFILING IDENTIFIES THE CYTOSKELETAL ORGANIZER EZRIN AND THE DEVELOPMENTAL HOMEOPROTEIN SIX-1 AS KEY METASTATIC REGULATORS. *NATURE MEDICINE* 10 (2): 175-181.

YUN, CHC; OH, SY; ZIZAK, M; STEPLOCK, D; TSAO, S; TSE, CM; WEINMAN, EJ; DONOWITZ, M. 1997. CAMP-MEDIATED INHIBITION OF THE EPITHELIAL BRUSH BORDER NA+/H+ EXCHANGER, NHE3, REQUIRES AN ASSOCIATED REGULATORY PROTEIN (VOL 94, PG 3010, 1997). *PROCEEDINGS OF THE NATIONAL ACADEMY OF SCIENCES OF THE UNITED STATES OF AMERICA* 94 (18): 10006-10006.

ZHOU, RH; CAO, XW; WATSON, C; MIAO, Y; GUO, Z; FORTE, JG; YAO, XB. 2003. CHARACTERIZATION OF PROTEIN KINASE A-MEDIATED PHOSPHORYLATION OF EZRIN IN GASTRIC PARIETAL CELL ACTIVATION. *JOURNAL OF BIOLOGICAL CHEMISTRY* 278 (37): 35651-35659.

ZHOU, RH; ZHU, LX; KODANI, A; HAUSER, P; YAO, XB; FORTE, JG. 2005. PHOSPHORYLATION OF EZRIN ON THREONINE 567 PRODUCES A CHANGE IN SECRETORY PHENOTYPE AND REPOLARIZES THE GASTRIC PARIETAL CELL. *JOURNAL OF CELL SCIENCE* 118 (19): 4381-4391.

ZHU, LX; LIU, YC; FORTE, JG. 2005. EZRIN OLIGOMERS ARE THE MEMBRANE-BOUND DORMANT FORM IN GASTRIC PARIETAL CELLS. *AMERICAN JOURNAL OF PHYSIOLOGY-CELL PHYSIOLOGY* 288 (6): C1242-C1254.